



저작자표시-비영리-변경금지 2.0 대한민국

이용자는 아래의 조건을 따르는 경우에 한하여 자유롭게

- 이 저작물을 복제, 배포, 전송, 전시, 공연 및 방송할 수 있습니다.

다음과 같은 조건을 따라야 합니다:



저작자표시. 귀하는 원저작자를 표시하여야 합니다.



비영리. 귀하는 이 저작물을 영리 목적으로 이용할 수 없습니다.



변경금지. 귀하는 이 저작물을 개작, 변형 또는 가공할 수 없습니다.

- 귀하는, 이 저작물의 재이용이나 배포의 경우, 이 저작물에 적용된 이용허락조건을 명확하게 나타내어야 합니다.
- 저작권자로부터 별도의 허가를 받으면 이러한 조건들은 적용되지 않습니다.

저작권법에 따른 이용자의 권리는 위의 내용에 의하여 영향을 받지 않습니다.

이것은 [이용허락규약\(Legal Code\)](#)을 이해하기 쉽게 요약한 것입니다.

[Disclaimer](#)

A Dissertation for the Degree of Doctor of Philosophy

Functional Analysis of EGF, IGF-I, VEGF
and CSF2 on Development of Porcine
Conceptus Trophectoderm during Early
Pregnancy

임신초기 돼지 영양외배엽 세포의 발달에 미치는
EGF, IGF-I, VEGF 및 CSF2의 기능분석 연구

February, 2014

By

WOOYOUNG JEONG

WCU Biomodulation Major

Department of Agricultural Biotechnology

Graduate School, Seoul National University

ABSTRACT

Functional Analysis of EGF, IGF-I, VEGF and CSF2 on Development of Porcine Conceptus Trophectoderm during Early Pregnancy

Wooyoung Jeong

WCU Biomodulation Major

Department of Agricultural Biotechnology

The Graduate School

Seoul National University

The majority of early conceptus mortality in pregnancy occurs during the peri-implantation stage, suggesting that this period is important for conceptus viability and the establishment of pregnancy. Successful establishment of pregnancy in all mammalian species depends on the orchestrated molecular events that transpire at the conceptus-uterine interface during the peri-implantation phase. This maternal-conceptus interaction is especially crucial in pigs because in them non-invasive epitheliochorial placentation occurs, in which the pre-implantation phase is prolonged.

During the pre-implantation period, conceptus survival and the establishment of pregnancy are known to depend on the developing conceptus receiving an adequate supply of histotroph, which contains a wide range of nutrients

and growth factors. Evidence links epidermal growth factor (EGF), insulin-like growth factor-I (IGF-I), vascular endothelial growth factor (VEGF), and colony-stimulating factor 2 (CSF2) to embryogenesis or implantation in various mammalian species; however, in the case of pig, little is known about such functions of these growth factors, especially their regulatory mechanisms at the maternal-conceptus interface. Therefore, the objectives of this study were to determine: 1) the temporal and cell-specific expression of EGF, IGF-I, VEGF, and CSF2 signaling systems in the porcine endometrium during the estrous cycle and early pregnancy; 2) the potential intracellular signaling pathways responsible for the activities of these four factors in primary porcine trophoderm (pTr) cells; and 3) the changes in cellular activities induced by these promising factors.

First, the functional effect and cellular signaling cascades in pTr cells induced by EGF, which exhibits potential growth-promoting activities on the conceptus and endometrium, were investigated. *EGFR* mRNA and protein were abundant in endometrial luminal epithelia (LE) and glandular epithelia (GE), stratum compactum stroma, and conceptus trophoderm on Days 13-14 of pregnancy, but not in any other cells of the uterus. EGF treatment of pTr cells increased the abundance of phosphorylated (p)-AKT1, p-ERK1/2 MAPK and p-P90RSK in the nucleus and/or cytoplasm when compared with the levels in control cells. Furthermore, EGF-stimulated phosphorylation of AKT1 and ERK1/2 MAPK were inhibited in pTr cells transfected with an EGFR siRNA, and compared with control siRNA-transfected pTr cells, the EGFR siRNA-transfected pTr cells exhibited an increase in the expression of gene encoding *interferon (IFN)- δ* and *transforming growth factor (TGF)*

β-1; by contrast, no effect was detected on the expression of the gene encoding *IFN-γ*. Moreover, EGF stimulated the proliferation and migration of pTr cells, but these stimulatory effects were blocked by pharmacological inhibitors such as SB203580 (a p38 inhibitor), U0126 (a MAPK inhibitor), rapamycin (an MTOR inhibitor), and LY294002 (a PI3K inhibitor).

Second, IGF-I was examined. IGF-I is another promising growth factor that is known to play key roles in reproductive processes; however, little is known about IGF-I-induced functional effects and regulatory mechanisms during peri-implantation in pigs. In this study, endometrial *type I IGF receptor (IGF-IR)* mRNA was determined to increase substantially during early pregnancy relative to the level during the estrous cycle, and the mRNAs of both *IGF-I* and *IGF-IR* were abundant in endometrial LE and GE, stroma and conceptus trophoctoderm on Day 12 of pregnancy. Moreover, IGF-I treatment potently increased the amounts of p-AKT1 and ERK1/2 MAPK in the nucleus and cytoplasm and of RPS6 in the cytosol when compared with the amounts in untreated pTr cells, and IGF-I-induced activation of AKT1 and ERK1/2 was blocked by LY294002. Furthermore, IGF-I strongly stimulated both the proliferation and the migration of pTr cells, but these effects were inhibited by SB203580, U0126, rapamycin and LY294002.

Third, this study focused on VEGF, which was identified as a potential mediator of the fetal-maternal dialog that regulates the development of the peri-implantation porcine conceptus. In addition to its known angiogenic effects, VEGF has been suggested to play roles in the development of the early embryo, but VEGF-

induced effects on the peri-implantation conceptus remain unknown. Results of this study revealed that endometrial *VEGF*, *VEGF receptor (VEGFR)-1*, and *VEGFR-2* mRNA levels in endometrial LE and GE, endothelial blood vessels, and scattered cells in the stroma were more abundant during the peri-implantation period of pregnancy than during the estrous cycle. Moreover, VEGF treatment of pTr cells increased the abundance of p-AKT1, p-ERK1/2, p-p70RSK, p-RPS6 and p-4EBP1, and the addition of LY294002 suppressed VEGF-induced phosphorylation of ERK1/2 and AKT1. Furthermore, VEGF potently stimulated both the proliferation and the migration of pTr cells, but these effects were inhibited in the presence of SB203580, U0126, rapamycin and LY294002.

The fourth promising cytokine studied was CSF2, which is also known as granulocyte-macrophage colony-stimulating factor (GM-CSF). CSF2 plays a role in facilitating mammalian early embryonic development. In this study, endometrial *CSF2* mRNA expression was determined to be increased during the peri-implantation period relative to the mRNA level during the estrous cycle. In pTr cells, CSF2 significantly induced the activation of AKT1, ERK1/2, MTOR, p70RSK, and RPS6, but not of STAT3, and the addition of LY294002 abolished CSF2-induced increases in p-ERK1/2, p-MTOR, and p-AKT1 levels. Furthermore, CSF2 strongly stimulated pTr cell proliferation, an effect that was blocked by U0126, rapamycin and LY294002.

Collectively, these results provide new insights into the potential mediators that regulate the development of the peri-implantation conceptus at the fetal-maternal interface. These results indicate that endometrial- and/or conceptus derived EGF, IGF-

I, VEGF, and CSF2 critically affect the growth and development of porcine trophoctoderm cells, and that these stimulatory effects are coordinately regulated by multiple cellular signaling cascades including the PI3K-AKT and ERK1/2 MAPK pathways during early pregnancy in pigs.

Keywords: trophoctoderm cells, peri-implantation, EGF, IGF-I, VEGF, CSF2

Student Number: 2010-24127

CONTENTS

ABSTRACT.....	i
CONTENTS.....	vi
LIST OF FIGURES	x
LIST OF TABLES.....	xvii
LIST OF ABBREVIATIONS	xviii
CHAPTER 1. General Introduction.....	1
CHAPTER 2. Literature Review	6
1. Estrous Cycle and Early Pregnancy.....	7
1.1. Estrous Cycle.....	7
1.2. Pre-Implantation Period	9
1.3. Opening of the Implantation Window and Implantation.....	10
2. Physiology of the Porcine Conceptus during Peri-Implantation	12
2.1. Early Conceptus Development	12
2.2. Maternal Recognition of Pregnancy	12
2.3. Conceptus Trophoblastic Elongation.....	13
2.4. Conceptus Apposition and Attachment to the Uterine Luminal Epithelium	15
3. Uterine Microenvironment during Early Pregnancy	16
3.1. Maternal-Conceptus Interactions	16
3.2. Embryonic Factors	17
3.3. Uterine Factors	18
4. Growth Factors and Cytokines Regulating Conceptus Cellular Processes	19
5. Promising Uterine Factors Affecting Conceptus Development and Implantation.....	21

5.1. Epidermal Growth Factor (EGF)	21
5.2. Insulin-Like Growth Factor-I (IGF-I)	22
5.3. Vascular Endothelial Growth Factor (VEGF)	23
5.4. Colony-Stimulating Factor 2 (CSF2).....	24

CHAPTER 3. Epidermal Growth Factor Stimulates Proliferation and Migration of Porcine Trophectoderm Cells Through Protooncogenic Protein Kinase 1 and Extracellular-Signal-Regulated Kinases 1/2 Mitogen-Activated Protein Kinase Signal Transduction Cascades during Early Pregnancy	27
1. Abstract.....	28
2. Introduction	30
3. Materials and Methods.....	34
4. Results	44
5. Discussion	61

CHAPTER 4. Insulin-Like Growth Factor I Induces Proliferation and Migration of Porcine Trophectoderm Cells through Multiple Cell Signaling Pathways, Including Protooncogenic Protein Kinase 1 and Mitogen-Activated Protein Kinase	67
1. Abstract.....	68
2. Introduction	70
3. Materials and Methods.....	74
4. Results	82
5. Discussion	96

CHAPTER 5. Stimulatory Effect of Vascular Endothelial Growth Factor on Proliferation and Migration of Porcine Trophectoderm Cells and Their Regulation by the Phosphatidylinositol-3-Kinase-AKT and Mitogen-Activated Protein Kinase Cell Signaling Pathways.....	103
1. Abstract.....	104
2. Introduction	106

3. Materials and Methods.....	110
4. Results	118
5. Discussion	133
CHAPTER 6. Proliferation-Stimulating Effect of Colony Stimulating Factor 2 on Porcine Trophectoderm Cells is Mediated by Activation of Phosphatidylinositol 3-Kinase and Extracellular Signal-Regulated Kinase 1/2 Mitogen-Activated Protein Kinase	139
1. Abstract.....	140
2. Introduction	142
3. Materials and Methods.....	146
4. Results	152
5. Discussion	162
CHAPTER 7. AHCYL1 Is Mediated by Estrogen-Induced ERK1/2 MAPK Cell Signaling and MicroRNA Regulation to Effect Functional Aspects of the Avian Oviduct	168
1. Abstract.....	169
2. Introduction	170
3. Materials and Methods.....	173
4. Results	182
5. Discussion	202
CHAPTER 8. Paradoxical Expression of AHCYL1 Affecting Ovarian Carcinogenesis between Chickens and Women.....	208
1. Abstract.....	209
2. Introduction	211
3. Materials and Methods.....	213
4. Results	222
5. Discussion	241

CHAPTER 9. Cell-Specific and Temporal Aspects of Gene Expression in the Chicken Oviduct at Different Stages of the Laying Cycle	245
1. Abstract.....	246
2. Introduction	247
3. Materials and Methods.....	249
4. Results	254
5. Discussion	269
 CHAPTER 10. Recrudescence Mechanism and Gene Expression Profile of the Reproductive Tracts in Chicken during the Molting Period	 276
1. Abstract.....	277
2. Introduction	279
3. Materials and Methods.....	283
4. Results	292
5. Discussion	314
 CHAPTER 11. Conclusion.....	 323
REFERENCES	331
초록.....	376
ACKNOWLEDGEMENTS	380

LIST OF FIGURES

CHAPTER 3

Fig. 3-1	Steady-state levels of <i>EGFR</i> mRNA in endometria from cyclic and pregnant gilts as determined by quantitative PCR analysis	50
Fig. 3-2	<i>In situ</i> hybridization and immunohistochemical analyses of <i>EGFR</i> mRNA and protein in endometria of cyclic and pregnant gilts	51
Fig. 3-3	Phosphorylation of AKT1, ERK1/2 MAPK and P90RSK in response to EGF in pTr cells	53
Fig. 3-4	Immunocytochemical localization of p-AKT1, p-ERK1/2 MAPK and p-P90RSK protein in pTr cells.....	55
Fig. 3-5	EGFR knockdown in the porcine trophectoderm cells.....	56
Fig. 3-6	Proliferation of pTr cells in response to EGF through various signal transduction cascades.....	58
Fig. 3-7	Migration of pTr cells in response to EGF through various signal transduction cascades.....	59
Fig. 3-8	Schematic illustrating the current working hypothesis on EGF-induced PI3K-AKT1 or ERK1/2 MAPK-P90RSK signal transduction cascades in pTr cells during the peri-implantation period	60

CHAPTER 4

Fig. 4-1	Relative quantification of expression of <i>IGF-I</i> and <i>IGF-IR</i> mRNAs in endometria during the estrous cycle and pregnancy by quantitative RT-PCR analysis	87
----------	--------------------------------------------------------------------------------------------------------------------------------------------------------------------------	----

Fig. 4-2	<i>In situ</i> hybridization analyses of <i>IGF-I</i> and <i>IGF-IR</i> mRNAs in the uterine endometrium during the estrous cycle and pregnancy in gilts.	88
Fig. 4-3	IGF-I increases the abundance of phosphorylated AKT1, ERK1/2 and RPS6 proteins and stimulates migration and proliferation of pTr cells	90
Fig. 4-4	Inhibition of IGF-I-induced AKT1 and ERK1/2 phosphorylation in pTr cells.....	91
Fig. 4-5	Immunofluorescence detection of p-AKT1, p-ERK1/2 and p-RPS6 proteins in IGF-I treated pTr cells	92
Fig. 4-6	IGF-I stimulates proliferation of pTr cells through various signal transduction cascades.....	93
Fig. 4-7	IGF-I stimulates migration of pTr cells through various signal transduction cascades.....	94
Fig. 4-8	Schematic illustrating the current working hypothesis on IGF-I induced signaling pathways responsible for pTr cell proliferation and/or migration.....	95

CHAPTER 5

Fig. 5-1	Relative quantification and localization of <i>VEGF</i> mRNAs in endometria of gilts during the estrous cycle and pregnancy by quantitative RT-PCR and <i>in situ</i> hybridization analyses.....	123
Fig. 5-2	Relative quantification and localization of <i>VEGFR-1</i> and <i>VEGFR-2</i> mRNAs in endometria of gilts during the estrous cycle and pregnancy by quantitative RT-PCR and <i>in situ</i> hybridization analyses	125

Fig. 5-3	VEGF influences the abundance of phosphorylated AKT1, ERK1/2, P70RSK, RPS6 and 4EBP1 proteins and stimulates migration and proliferation of pTr cells	127
Fig. 5-4	Inhibition of VEGF-induced AKT1 and ERK1/2 phosphorylation in pTr cells.....	129
Fig. 5-5	VEGF stimulates proliferation of pTr cells through various signal transduction cascades.....	130
Fig. 5-6	VEGF stimulates migration of pTr cells through various signal transduction cascades.....	131
Fig. 5-7	Schematic illustrating the current working hypothesis on VEGF-induced PI3K-AKT1 or ERK1/2 MAPK signal transduction cascades in pTr cells during the peri-implantation period	132

CHAPTER 6

Fig. 6-1	Relative quantification of <i>CSF2</i> mRNAs in porcine endometrium during the estrous cycle and pregnancy.....	156
Fig. 6-2	CSF2 increases the abundance of phosphorylated AKT1, ERK1/2, MTOR, p70RSK and RPS6 proteins and stimulates proliferation of pTr cells.....	157
Fig. 6-3	Inhibition of CSF2-induced AKT1 and ERK1/2 phosphorylation in pTr cells.....	159
Fig. 6-4	CSF2 stimulates proliferation of pTr cells through PI3K-MTOR and ERK1/2 MAPK pathways	160
Fig. 6-5	Schematic illustrating the current working hypothesis on CSF2-induced PI3K-AKT1 or ERK1/2 MAPK-P790RSK signaling pathways responsible for pTr cell proliferation.....	161

CHAPTER 7

Fig. 7-1	Expression of <i>AHCYL1</i> in chickens.....	190
Fig. 7-2	Effect of DES on tissue specific expression of chicken <i>AHCYL1</i>	191
Fig. 7-3	DES-induced phosphorylation of ERK1/2, stimulation of <i>AHCYL1</i> and calcium release in chicken oviduct epithelial cells.....	193
Fig. 7-4	<i>AHCYL1</i> knockdown decreased expression of genes associated with oviduct development and production of egg white proteins. .	195
Fig. 7-5	<i>In vitro</i> target assay of <i>miR-124a</i> , <i>miR-1602</i> , <i>miR-1612</i> , <i>miR-1669</i> , <i>miR-1710</i> and <i>miR-1782</i> on <i>AHCYL1</i> transcript.....	197
Fig. 7-6	Schematic illustrating the current working hypothesis on estrogen- induced ERK1/2 MAPK signaling cascades in chicken oviduct cells	199

CHAPTER 8

Fig. 8-1	Expression and quantitation of <i>AHCYL1</i> mRNA in normal and cancerous ovaries from hens.....	228
Fig. 8-2	Expression of <i>AHCYL1</i> mRNA and protein is unique to glandular epithelium of cancerous ovaries from hens.	229
Fig. 8-3	Differential expression of <i>AHCYL1</i> protein in normal and cancerous ovarian cells from hens.....	231
Fig. 8-4	Bisulfite sequencing of CpG sites in 5' promoter upstream of the transcription start site for the <i>AHCYL1</i> gene.....	232
Fig. 8-5	Differential localization of <i>AHCYL1</i> protein in human immortalized ovarian carcinoma cells.....	233

Fig. 8-6	Immunohistochemical expression of AHCYL1 protein in normal and cancerous ovaries from women.	234
Fig. 8-7	Histological types of chicken ovarian cancers used in this study..	235
Fig. 8-8	Effects of DES on AHCYL1 mRNA and protein expression in the chicken oviduct.	236

CHAPTER 9

Fig. 9-1	Identification of genes that changed significantly in the magnum and the shell gland of the oviduct during the egg laying cycle in hens	257
Fig. 9-2	Functional categorization of the genes that changed in the magnum and shell gland during interval from ovulation to oviposition in laying hens.	259
Fig. 9-3	Comparison of relative expression of mRNAs for <i>ACPI</i> , <i>CALBI</i> and <i>CYP26A1</i> which changed significantly in the oviduct of hens during the egg laying cycle based on quantitative RT-PCR analyses.	260
Fig. 9-4	Comparison of relative expression of mRNAs for <i>PENK</i> , <i>RCANI</i> and <i>SPP1</i> which changed significantly in the oviduct of hens during the egg laying cycle based on quantitative RT-PCR analyses	261
Fig. 9-5	Cell-specific localization of mRNAs for <i>ACPI</i> , <i>CALBI</i> and <i>CYP26A1</i> in the magnum are presented for oviducts of hens at 3 h and 20 h post-ovulation.....	262
Fig. 9-6	Cell-specific localization of mRNAs for <i>ACPI</i> , <i>CALBI</i> and <i>CYP26A1</i> in the shell gland of oviducts of hens are presented for 3 h and 20 h post-ovulation.....	263

Fig. 9-7 Cell-specific localization of mRNAs for *PENK*, *RCANI* and *SPP1* in the magnum are presented for oviducts of hens at 3 h and 20 h post-ovulation.264

Fig. 9-8 Cell-specific localization of mRNAs for *PENK*, *RCANI* and *SPP1* in the shell gland of oviducts of hens are presented for 3 h and 20 h post-ovulation.265

CHAPTER 10

Fig. 10-1 Establishment of an in vivo experimental model of degeneration and recrudescence of the chicken oviduct299

Fig. 10-2 Histological evaluation of ovarian and oviductal tissues at different days of the molting and recrudescence periods.....301

Fig. 10-3 TUNEL (TdT-Mediated dUTP Nick End Labeling) stained cells in the magnum of hens fed a high zinc diet or a normal diet302

Fig. 10-4 Immunohistochemical staining for detection of cytokeratin, vimentin and PCNA in cells of the magnum from each of the days during the molting and recrudescence processes303

Fig. 10-5 Identification of significant up- or down-regulated genes on each day during regression and regeneration of the oviduct.304

Fig. 10-6 Functional categorization of differentially expressed genes found to be associated in the cellular and molecular functions306

Fig. 10-7 Validation of microarray gene expression data by quantitative RT-PCR analysis.307

Fig. 10-8 Cell-specific localization of mRNAs for selected genes for which expression changed significantly in the magnum of hens at different days during the pre- and post-molting periods.....308

Fig. 10-9	<i>In vitro</i> target assay for effects of the chicken <i>miR-1689*</i> on expression of the <i>Sp1</i> transcript.....	309
Fig. 10-10	<i>In vitro</i> target assay for effects of chicken <i>miR-17-3p</i> , <i>miR-22*</i> and <i>miR-1764</i> on expression of the <i>STAT1</i> transcript.....	310
Fig. 10-11	<i>In vitro</i> target assay for effects of the chicken <i>miR-1562</i> on expression of the <i>ANGPTL3</i> transcript.....	312
Fig. 10-12	<i>In vitro</i> target assay for expression of the chicken <i>miR-138</i> on expression of the <i>p20K</i> transcript.....	313

CHAPTER 11

Fig. 11-1	A schematic illustration of the mechanisms by which the selected growth factors affect various intracellular signaling cascades responsible for the cellular activities of pTr cells during the peri-implantation period.....	330
-----------	-------------------------------------------------------------------------------------------------------------------------------------------------------------------------------------------------------------------------------	-----

LIST OF TABLES

CHAPTER 7

Fig. 7-1	Pairwise comparison of AHCYL1 proteins between chicken, mammalian and fish species	200
Fig. 7-2	Primers used for quantitative RT-PCR	201

CHAPTER 8

Fig. 8-1	Putative protein-binding sites within the upstream 5' promoter region of the <i>AHCYL1</i> gene.....	238
Fig. 8-2	Multivariate linear logistic regression analysis for factors affecting overall response.	239
Fig. 8-3	Multivariate Cox's proportional hazard analysis for factors affecting progression-free survival.	240

CHAPTER 9

Fig. 9-1	Primers used for quantitative RT-PCR analysis.	266
Fig. 9-2	Primers used for generating probes for in situ hybridization analysis.	267
Fig. 9-3	The fold-changes in expression of six genes (<i>ACPI</i> , <i>CALBI</i> , <i>CYP26A1</i> , <i>PENK</i> , <i>RCANI</i> and <i>SPP1</i>) detected using quantitative RT-PCR and microarray analyses.	268

LIST OF ABBREVIATION

4EBP1	Eukaryotic initiation factor 4E binding protein 1
APES	3-aminopropyltriethoxysilane
BrdU	5-bromo-2'-deoxyuridine
BSA	Bovine serum albumin
cDNA	Complementary DNA
CSF2	Colony-stimulating factor 2
CL	Corpus luteum
CSF1	Colony stimulating factor 1
CSF2	Colony stimulating factor 2
DAPI	4',6-diamidino-2-phenylindole
DEPC	Diethylpyrocarbonate
DIG	Digoxigenin
DNA	Deoxyribonucleic acid
dNTP	Doxyribonucleotid triphosphate
ECM	Extracellular matrix
EDTA	Ethylenediaminetetraacetic acid
EGF	Epidermal growth factor
EGFR	Epidermal growth factor receptor
ErbB	Erythroblastic leukemia viral oncogene homolog
ERK1/2	Extracellular signal-regulated kinase 1/2
EVT	Extravillous trophoblst

FGF7	Fibroblast growth factor 7
Flk-1	Fetal liver kinase-1
Flt	c-fms-like tyrosine kinase
FSH	Follicle stimulating hormone
GAPDH	Glyceraldehyde-3-phosphate dehydrogenase
GE	Glandular epithelium
GnRH	Gonadotropin-releasing hormone
HGF	Hepatocyte growth factor
ICM	Inner cell mass
IFND	Interferon delta (δ)
IFNG	Interferon gamma (γ)
IFNT	Interferon tau (τ)
IGF-I	Insulin-like growth factor-I
IGF-IR	Type I IGF receptor
IGF-II	Insulin-like growth factor-II
IGF-IIR	Type II IGF receptor
IgG	Immunoglobulin G
IHC	Immunohistochemistry
IL-1β	Interleukin-1 beta (β)
IL-1R1	Interleukin-1 receptor type 1
IL-1R2	Interleukin-1 receptor type 2
IL-6	Interleukin-6
KDR	Kinase domain-containing receptor

LAP	Latency-associated peptide
LE	Luminal epithelium
LH	Luteinizing hormone
LIF	Leukaemia inhibitory factor
LSM	Least-square means
mRNA	Messenger RNA
MAPK	Mitogen-activated protein kinase
MUC1	Mucin 1
MTOR	Mechanistic target of rapamycin
PBS	Phosphate buffered saline
PDGF	Platelet-derived growth factor
PGE	Prostaglandin E
PGF	Prostaglandin F
PI3K	Phosphatidylinositol-3 kinase
pTr	Porcine trophectoderm
qRT-PCR	Quantitative reverse transcriptase-polymerase chain reaction
RNA	Ribonucleic acid
RPS6	Ribosomal protein S6
RSK	Ribosomal S6 protein kinase
RT-PCR	Reverse transcriptase-polymerase chain reaction
SAS	Statistical analysis system
SDS-PAGE	Sodium dodecyl sulfate-polyacrylamide gel electrophoresis
SPP1	Secreted phosphoprotein 1

SSC	Standard saline citrate
STAT3	Signal transducer and activator of transcription 3
TGFα	Transforming growth factor alpha
TGFβ	Transforming growth factor beta
TMB	Tetramethylbenzidine
tRNA	Transfer RNA
TUBA	Alpha-tubulin
VEGF	Vascular endothelial growth factor
VEGFR-1	VEGF receptor-1
VEGFR-2	VEGF receptor-2

CHAPTER 1

General Introduction

Implantation is the process by which an activated blastocyst establishes a close physical- and physiological contact with the maternal endometrium to form the placenta that functions as the interface between the fetus and the maternal circulation. Successful implantation and the maintenance of pregnancy require temporal synchrony between early embryonic development leading to blastocyst formation and increased uterine receptivity, and a well-organized reciprocal dialog between the conceptus (embryo-fetus and associated extraembryonic membranes) and the maternal uterus must be established during the pre-implantation period (Tranguch et al., 2005). During the pre-implantation period, a substantial number of conceptuses die because of asynchronous development of the uterus and/or conceptus, failure of pregnancy recognition signaling, and inappropriate implantation, which eventually result in poor pregnancy rates across species (Lawson et al., 1983; Pope, 1988). In pigs, 20-30% of early embryonic deaths occur during early pregnancy, indicating that the pre-implantation period is critical for establishment and maintenance of pregnancy (Pope, 1988; Pope et al., 1986).

During the peri-implantation period, the developing conceptus signals its presence to the endometrium and thereby prolongs the life span of the corpus luteum (CL) and maintains pregnancy. In addition to the signal required for maternal pregnancy recognition, the conceptus secretes a variety of molecules including interferons (INFs), prostaglandins (PGs), growth factors, cytokines, and other as yet unknown factors (Geisert and Yelich, 1997; Jaeger et al., 2001; Lefevre et al., 1998; Tuo et al., 1996). In response to these factors, the uterine endometrium undergoes

morphological changes and produces various molecules that are either secreted by uterine epithelia or are transported into the uterine lumen and are collectively referred to as histotroph, which is required for conceptus development and the uterus's receptivity for implantation (Bazer, 1975; Kane et al., 1997). Histotroph includes numerous factors including lipids, ions, amino acids, sugars, growth factors, cytokines, hormones, enzymes, adhesion proteins, and transport proteins. Developing pre-implantation embryos depend on a sufficient supply of histotroph for survival, growth, and development. Studies conducted using the uterine-gland knockout ewe (UGKO) model demonstrated that secretions of the uterine glandular epithelium (GE) were required for survival, elongation and pregnancy-recognition signaling of the peri-implantation conceptus (Gray et al., 2002; Gray et al., 2001c).

The aforementioned coordinated interactions of various factors derived from the conceptus or the uterus are especially critical in pigs because non-invasive epitheliochorial implantation occurs in them, during which the pre-attachment phase is prolonged (Aplin and Kimber, 2004). In contrast to species that have the invasive type of implantation characterized by the nidation of the blastocyst into the uterine stroma, in pigs, implantation is superficial and the blastocyst remains within the uterine lumen. Before attaching to uterine epithelia, porcine blastocysts rapidly elongate by a process involving the transformation of a spherical blastocyst into a filamentous conceptus (Bazer et al., 2009; Guillomot, 1995). Typically, the conceptuses that elongate the most establish the largest surface contacts with the uterine epithelia to exchange nutrients and gases and thus have the highest chance of survival, emphasizing the

importance of conceptus development during the peri-implantation period in pigs (Burton et al., 2007).

How implantation fails because of inappropriately developed conceptuses is not well-understood, and elucidating the molecular and cellular processes required for these events should provide key insights into human and animal reproduction. Insufficient delivery of histotroph to the developing conceptus results in intrauterine growth restriction, a major social and economic problem of global importance (Bazer et al., 2012a). Among the components of histotroph, growth factors are known to orchestrate various changes in the endometrium and/or conceptus to establish an optimal uterine microenvironment required for appropriate conceptus development (Kane et al., 1997; Schultz and Heyner, 1993).

This study was focused on four promising factors involved in conceptus-maternal interaction; epidermal growth factor (EGF), insulin-like growth factor I (IGF-I), vascular endothelial growth factor (VEGF), and colony-stimulating factor 2 (CSF2). These factors have been hypothesized to be involved in regulating diverse aspects of reproductive physiology, and to either directly or indirectly regulate the growth and development of conceptus during the peri-implantation period. Previous studies conducted using pigs revealed that the levels of *EGF*, *IGF-I*, *VEGF*, and *CSF2* mRNA expression in the endometrial epithelia and/or conceptus trophoblast increased during the peri-implantation period when the conceptus is elongating. Moreover, knockout mice featuring a disrupted VEGF or CSF2 system exhibited

embryonic developmental abnormalities and/or early embryonic lethality (Carmeliet et al., 1996; Ferrara et al., 1996; Fong et al., 1995; Pollard, 1997; Robertson et al., 2001). Furthermore, providing recombinant EGF, VEGF, or CSF2 to embryos in *in vitro* cultures enhanced their developmental ability and implantation rate after embryo transfer and also rescued deficiencies in placental structure and fetal growth (Biswas et al., 2011; Einspanier et al., 2002; Hannan et al., 2011; Robertson et al., 2001; Sjoblom et al., 2005). Therefore, shortages of these factors during early pregnancy result in poor outcomes in pregnancy and prenatal- and postnatal growth and health. Despite these hypothesized roles and functions of these promising growth factors, little is known about the cellular signaling pathways that are stimulated by the selected factors in porcine trophoctoderm (pTr) cells and about how these factors stimulate conceptus development during early pregnancy.

Therefore, this study was conducted to determine the molecular mechanisms by which the four selected uterine factors activate the intracellular signaling cascades involved in orchestrating conceptus development during the peri-implantation period. Chapter 2 reviews the general characteristics of the estrous cycle and early pregnancy, the developmental process of the peri-implantation porcine embryo, maternal-conceptus interaction, and the four promising factors that affect conceptus development. The changes that were detected in the cellular activities and intracellular signaling pathways in the primary pTr cells in response to EGF, IGF-I, VEGF, and CSF2 are described in Chapter 3, 4, 5, and 6, respectively.

CHAPTER 2

Literature Review

1. Estrous Cycle and Early Pregnancy

1.1. Estrous Cycle

The estrous cycle is the recurring cycle that passes through a luteal- and a follicular phase in all non-pregnant placental mammals other than humans and higher primates. The estrous cycle starts after puberty, and it is often halted in sexually mature females during anestrus phases (absence of cycling) in seasonal breeders or during pregnancy. The cycle is precisely regulated through sequential changes and reciprocal interactions of circulating reproductive hormones, including gonadotropin-releasing hormone (GnRH), follicle stimulating hormone (FSH), luteinizing hormone (LH), estrogen and progesterone, which are derived from the hypothalamus, anterior pituitary and ovary (Jabbour et al., 2006; Slayden and Brenner, 2004).

The period of the estrous cycle comprises four phases; estrus, metestrus, diestrus, and proestrus. Proestrus results from CL regression, which leads to reduced plasma progesterone and increased estrogens levels concomitant with the maturation of growing follicles. Estrus is the result of mature follicles producing peak levels of estrogens, whose effect on the hypothalamus causes a surge of GnRH release and leads to the secretion of FSH and LH. A surge-release of FSH and LH stimulates the growth of new follicles, which ultimately results in ovulation and luteinization. Continued proteasomal degradation of the theca interna outward near the apex of the follicle leads to the formation of a hole and the expulsion of the oocyte. Ovulation

normally occurs toward the end of estrus. Metestrus is characterized by declining plasma estrogen concentrations after ovulation and the initiation of progesterone production by CL. In diestrus, increased natural progesterone levels induce endometrial glandular secretions that provide an environment suitable for initial conceptus development in the event that fertilization is successful. However, if viable embryos are not present in the uterus, plasma progesterone levels begin to decrease rapidly and prostaglandin F₂ α (PGF₂ α) is released, which results in the recruitment and maturation of the next group of developing follicles (Pharriss et al., 1972). The estrous cycle lasts for approximately 17 days in sheep, 21 days in cattle, and 21 days in pigs (Henricks et al., 1972; Oxender et al., 1972; Schrick et al., 1993).

In humans and certain primates, a menstrual cycle replaces the estrous cycle. During the menstrual cycle, the endometrium thickens before ovulation and it is shed through menstruation when fertilization does not occur. However, in animals that have an estrous cycle, the endometrium is reabsorbed by the uterus if conception does not occur during that cycle. Another distinction is sexual activity; mammals that have menstrual cycles can engage in sexual activity at any time during the cycle, whereas the females of species that have the estrous cycles tend to be sexually active only around the period of ovulation. Polyestrous animals such as cats, cows, and pigs can go into an estrous cycle several times a year. By contrast, in seasonal breeders, the estrous cycle occurs during a specific time of the year, and these breeders can be divided into short-day breeders, which are sexually active in fall or winter, and long-day breeders, which are sexually active in spring and summer.

1.2. Pre-Implantation Period

The pre-implantation embryo undergoes numerous mitotic cell divisions and morphological changes during the period between fertilization and implantation. The developing pre-implantation embryo is unique in that it develops in a fluid environment in a free-floating state, in the absence of direct cellular contact with the uterus for 1-2 weeks (depending on the species) before implantation. A substantial loss of pre-implantation embryos commonly occurs in several mammals. Abnormal regulation of the events before and during implantation may often be a cause of poor pregnancy rates in eutherian mammals.

The pre-implantation period is marked by several fundamental transitions that are remarkably similar across species. Following fertilization, the fertilized single-cell ovum progresses down the fallopian tube and enters the uterus. During this time, the zygote undergoes mitotic divisions that are called cleavages. The first cleavage is controlled by maternal mRNA and the cleavage produces 2 cells, which are called blastomeres. Further divisions generate 4, 8, and finally 16 blastomeres that form a compact ball of cells known as the morula. The blastomere compaction that occurs in this stage enables greater cell-cell interaction, and this process is a prerequisite for the segregation of the internal cells that form the inner cell mass (ICM). Eventually, a differentiated tissue called as the blastocyst is formed before implantation is initiated.

At the early blastocyst stage, cells first undergo a process that ultimately decides cell fates; various genetic and cellular interactions determine whether these earliest stem cells differentiate into the ICM or the trophoctoderm. The pluripotent ICM is the bundle of cells that will generate future cell lineages leading to the endoderm, mesoderm, or ectoderm, eventually giving rise to the fetus. Conversely, a thin outer layer surrounding the ICM, the epithelial trophoctoderm, establishes the connection with the luminal epithelia (LE) of the maternal uterus and forms the placenta interface or other extra-embryonic membranes. The trophoctoderm is necessary for successful embryonic development because it mediates the transfer of nutrients from the mother to the embryo. Before implantation, the embryo at the blastocyst stage escapes from the zona pellucida, and the exposed trophoctoderm cells become capable of attaching to the endometrial epithelium that lines the uterus, and this results in implantation being initiated (Wang and Dey, 2006).

1.3. Opening of the Implantation Window and Implantation

To enable implantation, the uterus undergoes alterations that are necessary for the attachment of the conceptus trophoctoderm (Paria et al., 1993). The embryo reception-ready phase of the endometrium, a limited period during the initiation of implantation, is termed “implantation window” (Psychoyos, 1973). The implantation window is initiated by changes in the endometrium of the uterus that help transform not only the lining of the uterus, but also the composition and pattern of endometrial secretions (Wilcox et al., 1999). During this period, the blastocyst approaches the

endometrium and the endometrium is primed for blastocyst attachment, given that it has acquired the accurate morphological and functional state (Finn and Martin, 1974). The implantation window is a critical period of development in that it requires the establishment of reciprocal interactions between the maternal endometrium and the developing conceptus; dysregulation on the part of either the conceptus or the uterine endometrium results in the inability to establish pregnancy (Fazleabas et al., 2004; Spencer et al., 2007a).

Steroid hormones serve fundamental roles in the aforementioned changes. The progesterone receptor in the uterine LE is down-regulated immediately before the opening of the implantation window, and this is generally associated with the endometrial transcriptional changes that are necessary for uterine receptivity and lead to implantation in humans (Lessey et al., 1988; Lessey et al., 1996) and in domestic animals (Geisert et al., 1994; Hartt et al., 2005; Meikle et al., 2001; Spencer and Bazer, 1995). Estrogen stimulation is critical for uterine receptivity because it exerts protective effects related to the CL and induces the endometrial alterations required for conceptus attachment.

Implantation is the process by which an activated blastocyst establishes a close physical- and physiological contact with the maternal endometrium to form the placenta that serves as the interface between the fetus and the maternal circulation. This process varies between species according to three placental types, the hemochorial (humans, rodents, and non-human primates), epitheliochorial (horses,

cows, sheep, and pigs), and endotheliochorial (most carnivores) types. Successful implantation depends on the embryo developing to the blastocyst stage in synchrony with the differentiation of the uterus to the receptive state, which is followed by two-way interactions between the blastocyst and the uterine LE (Psychoyos, 1973).

2. Physiology of the Porcine Conceptus during Peri-Implantation

2.1. Early Conceptus Development

Following fertilization, cleavage starts shortly after nuclear division and then subsequent divisions occur, allowing the porcine embryo to reach the 4-cell stage within 24 h after fertilization. Blastomere development beyond the 4-cell stage coincides with the activation of embryonic genome expression (Telford et al., 1990; Tomanek et al., 1989). Morphological differentiation including compaction and blastulation occurs within the conceptus by Day 6 after fertilization (Reima et al., 1993). The blastocyst forms on Day 8 after fertilization, and the conceptus now features a distinct trophoctodermal cell layer and an ICM within the blastocoele (Geisert et al., 1982a). Next, hatching from the zona pellucida on Days 7-8 of pregnancy allows the morphological variation of conceptus into spherical, tubular, and filamentous forms between Days 11 and 12 of pregnancy.

2.2. Maternal Recognition of Pregnancy

Maternal recognition of pregnancy is the process by which the early conceptus releases signaling molecules that induce a molecular cascade of events to lengthen the lifespan of the CL (Geisert et al., 1990). Protecting the CL promotes continued progesterone production, which allows the maintenance of myometrial quiescence and endometrial histotroph production (Nara et al., 1981).

During early pregnancy, porcine conceptuses express enzymes that convert steroid precursors into estrogen and secrete estrogen into the uterine lumen on Days 11-12 of pregnancy (Bazer et al., 1986; Perry et al., 1973; Perry et al., 1976). Secreted estrogen activates the mechanism required to direct prostaglandin $F_{2\alpha}$ ($PGF_{2\alpha}$) secretion away from the uterine vasculature and into the uterine lumen, this is called the endocrine-exocrine theory of maternal recognition. In pregnant gilts, $PGF_{2\alpha}$ secreted into the uterine lumen is converted into an inactive form that cannot cause luteolysis. Prostaglandin E2 (PGE_2) has also been shown to enhance CL performance and is considered to function as a luteotrophic agent during pregnancy in the pig (Ford and Christenson, 1991). In addition to estrogen, PGE_2 dramatically increases in uterine flushings during the time of maternal recognition of pregnancy in the pig (Geisert et al., 1982b). Injections of exogenous estrogen into gilts between Days 11 and 16 of the estrous cycle have been established to prolong the life of the CL and induce pseudopregnancy (Frank et al., 1977; Geisert et al., 1982b).

2.3. Conceptus Trophoblastic Elongation

In contrast to species that feature the invasive type of implantation, in pigs, which have an epitheliochorial placenta, the elongation of conceptus is critical for establishing a large surface area for nutrient and gas exchange (Burton et al., 2007). Trophoblastic elongation in pigs is characterized by a series of morphological transformations. On approximately Day 10 of pregnancy, the 2-3 mm-sized spherical porcine conceptuses grow in diameter (Geisert et al., 1982b) and continue to expand until reaching a diameter of approximately 9-10 mm diameter (Geisert et al., 1982b; Pusateri et al., 1990). Next, the spherical conceptus initiates a process of rapid trophoblastic elongation between Days 11 and 12 of pregnancy (Geisert et al., 1982b), which occurs concomitantly with the synthesis and release of estrogen by the conceptus (Bazer et al., 1986; Geisert et al., 1982b; Ross et al., 2003). The spherical conceptus becomes ovoid and tubular, and eventually becomes filamentous in shape and 150-200 mm long. This rapid transformation results mainly from a process in which the cytoskeletal rearrangements of filamentous actin cause trophectodermal migration (Geisert et al., 1982a; Mattson et al., 1990; Pusateri et al., 1990).

Trophoblastic elongation is critical because the conceptus expansion ensures that sufficient uterine space is retained for placentation (Geisert and Yelich, 1997; Stroband and Van der Lende, 1990) and that maternal recognition signal is efficiently delivered throughout the uterine lumen (Dziuk, 1968; Polge et al., 1966). Typically, the conceptuses that elongate the most acquire the greatest uterine surface contact and, consequently, have the highest chance of survival.

2.4. Conceptus Apposition and Attachment to the Uterine Luminal Epithelium

Pregnant gilts develop an epitheliochorial placenta that preserves the uterine LE cells, which are not destroyed as in other species and instead contribute to the apposition and attachment of the trophoctoderm (Burghardt et al., 1997). Following trophoblastic elongation and the secretion of embryonic estrogen, porcine filamentous conceptuses remain free-floating until Days 13-14 of pregnancy, after which they establish the initial attachment to the uterine LE, and the completion of implantation results in the interdigitation of the uterine LE and the trophoctoderm by Day 24 of pregnancy (Dantzer, 1985; Keys and King, 1990; Perry, 1981).

The initial low-affinity attachment is mediated by carbohydrate ligand-binding molecules such as selectins and galectins (Bazer et al., 2009; Ziecik et al., 2011). Furthermore, stable adhesions is required between integrins and the extracellular matrix (ECM) expressing specific ligands and receptors necessary for uterine receptivity and conceptus attachment (Hynes, 1992; Lessey, 1995). The attachment of the trophoctoderm to the ECM in the uterus involves various factors including fibronectin, secreted phosphoprotein (SPP1), laminin and transforming growth factor (TGF)- β latency-associated peptide (LAP) (Garlow et al., 2002; Jaeger et al., 2001). Another factor, the cell-surface mucin 1 (MUC-1), can also affect trophoctoderm adhesion to the LE through its ability to prevent integrin binding between the trophoctoderm and the uterine epithelium (Surveyor et al., 1995).

3. Uterine Microenvironment during Early Pregnancy

3.1. Maternal-Conceptus Interactions

Successful conceptus development and the establishment of a functional placenta and maintenance of pregnancy are the results of effective dialog between an implantation-competent blastocyst and a receptive uterus. The pre-implantation period is critical stage because during that period this maternal-conceptus network is established. Abnormal regulation of the events before implantation may often cause pre-implantation embryonic loss and poor pregnancy rates in eutherian mammals, particularly in livestock species such as the pig; in pigs, non-invasive implantation occurs and a pre-attachment phase is followed by prolonged apposition and attachment, indicating that well-organized intercellular communication is crucial (Aplin and Kimber, 2004).

Over the past decades, diverse embryonic- and maternal factors that affect the pre-implantation and implantation processes have been identified, including growth factors, cytokines, ions, glucose, fructose, amino acids, and ovarian hormones (Geisert et al., 1982b). In the absence of uterine glands, pregnancy fails early in the peri-implantation period in sheep, indicating that uterine glands and their secretions are essential for the peri-implantation and implantation processes such as the survival and development of the conceptus (Allison Gray et al., 2000; Gray et al., 2001c).

3.2. Embryonic Factors

Recent advances in molecular biological approaches have led to the discovery of numerous molecules involved in embryo-uterine interactions. Between Days 11 and 12 of pregnancy, the porcine conceptus synthesizes and secretes estrogen, which acts as an initial signal that enables maternal recognition of pregnancy (Geisert et al., 1982b). Conceptus-derived estrogen has been suggested to convert $\text{PGF}_{2\alpha}$ secretion from endocrine to exocrine secretion and thereby prevent the development of the endometrial luteolytic mechanism (Spencer and Bazer, 2004a). This anti-luteolytic effect of blastocyst-derived estrogen results in the maintenance of a functional CL and the secretion of progesterone, which is required to maintain a uterine environment. Introduction of exogenous estrogen on Days 11-15 of the estrous cycle leads to CL maintenance for a period equivalent to or slightly longer than pregnancy. The changes induced by conceptus-derived estrogen occur concurrently with dramatic gene expression changes and the initiation of phenotypic changes that enable the conceptus to survive in a uterine environment (Choi et al., 1996; Yelich et al., 1997b).

Available results indicate that two interferons (IFNs) derived from the porcine trophoblast, IFNG (IFN- γ) and IFND (IFN- δ), play critical roles during early pregnancy in pigs, by stimulating the remodeling and/or depolarization of endometrial epithelial cells, a prerequisite for implantation and the establishment of a functional placenta (Cencic et al., 2003). Moreover, during the peri-implantation period, the

conceptus also synthesizes and secretes a variety of molecules such as growth factors (e.g. IGFs, EGF, TGFs), cytokines (e.g., interleukins (ILs), CSFs), protease (e.g., matrix metalloprotein protease, tissue inhibitor of metalloproteinase), prostaglandins, hormones (e.g., corticotrophin-releasing hormone), and other unknown factors (Geisert and Yelich, 1997; Lefevre et al., 1998; Tuo et al., 1996). In response to these factors, the uterine endometrium undergoes morphological- and functional changes and secretes various factors to induce the development of conceptus and to become receptive to it.

3.3. Uterine factors

Coinciding with conceptus changes, numerous genes are expressed in a spatiotemporally specific manner by uterine LE, GE and stromal cells; these genes encode secretory molecules and transporters of nutrients secreted within the uterine lumen. The complex mixture of uterine luminal secretions and molecules transported into the uterine lumen is referred to as histotroph, which orchestrate embryonic cellular activities including cell division, gene expression, and metabolism during the peri-implantation period of pregnancy. The pre-implantation embryo develops in a fluid environment that contains ahistotroph, and the development occurs in free-floating state, in absence of direct cellular contact with the uterus. Conceptuses may fail to develop because of failing to respond to histotroph, which includes a variety of molecules such as hormones, cytokines, growth factors, proteins, ions, lymphokines, enzymes, amino acids, glucose, vitamins, and other molecules. Histotroph

components increase in the uterine lumen immediately following the release of estrogens from the conceptus on Day 11 of pregnancy (Geisert et al., 1982c).

4. Growth Factors and Cytokines Regulating Conceptus Cellular Processes

Among histotroph components, growth factors are known to be required for numerous key cellular events such as proliferation, polarity, differentiation, and survival and for the development of the conceptus (Kane et al., 1997; Schultz and Heyner, 1993). IGFs have been well characterized throughout early pregnancy in the pig. The expression of the porcine conceptus gene encoding IGF-I increases steadily during the pre-elongation stages and peaks at the time of conceptus elongation (Letcher et al., 1989). Kim et al. demonstrated that IGF-II markedly increased the migration of ovine trophoderm cells (Kim et al., 2008). EGF and TGF α are additional growth factors that can affect conceptus development (Vaughan et al., 1992a). Another family of growth factors that have been extensively investigated during conceptus-maternal interaction is the TGF β family, which contains three isoforms (TGF β -1, -2 and -3). The expression of genes encoding all three TGF β isoforms and TGF β receptors tends to increase in the porcine conceptus trophoderm and uterine LE during the period of rapid morphological change in conceptus development (Gupta et al., 1996; Gupta et al., 1998; Yelich et al., 1997a). Placental estrogens act on the endometrial epithelia to increase the expression of

another specific growth factor, fibroblast growth factor-7 (FGF-7), that acts on the trophoctoderm to stimulate cell proliferation as well as conceptus development (Ka et al., 2001).

Several cytokines have also been reported to be involved in regulating conceptus development and the establishment of pregnancy. IL-1 β is known to induce the gene expression for the increase of PGE and cell membrane fluidity necessary for trophoctoderm remodeling (Guan et al., 1998; Kol et al., 2002). Modric et al. further indicated that the expression of IL-6 gene in the pre-implantation porcine conceptus peaked on Day 12 (Modric et al., 2000). CSF-1 is a factor that is expressed in conceptuses as early as Days 10-12 of pregnancy (Tuo et al., 1995). A previous study conducted using mice lacking the CSF-1 gene indicated that conceptus-produced CSF-1 is required for successful female fertility (Wiktor-Jedrzejczak et al., 1990). Leukaemia-inhibitory factor (LIF) is another cytokine that has been proposed to facilitate conceptus-uterine communication (Anegon et al., 1994). Modric et al. indicated that LIF levels in porcine uterine-luminal flushings peaks at the time that rapid trophoblastic elongation is initiated and that LIF likely exerts direct effects through LIF-receptor β on both pre- and post-elongation conceptuses (Modric et al., 2000).

A collection of growth factors and cytokines produced locally at the maternal-conceptus interface has been implicated in regulating trophoblast migration and/or invasion (Cohen and Bischof, 2007); however, the mechanisms that link these

factors to intracellular signal transduction are still only partially understood. A few studies have linked growth factor-induced intracellular signaling pathways to cellular activities in the trophoblast. IGF-II is known to stimulate the migration of human extravillous trophoblast (EVT) cells by activating the MAPK signaling pathway (Gleeson et al., 2001; McKinnon et al., 2001). Moreover, Kim et al. demonstrated that ovine IGF-II stimulates the migration of trophoblast cells by activating both PI3K and MAPK signaling pathways (Kim et al., 2008). Furthermore, hepatocyte growth factor (HGF) has been demonstrated to induce PI3K-dependent migration in the SGHPL-4 human trophoblast (Cartwright et al., 2002), and Qiu et al. suggested that both PI3K and MAPK pathways are required in EGF-induced EVT migration in human (Qiu et al., 2004a).

5. Promising Uterine Factors Affecting Conceptus Development and Implantation

5.1. Epidermal Growth Factor (EGF)

EGF is a multifunctional growth factor that plays a role in a variety of basic cellular activities such as cell growth, proliferation, and differentiation (Bass et al., 1994; Carpenter and Cohen, 1990; Haase et al., 2003; Pedersen et al., 1994). EGF has also been confirmed to function as a potent stimulatory growth factor in the development of the placenta by inducing the proliferation, survival, differentiation,

and invasion/migration of the trophoblast in diverse species (Barber et al., 2005; Bass et al., 1994; Biadasiewicz et al., 2011; Henic et al., 2006; Joslin et al., 2007; Li and Zhuang, 1997; Llimargas and Casanova, 1999).

In various cellular systems, the binding of EGF to EGF receptor (EGFR) activates myriad intracellular signaling pathways including the PLC γ /protein kinase C, MAPK and PI3K pathways, resulting in the transcriptional regulation of target genes involved in numerous cellular activities (Squires et al., 2003; Thomas et al., 2003; Wieduwilt and Moasser, 2008). Furthermore, administering exogenous estrogen stimulated the binding of EGF to EGFR in immature rats and exerted mitogenic effects in ovariectomized mice, raising the possibility that EGF participates in estrogen-induced uterine growth and differentiation (Mukku and Stancel, 1985; Nelson et al., 1991). Whereas porcine EGF is considered to contribute to early conceptus development because its gene is expressed at that stage, little is known about the EGF-EGFR system in the porcine uterus in terms of the regulatory mechanisms through which EGF affects conceptus development.

5.2. Insulin-Like Growth Factor-I (IGF-I)

IGF-I exerts mitogenic and insulin-like metabolic effects by binding to type I IGF receptor (IGF-IR) and type II IGF receptor (IGF-IIR), respectively (Jones and Clemmons, 1995; Rechler and Nissley, 1985). IGFs circulate at high concentrations and stimulate protein synthesis, but their actions are tissue- and cell-

dependent, and thus IGFs are considered paracrine or autocrine factors rather than endocrine factors (Denley et al., 2005; Miese-Looy et al., 2012). In pigs, IGF-I and its specific receptors are expressed in the uterine endometrium throughout the peri-implantation period and in the embryo during the pre-elongation stages (Green et al., 1995; Letcher et al., 1989; Simmen et al., 1990). Moreover, the expression of uterine *IGF-I* transcripts and the concentration of secreted IGF-I in uterine flushings both peak when the conceptus elongates rapidly and secretes estrogen (Geisert et al., 2001; Green et al., 1996; Miese-Looy et al., 2012; Simmen et al., 1992).

Available evidence suggests that IGFs are highly relevant to peri-implantation events during early pregnancy. Recently, a study conducted using ovine trophectoderm cells demonstrated that IGF-II, another member of the IGF family, stimulated cell migration by activating multiple signaling pathways (Kim et al., 2008). However, despite the spatiotemporally matching expression of IGF-I, potential novel functions of IGF-I during the peri-implantation period and molecular mechanisms linked to the IGF-I system are poorly understood.

5.3. Vascular Endothelial Growth Factor (VEGF)

VEGF, also known as VEGF-A, is a heparin-binding glycoprotein that plays a critical role in angiogenesis in a variety of tissues (Charnock-Jones et al., 1993; Cullinan-Bove and Koos, 1993; Das et al., 1997; Ferrara et al., 2003). VEGF activates intracellular signaling cascades by binding to VEGF receptor (VEGFR)-1 (c-fms-like

tyrosine kinase, Flt-1) or VEGFR-2 (fetal liver kinase-1/kinase domain-containing receptor, Flk-1/KDR) (Robinson and Stringer, 2001; Waltenberger et al., 1994).

VEGF is known to be present in the uterus of various mammals and to participate in the processes of early embryonic development and implantation (Charnock-Jones et al., 1993; Cullinan-Bove and Koos, 1993; Greb et al., 1997; Reynolds et al., 1998; Winther et al., 1999). Knockout mice featuring a disrupted VEGF or VEGFR system show embryonic developmental abnormalities and/or early embryonic lethality (Carmeliet et al., 1996; Ferrara et al., 1996; Fong et al., 1995). Moreover, adding recombinant VEGF to *in vitro* culture media can stimulate the outgrowth of mouse blastocysts and increase blastocyst cell number (Biswas et al., 2011; Einspanier et al., 2002; Hannan et al., 2011).

VEGF-induced vascular remodeling is undoubtedly crucial for the rapid morphological changes of the endometrium during early pregnancy. However, the VEGF-VEGFR system is detected in peri-implantation trophoblast cells, where no angiogenesis occurring, suggesting that VEGF exhibits other novel functions in blastocysts and conceptuses during the peri-implantation period.

5.4. Colony-Stimulating Factor 2 (CSF2)

CSF2 is a multifunctional cytokine that is hypothesized to be responsible for the survival, proliferation, and differentiation of granulocytes and macrophages

(Gasson, 1991; Rapoport et al., 1992; Robertson et al., 1994). CSF2 is considered to be involved in regulating diverse aspects of reproductive physiology, including pre-implantation embryo development, implantation, and placental development (Robertson, 2007).

In humans and mice, CSF2 synthesis remains high following fertilization, and then declines at the time of blastocyst implantation (Robertson et al., 1996; Tremellen et al., 1998). Moreover, the expression of CSF2 receptor is detectable at the time of fertilization and during subsequent stages of blastocyst development (Robertson et al., 2001; Sjoblom et al., 2002). Mice deficient in CSF2 develop blastocysts featuring a reduced numbers of cells, which is linked to impaired placental structure and increased mortality of early conceptuses (Pollard, 1997; Robertson et al., 2001). Exogenous CSF2 increases the rate at which the blastocyst stage is reached and promotes the subsequent development of *in vitro* cultured blastocysts across several species (Diaz-Cueto and Gerton, 2001; Hardy and Spanos, 2002; Robertson, 2007; Sjoblom et al., 1999). Furthermore, adding CSF to *in vitro* culture media rescued deficiencies in placental structure and fetal growth, and also improved postnatal development of mouse pups (Robertson et al., 2001; Sjoblom et al., 2005).

Evidence suggests that CSF2 promotes the proliferation of bovine trophoctoderm cells before and during the peri-implantation period of pregnancy (Michael et al., 2006). Moreover, before and after the attachment phase of implantation in cows, conceptus-derived secretions including estrogens and IFN-tau

(IFNT) stimulate the expression of CSF2 by the uterine epithelia (Michael et al., 2006; Robertson, 2007). This evidence identifies porcine CSF2 as a promising factor that stimulates conceptus development.

CHAPTER 3

Epidermal Growth Factor Stimulates Proliferation and Migration of Porcine Trophectoderm Cells Through Protooncogenic Protein Kinase 1 and Extracellular-Signal-Regulated Kinases 1/2 Mitogen-Activated Protein Kinase Signal Transduction Cascades During Early Pregnancy

1. Abstract

For successful implantation and establishment of early epitheliochorial placentation, porcine conceptuses require histotroph, including nutrients and growth factors, secreted by or transported into the lumen of the uterus. Epidermal growth factor (EGF), an essential component of histotroph, is known to have potential growth-promoting activities on the conceptus and uterine endometrium. However, little is known about its effects to transactivate cell signaling cascades responsible for proliferation, growth and differentiation of conceptus trophoctoderm. In the present study, *EGFR* mRNA and protein were abundant in endometrial luminal and glandular epithelia, stratum compactum stroma and conceptus trophoctoderm on d 13–14 of pregnancy, but not in any other cells of the uterus or conceptus. In addition, primary porcine trophoctoderm (pTr) cells treated with EGF exhibited increased abundance of phosphorylated (p)-AKT1, p-ERK1/2 MAPK and p-P90RSK over basal levels within 5 min, and effect that was maintained to between 30 and 120 min. Immunofluorescence microscopy revealed abundant amounts of p-ERK1/2 MAPK and p-AKT1 proteins in the nucleus and, to a lesser extent, in the cytoplasm of pTr cells treated with EGF as compared to control cells. Furthermore, the abundance of p-AKT1 and p-ERK1/2 MAPK proteins was inhibited in control and EGF-treated pTr cells transfected with *EGFR* siRNA. Compared to the control siRNA transfected pTr cells, pTr cells transfected with *EGFR* siRNA exhibited an increase in expression of *IFND* and *TGFBI*, but there was no effect of expression of *IFNG*. Further, EGF stimulated proliferation and migration of pTr cells through activation of the PI3K-

AKT1 and ERK1/2 MAPK-P90RSK cell signaling pathways. Collectively, these results support the hypothesis that EGF coordinately activates multiple cell signaling pathways critical to proliferation, migration and survival of trophoblast cells that are critical to development of porcine conceptuses during implantation and placentation.

2. Introduction

Epidermal growth factor (EGF) is a 6 kDa protein consisting of 53 amino acid residues and three intra-molecular disulfide bridges that plays pivotal roles in a variety of biological processes such as cell growth, proliferation, and differentiation (Carpenter and Cohen, 1990). After binding to its cognate EGF receptor (EGFR), which is a transmembrane glycoprotein member of the ERBB family of receptor tyrosine kinases, EGF induces autophosphorylation of EGFR-bound kinases and subsequently relays signals via a series of transcription factors to transactivate expression of target genes (Herbst, 2004). EGF has been implicated in development of human placental-trophoblast microenvironment in many ways, including trophoblast proliferation, survival, differentiation, invasion and/or migration (Barber et al., 2005; Bass et al., 1994; Biadasiewicz et al., 2011; Li and Zhuang, 1997). Also, it has been shown that EGF-EGFR system activates the mitogen-activated protein kinase (MAPK) and the phosphatidylinositol 3-kinase (PI3K)/AKT pathways, suggesting that activation of these signaling pathways are important for human placentation and implantation (Knofler, 2010; Squires et al., 2003).

In the porcine uterus, implantation is initiated with apposition and attachment of conceptus (embryo/fetus and associated membranes) trophoctoderm to uterine luminal (LE) epithelium (Bazer et al., 2010). Indeed, the porcine conceptus undergoes dramatic morphological changes requiring proliferation, migration and differentiation of trophoctoderm cells in preparation for implantation and placentation

during the peri-implantation period of pregnancy (Bazer et al., 2009). Following the morphological differentiation and cellular polarization within the blastocyst stage, the porcine conceptus dramatically elongates from 5 to 150 mm in length and also secretes the maternal recognition signal between days 10 and 12 of pregnancy (Bazer and Thatcher, 1977; Geisert et al., 1982b). The free-floating filamentous conceptus starts initial attachments to the uterine LE by 13 day of pregnancy, and implantation is complete by 24 day of pregnancy (Geisert and Yelich, 1997; Keys and King, 1990). This process requires histotroph, which includes a number of essential molecules such as nutrients, growth factors, hormones, cytokines, lipids, ions, and sugars that are either transported into or secreted into the uterine lumen by uterine epithelia for establishment and maintenance of pregnancy (Bazer et al., 2010). Of these components of histotroph, growth factors are required for many key events such as proliferation, polarity, differentiation, survival and development of the conceptus (Schultz and Heyner, 1993; Simmen and Simmen, 1991). Therefore, deficiencies of these growth factors and nutrients during early pregnancy result in poor pregnancy outcomes, as well as poor postnatal growth and health (Bazer, 1975; Wu et al., 2004). For instance, studies of the uterine gland knockout ewe model demonstrated the requirement for components of histotroph from uterine glandular (GE) epithelium for survival and normal development of the conceptus, as well as pregnancy recognition signaling (Gray et al., 2002). Our previous studies with pigs revealed that nutrients such as glucose, arginine, leucine, and glutamine in the uterine lumen coordinately activate proto-oncogenic protein kinase Akt 1 (AKT1), mechanistic target of rapamycin (MTOR), ribosomal protein S6K (RPS6K), and ribosomal protein S6

(RPS6) cell signaling to stimulate hypertrophy, hyperplasia, and migration of ovine trophoctoderm cells during the peri-implantation period of pregnancy (Kim et al., 2013).

As compared with classical hormones, growth factors have unique features in that their sites of synthesis and sites of action are restricted to defined glands or tissues (Carpenter and Cohen, 1990). Since EGF was discovered and characterized by Stanley Cohen, who won Nobel Prize in Physiology and Medicine in 1986, numerous studies in humans and mice have elucidated biological functions of EGF. During the female reproductive cycle, the expression of EGF and EGFR is predominantly in pregnant uteri of various mammalian species such as human (Chegini et al., 1986; Smith et al., 1991) and mouse (Das et al., 1994) and associated with proliferation and differentiation of cells and uterine remodeling for implantation and placentation. However, little is known about EGF and EGFR in the porcine uterus regarding regulatory mechanisms whereby EGF affects uterine functions and development of the conceptus. Although failures of implantation and placentation due to underdeveloped conceptuses are not well-understood, a better understanding of molecular and cellular processes required for these events will provide important insights into human and animal reproduction. Insufficient delivery of histotroph, including growth factors and nutrients, to the developing conceptus results in intrauterine growth restriction, a significant social and economic problem of global importance (Bazer et al., 2012a). Furthermore, despite the hypothesized roles and functions of the EGF-EGFR system, little is known about cell signaling pathways stimulated by EGF in

porcine conceptus trophoderm cells and how EGF stimulates conceptus development during pregnancy. Therefore, the present study was conducted to determine the molecular mechanisms by which EGF activates the PI3K-AKT1 or ERK1/2 MAPK cell signal transduction pathway for proliferation, migration and gene expression by pig trophoderm cells.

3. Materials and Methods

Experimental Animals and Animal Care

Sexually mature gilts of similar age, weight, and genetic background were observed daily for estrus (day 0) and exhibited at least two estrous cycles of normal duration (18-21 days) before being used in this study. All experimental and surgical procedures were in compliance with the Guide for Care and Use of Agricultural Animals in Teaching and Research and approved by the Institutional Animal Care and Use Committee of Texas A&M University.

Experimental Design and Tissue Collection

To evaluate the effects of pregnancy on expression of EGFR, ERK1/2 MAPK-P90RSK and PI3K-AKT1, gilts were assigned randomly to either cyclic or pregnant status. Those in the pregnant group were bred when detected in estrus and 12 and 24 h later. Gilts were ovariectomized on either d 9, 12, or 15 of the estrous cycle or on d 9, 12, 13, 14, 15 or 20 of pregnancy (n = 3-4 pigs per day per status). For confirmation of pregnancy prior to implantation, the lumen of each uterine horn was flushed with 20 ml of physiological saline on d 9-15 of pregnancy and examined for the presence of morphologically normal conceptuses. Uteri from gilts on d 9-15 of the estrous cycle were processed in the same way. Several sections (~0.5 cm) of the entire uterine wall from the middle of each uterine horn were fixed in fresh 4%

paraformaldehyde in PBS (pH 7.2) and embedded in Paraplast-Plus (Oxford Laboratory, St. Louis, MO, USA).

Cell culture

Mononuclear porcine trophectoderm (pTr) cells from d 12 pig conceptuses were cultured and used in the present *in vitro* studies as described previously (Ka et al., 2001). For experiments, monolayer cultures of pTr cells were grown in culture medium to 80% confluence in 100-mm tissue culture dishes. Cells were serum starved for 24 h, and then treated with recombinant human pro-EGF (100 ng/ml; R&D Systems, Inc., Minneapolis, MN, USA) for 0, 5, 15, 30, 60 or 120 min. Based on preliminary dose-response experiments, 100 ng/ml (0.0089 nM) EGF was selected for use in all experiments in the present study. This design was replicated in three independent experiments.

RNA Isolation

Total cellular RNA was isolated from endometrium from cyclic and pregnant gilts using Trizol reagent (Invitrogen, Carlsbad, CA, USA) and purified using an RNeasy Mini Kit (Qiagen, Hilden, Germany) according to the manufacturer's recommendations. The quantity and quality of total RNA was determined by spectrometry and denaturing agarose gel electrophoresis, respectively.

Cloning of partial cDNA for porcine EGF receptor

Complementary DNA was synthesized using AccuPower® RT PreMix (Bioneer, Daejeon, Korea). A partial cDNA for porcine *EGFR* mRNA was amplified using specific primers based on data for porcine *EGFR* mRNA (GenBank accession no. AY117054.1; forward, 5'- GAA TCG CAG GAG AAA ACA GC-3'; reverse, 5'- CCT CAA GAG AGC TTG GTT GG-3'). The partial cDNAs for *EGFR* were gel-extracted and cloned into TOPO TA cloning vector (Invitrogen, Carlsbad, CA, USA).

Quantitative PCR Analysis

Specific primers for porcine *EGFR* (forward: 5'- AGC GAA AAA GAG TGC AAA GC -3'; reverse: 5'- ATG CAG TCT CTG GGT TCA GG-3'), *IFND* (forward: 5'- TCT GCT CCA TCT CTG TTT GC-3'; reverse: 5'- CCC TCT TCT CTA CGC AAT GG-3'), *IFNG* (forward: 5'- TGG GAA ACT GAA TGA CTT CG-3'; reverse: 5'- GAG TTC ACT GAT GGC TTT GC-3') and *TGFBI* (forward: 5'- GGC TGT CCT TTG ATG TCA CC-3'; reverse: 5'- GGC GAA AAC CCT CTA TAG CC-3') were designed from sequences in the GenBank data base using Primer 3 (ver.4.0.0). All primers were synthesized by Bioneer Inc. (Daejeon, Korea). Gene expression levels were measured using SYBR® Green (Sigma, St. Louis, MO, USA) and a StepOnePlus™ Real-Time PCR System (Applied Biosystems, Foster City, CA, USA). The PCR conditions were 95°C for 3 min, followed by 40 cycles at 95°C for 20 sec, 64°C for 40 sec, and 72°C for 1 min using a melting curve program

(increasing the temperature from 55°C to 95°C at 0.5°C per 10 sec) and continuous fluorescence measurements. Sequence-specific products were identified by generating a melting curve in which the C_T value represented the cycle number at which a fluorescent signal was significantly greater than background, and relative gene expression was quantified using the $2^{-\Delta\Delta CT}$ method. The gene glyceraldehydes-3-phosphate dehydrogenase (*GAPDH*) was used as endogenous control to standardize the amount of RNA in each reaction.

In situ Hybridization Analysis

After verification of the sequences, the plasmids containing gene sequences were amplified with T7- and SP6-specific primers (T7:5'-TGT AAT ACG ACT CAC TAT AGG G-3'; SP6:5'-CTA TTT AGG TGA CAC TAT AGA AT-3') then digoxigenin (DIG)-labeled RNA probes were transcribed using a DIG RNA labeling kit (Roche, Indianapolis, IN, USA). The tissue sections were deparaffinized, rehydrated, and treated with 1% Triton X-100 in PBS for 20 min and washed two times in DEPC-treated PBS. After post-fixation in 4% paraformaldehyde, sections were incubated in a prehybridization mixture containing 50% formamide and 4X standard saline citrate (SSC) for at least 10 min at room temperature. After hybridization and blocking steps, the sections were incubated overnight with sheep anti-DIG antibody conjugated to alkaline phosphatase (Roche, Indianapolis, IN, USA). The signal was visualized by exposure to a solution containing 0.4 mM 5-bromo-4-chloro-3-indolyl phosphate, 0.4 mM nitroblue tetrazolium, and 2 mM levamisole

(Sigma, St. Louis, MO, USA).

Immunohistochemistry

Immunohistochemical localization of EGFR protein in the porcine uteri was performed as described previously (Song et al., 2007a). Rabbit anti-human EGFR polyclonal antibody (catalog number: 2963) purchased from Cell Signaling Technology, Inc. (Danvers, MA, USA) was used at a 1:200 dilution. Antigen retrieval was performed using the boiling citrate method. Negative controls included substitution of the primary antibody with purified non-immune rabbit IgG at the same final concentration.

Western Blot Analyses

Concentrations of protein in whole-cell extracts were determined using the Bradford protein assay (Bio-Rad, Hercules, CA, USA) with bovine serum albumin (BSA) as the standard. Proteins were denatured, separated using SDS-PAGE and transferred to nitrocellulose. Blots were developed using enhanced chemiluminescence detection (SuperSignal West Pico; Pierce, Rockford, IL, USA) and quantified by measuring the intensity of light emitted from correctly sized bands under ultraviolet light using a ChemiDoc EQ system and Quantity One software (Bio-Rad, Hercules, CA, USA). Immunoreactive proteins were detected using rabbit anti-mouse polyclonal antibodies against p-AKT1 and AKT1 at a 1:1000 dilution and 10%

SDS/PAGE gel; rabbit anti-human polyclonal antibodies against p-P90RSK and P90RSK at a 1:1000 dilution and 10% SDS/PAGE gel; rabbit anti-human polyclonal p-ERK1/2 MAPK and rabbit anti-human monoclonal ERK1/2 MAPK IgG, each at a 1:1000 dilution, and 12% SDS/PAGE gel; rabbit anti-human polyclonal EGFR IgG at a 1:1000 dilution, and 6% SDS/PAGE gel. As a loading control, mouse anti- α -tubulin (TUBA) was used to normalize results from detection of proteins by western blotting. All antibodies were from Cell Signaling Technology (Danvers, MA, USA). Multiple exposures of each western blot were performed to ensure linearity of chemiluminescent signals.

Immunofluorescence microscopy

The effects of EGF on phosphorylation of AKT1, ERK1/2 MAPK and P90RSK were determined by immunofluorescence microscopy. Cells were probed with rabbit anti-human polyclonal p-AKT1 (Ser473) IgG at a 1:200 dilution, rabbit anti-human polyclonal p-ERK1/2 MAPK (Ser217/221) IgG at a 1:200 dilution, or rabbit anti-human polyclonal p-P90RSK (Thr573) IgG at a 1:200 dilution. They were then incubated with goat anti-rabbit IgG Alexa 488 (Chemicon, Temecula, CA, USA) at a 1:200 dilution for 1 h at room temperature. Cells then were washed and overlaid with Prolong® Gold Antifade reagent with DAPI. For each primary antibody, images were captured using a Zeiss confocal microscope LSM710 (Carl Zeiss, Jena, German) fitted with a digital microscope camera AxioCam using Zen 2009 software.

Target-specific siRNAs for EGFR knockdown

For messenger RNA sequences of pig EGFR (AY117054.1), two potential small interfering RNA target sites were determined using the Invitrogen design program. The most effective target sequence (CAG ATC GCA AAG GGC ATG A) was screened out and synthesized. Silencer Negative Control 1 siRNA (Ambion, Austin, TX, USA), with no homology to any known gene, was used as a negative control. Down-regulation of EGFR expression was confirmed by quantitative PCR and Western blotting analyses.

Transfection

The pTr cells were treated with specific EGFR siRNA or controls that included naive treatment (no siRNA or Lipofectamine 2000) and mock treatment (Lipofectamine 2000 only). Transfection of siRNA was performed according to the manufacturer's instructions. For the 48 h after EGFR siRNA transfection, pTr cells were serum starved, and then EGF (100 ng/ml) was added to the culture medium. The incubation was continued for either 5 or 15 min. Using green fluorescein conjugate control siRNA duplexes (Cell Signaling Technology, Danvers, MA, USA), it was estimated that more than 95% of the cells were transfected successfully.

Proliferation assay

Proliferation assays were conducted using Cell Proliferation ELISA, BrdU kit (Roche, Basel, Switzerland) according to the manufacturer's recommendations. Briefly, pTr cells were seeded in a 96-well microplate (tissue culture grade, flat bottom), and then incubated for 24 h in serum-free DMEM/F-12. Cells were then treated with recombinant EGF protein and various treatments in a final volume of 100 μ l/well. After 24 h of incubation, 10 μ M BrdU was added to the cell culture and the cells were reincubated for additional 24 h at 37°C. After labeling of cells with BrdU, the fixed cells were incubated with anti-BrdU-POD working solution for 90 min. The anti-BrdU-POD binds to the BrdU incorporated in newly synthesized cellular DNA and these immune complexes were detected by the reaction to TMB substrate solution. The absorbance values of the reaction product were quantified by measuring the absorbance at the 370 nm using an ELISA reader (Bio-Rad, Seoul, Korea).

Migration assay

The pTr cells (50,000 cells per 100 μ l serum and insulin-free DMEM) were seeded on 8- μ m pore Transwell inserts (Corning Costar no. 3422; Corning, Inc., Corning, NY, USA) and treatments added to each well (n = 3 wells per treatment). After 12 h, cells on the upper side of the inserts were removed with a cotton swab. For evaluation of cells that migrated onto the lower surface, inserts were fixed in 50% ethanol for 5 min. The Transwell membranes were then removed, placed on a glass slide with the side containing cells facing up, overlaid with prolong antifade mounting reagent with 4',6-diamidino-2-phenylindole, and overlaid with a coverslip

(Invitrogen-Molecular Probes, Eugene, OR, USA). Migrated cells were counted systematically in five nonoverlapping locations, which covered approximately 70% of the insert membrane growth area, using a Zeiss confocal microscope LSM710 (Carl Zeiss, Jena, German) fitted with a digital microscope camera AxioCam using Zen 2009 software. The entire experiment was repeated at least three times.

Reagents

Rabbit anti-human polyclonal antibodies against EGFR (catalog number: 2963), p-ERK1/2 MAPK (catalog number: 9101), p-P90RSK (catalog number: 9346), P90RSK (catalog number: 9347), rabbit anti-human monoclonal antibody against ERK1/2 MAPK (catalog number: 4695) and rabbit anti-mouse polyclonal antibodies against p-AKT1 (catalog number: 9271), AKT1 (catalog number: 9272) were purchased from Cell Signaling Technology, Inc. (Danvers, MA, USA). Inhibitors for PI3K (LY294002, catalog number: 9901), MEK1/2 (U0126, catalog number: 9903), P38 MAPK (SB203580, catalog number: 5633) and MTOR (Rapamycin, catalog number: 5633) were also obtained from Cell Signaling Technology, Inc. (Danvers, MA, USA).

Statistical Analyses

All quantitative data were subjected to least squares ANOVA using the General Linear Model procedures of the Statistical Analysis System (SAS Institute

Inc., Cary, NC, USA). Western blot data were corrected for differences in sample loading using the TUBA data as a covariate. All tests of significance were performed using the appropriate error terms according to the expectation of the mean squares for error. A *P* value less than or equal to 0.05 was considered significant. Data are presented as least-square means (LSMs) with SEs.

4. Results

Effects of estrous cycle and pregnancy on expression of EGFR mRNA and protein in porcine endometria

It is known that EGF protein is present in the porcine uterine lumen (Brigstock et al., 1996; Kim et al., 2009; Vaughan et al., 1992b); therefore, this study focused on temporal and cell-specific patterns of expression of EGFR mRNA and protein during the estrous cycle and pregnancy in gilts. Steady-state levels of uterine *EGFR* mRNA were determined by quantitative PCR analysis (Figure 3-1). In cyclic gilts, steady-state levels of *EGFR* mRNA in the uterus were low and unaffected by day of the estrous cycle. However, *EGFR* mRNA increased 71.6-fold between d 9 and d 14 of pregnancy ($P < 0.05$ or $P < 0.01$) and then declined to d 15 and was not detectable thereafter which supports results of a previous study (Kim et al., 2009). *In situ* hybridization analysis revealed that that *EGFR* mRNA was expressed at low abundance in uterine LE and GE between d 9 and d 15 of the estrous cycle (Figure 3-2A). Similarly, *EGFR* mRNA was weakly expressed in endometrial LE between d 9 and d 12 of pregnancy, but was abundantly expressed only in uterine LE, GE and stratum compactum stroma, as well as conceptus trophectoderm on d 13 and d 14 of pregnancy. On d 20 of pregnancy, *EGFR* mRNA was detectable in low abundance only in uterine LE. In addition, immunohistochemical analysis failed to detect EGFR protein in uteri of cyclic gilts on any day studied or uteri of pregnant gilts on d 9 and d 20, but EGFR protein was localized to uterine LE, GE and stratum compactum stroma

between d 12 and d 14 of pregnancy (Figure 3-2B). Thus, collectively, EGFR mRNA and protein expression is limited to uterine LE, GE and stratum compactum stroma, and conceptus trophoctoderm during the peri-implantation period of pregnancy when the conceptus is undergoing rapid elongation to the fully developed filamentous form.

EGF activates PI3K-AKT1 or ERK1/2 MAPK-P90RSK signal transduction pathways in porcine trophoctoderm cells

Western blot analyses of pTr cell extracts using antibodies to phosphorylated target proteins revealed that EGF increased the abundance of phosphorylated AKT1 (p-AKT1) 6.5-fold within 5 min over basal levels ($P < 0.01$), and this phosphorylated status was maintained to 120 min (Figure 3-3A). As compared to basal values, EGF increased phosphorylated ERK1/2 MAPK (p-ERK1/2 MAPK) by 2.0-fold within 5 min ($P < 0.001$) and the increases were sustained to 30 min (Figure 3-3B). EGF also stimulated phosphorylated P90RSK (p-P90RSK) by 6.5-fold ($P < 0.01$) over basal levels within 5 min, and the effect was maintained to 120 min (Figure 3-3C). To determine the cell signaling pathways mediating effects of EGF on AKT1 and ERK1/2 MAPK, pTr cells were pretreated with pharmacological inhibitors of PI3K (20 μ M LY294002) and ERK1/2 MAPK activity (20 μ M U0126), respectively. Induction of p-AKT1 and p-ERK1/2 MAPK by EGF was blocked by each of those inhibitors ($P < 0.01$ or $P < 0.001$) (Figure 3-3D and 3-3E). These results suggest that activation of the PI3K and ERK1/2 MAPK cell signaling pathways by EGF are required for phosphorylation of both AKT1 and P90RSK in the EGF-induced

cell signaling cascade.

Localization of p-AKT1, p-ERK1/2 MAPK and p-P90RSK by EGF in porcine trophectoderm cells

The effects of EGF on the phosphorylation of AKT1, ERK1/2 MAPK and P90RSK proteins were determined by immunofluorescence analyses (Figure 3-4). The pTr cells were incubated for 30 min with 100 ng/ml EGF. Untreated pTr cells had low basal levels of p-AKT1, p-ERK1/2 MAPK and p-P90RSK in the cytosol and nucleus, but EGF-treated pTr cells had abundant amounts of p-ERK1/2 MAPK, p-AKT1 and p-P90RSK proteins in the nuclear compartment and to a lesser extent, in the cytoplasm. These results suggest that activated ERK1/2 and AKT proteins translocate to the nucleus and activate specific transcription factors such as P90RSK family proteins. P90RSK is known to have important roles in various cellular events by phosphorylating ribosomal proteins which are typically activated through the PI3K-AKT1-MTOR or ERK1/2 MAPK pathways to increase mRNA translation and protein synthesis in the cytoplasm.

EGFR-PI3K-AKT1 and EGFR-ERK1/2 MAPK-P90RSK cell signaling pathways in porcine trophectoderm cells in response to EGF

As illustrated in Figures 3-5A and 3-5B, *EGFR* mRNA and protein in pTr cells were decreased by 21- ($P < 0.05$), 39- ($P < 0.001$) and 39% ($P < 0.001$) at 48 h

post-transfection with EGFR siRNA at 10-, 25- and 50 nM, respectively. Cells transfected with the EGFR-specific siRNA (50 nM) had less EGFR mRNA and protein as compared to naïve ($P < 0.001$) and mock-treated cells ($P < 0.05$) and cells transfected with control siRNA ($P < 0.001$). Additionally, as shown in Figure 3-5C, amounts of p-AKT1 and p-ERK1/2 proteins were reduced 81 and 43% in pTr cells after transfection with EGFR siRNA at 50 nM, irrespective of EGF treatment. However, there was no significant decrease in p-P90RSK protein in these cells in response to EGFR siRNA transfection. These results demonstrate that EGFR-AKT1 and EGFR-ERK1/2 signaling pathways are stimulated by EGF in pTr cells. It was also of interest to determine effects of EGFR siRNA on expression of genes associated with the conceptus trophoctoderm during the peri-implantation period of pregnancy in pigs. Accordingly, quantitative PCR analyses was used to determine relative effects of EGFR siRNA, control siRNA, naïve and mock transfection on expression of *interferon delta (IFND)*, *interferon gamma (IFNG)*, and *transforming growth factor beta 1(TGFBI)*. As illustrated in Figure 3-5D, EGFR siRNA treatment increased expression of *IFND* and *TGFBI* by 1.3- ($P < 0.05$) and 1.5-fold ($P < 0.01$), respectively. But, expression of *IFNG* mRNA was not affected by the siRNA treatment. These results indicate that EGF-EGFR system regulates two important genes involved in development of conceptus trophoctoderm and implantation events at the maternal-fetal interface during pregnancy.

Effect of EGF on proliferation of porcine trophoctoderm cells

Cell proliferation assays were conducted to investigate biological effects of EGF on pTr cells. EGF increased pTr cell numbers by approximately 177% ($P < 0.05$) (Figure 3-6). However, when EGF was combined with U0126 and LY294002, there was no increased pTr cell numbers ($P < 0.05$). Treatment of pTr cells with U0126 and LY294002 in the absence of EGF also inhibited proliferation of pTr cells. To examine involvement of other transcription factors, pharmacological inhibitors of P38 MAPK (SB203580) and MTOR (rapamycin) were used. Interestingly both inhibitors blocked effects of EGF on proliferation of pTr cells ($P < 0.05$). These results support our hypothesis that EGF from endometrial LE and GE acts in a paracrine manner on conceptus trophoctoderm to stimulate cell proliferation through the PI3K-AKT1-MTOR and ERK1/2 MAPK or P38 MAPK pathways.

Effect of EGF on migration of porcine trophoctoderm cells

To investigate another functional effect of EGF on pTr cells, cell migration assays were conducted. As shown in Figure 3-7, treatment of pTr cells with EGF increased their migration approximately 601% ($P < 0.01$). Meanwhile, treatment of pTr cells with either SB203580, U0126 or rapamycin decreased migration of these cells in response to EGF by 56-, 50-, and 54%, respectively ($P < 0.05$) as compared with EGF treatment alone. Interestingly, LY294002 decreased effects of EGF on migration of pTr cells about 80% ($P < 0.001$). Of particular note, treatment of the pTr cells with the inhibitors alone for 12 h did not affect cell migration. Collectively, these results strongly support our hypothesis that EGF from endometrial LE and GE acts in

a paracrine manner on conceptus trophoctoderm to stimulate cell migration via activation of PI3K-AKT1 and MAPK signaling cascades.

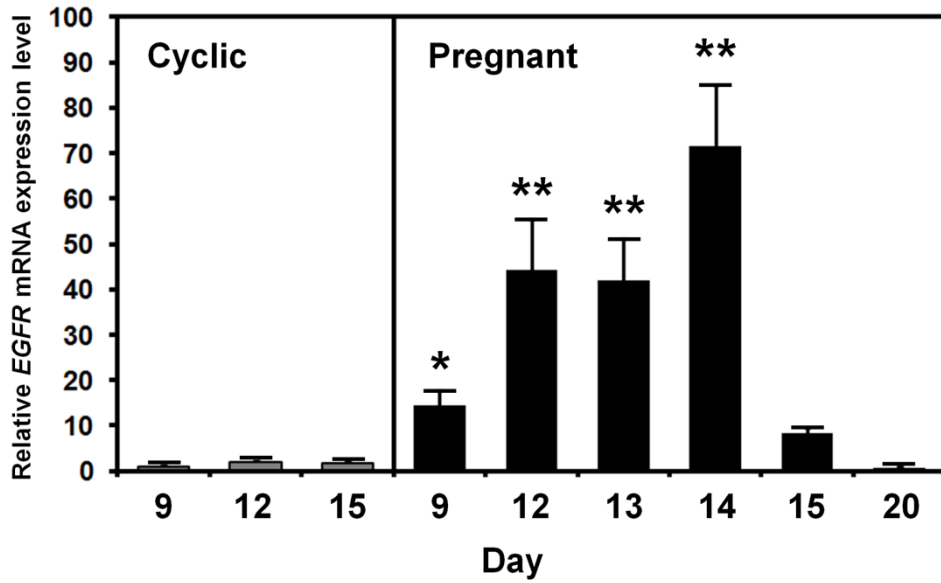
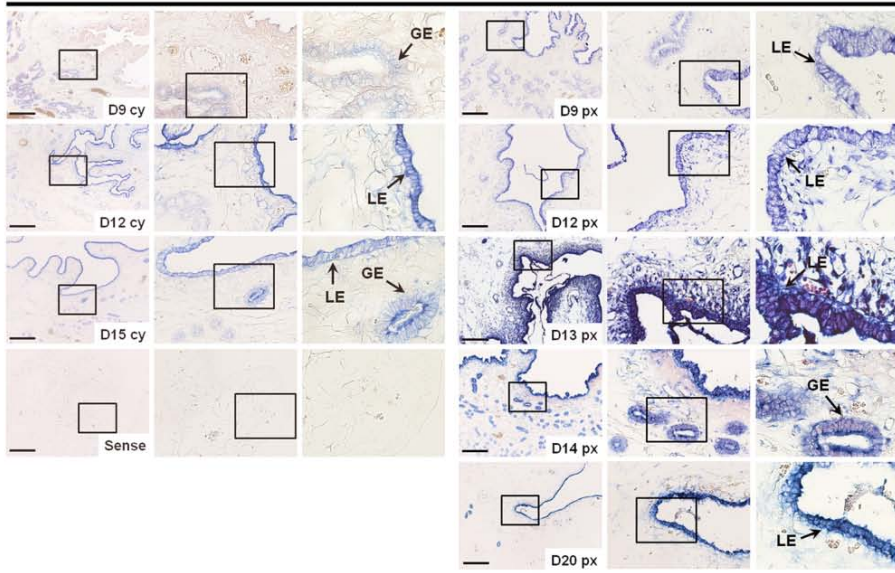


Figure 3-1. Steady-state levels of *EGFR* mRNA in endometria from cyclic and pregnant gilts as determined by quantitative PCR analysis. *EGFR* mRNA was affected ($P < 0.05$ or $P < 0.01$) by day, status, and their interaction when values for d 9, 12, and 15 of the estrous cycle and pregnancy were analyzed. Effects of day of the estrous cycle were not significant; however, effects of day of pregnancy on *EGFR* mRNA were significant ($P < 0.01$) as values increased between d 9 and d 14, before declining on d 15 and d 20. The asterisks denote statistically significant differences ($P < 0.01$ and * $P < 0.05$).**

[A]

EGFR



[B]

EGFR

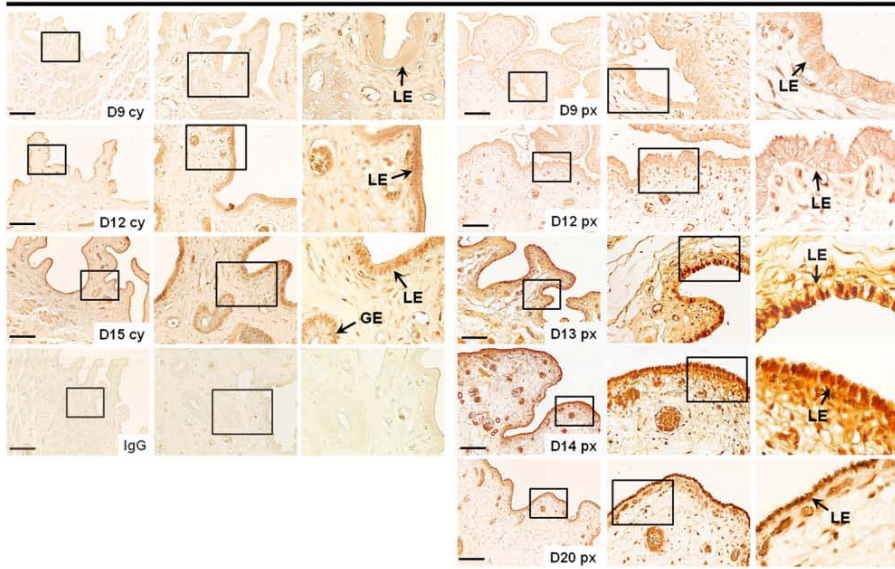


Figure 3-2. *In situ* hybridization and immunohistochemical analyses of EGFR mRNA and protein in endometria of cyclic and pregnant gilts. [A] *In situ* hybridization analyses of *EGFR* mRNAs in the porcine uteri. Cross-sections of the uterine wall of cyclic and pregnant gilts were hybridized with antisense or sense porcine *EGFR* cRNA probes. [B] Immunoreactive *EGFR* protein in the porcine uteri. For the IgG control, normal rabbit IgG was substituted for the primary antibody. Sections were not counterstained. Legend: cy, cyclic; px, pregnant; LE, luminal epithelium; GE, glandular epithelium. Scale bar represents 100 μ m. Images were captured at 10X, 40X and 100X objective magnifications.

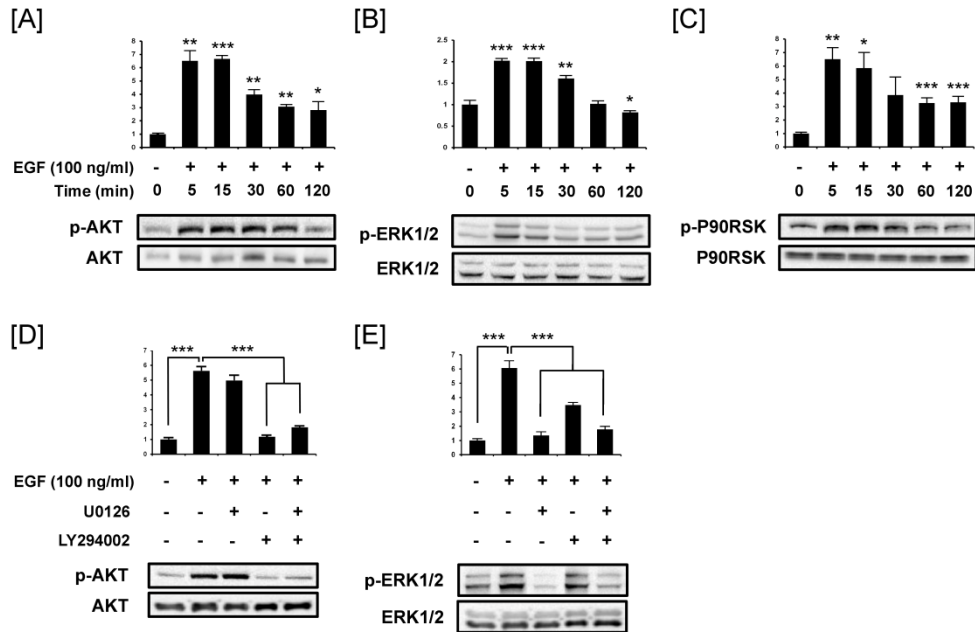


Figure 3-3. Phosphorylation of AKT1, ERK1/2 MAPK and P90RSK in response to EGF in pTr cells. [A-C] Analysis of time-dependent effects of EGF on phosphorylation of AKT1, ERK1/2 MAPK and P90RSK. Monolayers of 80% confluent pTr cells were serum-starved for 24 h and then treated with EGF (100 ng/ml) for the times indicated. Blots were imaged to calculate the normalized values presented in the graph (top) by measurements of levels phosphorylated protein relative to total protein. The bars represent the relative abundance of phosphorylated protein. Representative Western blots for p-AKT1, p-ERK1/2 MAPK and p-P90RSK (middle) and total AKT1, ERK1/2 MAPK and P90RSK (bottom; visualized with total AKT1 antibody after stripping the same blot). [D-E] Inhibition of AKT1 and ERK1/2 MAPK by the pharmacological inhibitors LY294002 and U0126, respectively. Serum starved pTr cells were pretreated with either 20 μ M LY294002 or 20 μ M U0126 for 30 min

and then stimulated with EGF (100 ng/ml) for 15 min. Representative results from western blots for p-AKT1 and p-ERK1/2 MAPK (middle), total AKT1 and total ERK1/2 MAPK are presented. Blots were imaged to calculate the normalized values presented in the graph (top) by measurements of levels p-AKT1 and p-ERK1/2 MAPK relative to total AKT1 and total ERK1/2 MAPK. The bars represent the relative abundance of phosphorylated protein. The asterisks denote statistically significant differences ($***P < 0.001$, $**P < 0.01$, and $*P < 0.05$).

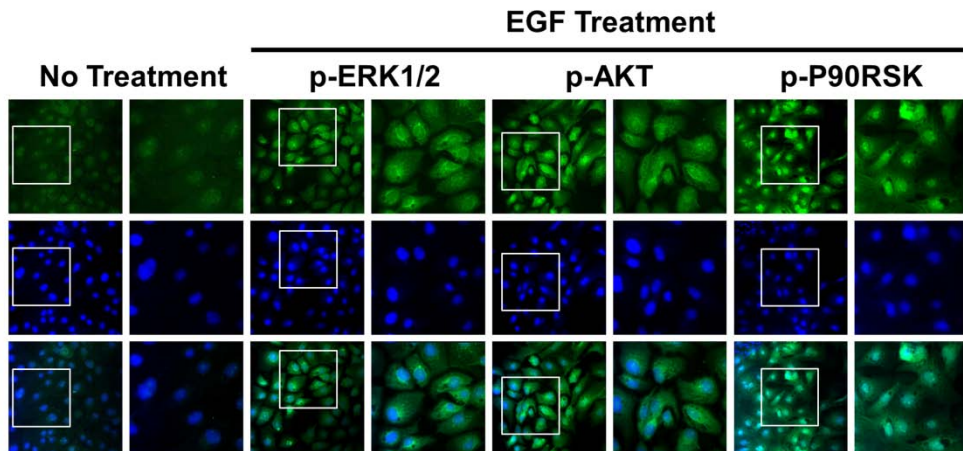


Figure 3-4. Immunocytochemical localization of p-AKT1, p-ERK1/2 MAPK and p-P90RSK protein in pTr cells. Immunoreactive p-AKT1, p-ERK1/2 MAPK and p-P90RSK proteins were localized in very low abundance to the nucleus and cytoplasm of untreated pTr cells, whereas pTr cells treated with EGF had abundant amounts of p-AKT1, p-ERK1/2 MAPK and p-P90RSK proteins in the nucleus. Activated p-P90RSK was localized to the nucleus and to a lesser extent in cytoplasm where it is involved in mRNA translation in the ribosomes. Images were captured at 20X and 40X objective magnification.

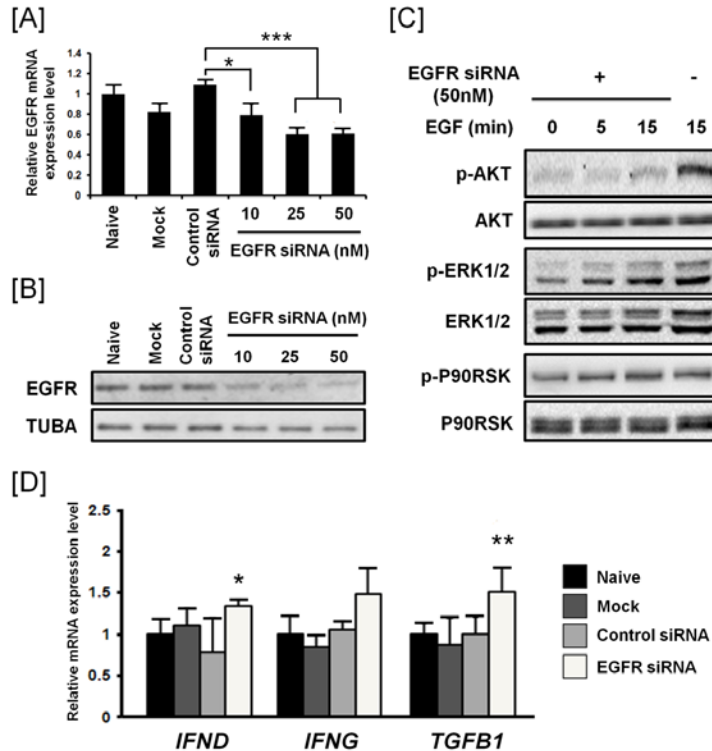


Figure 3-5. EGFR knockdown in the porcine trophoblast cells. [A-B] In the control group (naïve, mock and control siRNA treatments) and EGFR silencing group (dose-dependent manner), *EGFR* mRNA and protein levels were measured using quantitative RT-PCR and western blot analyses. Blots were imaged to calculate the normalized values presented as levels of EGFR protein relative to TUBA (alpha-tubulin) protein. [C] Effects of EGF combined with EGFR siRNA treatment on phosphorylation of AKT1, ERK1/2 MAPK and P90RSK in pTr cells. [D] The effects of EGF treatment on control pTr cells with naïve mock and control siRNA treatment and pTr cells in which EGFR was silenced. Total RNA isolated from pTr cells treated with EGFR siRNA (50 nM) affected expression of *IFND* and *TGFB1*, but not *IFNG*

mRNAs as determined using quantitative RT-PCR analyses. All quantitative data are presented as the LSM with overall SEM. The asterisk denotes a significant effect ($***P < 0.001$, $**P < 0.01$ and $*P < 0.05$). Legend: IFND, interferon delta; IFNG, interferon gamma; TGFB1, transforming growth factor beta 1.

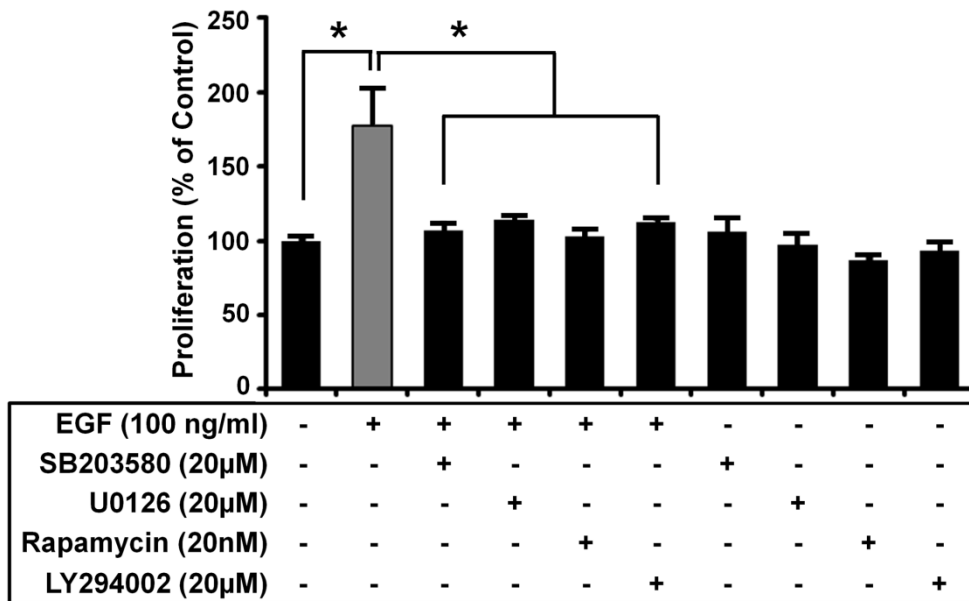


Figure 3-6. Proliferation of pTr cells in response to EGF through various signal transduction cascades. The pTr cells were cultured in a transwell plate (n=3 wells per treatment) and treated with recombinant human EGF (100 ng/ml), SB203580 (20 μM), U0126 (20 μM), Rapamycin (20 nM) or LY294002 (20 μM) or their combination. Cell numbers were determined after 48 h of incubation, and data are expressed as a percentage relative to nontreated control pTr cells (100%). All quantitative data are presented as the LSM with overall SEM. Asterisks denote an effect of treatment (* $P < 0.05$).

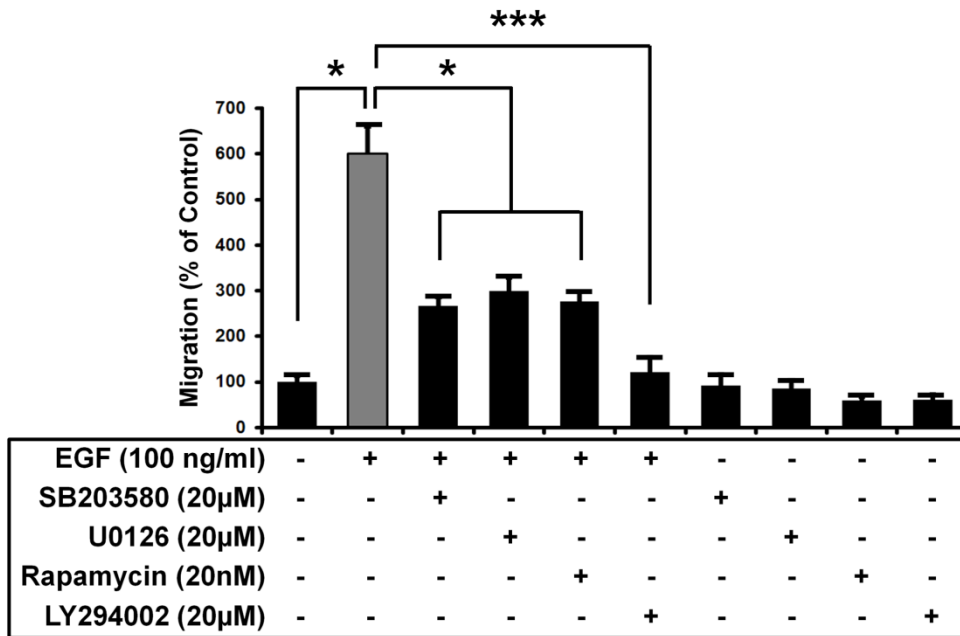


Figure 3-7. Migration of pTr cells in response to EGF through various signal transduction cascades. The pTr cells were cultured in a transwell plate (n=3 wells per treatment) and treated with recombinant human EGF (100 ng/ml), SB203580 (20 μM), U0126 (20 μM), Rapamycin (20 nM) or LY294002 (20 μM) or their combination. Cell migration was determined after 12 h treatment and data are expressed at a percentage relative to nontreated control cells (100%). EGF stimulated ($P < 0.01$) and the inhibitors blocked ($P < 0.05$ or $P < 0.001$) the effect of EGF on cell migration. The asterisks denote an effect of treatment ($***P < 0.001$ and $*P < 0.05$).

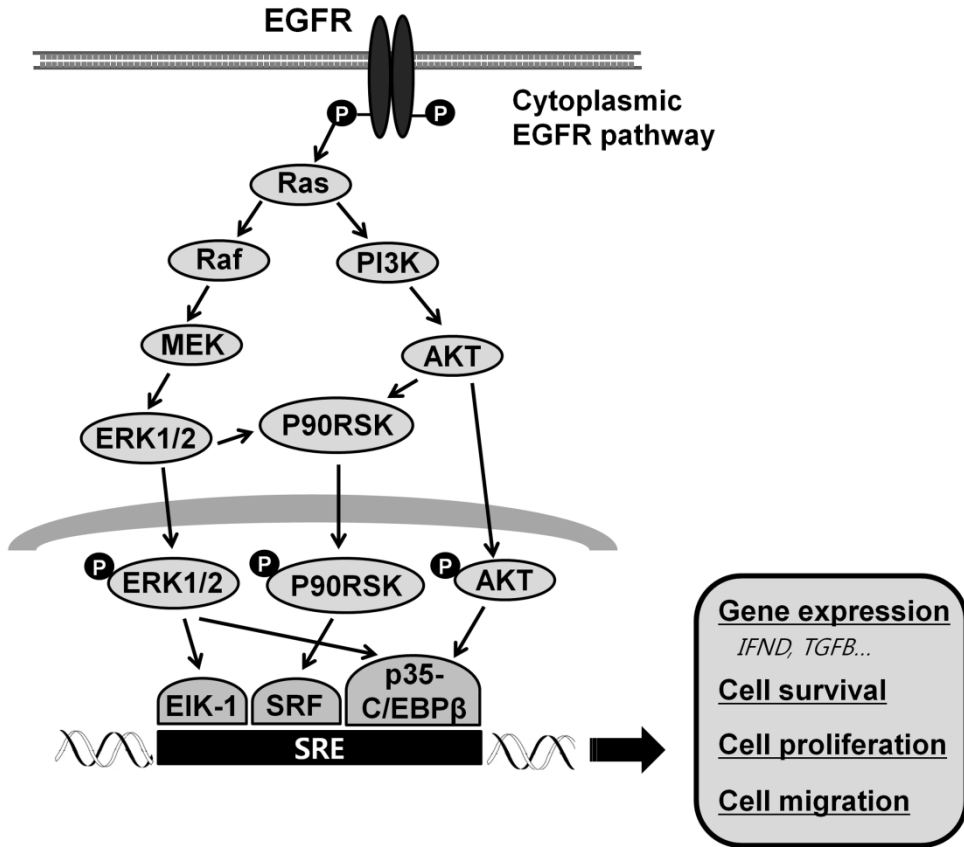


Figure 3-8. Schematic illustrating the current working hypothesis on EGF-induced PI3K-AKT1 or ERK1/2 MAPK-P90RSK signal transduction cascades in pTr cells during the peri-implantation period.

5. Discussion

Results of the present study demonstrate key roles for EGF in stimulating proliferation and migration of pTr cells through the PI3K-AKT1 and ERK1/2 MAPK signaling cascades (see Figure 3-8). These novel findings support our hypothesis that EGF influences migration, survival, and development of porcine conceptuses and that appropriate amounts of EGF are critical for implantation events during the peri-implantation period of pregnancy. For the successful establishment of pregnancy, well-organized and functional interactions at the maternal-conceptus interface are indispensable in mammals. This is especially important in pigs in which conceptuses must achieve contact with a maximum amount of uterine endometrial surface area for the exchange of histotroph and gases across a true epitheliochorial placenta (Song et al., 2011a). The histotroph includes nutrients and growth factors that play pivotal roles in mechanisms for secretion of hormones, cell signaling cascades and various developmental events such as growth and development of the conceptus.

Among essential growth factors during early pregnancy, EGF is known to influence uterine capacity since location of the gene for the EGF precursor is very near a quantitative trait locus for uterine capacity in pigs (Kim et al., 2001). Both EGF and EGFR are expressed in pregnant uteri of various mammalian species such as human (Chegini et al., 1986; Smith et al., 1991), baboon (Slowey et al., 1994), rhesus monkey (Yue et al., 2000), rabbit (Hofmann and Anderson, 1990), mouse (Das et al., 1994) and pigs (Kennedy et al., 1994; Kim et al., 2001; Kim et al., 2009; Wollenhaupt

et al., 2004), and it is present at high concentration in various body fluids. In pigs, EGF is expressed predominantly by uterine GE and columnar epithelial cells of the oviduct (Kennedy et al., 1994). In uteri of pregnant gilts, *EGF* mRNA expression is greatest on d 15 and declines to low levels by d 30, and is then sustained at this low level for the remainder of gestation (Kim et al., 2009). In addition, the temporal pattern of expression of *Egf* mRNA in uteri of rats suggests that EGF plays an important role in implantation and placentation (Aflalo et al., 2007). Administration of recombinant EGF protein stimulates endometrial stromal cell proliferation in humans (Hammond et al., 1993) when expression of EGFR is also abundant during the period of implantation (Kim et al., 2009). In the present study, EGFR mRNA and protein were barely detectable in uterine LE of cyclic and pregnant gilts; however, both increased significantly in uterine LE and GE between d 12 and d 14 of pregnancy before declining subsequently. These results indicate that EGF and EGFR in uteri of gilts during the period of implantation play key roles in the establishment of uterine capacity for establishment and maintenance of pregnancy.

In mammals, uterine remodeling for implantation is regulated primarily by both estrogen and progesterone which influence proliferation and differentiation of cells of the uterus by inducing synthesis and secretion of growth factors and cytokines (Stewart and Cullinan, 1997). During the peri-implantation period in pregnant gilts, balanced concentrations of estradiol-17 β (E2) from the conceptus and progesterone from the corpora lutea appear to be essential for expression of the EGF-EGFR system (Wollenhaupt et al., 2004). Several reports support this idea. For instance,

administration of E2 to immature female rats stimulates binding of EGF to EGFR and EGF-dependent tyrosine kinase activity as well as expression of *Egfr* expression in cells of the uterus (Mukku and Stancel, 1985). Furthermore, administration of exogenous EGF to ovariectomized mice had mitogenic effects and both E2 and EGF induced estrogen-inducible secretory proteins by transactivation of estrogen receptor alpha, which hints at participation of EGF in E2-induced uterine growth and differentiation (Nelson et al., 1991). In the present study, expression of *EGFR* mRNA was weakly detected in uterine LE and GE between d 12 and d 15 of the estrous cycle. Because circulating concentrations of both E2 and EGF at d 12 (mid-period) are lower than at d 20 of the estrous cycle (proestrus/estrus) (Wollenhaupt et al., 2004), our finding very low expression of EGFR during the early and mid-phases of the estrous cycle suggest that estrogen may regulate expression of the EGF-EGFR system. EGFR is abundant in endometrial LE and GE, and to a lesser extent, stromal cells between d 12 and d 14 of pregnancy when peri-implantation pig conceptuses secrete significant amounts of estrogen (Fischer et al., 1985; Geisert et al., 1982b; Robertson and King, 1974). During this period, the secreted estrogens act as the maternal recognition of pregnancy signal in swine and exert effects through cognate receptor on gene expression by uterine epithelial and stromal cells to induce uterine remodeling for implantation (Bazer and Thatcher, 1977). Indeed, placental estrogens act on the endometrial epithelia in a paracrine manner to increase expression of specific growth factors, including insulin-like growth factor one (IGF-I) (Persson et al., 1997) and fibroblast growth factor seven (FGF-7; also termed keratinocyte growth factor or KGF) (Ka et al., 2001; Ka et al., 2000), and secreted phosphoprotein 1 (SPP1, also known as

osteopontin) (White et al., 2005) that acts on the trophoctoderm to stimulate proliferation, migration and attachment to uterine LE.

Although the PI3K-AKT1 cell signaling pathway has emerged as a critical component of EGF-EGRF signaling system in human extravillous trophoblast during implantation (Qiu et al., 2004a, b), little is known of the signaling events mediated by EGF-EGFR system in the porcine conceptus during the peri-implantation period of pregnancy. Results of the present study demonstrated that EGF induces activation of AKT1 through phosphorylation and that LY294002 (pharmacological inhibitors of PI3K-AKT1) blocked the ability of EGF to increase proliferation and migration of pTr cells. Results of the present study also indicate that EGF induces phosphorylation of ERK1/2 MAPK-P90RSK in pTr cells. The ERK1/2 MAPK cell signaling cascade mediates mitogenic signaling in response to EGF to stimulate downstream targets in migration and invasion of trophoblast cells in humans (Qiu et al., 2004a, b). Among the three well-characterized MAPKs, the ERK1/2 MAPK pathway plays an essential role in trophoblast differentiation and placental development in humans and mice during early pregnancy (Daoud et al., 2005b; Wang et al., 2004a). In the present study, EGF induced maximum increases in phosphorylation of both ERK1/2 MAPK and P90RSK and treatment of pTr cells with U0126 (pharmacological inhibitors for ERK1/2 MAPK activity) blocked effects of EGF to increase proliferation and migration of pTr cells. In addition to activation of PI3K-AKT1 and ERK1/2 MAPK-P90RSK cell signaling pathways, EGF increased proliferation and migration of pTr cells via the MTOR and P38 MAPK cell signaling pathways, and these effects of EGF

could be blocked by treatment with rapamycin and SB203580, respectively. These results support our hypothesis that EGF from uterine LE and GE acts in a paracrine manner on conceptus trophoctoderm to stimulate cell proliferation and migration through the PI3K-AKT1-MTOR and ERK1/2 or P38 MAPK pathways; however, this requires further investigation.

Results of the present study also demonstrated that p-AKT1 and p-ERK1/2 MAPK proteins were inhibited significantly in pTr cells by EGFR knock down indicating the EGFR-AKT1 and EGFR-ERK1/2 MAPK signaling pathways are stimulated by EGF in pTr cells. In addition, EGFR knock down in pTr cells lead to increased expression of implantation-related genes, specifically *IFND* and *TGFBI*, but not *IFNG* in pTr cells. These results indicate that the EGF-EGFR system may regulate important genes involved in the development of the conceptus trophoctoderm and implantation events at the maternal-conceptus interface during early pregnancy. Spatio-temporal regulation of expression of these genes by EGF requires further investigation to better understand specific functions and regulatory mechanisms associated with development of the pig conceptus development and implantation, as well as placentation.

Collectively, EGF activates PI3K-AKT1 and stimulates ERK1/2 MAPK-P90RSK cell signaling pathways to effect proliferation, migration and gene expression by trophoctoderm of the pig conceptus during the peri-implantation period of pregnancy. These results provide important insights into mechanisms by which EGF

regulates conceptus development during the peri-implantation period of pregnancy in pigs.

CHAPTER 4

Insulin-Like Growth Factor I Induces Proliferation and Migration of Porcine Trophectoderm Cells through Multiple Cell Signaling Pathways, Including Protooncogenic Protein Kinase 1 and Mitogen-Activated Protein Kinase

1. Abstract

During early pregnancy, the developing conceptus is dependent upon a wide range of growth factors and nutrients that are secreted by or transported by uterine epithelia into the uterus at the maternal-conceptus interface for successful implantation and placentation. Among these factors, insulin-like growth factor-I (IGF-I) is known to play an important role in development of the early embryo and uterine endometrium. However, few studies have been conducted with pigs to determine IGF-I-induced functional effects on peri-implantation embryos such as activation of cell signaling cascades responsible for growth, proliferation and differentiation of cells of the conceptus. Therefore, the aim of this study was to examine the functional role of IGF-I on primary porcine trophectoderm (pTr) cells and to assess potential signaling pathways responsible for biological activities of IGF-1. In the present study, expression of *endometrial type I IGF receptor (IGF-IR)* mRNA increased significantly from Day 10 to Day 12 of pregnancy and the increase was greater for pregnant than cyclic gilts. Both *IGF-I* and *IGF-IR* mRNA were abundant in endometrial luminal and glandular epithelia, stratum compactum stroma and conceptus trophectoderm on Day 12 of pregnancy. In addition, IGF-I significantly induced phosphorylation of AKT1, ERK1/2 and RPS6 in a time- and concentration-dependent manner in pTr cells. Immunofluorescence microscopy revealed that IGF-I treated pTr cells exhibited increased abundance of phosphorylated (p)-AKT1 and p-ERK1/2 MAPK proteins in the nucleus and cytoplasm, and p-RPS6 proteins in the cytosol as compared to none-treated pTr cells. In the presence of the MAPK inhibitor (U0126), IGF-I-induced

AKT1 phosphorylation was not affected, whereas the PI3K inhibitor (LY294002) decreased IGF-I-induced phosphorylation of ERK1/2 and AKT1 proteins, and both the PI3K-AKT1 and ERK1/2 MAPK pathways were blocked by LY294002. Furthermore, IGF-I significantly stimulated both proliferation and migration of pTr cells, but these effects were inhibited by SB203580, U0126, rapamycin and LY294002. Taken together, these results indicate that IGF-I coordinately regulates multiple cell signaling pathways including PI3K-AKT1-RPS6 and ERK1/2 MAPK signaling pathways that are critical to proliferation, migration and survival of trophectoderm cells during early pregnancy in pigs.

2. Introduction

As in any eutherian mammal, successful establishment and maintenance of pregnancy in the pig follows a well-organized reciprocal communication between the developing conceptus and maternal uterus to support pregnancy recognition, implantation, placentation and exchange of nutrients and gases (Bazer et al., 2012b). The peri-implantation period is one of the most critical stage of pregnancy for initiation of the maternal-conceptus dialogue, and it is also the period when the majority of conceptus mortality and reduction in litter size occurs in pigs (Stroband and Van der Lende, 1990). During this period, the spherical porcine blastocyst dramatically elongates to tubular and filamentous forms between Days 10 and 12 of pregnancy, and then comes in close proximity and begins to make attachment to the uterine luminal epithelium (LE) by Day 13 of pregnancy to establish a diffuse epitheliochorial type of placenta in which uterine LE is not destroyed during placental invasion as in other species (Burghardt et al., 1997; Geisert et al., 1982b; Geisert and Yelich, 1997; Keys and King, 1990; Leiser and Kaufmann, 1994). This process is especially important in pigs as it maximizes placenta-uterine surface area of contact for the efficient transfer of nutrients and gases between the maternal and conceptus vascular system (Song et al., 2011a; Stroband and Van der Lende, 1990).

During the peri-implantation period of pregnancy, the free-floating conceptus develops in the absence of direct contact with the uterine LE, so uterine secretions are essential for growth and development of conceptus. Many factors

including growth factors, cytokines, enzymes, hormones, ions and nutrients in uterine secretions make up what is called as histotroph. Histotroph is implicated in regulation of functional local interactions at the maternal-conceptus interface during the peri-implantation period of pregnancy (Carson et al., 2000; Gray et al., 2001a; Gray et al., 2001c; Lim et al., 2002; Spencer and Bazer, 2004b; Spencer et al., 2007b). Histotroph includes important growth factors for conceptus development and implantation that are expressed by uterine epithelia in a temporal and cell-specific manner, as well as secretions from the peri-implantation conceptus (Kane et al., 1997).

The insulin-like growth factors (IGFs), IGF-I and IGF-II, are single chain polypeptides which have structural homology with proinsulin (Heyner et al., 1989; Kaye et al., 1992). IGF-I and IGF-II have mitogenic and insulin-like metabolic effects that regulate a variety of fundamental cell properties by binding to type I IGF receptors (IGF-IR) and type II IGF receptors (IGF-IIR), respectively on the cell surface (Jones and Clemmons, 1995; Rechler and Nissley, 1985). The IGFs are significant regulators of conceptus and placental development during the peri-implantation period of pregnancy in humans, rodents, and domestic animals (Binoux, 1995; Gluckman, 1986; Irwin et al., 1999; Kim et al., 2008; Wathes et al., 1998; Watson et al., 1999). Results from studies of humans and mice suggest that IGF-I and IGF-II play important roles in stimulating protein synthesis, growth and development of the conceptus by regulating migration and proliferation of trophoblast cells (DeChiara et al., 1990; Gardner and Kaye, 1991; Harvey and Kaye, 1988, 1990, 1991, 1992a, b, c; Zwijsen et al., 2000). In domestic mammals such as cattle and sheep,

IGFs and their receptors are expressed in the uterus, oviduct and conceptus during the peri-implantation period of pregnancy and regulate growth and development of blastocysts, as well as endometrial gland morphogenesis for implantation and placentation (Ko et al., 1991; Robinson et al., 2000; Watson et al., 1992). Furthermore, our previous study with ovine trophoblast cells revealed that IGF-II stimulates migration via multiple cell signaling pathways (Kim et al., 2008).

In pigs, IGF-I, IGF-II and their specific receptors are expressed in the endometrium throughout peri-implantation period of conceptus development (Green et al., 1995; Simmen et al., 1990). Endometrial *IGF-II* transcripts increase as pregnancy progresses, whereas *IGF-I* transcripts in the uterus and secretory IGF-I protein in uterine flushings are greatest on Day 12 of pregnancy, coinciding with the time of conceptus elongation and secretion of estrogen for pregnancy recognition signaling (Geisert et al., 2001; Miese-Looy et al., 2012; Simmen et al., 1992). Also, enhanced release of porcine IGF-I stimulates embryonic protein synthesis, and expression of genes such as cytochrome P450 aromatase for secretion of estrogens by the conceptus (Estrada et al., 1991; Green et al., 1995; Hofig et al., 1991; Ko et al., 1994). Available evidence suggests that IGF-I is highly relevant to peri-implantation events during early pregnancy in pigs. However, regardless of spatial and temporal expression of IGF-I, potential novel functions of IGF-I during early pregnancy and molecular mechanisms that link the IGF-I system to peri-implantation processes are poorly understood.

This study tested the hypothesis that IGF-I from the endometrium and/or conceptus functions through multiple cell signaling pathways critical to proliferation, migration and survival of porcine trophectoderm (pTr) cells during implantation and placentation. Therefore, the specific objectives of this study were to determine: 1) the temporal and cell-specific expression of IGF-I and IGF-IR in porcine endometrium during the estrous cycle and early pregnancy; 2) effects of IGF-I on transactivation of PI3K-AKT1 and ERK1/2 MAPK signaling pathways in pTr cells; and 3) functional effects of IGF-I on proliferation and migration of pTr cells.

3. Materials and Methods

Experimental Animals and Animal Care

Sexually mature gilts of similar age, weight, and genetic background were observed daily for estrus (Day 0) and exhibited at least two estrous cycles of normal duration (18-21 days) before being used in this study. All experimental and surgical procedures were in compliance with the Guide for Care and Use of Agricultural Animals in Teaching and Research and approved by the Institutional Animal Care and Use Committee of Texas A&M University.

Experimental Design and Tissue Collection

Gilts were assigned randomly to either cyclic or pregnant status. Those in the pregnant group were bred when detected in estrus and 12 and 24 h later. Gilts were ovariectomized on either Day 9, 12, or 15 of the estrous cycle or on Day 9, 12, 13, 14 or 20 of pregnancy (n = 3-4 pigs per day per status). For confirmation of pregnancy prior to implantation, the lumen of each uterine horn was flushed with 20 ml of physiological saline and examined for the presence of morphologically normal conceptuses. Uteri from cyclic and pregnant gilts were processed to obtain several sections (~0.5 cm) from the entire uterine wall in the middle of each uterine horn, fix the tissue in fresh 4% paraformaldehyde in PBS (pH 7.2) and embed the tissue in Paraplast-Plus (Oxford Laboratory, St. Louis, MO, USA).

Cell culture

Mononuclear porcine trophoblast (pTr) cells from Day 12 pig conceptuses were cultured and used in the present *in vitro* studies as described previously (Ka et al., 2001). For experiments, monolayer cultures of pTr cells were grown in culture medium to 80% confluence in 100-mm tissue culture dishes. Cells were serum starved for 24 h, and then treated with recombinant human IGF-I (100 ng/ml; R&D Systems, Inc., Minneapolis, MN, USA) for 0, 5, 15, 30, 60 or 120 min. Based on preliminary dose-response experiments, 100 ng/ml (1.33 nM) IGF-I was selected for use in all experiments in the present study. This design was replicated in three independent experiments.

RNA Isolation

Total cellular RNA was isolated from endometrium from cyclic and pregnant gilts using Trizol reagent (Invitrogen, Carlsbad, CA, USA) and purified using an RNeasy Mini Kit (Qiagen, Hilden, Germany) according to the manufacturer's recommendations. The quantity and quality of total RNA was determined by spectrometry and denaturing agarose gel electrophoresis, respectively.

Cloning of partial cDNA for porcine IGF-I and IGF-I receptor

Complementary DNA was synthesized using AccuPower® RT PreMix (Bioneer, Daejeon, Korea). Partial cDNAs for porcine *IGF-I* and *IGF-I receptor* mRNAs were amplified using specific primers based on data for porcine *IGF-I* (GenBank accession no. NM_214256.1; forward, 5'- TGC ACA TCA CAT CCT CTT CG -3'; reverse, 5'- TGT ACT TCC TTC TGA GCC TTG G -3') and *IGF-I receptor* mRNA (GenBank accession no. NM _214172.1; forward, 5'- CAG TCC TAG CAC CTC CAA GC -3'; reverse, 5'- GCT GAT GAT CTC CAG GAA GG -3'). The partial cDNAs for *IGF-I* and *IGFI receptor* were gel-extracted and cloned into a TOPO TA cloning vector (Invitrogen, Carlsbad, CA, USA).

Quantitative PCR Analysis

Specific primers for porcine *IGF-I* (forward: 5'- CTC TCC TTC ACC AGC TCT GC -3'; reverse: 5'- GCC TCC TCA GAT CAC AGC TC -3') and *IGF-I receptor* (forward: 5'- TCC TAG CAC CTC CAA GCC TA -3'; reverse: 5'- GTC TTC GGC CAC CAT ACA GT -3') were designed from sequences in the GenBank data base using Primer 3 (ver.4.0.0). All primers were synthesized by Bioneer Inc. (Daejeon, Korea). Gene expression levels were measured using SYBR® Green (Sigma, St. Louis, MO, USA) and a StepOnePlus™ Real-Time PCR System (Applied Biosystems, Foster City, CA, USA). The PCR conditions were 95°C for 3 min, followed by 40 cycles at 95°C for 20 sec, 64°C for 40 sec, and 72°C for 1 min using a melting curve program (increasing the temperature from 55°C to 95°C at 0.5°C per 10 sec) and continuous fluorescence measurements. Sequence-specific products were

identified by generating a melting curve in which the C_T value represented the cycle number at which a fluorescent signal was significantly greater than background, and relative gene expression was quantified using the $2^{-\Delta\Delta C_T}$ method. The glyceraldehydes-3-phosphate dehydrogenase (*GAPDH*) gene was used as the endogenous control to standardize the amount of RNA in each reaction.

In situ Hybridization Analysis

After verification of the sequences, the plasmids containing gene sequences were amplified with T7- and SP6-specific primers (T7:5'-TGT AAT ACG ACT CAC TAT AGG G-3'; SP6:5'-CTA TTT AGG TGA CAC TAT AGA AT-3') then digoxigenin (DIG)-labeled RNA probes were transcribed using a DIG RNA labeling kit (Roche Applied Science, Indianapolis, IN). The tissue sections were deparaffinized, rehydrated, and treated with 1% Triton X-100 in PBS for 20 min and washed two times in DEPC-treated PBS. After post-fixation in 4% paraformaldehyde, sections were incubated in a prehybridization mixture containing 50% formamide and 4X standard saline citrate (SSC) for at least 10 min at room temperature. After hybridization and blocking steps, the sections were incubated overnight with sheep anti-DIG antibody conjugated to alkaline phosphatase (Roche, Indianapolis, IN, USA). The signal was visualized by exposure to a solution containing 0.4 mM 5-bromo-4-chloro-3-indolyl phosphate, 0.4 mM nitroblue tetrazolium, and 2 mM levamisole (Sigma, St. Louis, MO, USA).

Western Blot Analyses

Concentrations of protein in whole-cell extracts were determined using the Bradford protein assay (Bio-Rad, Hercules, CA, USA) with bovine serum albumin (BSA) as the standard. Proteins were denatured, separated using SDS-PAGE and transferred to nitrocellulose. Blots were developed using enhanced chemiluminescence detection (SuperSignal West Pico; Pierce, Rockford, IL, USA) and quantified by measuring the intensity of light emitted from correctly sized bands under ultraviolet light using a ChemiDoc EQ system and Quantity One software (Bio-Rad, Hercules, CA, USA). Immunoreactive proteins were detected using rabbit anti-mouse polyclonal antibodies against p-AKT1 and AKT1 at a 1:1000 dilution and 10% SDS/PAGE gel; rabbit anti-human polyclonal antibodies against p-RPS6 and rabbit anti-human monoclonal antibodies against RPS6 at a 1:1000 dilution and 10% SDS/PAGE gel; rabbit anti-human polyclonal p-ERK1/2 MAPK and rabbit anti-human monoclonal ERK1/2 MAPK IgG, each at a 1:1000 dilution, and 12% SDS/PAGE gel. As a loading control, mouse anti- α -tubulin (TUBA) was used to normalize results from detection of proteins by western blotting. All antibodies were from Cell Signaling Technology (Danvers, MA, USA). Multiple exposures of each western blot were performed to ensure linearity of chemiluminescent signals.

Immunofluorescence microscopy

The effects of IGF-I on phosphorylation of AKT1, ERK1/2 MAPK and

RPS6 were determined by immunofluorescence microscopy. Cells were probed with rabbit anti-human polyclonal p-AKT1 (Ser473) IgG at a 1:200 dilution, rabbit anti-human polyclonal p-ERK1/2 MAPK (Ser217/221) IgG at a 1:200 dilution, or rabbit anti-human polyclonal p-RPS6 (Ser235/236) IgG at a 1:200 dilution. They were then incubated with goat anti-rabbit IgG Alexa 488 (Chemicon, Temecula, CA, USA) at a 1:200 dilution for 1 h at room temperature. Cells were then washed and overlaid with Prolong® Gold Antifade reagent with DAPI. For each primary antibody, images were captured using a Zeiss confocal microscope LSM710 (Carl Zeiss, Jena, German) fitted with a digital microscope camera AxioCam using Zen 2009 software.

Proliferation assay

Proliferation assays were conducted using Cell Proliferation ELISA, BrdU kit (Roche, Indianapolis, IN, USA) according to the manufacturer's recommendations. Briefly, pTr cells were seeded in a 96-well microplate (tissue culture grade, flat bottom), and then incubated for 24 h in serum-free DMEM/F-12. Cells were then treated with recombinant IGF-I protein and various treatments in a final volume of 100 µl/well. After 24 h of incubation, 10 µM BrdU was added to the cell culture and the cells were reincubated for additional 24 h at 37°C. After labeling of cells with BrdU, the fixed cells were incubated with anti-BrdU-POD working solution for 90 min. The anti-BrdU-POD binds to the BrdU incorporated in newly synthesized cellular DNA and these immune complexes were detected by the reaction to TMB substrate solution. The absorbance values of the reaction product were quantified by

measuring the absorbance at 370 nm using an ELISA reader (Bio-Rad, Seoul, Korea).

Migration assay

The pTr cells (50,000 cells per 100 μ l serum and insulin-free DMEM) were seeded on 8- μ m pore Transwell inserts (Corning Costar no. 3422; Corning, Inc., Corning, NY, USA) and treatments added to each well (n = 3 wells per treatment). After 12 h, cells on the upper side of the inserts were removed with a cotton swab. For evaluation of cells that migrated onto the lower surface, inserts were fixed in 50% ethanol for 5 min. The transwell membranes were then removed, placed on a glass slide with the side containing cells facing up, overlaid with prolong antifade mounting reagent with 4',6-diamidino-2-phenylindole, and overlaid with a coverslip (Invitrogen Molecular Probes, Eugene, OR, USA). Migrated cells were counted systematically in five non-overlapping locations, which covered approximately 70% of the insert membrane growth area, using a Zeiss confocal microscope LSM710 (Carl Zeiss, Jena, German) fitted with a digital microscope camera AxioCam using Zen 2009 software. The entire experiment was repeated at least three times.

Reagents

Rabbit anti-human polyclonal antibodies against p-ERK1/2 MAPK (catalog number: 9101) and p-RPS6 (catalog number: 2211), and rabbit anti-human monoclonal antibody against RPS6 (catalog number: 2217) and ERK1/2 MAPK

(catalog number: 4695), and rabbit anti-mouse polyclonal antibodies against p-AKT1 (catalog number: 9271), AKT1 (catalog number: 9272) were purchased from Cell Signaling Technology, Inc. (Danvers, MA, USA). Inhibitors for PI3K (LY294002, catalog number: 9901), MEK1/2 (U0126, catalog number: 9903), P38 MAPK (SB203580, catalog number: 5633) and MTOR (Rapamycin, catalog number: 5633) were also obtained from Cell Signaling Technology, Inc. (Danvers, MA, USA).

Statistical Analyses

All quantitative data were subjected to least squares ANOVA using the General Linear Model procedures of the Statistical Analysis System (SAS Institute Inc., Cary, NC, USA). Western blot data were corrected for differences in sample loading using the TUBA data as a covariate. All tests of significance were performed using the appropriate error terms according to the expectation of the mean squares for error. A *P* value less than or equal to 0.05 was considered significant. Data are presented as least-square means (LSMs) with SEs.

4. Results

Temporal and cell-specific expression of IGF-I and type I IGF receptor mRNA in porcine endometria during the estrous cycle and pregnancy

Uterine *IGF-I* and *IGF-IR* mRNA levels in cyclic and pregnant pigs were determined by quantitative RT-PCR analysis (Figure 4-1). Steady-state levels of *IGF-I* mRNA in the uterus were not affected by day of the estrous cycle (day, $P > 0.05$), but level of *IGF-I* mRNA on Day 9 of pregnancy was lower ($P < 0.01$) than those on Day 9 of the estrous cycle. Expression of *IGF-I* mRNA increased 1.6-fold on Day 14 of pregnancy ($P < 0.05$) and then decline to d 20 of pregnancy ($P < 0.01$). No significant differences were found in *IGF-IR* transcripts due to day of the estrous cycle (day, $P > 0.05$), but *IGF-IR* mRNA levels increased 2.8-fold between Days 9 and 12 of pregnancy ($P < 0.01$) and then declined to Day 20 of pregnancy. *In situ* hybridization analysis was used to detect cell-specific localization of *IGF-I* and *IGF-IR* mRNAs in pig endometria during the estrous cycle and pregnancy (Figure 4-2). There was no difference in abundance of *IGF-I* mRNA in stratum compactum stroma, uterine luminal epithelial cells (LE) and glandular epithelial cells (GE) between Days 9 and 15 of estrous cycle. In pregnant gilts, *IGF-I* mRNA expression tended to increase in GE between Days 9 and 12, and was abundant in stratum compactum stroma, uterine LE, as well as conceptus trophoctoderm on Days 13 and 14. In cyclic gilts, there was strong expression of *IGF-IR* mRNA in uterine LE and GE. Similarly, *IGF-IR* mRNA was localized primarily to uterine LE and GE during pregnancy, and expression of

IGF-IR mRNA in stratum compactum stroma, LE and GE tended to increase between Days 9 and d 12 of pregnancy. On Days 13 and 14 of pregnancy, *IGF-IR* mRNA was also detectable in conceptus trophoctoderm, and relatively lower levels of *IGF-IR* mRNA were detected in stratum compactum stroma, uterine LE and GE on Day 20 of pregnancy. Collectively, these results demonstrate that *IGF-I* and *IGF-IR* mRNAs are abundant in uterine LE, GE, stratum compactum stroma, and conceptus trophoctoderm during the peri-implantation period of pregnancy.

IGF-I activates AKT1, ERK1/2 and RPS6 phosphorylation and stimulates migration and proliferation of porcine trophoctoderm (pTr) cells

IGF-I stimulated phosphorylation of AKT1, ERK1/2 as well as RPS6 in a dose-dependent manner (Figure 4-3A). Under the same specific culture conditions, we the effects of different concentrations of IGF-I (0, 0.1, 1, 20, 100 ng/ml) on proliferation and migration of pTr cells were measured (Figure 4-3B and 4-3C). IGF-I at 100 ng/ml increased pTr cell proliferation by approximately 163% ($P < 0.05$). Similarly, IGF-I stimulated migration of pTr cells approximately 421% ($P < 0.001$) and 463% ($P < 0.001$) at 20 ng/ml and 100 ng/ml, respectively. Based on results from our dose-response experiments, IGF-I was used at 100 ng/ml in experiments to determine cell signaling pathways. IGF-I increased the abundance of phosphorylated AKT1 (p-AKT1) in a time-dependent manner, reaching 6.6-fold ($P < 0.001$) at 60 min after treatment (Figure 4-3D). As compared to basal values, IGF-I stimulated a rapid 4.1-fold ($P < 0.01$) increase in phosphorylated ERK1/2 MAPK (p-ERK1/2 MAPK)

within 5 min post-treatment, and this level of phosphorylation was maintained to 120 min (Figure 4-3E). Within 30 min after IGF-I treatment, phosphorylated RPS6 (p-RPS6) increased 6.6-fold ($P < 0.001$), and then gradually decreased through 120 min, but remained higher than at basal levels (Figure 4-3F).

IGF-I activates PI3K-AKT1 and ERK1/2 MAPK signal transduction pathways in porcine trophectoderm cells

Effects of IGF-I on PI3K-AKT1 and MAPK cell signal transduction in pTr cells were investigated using pharmacological inhibitors of PI3K (20 μ M LY294002) and ERK1/2 MAPK activity (20 μ M U0126). Serum starved pTr cells were incubated with either LY294002 (20 μ M) or U0126 (20 μ M) 1 h prior to treatment with IGF-I (100 ng/ml). IGF-I-induced phosphorylation of AKT1 was completely inhibited by the PI3K inhibitor ($P < 0.001$), while U0126 did not affect the abundance of IGF-I-induced p-AKT1 protein ($P > 0.05$) (Figure 4-4A). IGF-I-induced increases in phospho-ERK1/2 were blocked by both U0126 ($P < 0.001$) and LY294002 ($P < 0.001$) (Figure 4-4B). These results suggest that IGF-I induce activation of both PI3K-AKT1 and ERK1/2 MAPK cell signaling pathways in pTr cells, and that ERK1/2 MAPK is a down-stream target of PI3K in the regulation of the IGF-I-induced cell signaling cascade.

Immunolocalization of p-AKT1, p-ERK1/2 and p-RPS6 by IGF-I in porcine trophectoderm cells

The positive immunoreactions for p-AKT1, p-ERK1/2 and p-RPS6 revealed the effects of IGF-I on the phosphorylation of AKT1, ERK1/2 and RPS6 proteins in pTr cells (Figure 4-5). Serum starved pTr cells were treated with 100 ng/ml IGF-I for 30 min, and then incubated with antibodies specific for p-AKT1, p-ERK1/2 and p-RPS6. Immunoreactive p-AKT1, p-ERK1/2 and p-RPS6 were present at low basal intensity within the cytosol and nucleus in control cultures. But, IGF-I treated pTr cells exhibited a significant increase in p-AKT1 and p-ERK1/2 protein in the cytoplasm, and to a lesser extent, the nucleus. Phosphorylated RPS6 protein also increased in response to IGF-I, and the increase was most abundant at the cytoplasm, especially the perinuclear cytoplasmic regions. These results suggest that IGF-I activates AKT1 and ERK1/2 proteins by phosphorylation and, they induce activation of RPS6 protein in the cytoplasm to increase mRNA translation for proteins.

Proliferation of pTr cells in response to IGF-I through various signal transduction cascades

To confirm whether PI3K-AKT1 and ERK1/2 MAPK signal transduction pathways are involved in effects of IGF-I on proliferation of pTr cells, cell proliferation assays were conducted in the presence or absence of IGF-I (100 ng/ml), U0126 or LY294002. As shown in Figure 4-6, IGF-I increased pTr cell numbers by approximately 166% ($P < 0.05$). However, pretreatment with U0126 or LY294002 plus IGF-I reduced pTr cell numbers ($P < 0.001$) as compared to IGF-I treatment

alone. To examine involvement of other intracellular messengers, pharmacological inhibitors of P38 MAPK (SB203580) and FRAP/mTOR activity (rapamycin) were used. Interestingly both of those inhibitors also blocked effects of IGF-I on proliferation of pTr cells ($P < 0.001$ or $P < 0.05$). These results suggest that activation of PI3K-AKT1-FRAP and ERK1/2 or P38 MAPK signaling pathways play an important role in stimulation of pTr cell proliferation in response to IGF-I from endometrial and/or conceptus tissues.

Migration of pTr cells in response to IGF-I through various signal transduction cascades

Using transwell plates, functional effects of IGF-I on pTr cell migration were investigated. As shown in Figure 4-7, treatment of pTr cells with IGF-I alone stimulated cell migration approximately 501% ($P < 0.001$), but SB203580, U0126, rapamycin and LY294002 inhibited the stimulatory effects of IGF-I on pTr cell migration to 206-, 181-, 276-, and 300%, respectively ($P < 0.01$). As expected, in the absence of IGF-I, treatment of the cells with the inhibitors only had no effect on pTr cell migration. Taken together, these results suggest that IGF-I from endometria and/or conceptus tissues act in a paracrine or autocrine manner to stimulate pTr cell migration via activation of PI3K-AKT1-FRAP and ERK1/2 or P38 MAPK signaling pathways.

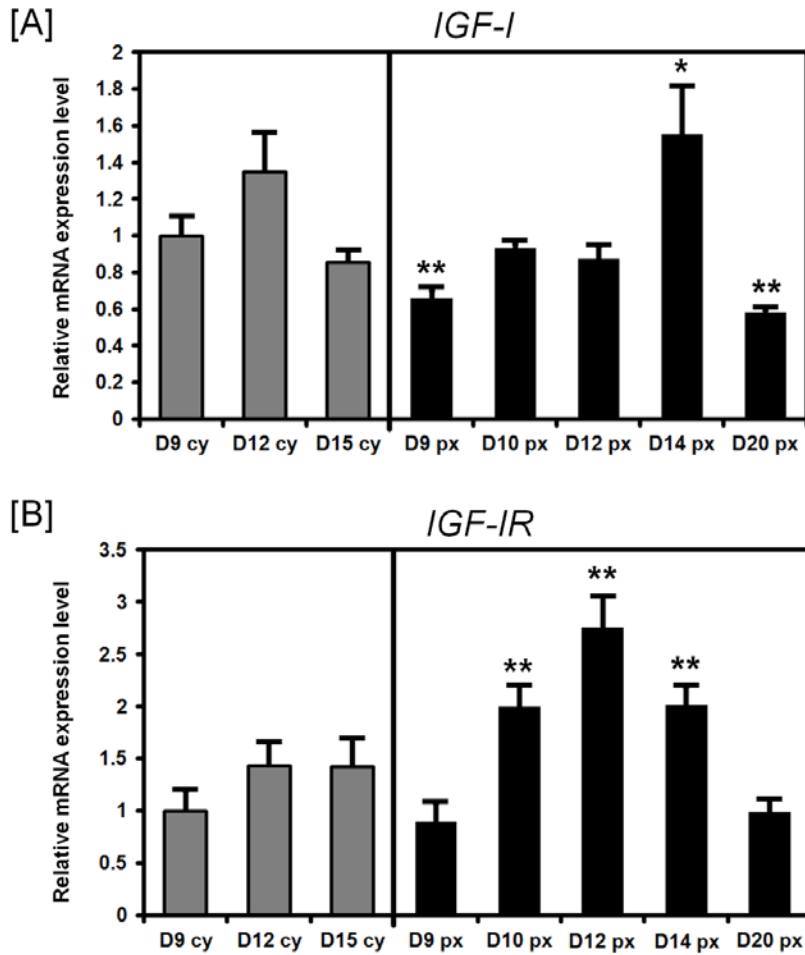
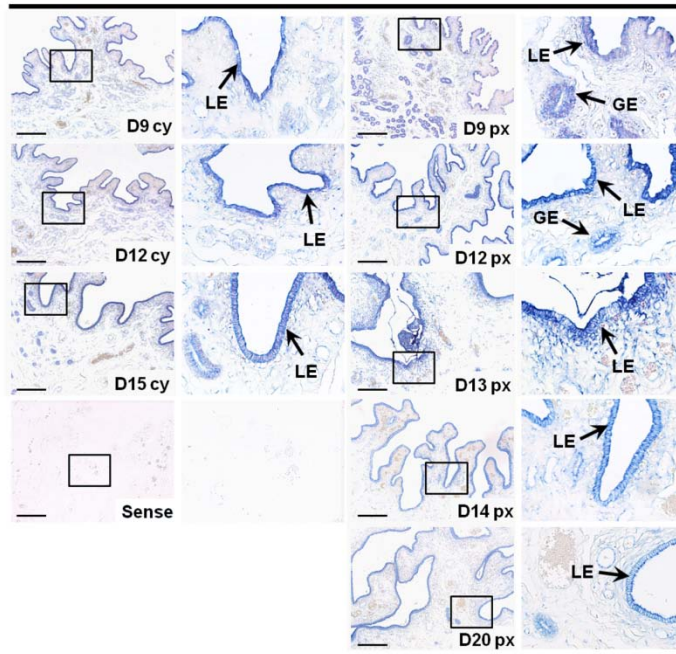


Figure 4-1. Relative quantification of expression of *IGF-I* and *IGF-IR* mRNAs in endometria during the estrous cycle and pregnancy by quantitative RT-PCR analysis. [A] Expression of *IGF-I* mRNAs in endometria from cyclic and pregnant gilts. [B] Expression of *IGF-IR* mRNAs in endometria from cyclic and pregnant gilts. *IGF-I* and *IGF-IR* mRNA levels were not affected by day of the estrous cycle, but effects of day of pregnancy on expression of *IGF-I* and *IGF-IR* mRNA were significant (day, $P < 0.05$ or 0.01). The asterisks denote statistically significant differences (** $P < 0.01$ and * $P < 0.05$).

[A]

IGF-I



[B]

IGF-IR

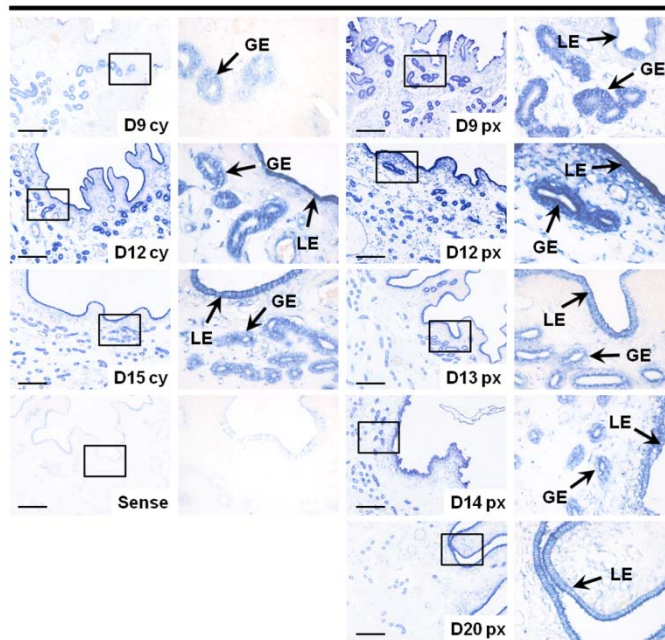


Figure 4-2. In situ hybridization analyses of *IGF-I* and *IGF-IR* mRNAs in the uterine endometrium during the estrous cycle and pregnancy in gilts. *In situ* hybridization analyses of *IGF-I* and *IGF-IR* mRNAs in the uterine endometrium during the estrous cycle and pregnancy in gilts. [A] *In situ* hybridization analyses of *IGF-I* mRNAs in the porcine uterus. [B] *In situ* hybridization analyses of *IGF-IR* mRNA in the porcine uterus. Cross-sections of the uterus from Day 12 of pregnancy were hybridized with DIG-labeled sense porcine *IGF-I* or *IGF-IR* cRNA probes as a negative control. Legend: cy, estrous cycle; px, pregnancy; LE, luminal epithelium; GE, glandular epithelium. Scale bar represents 100 μ m. Images were captured at 10X and 40X objective magnification.

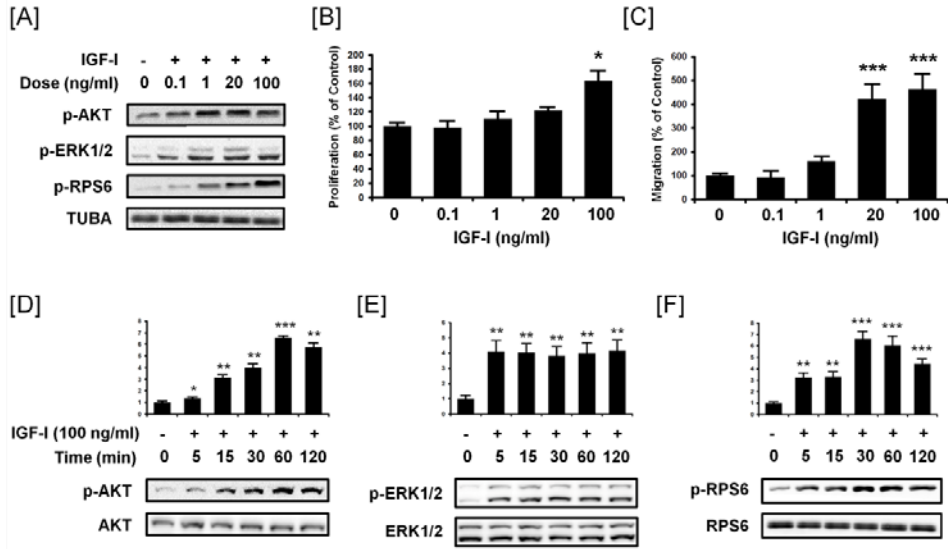


Figure 4-3. IGF-I increases the abundance of phosphorylated AKT1, ERK1/2 and RPS6 proteins and stimulates migration and proliferation of pTr cells. [A] Western blot analyses showing dose-dependent effects of IGF-I to increase the abundance of p-AKT1, p-ERK1/2 and p-RPS6 proteins in pTr cells *in vitro*. Tubulin-alpha (TUBA) was detected as a total protein control. [B] The effect of IGF-I (0, 0.1, 1, 20 and 100 ng/ml) on pTr cell proliferation. [C] The effect of IGF-I (0, 0.1, 1, 20 and 100 ng/ml) on pTr cell migration. [D] Detection of p-AKT1 and AKT1 between 0 and 120 min after treatment of pTr cells with IGF-I. [E] Detection of p-ERK1/2 and ERK1/2 between 0 and 120 min in pTr cells treated with IGF-I. [F] Detection of p-RPS6 and RPS6 between 0 and 120 min after treatment of pTr cells with IGF-I. Blots were imaged to calculate the normalized values presented in the *graph* by measurements of abundance of phosphorylated proteins relative to total protein. The asterisks denote statistically significant differences ($***P < 0.001$, $**P < 0.01$ and $*P < 0.05$).

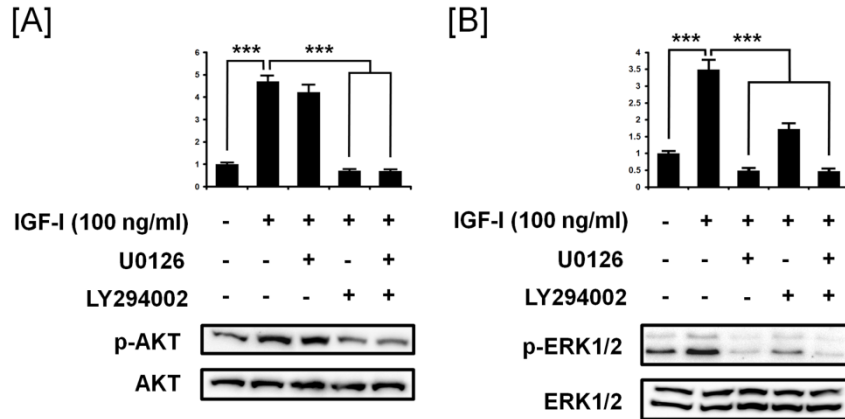


Figure 4-4. Inhibition of IGF-I-induced AKT1 and ERK1/2 phosphorylation in pTr cells. [A] The effects of the PI3K inhibitor (LY294002) on IGF-I-induced p-AKT1 and p-ERK1/2 proteins. [B] The effects of MAPK inhibitor (U0126) on IGF-I-induced phosphorylation of AKT1 and ERK1/2. Serum starved pTr cells were incubated with 20 μ M LY294002 or 20 μ M U0126 for 1 h and then stimulated with IGF-I for 30 min. Blots were imaged to calculate the normalized values presented in the *graph* by measurements of levels phosphorylated proteins relative to total proteins. The asterisks denote statistically significant differences (***) ($P < 0.001$).

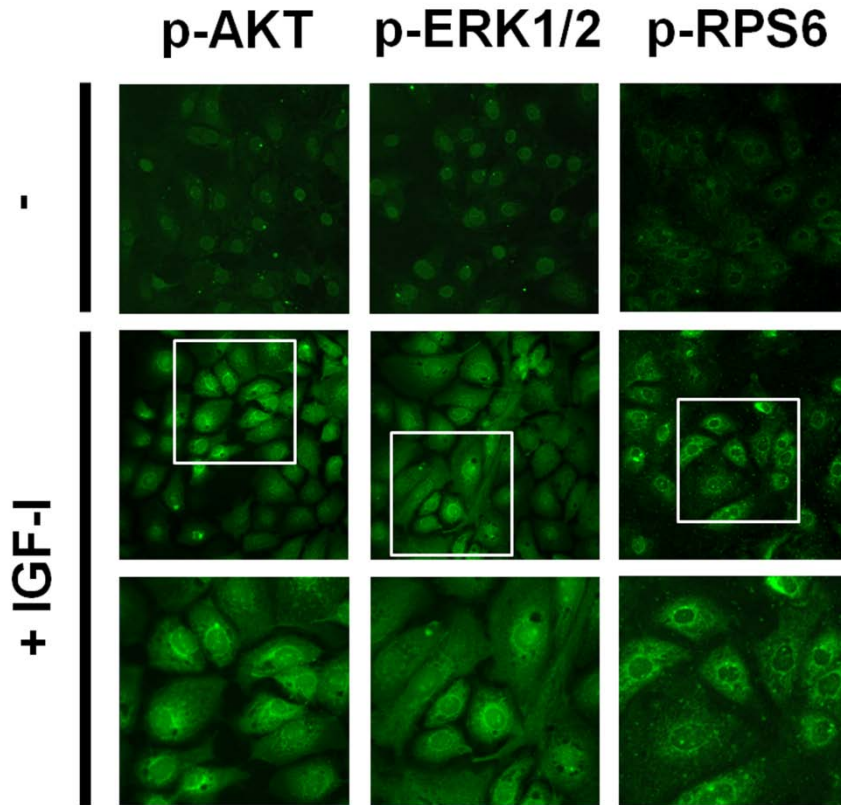


Figure 4-5. Immunofluorescence detection of p-AKT1, p-ERK1/2 and p-RPS6 proteins in IGF-I treated pTr cells. Basal levels of p-AKT1, p-ERK1/2 and p-RPS6 proteins were localized to the nucleus and cytoplasm of untreated pTr cells, whereas IGF-I treated pTr cells had abundant amounts of p-AKT1 and p-ERK1/2 in the cytoplasm and to a lesser extent, in the nuclei. Also IGF-I increased cytoplasmic levels of immunoreactive p-RPS6 proteins in cytoplasm, but not in the nucleus. Images were captured at 20X and 40X objective magnification.

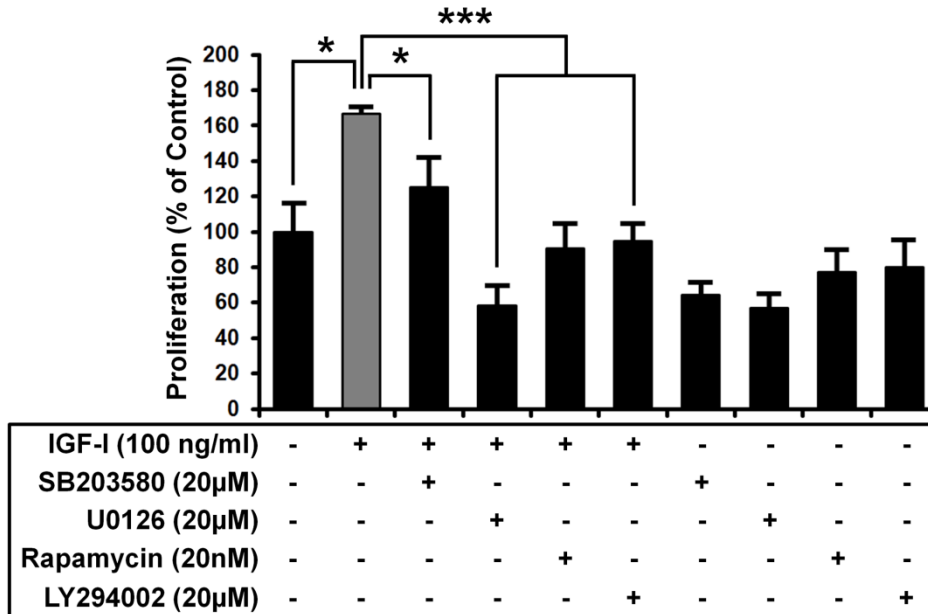


Figure 4-6. IGF-I stimulates proliferation of pTr cells through various signal transduction cascades. The pTr cells seeded in a 96-well microplate were treated with recombinant IGF-I (100 ng/ml), SB203580 (20 μM), U0126 (20 μM), Rapamycin (20 nM), LY294002 (20 μM), or their combination for 24 h in serum-free medium. After labeling of cells with BrdU for 24 h, cell numbers were determined by measuring the absorbance values of the reaction product. Data are expressed as a percentage relative to non-treated control pTr cells (100%). IGF-I stimulated ($P < 0.05$) pTr cell proliferation and the inhibitors blocked ($P < 0.001$ or $P < 0.05$) the effect of IGF-I on cell proliferation. The asterisks denote a significant effect of IGF-I treatment ($***P < 0.001$ and $*P < 0.05$).

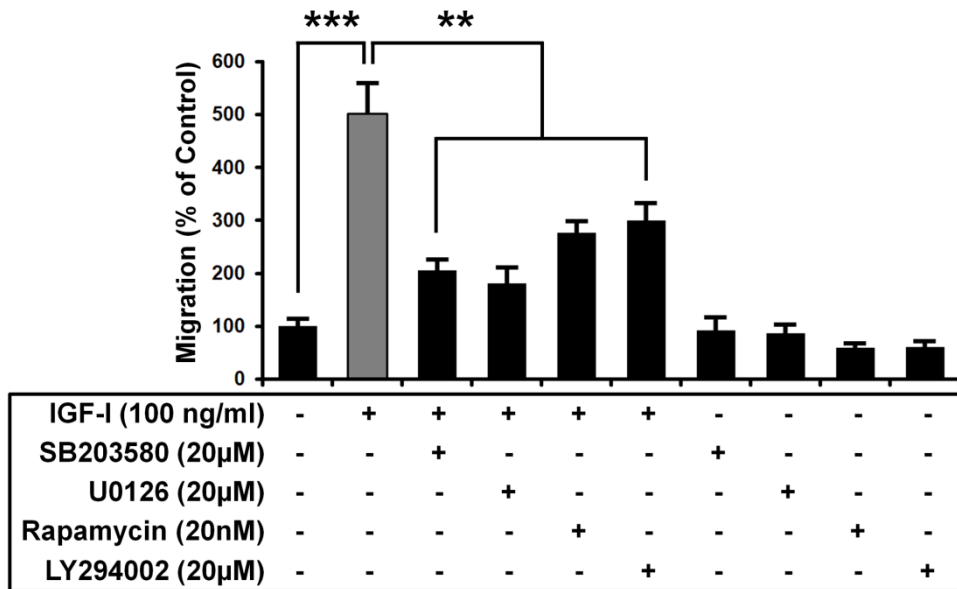


Figure 4-7. IGF-I stimulates migration of pTr cells through various signal transduction cascades. The pTr cells were cultured in a transwell plate (n = 3 wells per treatment) and treated with recombinant IGF-I (100 ng/ml), SB203580 (20 μM), U0126 (20 μM), Rapamycin (20 nM), LY294002 (20 μM), or their combination for 12 h in serum-free medium. Data are expressed at a percentage relative to non-treated control cells (100%). IGF-I stimulated ($P < 0.001$) and the inhibitors blocked ($P < 0.01$) the effect of IGF-I on cell migration. The asterisks denote an effect of treatment with IGF-I ($***P < 0.001$ and $**P < 0.01$).

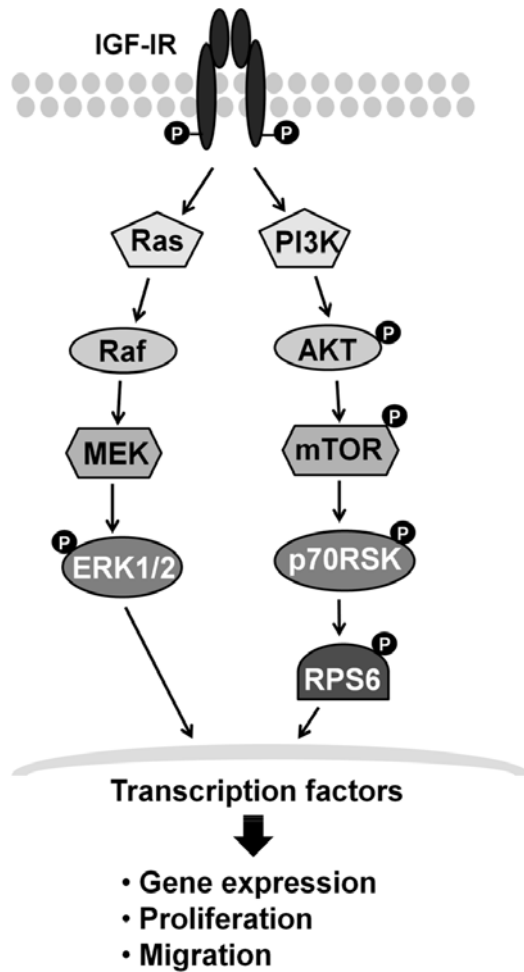


Figure 4-8. Schematic illustrating the current working hypothesis on IGF-I induced signaling pathways responsible for pTr cell proliferation and/or migration.

5. Discussion

The results of the present study demonstrate stimulatory effects of IGF-I on proliferation and migration of pTr cells through activation of PI3K-AKT1-RPS6 and/or ERK1/2 MAPK cell signaling pathways (see Figure 4-8). Results of the present study support our hypothesis that IGF-I from endometrial tissues and/or conceptus plays pivotal roles in implantation events by regulating the development of porcine conceptus during the early pregnancy.

During early pregnancy in pigs, the conceptus undergoes a dramatic morphological change as spherical blastocysts elongate to tubular and then filamentous forms, and the conceptus initiates implantation by attaching to the uterine LE. During this period, elongation and survival of conceptuses relies on reciprocal communication between the conceptus and endometrium. Successful establishment and maintenance of pregnancy are ultimately dependent upon a sufficient supply of histotrophic nutrition that includes growth factors, cytokines, ions, glucose, fructose and amino acids (Geisert et al., 1982b; Gray et al., 2001c; Guillomot, 1995). Evidence from studies with the uterine gland knockout ewe model revealed that uterine glands and their secretions are essential for conceptus survival, development, implantation and placentation during the early pregnancy (Allison Gray et al., 2000; Gray et al., 2001b; Spencer and Bazer, 2004b). Among these factors, IGF-I and IGF-II are highly implicated as promising growth factors in regulation of both embryonic and placental development during early pregnancy in most mammalian species (Clemmons, 1989;

Geisert et al., 1991; Maulik et al., 2006; Reynolds et al., 1997; Wathes et al., 1998). However, previous studies with pigs focused mainly on their concentrations in the endometrium during the estrous cycle and pregnancy and on its regulation by endocrine factors secreted from the porcine conceptus (Ashworth et al., 2005; Maulik et al., 2006; Simmen et al., 1992).

In pigs, IGF-I circulates at high concentrations in serum, and during pregnancy, it peaks at Day 12 of pregnancy, and declines as pregnancy progress (Simmen et al., 1992). Also IGF-I transcripts increase significantly in endometrial tissues on Day 12 of pregnancy as compared to Day 12 of the estrous cycle and the abundance of IGF-I occurs simultaneously with trophoblast elongation (Geisert et al., 2001; Green et al., 1996). On the other hand, endometrial IGF-II transcripts tend to increase as pregnancy progresses, suggesting that IGF-I is more important during the peri-implantation period of pregnancy in pigs (Geisert et al., 2001; Simmen et al., 1992). According to previous studies in primates, rodents and ruminants, IGFs in the maternal circulation do not cross the placenta, suggesting that the effects of IGFs in placental regions are highly localized (Han and Carter, 2000). IGF-I effects are tissue and cell dependent through binding to type I IGF receptors expressed abundantly on target cell surface membranes in the uterine endometrium (Dupont and Holzenberger, 2003; Simmen et al., 1992). Previous research identified both IGF-I ligand and receptor in uterine endometrium during the peri-implantation period of pregnancy, as well as in the embryo during pre-elongation stages which provides evidence for autocrine and/or paracrine effects of IGF-I (Letcher et al., 1989). In the present study,

expression of endometrial *IGF-I* and *IGF-IR* mRNA is not affected by day of the estrous cycle; but both mRNAs increased in endometrial LE and GE between Days 9 and 14 of pregnancy proliferation and migration of trophoblast cells allow for rapid elongation of the conceptus. These results provide evidence in support of our hypothesis that IGF-I and IGF-IR in endometria of gilts play essential roles in peri-implantational events, and that IGF-I acts in autocrine and paracrine manner to stimulate growth and development of the conceptus and perhaps prepares the uterus for implantation.

The increase of both *IGF-I* and *IGF-IR* mRNA in the endometrium during early pregnancy, as shown by others and in the present study, coincides temporally with the onset of elongation of porcine blastocysts and their secretion of estrogens for signaling pregnancy recognition. These results hint that the IGF-I system in the peri-implantation period is regulated by conceptus-derived estrogens that exert a local effect on the maternal endometrium together with circulating maternal steroids. Steroid hormones no doubt have a fundamental responsibility to mediate uterine remodeling for implantation by regulating endometrial secretions and uterine receptivity (Fischer et al., 1985). Among these hormones, the major hormone produced by the placenta of the pig that acts on the endometrium is estrogen. Around Day 12 of pregnancy, the porcine conceptus begins to secrete estrogen into the uterine environment, which causes a series of responses including variations in levels of steroid receptors and growth factors as well as acting as the signal for maternal recognition of pregnancy (Geisert et al., 1982b; Geisert et al., 1982c). The specific

timing and extent of estrogen secretion by the conceptus during early pregnancy has been shown to have dramatic effects on the ability of the conceptus to attach to the uterine LE, initiate implantation and subsequently develop. Estrogens also act on the endometrial epithelium in a paracrine manner to increase endometrial secretions. Exogenous administration of estrogen to cycling gilts increases endometrial secretory products and, in pregnancy gilts, placental estrogens also causes an increase in secretion of specific growth factors, which in turn act on the trophoctoderm to stimulate cell growth and development (Pusateri et al., 1990; Spencer and Bazer, 2004b). Several studies in pigs have also shown that estrogen stimulates uterine synthesis and/or endometrial secretion of IGF-I as well as expression of *IGF-I* mRNA in cells of the uterus (Sahlin et al., 1990; Simmen et al., 1990).

Although possible IGF signaling pathways during reproductive processes have been documented, currently, the exact cell signaling mechanisms activated by IGF-I in the porcine conceptus during the peri-implantation period are unknown. The PI3K-AKT1 cell signaling pathway is an evolutionarily conserved network that plays critical roles in regulation of cell proliferation and survival by transmitting signals arising from growth factor stimulation (Levine et al., 2006). IGF-I is known to stimulate the PI3K-AKT1 cell signaling pathway by activating Akt in the human endometrium and mouse uterus (Lathi et al., 2005; Toyofuku et al., 2006). Also, Kim *et al.* previously used ovine trophoctoderm cells to demonstrate that IGF-II stimulates cell migration through activation of the PI3K-AKT1 signaling pathway (Kim et al., 2008). Results of the present study demonstrated that IGF-I activates AKT1 within 5

min in pTr cells. In addition, immunoreactive p-AKT1 proteins were present at low levels in trophectoderm cells of early pregnant pigs, but were induced in nuclei and cytoplasm in response to IGF-I. For effective promotion of cell proliferation and growth, many growth factors and mitogens induce the phosphorylation of RPS6 which stimulates translation of mRNA transcripts encoding proteins such as cell cycle-related factors (Dufner and Thomas, 1999; Peterson and Schreiber, 1998). In the present study, cytoplasmic RPS6, the primary downstream target of AKT1-mTOR-p70RSK pathway, was also activated by IGF-I in pTr cells. Taken together, these results suggest that the PI3K-AKT1-RPS6 cell signaling pathway induced by IGF-I plays an essential role in conceptus development and implantation events in the pig.

Results of the present study demonstrated for the first time that the ERK1/2 MAPK pathway is also activated by IGF-I stimulation of pTr cells. The MAPK cascade is activated by diverse stimuli including growth factors and has been implicated in various cellular processes such as cell proliferation, differentiation, and migration in a number of model systems (Klemke et al., 1997; Seger and Krebs, 1995). In human extravillous trophoblast cells, several IGF family molecules, including IGF-II and insulin-like growth factor-binding protein-1 (IGFBP-1), stimulate cell migration through activation of MAPK cell signaling pathway (Gleeson et al., 2001; McKinnon et al., 2001). ERK1/2 MAPK, the most widely studied cascade among three well-characterized subfamilies of MAPK pathways, has been established as a major participant in differentiation processes, including embryonic and placental development (Fernandez-Serra et al., 2004b; Wang et al., 2004a). In the present study,

IGF-I induced a rapid increase in phosphorylation of ERK1/2 proteins, and these IGF-I-induced immunoreactive p-ERK1/2 proteins were abundant in nuclei and cytoplasm. These results suggest that activation of both PI3K-AKT1 and ERK1/2 MAPK cell signaling cascades are induced simultaneously by IGF-I in pTr cells.

Given the importance of both PI3K-AKT1 and ERK1/2 MAPK pathways in the regulation of IGF-I-induced effects on pTr cells, it was interested in examining possible cross-talk between PI3K-AKT1 and ERK1/2 MAPK cell signaling exists in pTr cells. In the present study, we found that MAPK inhibitor (U0126) inhibited IGF-I induction of highly phosphorylated ERK1/2 as well as IGF-I-induced proliferation and migration of pTr cells, but there was no significant effect on IGF-I-induced activation of the PI3K-AKT1 pathway. The PI3K inhibitor (LY294002) inhibited IGF-I-induced phosphorylation of AKT1 as well as IGF-I-induced proliferation and migration of pTr cells; however, IGF-I-induced phosphorylation of ERK1/2 was also inhibited by LY294002. Taken together, these results suggest that the ERK1/2 MAPK is a downstream target of PI3K-AKT1 in the pathway that regulates IGF-I-induced proliferation and migration of pTr cells. Also, as noted previously, activation of RPS6 protein occurs in response to IGF-I which suggests that phosphorylation of RPS6 protein is also a downstream target of cross-talk between the ERK1/2 MAPK and PI3K-AKT1 pathways.

Pharmacological inhibitors of FRAP/mTOR activity (rapamycin) and P38 MAPK activity (SB203580) abolished IGF-I-induced proliferation and migration of

pTr cells indicating a central role of mTOR and P38 MAPK cell signaling pathways in these processes. These results propose that IGF-I effects on proliferation and migration of pTr cells occurs in response to IGF-I, PI3K-AKT1-mTOR-(p70RSK) and ERK1/2 or P38 MAPK pathways that have common downstream targets such as RPS6. However, evidence for this requires further investigation.

In conclusion, IGF-I from endometrial and/or conceptus tissues regulates proliferation and migration of conceptus trophoctoderm in a paracrine or autocrine manner through PI3K-AKT1-mTOR-RPS6 and MAPK signal transduction cascades during the peri-implantation period. Results of the present study provide important insights into the mechanisms by which IGF-I regulates growth and development of the porcine conceptus during pregnancy. Further understanding of IGF-I induced cell signaling events that regulate development of the porcine conceptus will facilitate the development of intensive approaches to ameliorate peri-implantation embryonic death losses in pigs.

CHAPTER 5

Stimulatory Effect of Vascular Endothelial Growth Factor on Proliferation and Migration of Porcine Trophectoderm Cells and Their Regulation by the Phosphatidylinositol-3-Kinase-AKT and Mitogen-Activated Protein Kinase Cell Signaling Pathways

1. Abstract

Vascular endothelial growth factor (VEGF), a potent stimulator for angiogenesis, is likely to regulate implantation by stimulating endometrial angiogenesis and vascular permeability. In addition to known angiogenetic effects, VEGF has been suggested to participate in development of the early embryo as a mediator of fetal-maternal dialogue. Current studies have determined VEGF in terms of its role in endometrial vascular events, but VEGF-induced effects on the peri-implantation conceptus (embryo and extra-embryonic membranes) remains unknown. In the present study, endometrial *VEGF*, *VEGF receptor-1 (VEGFR-1)* and *VEGF receptor-2 (VEGFR-2)* mRNAs increased significantly during the peri-implantation period of pregnancy as compared to the estrous cycle. Expression of *VEGF*, *VEGFR-1* and *VEGFR-2* mRNAs was abundant in endometrial luminal and glandular epithelia, endothelial blood vessels and scattered cells in the stroma and conceptus trophoctoderm. In addition, pTr cells treated with VEGF exhibited increased abundance of phosphorylated (p)-AKT1, p-ERK1/2, p-p70RSK, p-RPS6 and p-4EBP1 in a time-dependent manner. The addition of U0126, an inhibitor of ERK1/2, inhibited VEGF-induced ERK1/2 phosphorylation, but AKT1 phosphorylation was not affected. The addition of LY294002, a PI3K inhibitor, decreased VEGF-induced phosphorylation of ERK1/2 and AKT1. Furthermore, VEGF significantly stimulated proliferation and migration of pTr cells, but these effects were blocked by SB203580, U0126, rapamycin and LY294002 which inhibit p38 MAPK, ERK1/2, mTOR and PI3K, respectively. These results suggest that VEGF is critical to successful growth

and development of porcine trophoderm during early pregnancy and that VEGF-induced stimulatory effect is coordinately regulated by multiple cell signaling pathways including PI3K-AKT1-mTOR and MAPK signaling pathways.

2. Introduction

The peri-implantation period represents a critical point in pregnancy when a well-organized dialogue between the endometrium and conceptus (embryo and its extra-embryonic membranes) must be established to ensure a suitable environment for implantation and conceptus development (Bazer et al., 2012b; Stroband and Van der Lende, 1990). Histotroph in uterine secretions is produced locally by the peri-implantation conceptus and/or uterine epithelia, and it is implicated in the interaction between the activated conceptus and receptive endometrium during early pregnancy (Carson et al., 2000; Gray et al., 2001a; Gray et al., 2001c; Kane et al., 1997; Lim et al., 2002; Spencer and Bazer, 2004b; Spencer et al., 2007b). Histotroph includes a wide range of molecules such as growth factors, cytokines, enzymes, hormones, prostaglandins, ions and nutrients (Geisert et al., 1982b; Gray et al., 2001c; Guillomot, 1995; Lim et al., 2002; Spencer and Bazer, 2004b).

Vascular endothelial growth factor (VEGF; also referred to as VEGF-A), a homodimeric heparin-binding glycoprotein, is one of the potent regulators participating in maternal-conceptus interactions. In humans, alternatively spliced variants, consisting of VEGF 121, 145, 165, 183, 189 and 206, were discovered (Houck et al., 1991; Jingjing et al., 1999; Poltorak et al., 1997). Among these isoforms, VEGF165 appears to be the primary isoform most frequently expressed (Charnock-Jones et al., 1993; Robinson and Stringer, 2001). The biological effects of VEGF are mediated via binding to high affinity tyrosine kinase receptors; VEGFR-1 (c-fms-like

tyrosine kinase, Flt-1) and VEGFR-2 (fetal liver kinase-1/kinase domain-containing receptor, Flk-1/KDR) (Ferrara et al., 2003). After binding to VEGFR-1 or VEGFR-2, VEGF induces their dimerization and autophosphorylation of receptor kinase, which activates intracellular signaling cascades. Although VEGF affinity is highest for VEGFR-1, VEGFR-2 has more potent angiogenetic activity in response to VEGF (Robinson and Stringer, 2001; Waltenberger et al., 1994).

VEGF plays a critical role in formation of new blood vessels and regulation of the permeability in a variety of tissues. VEGF in reproductive organs has been described in various species as a regulatory factor participating in mammalian reproduction (Charnock-Jones et al., 1993; Cullinan-Bove and Koos, 1993; Das et al., 1997; Ferrara et al., 2003). VEGF expression seems to correlate with implantation processes, by stimulating endothelial cell proliferation and vascular permeability (Das et al., 1997; Halder et al., 2000; Rabbani and Rogers, 2001). In early pregnancy, the endometrium undergoes rapid morphological and functional changes. VEGF-induced vascular remodeling is undoubtedly crucial for these processes. For example, increased blood supply via an enhanced endometrial vascular network is the first distinct mark for implantation and which is indispensable for successful establishment and maintenance of pregnancy. Also, during the peri-implantation phase, the endometrium and early conceptus induces angiogenesis at the implantation site, which provides an optimal environment for implantation and placentation (Reynolds and Redmer, 2001; Song et al., 2011a; Stroband and Van der Lende, 1990). Inadequate angiogenesis during the window of implantation results in a less receptive

endometrium, implantation failure and deficient placental formation. The VEGF-receptor system also plays an important role in early embryonic development. Gene knockout studies have shown that inactivation of a single allele for VEGF in mice results in embryonic abnormalities and early embryonic death (Carmeliet et al., 1996; Ferrara et al., 1996). Mice carrying disrupted VEGFR-1 and VEGFR-2 genes also experience developmental defects and early embryonic lethality (Fong et al., 1995).

During estrous cycle and pregnancy in pigs, the uterine VEGF-receptor system is expressed in glandular- and luminal epithelia, arteries, arterioles, and myometrial smooth muscle cells (Winther et al., 1999). Maternal blood flow increases on Days 12 and 13 of pregnancy when there are also significant increases in expression of *VEGF*, *VEGFR-1*, and *VEGFR-2* mRNAs in the porcine endometrium (Burghardt et al., 1997; Ford and Christenson, 1979; Geisert et al., 1982b; Geisert and Yelich, 1997; Keys and King, 1990; Leiser and Kaufmann, 1994; Welter et al., 2003; Wollenhaupt et al., 2004). These increases coincide temporally with the dramatic elongation of spherical and tubular blastocysts to the filamentous stage and secretion of estrogens by the trophoblast. Also, early embryonic transcripts for VEGF are detectable from the oocyte to the blastocyst stages and both VEGF receptors are expressed from the 1-cell to the blastocyst stages. The fact that expression of the VEGF-receptor system is detectable throughout the peri-implantation period in trophoblast cells, which are not endothelial cells and in which no angiogenesis occurs, raises the possibility that VEGF has non-angiogenetic roles in the trophectoderm. But, most studies have focused primarily on angiogenetic effects of the endometrial

VEGF-receptor system during the peri-implantation period of pregnancy.

In this study, it was determined whether VEGF, originally identified as an angiogenic factor, also plays a novel role in peri-implantation events by modulating development and function of trophoblast cells. This study tested the hypothesis that during early pregnancy in pigs, the VEGF-receptor system of both the endometrium and conceptus is critical for growth and development of porcine trophoblast (pTr) cells during the peri-implantation period of pregnancy. Therefore, 1) temporal and cell-specific expression of endometrial VEGF and its two receptors, VEGFR-1 and VEGFR-2, during the estrous cycle and early pregnancy in pigs; 2) stimulatory effects of VEGF on PI3K-AKT1 and MAPK cascades in pTr cells; and 3) functional effects of VEGF on proliferation and migration of pTr cells were determined.

3. Materials and Methods

Experimental Animals and Animal Care

Sexually mature gilts of similar age, weight, and genetic background were observed daily for estrus (Day 0) and exhibited at least two estrous cycles of normal duration (18-21 days) before being used in this study. All experimental and surgical procedures were in compliance with the Guide for Care and Use of Agricultural Animals in Teaching and Research and approved by the Institutional Animal Care and Use Committee of Texas A&M University.

Experimental Design and Tissue Collection

Gilts were assigned randomly to either cyclic or pregnant status. Those in the pregnant group were bred when detected in estrus and 12 and 24 h later. Gilts were ovariectomized on either Day 9, 12, or 15 of the estrous cycle or on Day 9, 10, 12, 13, 14, 15 or 20 of pregnancy (n = 3-4 pigs per day per status). For confirmation of pregnancy prior to implantation, the lumen of each uterine horn was flushed with 20 ml of physiological saline and examined for the presence of morphologically normal conceptuses. Uteri from cyclic and pregnant gilts were processed to obtain several sections (~0.5 cm) from the entire uterine wall in the middle of each uterine horn, fix the tissue in fresh 4% paraformaldehyde in PBS (pH 7.2) and the tissue embedded in Paraplast-Plus (Oxford Laboratory, St. Louis, MO, USA).

Cell culture

Mononuclear porcine trophoblast (pTr) cells from Day 12 pig conceptuses were cultured and used in the present *in vitro* studies as described previously (Ka et al., 2001). For experiments, monolayer cultures of pTr cells were grown in culture medium to 80% confluence in 100-mm tissue culture dishes. Cells were serum starved for 24 h, and then treated with recombinant human VEGF (R&D Systems, Inc., Minneapolis, MN, USA) for 0, 5, 15, 30, 60 or 120 min. Based on preliminary dose-response experiments, 20 ng/ml (1.05 nM) VEGF was selected for use in all experiments in the present study. This design was replicated in three independent experiments.

RNA Isolation

Total cellular RNA was isolated from endometrium of cyclic and pregnant gilts using Trizol reagent (Invitrogen, Carlsbad, CA) and purified using an RNeasy Mini Kit (Qiagen, Hilden, Germany) according to the manufacturer's recommendations. The quantity and quality of total RNA was determined by spectrometry and denaturing agarose gel electrophoresis, respectively.

Cloning of partial cDNA for porcine VEGF, VEGFR-1 and VEGFR-2

Complementary DNA was synthesized using AccuPower® RT PreMix

(Bioneer, Daejeon, Korea). Partial cDNAs for porcine *VEGF*, *VEGFR-1* and *VEGFR-2* mRNAs were amplified using specific primers based on data for porcine *VEGF* (GenBank accession no. NM_214084.1; forward, 5'- CGA AGT GGT GAA GTT CAT GG -3'; reverse, 5'- TCA CAT CTG CAA GTA CGT TCG -3'), *VEGFR-1* mRNA (GenBank accession no. AY566244.1; forward, 5'- ACA AAG ACC CCA AAG AAA GG -3'; reverse, 5'- GGG AGT GGA GTA CGT GAA GC -3') and *VEGFR-2* mRNA (GenBank accession no. AJ245446.1; forward, 5'- CAG AGT GGC TCT GAG GAA CG -3'; reverse, 5'- CTG GAT ACC TCG CAC AAA GG -3'). The partial cDNAs for *VEGF*, *VEGFR-1* and *VEGFR-2* were gel-extracted and cloned into the TOPO TA cloning vector (Invitrogen, Carlsbad, CA, USA).

Quantitative PCR Analysis

Specific primers for porcine *VEGF* (forward: 5'- CTA CCT CCA CCA TGC CAA GT -3'; reverse: 5'- ACA CAG GAC GGC TTG AAG AT -3'), *VEGFR-1* (forward: 5'- GAA AGG CCA AGA TTT GTG GA -3'; reverse: 5'- GGG AGT GGA GTA CGT GAA GC -3') and *VEGFR-2* (forward: 5'- TGA TCG GAA ATG ACA CTG GA -3'; reverse: 5'- TTG AAA TGG TCC CCA GAC AT -3') were designed from sequences in the GenBank data base using Primer 3 (ver.4.0.0). All primers were synthesized by Bioneer Inc. (Daejeon, Korea). Gene expression levels were measured using SYBR[®] Green (Sigma, St. Louis, MO, USA) and a StepOnePlus[™] Real-Time PCR System (Applied Biosystems, Foster City, CA, USA). The PCR conditions were 95°C for 3 min, followed by 40 cycles at 95°C for 20 sec,

64°C for 40 sec, and 72°C for 1 min using a melting curve program (increasing the temperature from 55°C to 95°C at 0.5°C per 10 sec) and continuous fluorescence measurements. Sequence-specific products were identified by generating a melting curve in which the C_T value represented the cycle number at which a fluorescent signal was significantly greater than background, and relative gene expression was quantified using the $2^{-\Delta\Delta C_T}$ method. The glyceraldehyde-3-phosphate dehydrogenase (*GAPDH*) gene was used as the endogenous control to standardize the amount of RNA in each reaction.

In situ Hybridization Analysis

After verification of the sequences, the plasmids containing gene sequences were amplified with T7- and SP6-specific primers (T7:5'-TGT AAT ACG ACT CAC TAT AGG G-3'; SP6:5'-CTA TTT AGG TGA CAC TAT AGA AT-3') then digoxigenin (DIG)-labeled RNA probes were transcribed using a DIG RNA labeling kit (Roche, Indianapolis, IN, USA). The tissue sections were deparaffinized, rehydrated, and treated with 1% Triton X-100 in PBS for 20 min and washed two times in DEPC-treated PBS. After post-fixation in 4% paraformaldehyde, sections were incubated in a prehybridization mixture containing 50% formamide and 4X standard saline citrate (SSC) for at least 10 min at room temperature. After hybridization and blocking steps, the sections were incubated overnight with sheep anti-DIG antibody conjugated to alkaline phosphatase (Roche, Indianapolis, IN, USA). The signal was visualized by exposure to a solution containing 0.4 mM 5-bromo-4-

chloro-3-indolyl phosphate, 0.4 mM nitroblue tetrazolium, and 2 mM levamisole (Sigma, St. Louis, MO, USA).

Western Blot Analyses

Concentrations of protein in whole-cell extracts were determined using the Bradford protein assay (Bio-Rad, Hercules, CA, USA) with bovine serum albumin (BSA) as the standard. Proteins were denatured, separated using SDS-PAGE and transferred to nitrocellulose. Blots were developed using enhanced chemiluminescence detection (SuperSignal West Pico; Pierce, Rockford, IL, USA) and quantified by measuring the intensity of light emitted from correctly sized bands under ultraviolet light using a ChemiDoc EQ system and Quantity One software (Bio-Rad, Hercules, CA, USA). Immunoreactive proteins were detected using rabbit anti-mouse polyclonal antibodies against p-AKT1 and AKT1 at a 1:1000 dilution and 10% SDS/PAGE gel; rabbit anti-human polyclonal antibodies against p-RPS6 and rabbit anti-human monoclonal antibodies against RPS6 at a 1:1000 dilution and 10% SDS/PAGE gel; rabbit anti-human polyclonal antibodies against p-p70RSK and p70 RSK at a 1:1000 dilution and 10% SDS/PAGE gel; rabbit anti-mouse polyclonal antibodies against p-4EBP1 and rabbit anti-human polyclonal antibodies against 4EBP1 at a 1:1000 dilution and 12% SDS/PAGE gel; rabbit anti-human polyclonal p-ERK1/2 MAPK and rabbit anti-human monoclonal ERK1/2 MAPK IgG, each at a 1:1000 dilution, and 12% SDS/PAGE gel. As a loading control, mouse anti- α -tubulin (TUBA) was used to normalize results from detection of proteins by western blotting.

All antibodies were from Cell Signaling Technology (Danvers, MA, USA). Multiple exposures of each western blot were performed to ensure linearity of chemiluminescent signals.

Proliferation assay

Proliferation assays were conducted using Cell Proliferation ELISA, BrdU kit (Roche, Indianapolis, IN, USA) according to the manufacturer's recommendations. Briefly, pTr cells were seeded in a 96-well microplate (tissue culture grade, flat bottom), and then incubated for 24 h in serum-free DMEM/F-12. Cells were then treated with recombinant VEGF protein and various treatments in a final volume of 100 μ l/well. After 24 h of incubation, 10 μ M BrdU was added to the cell culture and the cells were reincubated for an additional 24 h at 37°C. After labeling of cells with BrdU, the fixed cells were incubated with anti-BrdU-POD working solution for 90 min. The anti-BrdU-POD binds to the BrdU incorporated in newly synthesized cellular DNA and these immune complexes were detected by the reaction to TMB substrate solution. The absorbance values of the reaction product were quantified by measuring the absorbance at 370 nm using an ELISA reader (Bio-Rad, Seoul, Korea).

Migration assay

The pTr cells (50,000 cells per 100 μ l serum and insulin-free DMEM) were seeded on 8- μ m pore Transwell inserts (Corning Costar no. 3422; Corning, Inc.,

Corning, NY, USA) and treatments added to each well (n = 3 wells per treatment). After 12 h, cells on the upper side of the inserts were removed with a cotton swab. For evaluation of cells that migrated onto the lower surface, inserts were fixed in 50% ethanol for 5 min. The transwell membranes were then removed, placed on a glass slide with the side containing cells facing up, overlaid with prolong antifade mounting reagent with 4',6-diamidino-2-phenylindole, and overlaid with a coverslip (Invitrogen-Molecular Probes, Eugene, OR, USA). Migrated cells were counted systematically in five non-overlapping locations, which covered approximately 70% of the insert membrane growth area, using a Zeiss confocal microscope LSM710 (Carl Zeiss, Jena, German) fitted with a digital microscope camera AxioCam using Zen 2009 software. The entire experiment was repeated at least three times.

Reagents

Rabbit anti-human polyclonal antibodies against p-ERK1/2 MAPK (catalog number: 9101) and p-RPS6 (catalog number: 2211), p-p70RSK (catalog number: 9204), p70RSK (catalog number: 9202), 4EBP1 (catalog number: 9452), and rabbit anti-human monoclonal antibody against RPS6 (catalog number: 2217) and ERK1/2 MAPK (catalog number: 4695), and rabbit anti-mouse polyclonal antibodies against p-AKT1 (catalog number: 9271), AKT1 (catalog number: 9272), p-4EBP1 (catalog number: 9451) were purchased from Cell Signaling Technology, Inc. (Danvers, MA, USA). Inhibitors for PI3K (LY294002, catalog number: 9901), MEK1/2 (U0126, catalog number: 9903), P38 MAPK (SB203580, catalog number:

5633) and mTOR (Rapamycin, catalog number: 5633) were also obtained from Cell Signaling Technology, Inc. (Danvers, MA, USA).

Statistical Analyses

All quantitative data were subjected to least squares ANOVA using the General Linear Model procedures of the Statistical Analysis System (SAS Institute Inc., Cary, NC, USA). Western blot data were corrected for differences in sample loading using the TUBA data as a covariate. All tests of significance were performed using the appropriate error terms according to the expectation of the mean squares for error. A *P* value less than or equal to 0.05 was considered significant. Data are presented as least-square means (LSMs) with SEs.

4. Results

Changes in expression of endometrial VEGF, VEGFR-1 and VEGFR-2 mRNAs and their localization in porcine endometria during the estrous cycle and pregnancy

Uterine *VEGF* mRNA levels in cyclic and pregnant pigs were determined by quantitative RT-PCR analysis (Figure 5-1A). Steady-state levels of *VEGF* mRNA in the uterus were not affected by day of the estrous cycle (day, $P > 0.05$), but expression of *VEGF* mRNA on Day 12 and Day 15 of pregnancy was higher ($P < 0.001$ or $P < 0.01$) than on Day 12 and Day 15 of the estrous cycle. *In situ* hybridization analysis was used to detect cell-specific localization of *VEGF* mRNAs in pig endometria during the estrous cycle and pregnancy (Figure 5-1B). In cyclic gilts, *VEGF* mRNA was localized primarily to uterine luminal (LE) and glandular (GE) epithelial cells, and there was no significant difference in abundance of *VEGF* mRNA except for strong expression of endometrial *VEGF* mRNA in uterine GE on Day 9 of estrous cycle. Similarly, endometrial *VEGF* mRNA was localized primarily to uterine LE, GE and stratum compactum stroma during pregnancy, and expression of *VEGF* mRNA in LE and stratum compactum stroma tended to increase between Days 9 and 13 of pregnancy. As shown in Figure 5-2A, no significant differences were found in *VEGFR-1* and *VEGFR-2* transcripts due to day of the estrous cycle (day, $P > 0.05$), but *VEGFR-1* mRNA levels gradually increased 7.6-fold ($P < 0.001$) from Day 9 of pregnancy to Day 14 of pregnancy and, then declined to levels similar to Day 15 of estrous cycle on Day 20 of pregnancy (Figure 5-2A). *VEGFR-2* mRNA also increased

5.6-fold ($P < 0.001$) from Day 9 to Day 14 of pregnancy, and then decreased slightly on Day 20 of pregnancy, but remained higher than those on the same days of the estrous cycle (Figure 5-2B). *In situ* hybridization analysis was used to detect cell-specific localization of *VEGFR-1* and *VEGFR-2* mRNAs in pig endometria during the estrous cycle and pregnancy (Figure 5-2C and 5-2D). In cyclic gilts, there was low expression of *VEGFR-1* mRNA in uterine LE and GE. In pregnant gilts, *VEGFR-1* mRNA expression tended to increase in LE and scattered cells in stratum compactum stroma between Days 9 and 12, and on Days 12 and 13 of pregnancy, *VEGFR-1* mRNA was also detected in conceptus trophoctoderm, and relatively low levels of *VEGFR-1* mRNA were detected in uterine LE, GE and stromal cells on Day 20 of pregnancy. *VEGFR-2* mRNA expression tend to increase in uterine LE, GE and stratum compactum stroma between Day 9 and Day 12 of estrous cycle. In pregnant gilts, there was strong expression of *VEGFR-2* mRNA in uterine LE, GE, endothelial blood vessels and scattered cells in stratum compactum stroma. On Days 13 and 14 of pregnancy, *VEGFR-2* mRNA was also detectable in conceptus trophoctoderm. Taken together, these results demonstrated that *VEGF* and *VEGF receptors* are expressed abundantly in uterine LE, GE, and stratum compactum stroma, as well as conceptus trophoctoderm during the peri-implantation period of pregnancy in pigs.

Effect of VEGF on PI3K-AKT1 and MAPK cell signaling and on proliferation and migration of porcine trophoctoderm (pTr) cells

VEGF stimulated phosphorylation of AKT1 and ERK1/2 in pTr cells in a

dose-dependent manner (Figure 5-3A). Under the same specific culture conditions, dose-dependent effects of VEGF (0, 0.1, 1, 20, 100 ng/ml) on proliferation and migration of pTr cells were measured (Figure 5-3B and 5-3C). At 20 ng/ml or 100 ng/ml, VEGF increased pTr cell proliferation by approximately 148% and 149% ($P < 0.05$), respectively. Similarly, VEGF stimulated migration of pTr cells approximately 219% and 225% ($P < 0.01$) at 20 ng/ml and 100 ng/ml, respectively. Based on those results, VEGF was used at 20 ng/ml in experiments to determine its effects on cell signaling pathways. VEGF stimulated a rapid 2.8-fold and 4.1-fold ($P < 0.01$) increase in the abundance of phosphorylated AKT1 (p-AKT1) and phosphorylated ERK1/2 MAPK (p-ERK1/2 MAPK), respectively, within 5 min after treatment, and those levels of phosphorylation were maintained to 15 min (Figure 5-3D and 5-3E). VEGF also increased the abundance of phosphorylated p70RSK (p-p70RSK), phosphorylated RPS6 (p-RPS6) and phosphorylated 4EBP1 (p-4EBP1) in a time-dependent manner, reaching 5.4-fold, 8.4-fold and 3.3-fold ($P < 0.001$) respectively, at 30 min post-treatment, and then gradually decreased through 120 min, but remained higher than basal levels (Figure 5-3F-H).

Activation of PI3K-AKT1 and ERK1/2 MAPK signaling pathways in porcine trophoderm cells in response to VEGF

Effects of VEGF on PI3K-AKT1 and MAPK cell signal transduction in pTr cells were investigated using pharmacological inhibitors of PI3K (20 μ M LY294002) and ERK1/2 MAPK activity (20 μ M U0126). Serum starved pTr cells

were incubated with either LY294002 (20 μ M) or U0126 (20 μ M) for 1 h prior to treatment with VEGF (20 ng/ml). VEGF-induced phosphorylation of AKT1 was completely inhibited by the PI3K inhibitor ($P < 0.001$), while U0126 did not affect the abundance of VEGF-induced p-AKT1 protein ($P > 0.05$) (Figure 5-4A). VEGF-induced increases in phospho-ERK1/2 were blocked by both U0126 and LY294002 ($P < 0.001$) (Figure 5-4B). These results suggest that VEGF induces activation of both PI3K-AKT1 and ERK1/2 MAPK cell signaling pathways in pTr cells, and that ERK1/2 MAPK is a down-stream target of PI3K in the regulation of VEGF-induced cell signaling.

VEGF-induced proliferation of pTr cells through various signal transduction cascades

To confirm whether PI3K-AKT1 and ERK1/2 MAPK signal transduction pathways are involved in effects of VEGF on proliferation of pTr cells, cell proliferation assays were conducted in the presence or absence of VEGF (20 ng/ml), U0126 or LY294002. VEGF increased pTr cell numbers by approximately 134% ($P < 0.01$; Figure 5-5). However, pretreatment with U0126 or LY294002 plus VEGF reduced pTr cell numbers ($P < 0.001$) as compared to VEGF treatment alone. To examine involvement of other intracellular messengers, pharmacological inhibitors of P38 MAPK (SB203580) and FRAP/mTOR activity (rapamycin) were used. Interestingly, both of those inhibitors also blocked effects of VEGF on proliferation of pTr cells ($P < 0.001$). These results suggest that activation of PI3K-AKT1-p70RSK

and ERK1/2 or P38 MAPK signaling pathways play an important role in stimulation of pTr cell proliferation in response to VEGF from endometrial and/or conceptus tissues.

VEGF-induced migration of pTr cells through various signal transduction cascades

Using transwell plates, functional effects of VEGF on pTr cell migration were investigated. Treatment of pTr cells with VEGF alone stimulated cell migration approximately 201% ($P < 0.01$), but SB203580, U0126, rapamycin and LY294002 inhibited the stimulatory effects of VEGF on pTr cell migration to 126-, 81-, 146-, and 130%, respectively ($P < 0.001$ or $P < 0.01$; Figure 5-6). In the absence of VEGF, treatment of pTr cells with the inhibitors only had no effect on pTr cell migration. Taken together, these results indicate that VEGF from endometria and/or conceptus tissues acts in a paracrine or autocrine manner to stimulate pTr cell migration via activation of PI3K-AKT1-p70RSK and ERK1/2 or P38 MAPK signaling pathways.

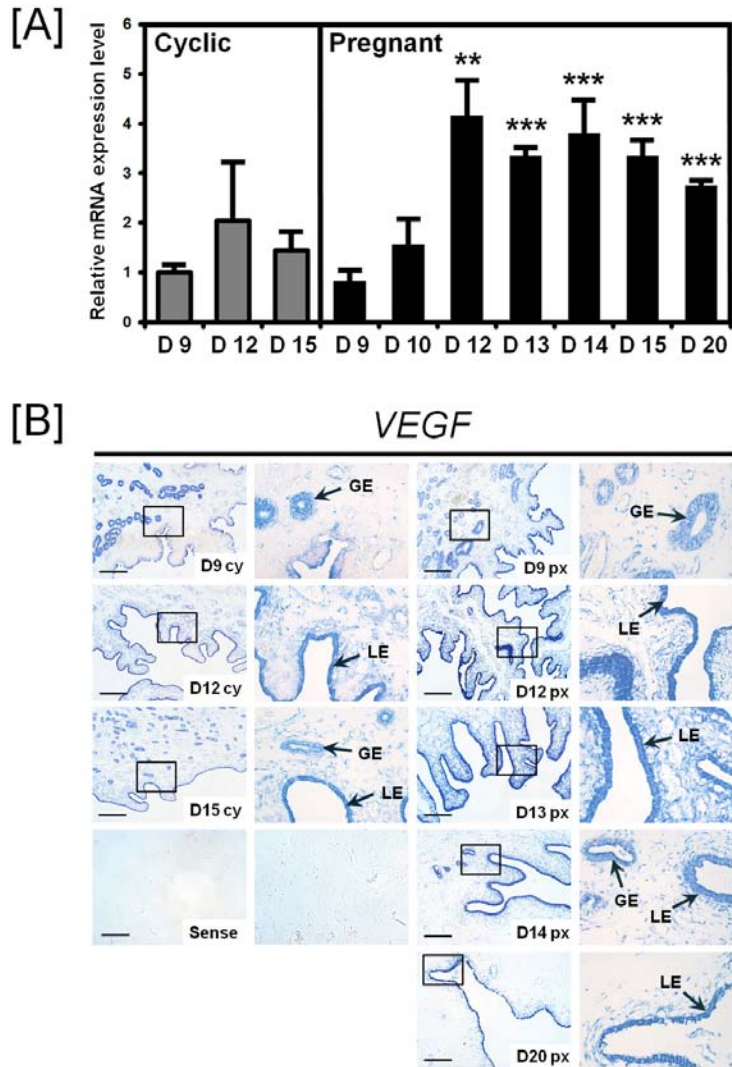
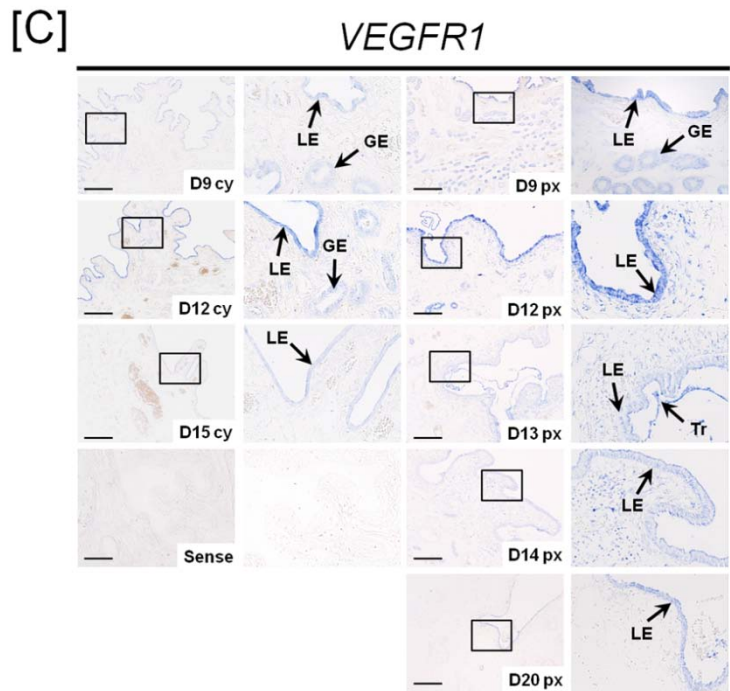
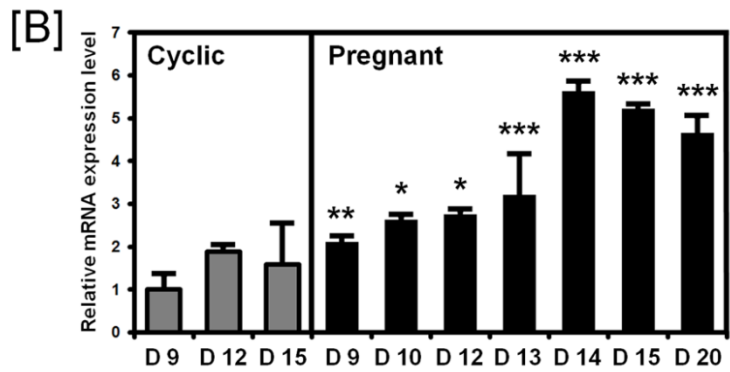
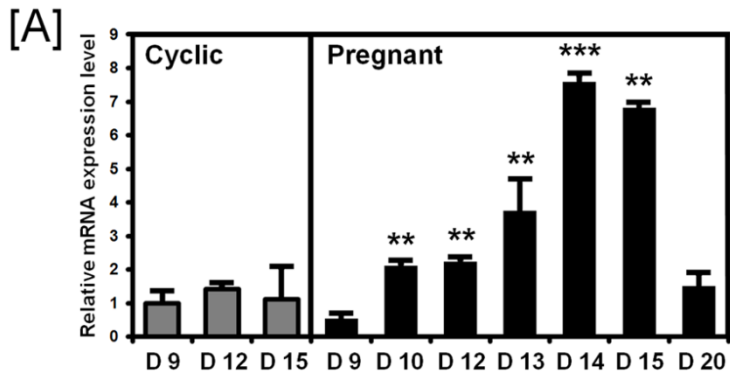


Figure 5-1. Relative quantification and localization of *VEGF* mRNAs in endometria of gilts during the estrous cycle and pregnancy by quantitative RT-PCR and *in situ* hybridization analyses. [A] Expression of *VEGF* mRNAs in endometria from cyclic and pregnant gilts. *VEGF* mRNA levels were not affected by day of the estrous cycle, but there were effects of day of pregnancy on expression of

VEGF mRNA (day, $P < 0.001$ or 0.01). The asterisks denote statistically significant differences ($***P < 0.001$ and $**P < 0.01$). [B] *In situ* hybridization analyses of *VEGF* mRNAs in the porcine uterus. Cross-sections of the uterus from Day 12 of pregnancy were hybridized with DIG-labeled sense porcine *VEGF* cRNA probes as a negative control. Legend: cy, estrous cycle; px, pregnancy; LE, luminal epithelium; GE, glandular epithelium. Scale bar represents 100 μm . Images were captured at 10X and 40 X objective magnifications.



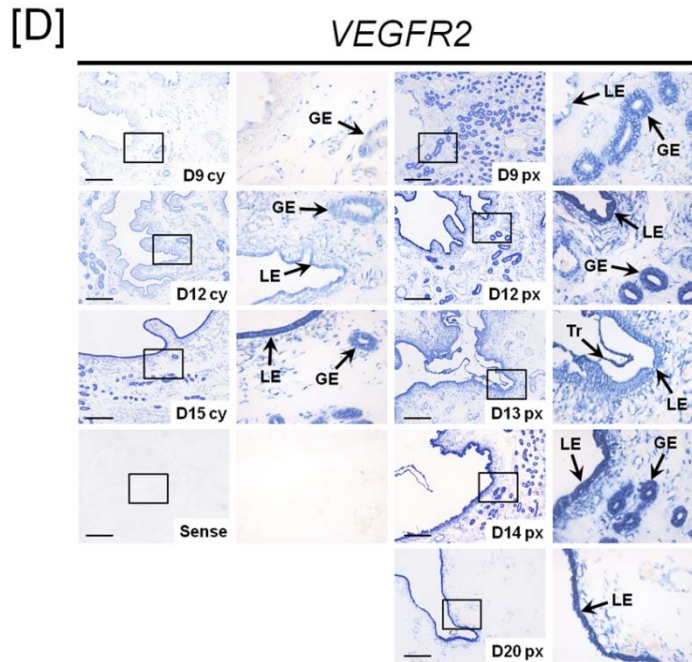


Figure 5-2. Relative quantification and localization of *VEGFR-1* and *VEGFR-2* mRNAs in endometria of gilts during the estrous cycle and pregnancy by quantitative RT-PCR and *in situ* hybridization analyses. [A] Expression of *VEGFR-1* mRNAs in endometria from cyclic and pregnant gilts. [B] Expression of *VEGFR-2* mRNAs in endometria from cyclic and pregnant gilts. The asterisks denote significant differences ($***P < 0.001$, $**P < 0.01$ and $*P < 0.05$). [C] *In situ* hybridization analyses of *VEGFR-1* mRNAs in the porcine uterus. [D] *In situ* hybridization analyses of *VEGFR-2* mRNAs in the porcine uterus. Cross-sections of uteri from Day 12 of pregnancy were hybridized with DIG-labeled sense porcine *VEGFR-1* or *VEGFR-2* cRNA probes as a negative control. Legend: cy, estrous cycle; px, pregnancy; LE, luminal epithelium; GE, glandular epithelium. Scale bar represents 100 μ m. Images were captured at 10X and 40 X objective magnifications.

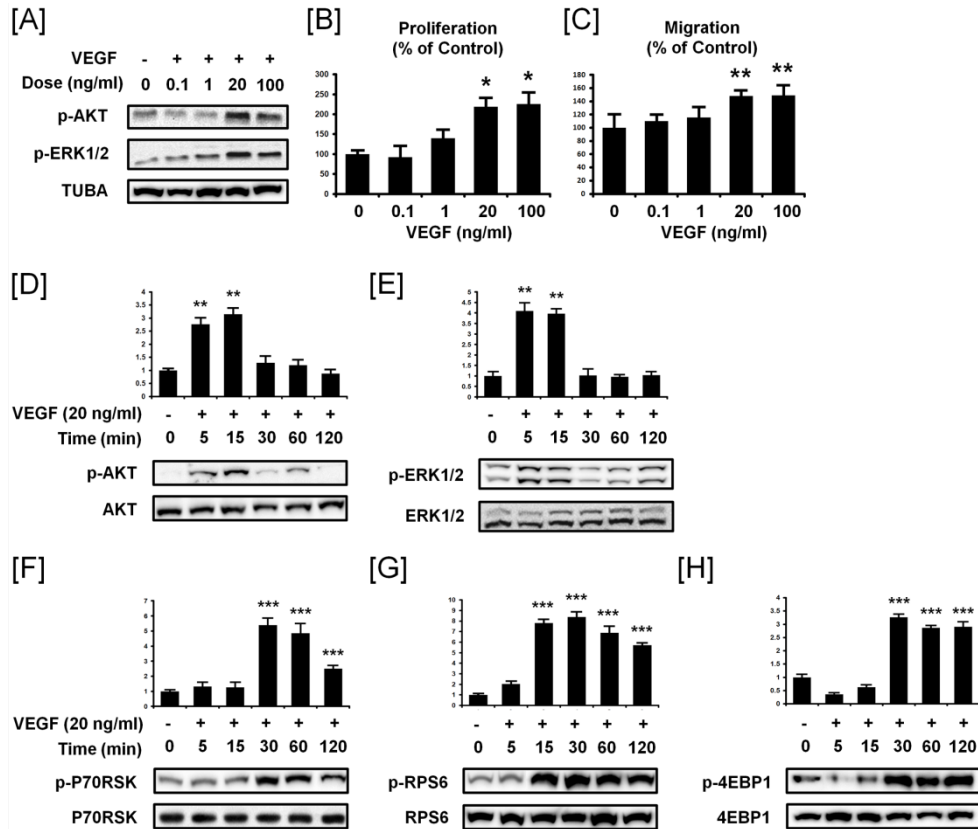


Figure 5-3. VEGF influences the abundance of phosphorylated AKT1, ERK1/2, P70RSK, RPS6 and 4EBP1 proteins and stimulates migration and proliferation of pTr cells. [A] Western blot analyses revealed dose-dependent effects of VEGF to increase the abundance of p-AKT1 and p-ERK1/2 proteins in pTr cells *in vitro*. Tubulin-alpha (TUBA) was the total protein control. [B] The effect of VEGF (0, 0.1, 1, 20 and 100 ng/ml) on pTr cell proliferation. [C] The effect of VEGF (0, 0.1, 1, 20 and 100 ng/ml) on pTr cell migration. [D] p-AKT1 and AKT1 were detected between 0 and 120 min after treatment of pTr cells with VEGF. [E] p-ERK1/2 and ERK1/2 were detected between 0 and 120 min in pTr cells treated with VEGF. [F] p-p70RSK and

p70RSK were detected between 0 and 120 min after treatment of pTr cells with VEGF. [G] p-RPS6 and RPS6 were detected between 0 and 120 min after treatment of pTr cells with VEGF. Blots were imaged to calculate the normalized values presented in the graph by measurements of abundance of phosphorylated proteins relative to total protein. The asterisks denote significant differences ($***P < 0.001$, $**P < 0.01$ and $*P < 0.05$).

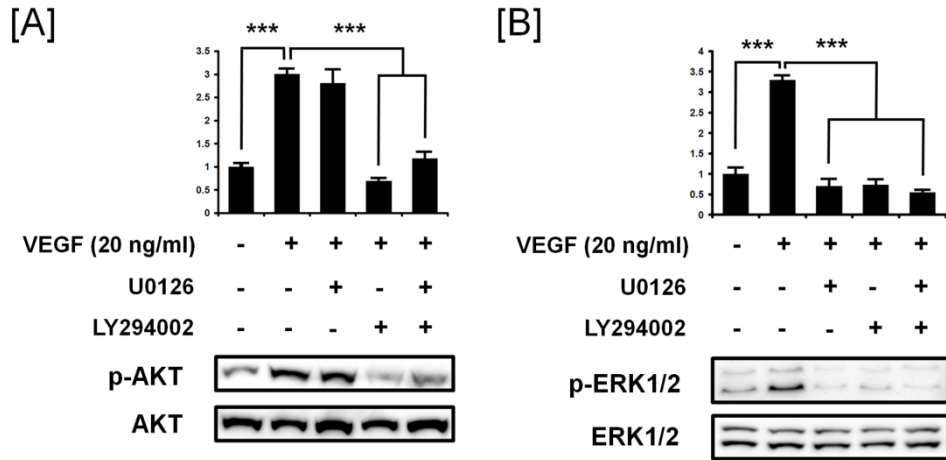


Figure 5-4. Inhibition of VEGF-induced AKT1 and ERK1/2 phosphorylation in pTr cells. [A] The effects of the PI3K inhibitor (LY294002) on VEGF-induced p-AKT1 and p-ERK1/2 proteins. [B] The effects of MAPK inhibitor (U0126) on VEGF-induced p-AKT1 and p-ERK1/2. Serum starved pTr cells were incubated with 20 μ M LY294002 or 20 μ M U0126 for 1 h and then stimulated with VEGF for 15 min. Blots were imaged to calculate the normalized values presented in the graph by measurements of levels phosphorylated proteins relative to total proteins. The asterisks denote significant differences (***) $P < 0.001$.

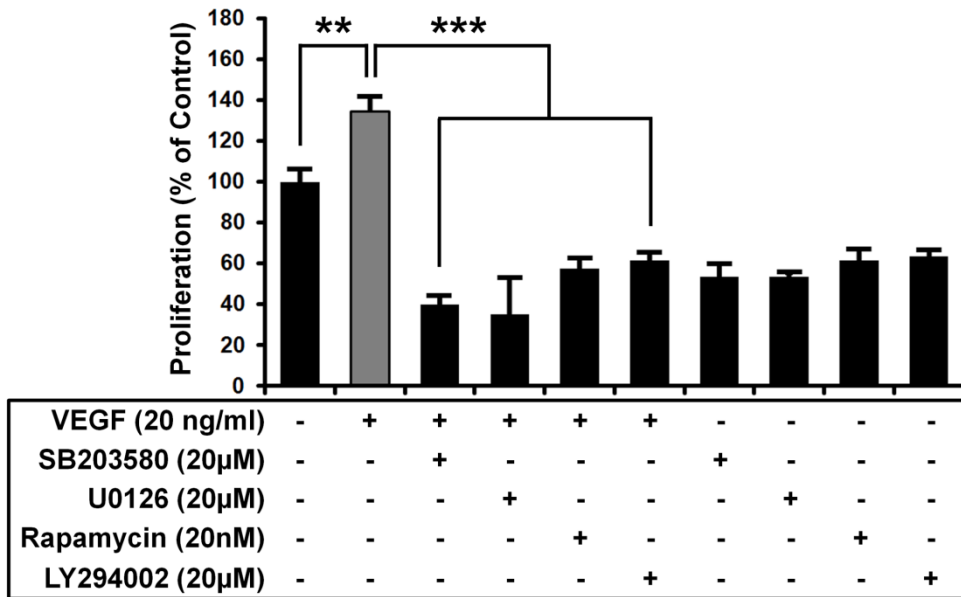


Figure 5-5. VEGF stimulates proliferation of pTr cells through various signal transduction cascades. The pTr cells seeded in a 96-well microplate were treated with recombinant VEGF (20 ng/ml), SB203580 (20 μM), U0126 (20 μM), Rapamycin (20 nM), LY294002 (20 μM), or their combination for 24 h in serum-free medium. After labeling cells with BrdU for 24 h, cell numbers were determined by measuring the absorbance values of the reaction product. Data are expressed as a percentage relative to non-treated control pTr cells (100%). VEGF stimulated ($P < 0.01$) pTr cell proliferation and the inhibitors blocked ($P < 0.001$) the effect of VEGF on cell proliferation. The asterisks denote an effect of VEGF treatment ($***P < 0.001$ and $**P < 0.01$).

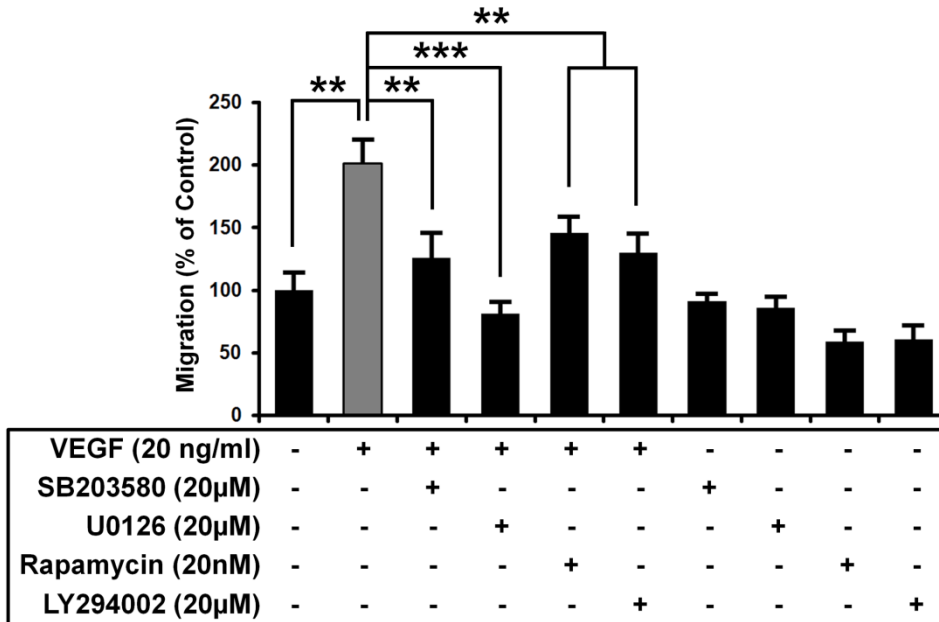


Figure 5-6. VEGF stimulates migration of pTr cells through various signal transduction cascades. The pTr cells were cultured in a transwell plate (n = 3 wells per treatment) and treated with recombinant VEGF (20 ng/ml), SB203580 (20 μM), U0126 (20 μM), Rapamycin (20 nM), LY294002 (20 μM), or their combination for 12 h in serum-free medium. Data are expressed at a percentage relative to non-treated control cells (100%). VEGF stimulated ($P < 0.01$) pTr cell migration and the inhibitors blocked ($P < 0.001$ or $P < 0.01$) the effect of VEGF on cell migration. The asterisks denote an effect of treatment with VEGF ($***P < 0.001$ and $**P < 0.01$).

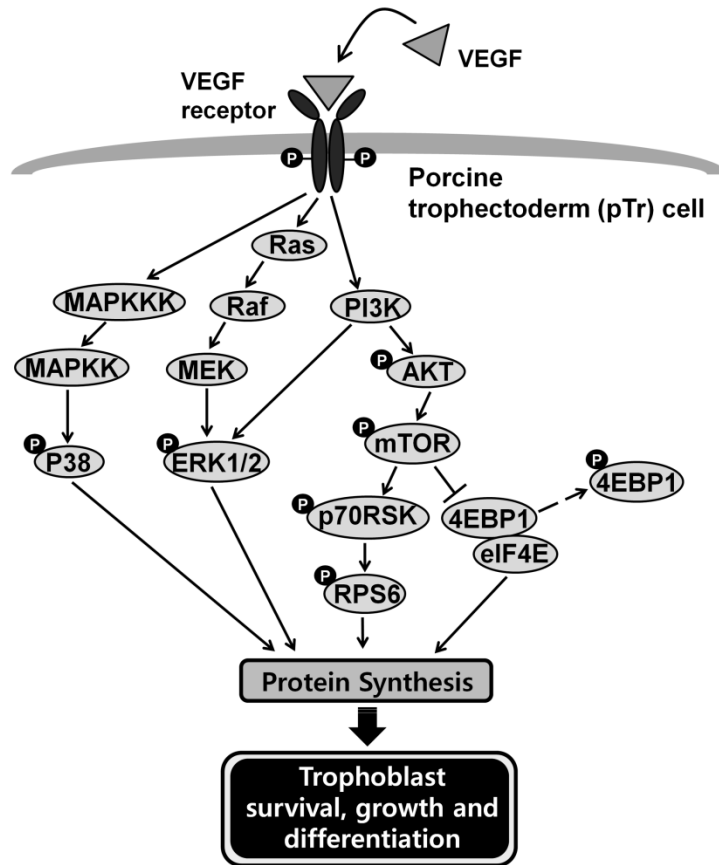


Figure 5-7. Schematic illustrating the current working hypothesis on VEGF-induced PI3K-AKT1 or ERK1/2 MAPK signal transduction cascades in pTr cells during the peri-implantation period. Endometrial- and/or trophoblastic VEGF induces phosphorylation of p70RSK-RPS6 and 4EBP1 via the PI3K-AKT1 cell signaling pathway. ERK1/2 and P38 MAPK signal transduction cascades also act in parallel to transduce VEGF signals. These VEGF-activated signaling pathways are likely involved in protein synthesis of growth- and/or development-related genes affecting proliferation and migration of porcine trophoblast.

5. Discussion

The results of this study revealed stimulatory effects of endometrial- and/or conceptus-derived VEGF on proliferation and migration of pTr cells via the PI3K-AKT1-mTOR and MAPK signaling pathways (see Figure 5-7). The results provide evidence for novel roles of VEGF in regulating development of porcine trophoctoderm during the peri-implantation period of pregnancy and indicate regulatory cell signaling mechanisms. Successful implantation requires a synchronized conceptus-maternal dialogue via locally produced mediators such as growth factor and cytokines. Deficiencies in those factors can result in implantation failure, defective placentation and developmental abnormalities. Previous studies with the uterine gland knockout sheep model emphasize the importance of secretions from uterine glands for implantation and placentation (Allison Gray et al., 2000; Gray et al., 2001b; Spencer and Bazer, 2004b). VEGF in the uterine cavity is likely to be an important regulator of implantation (Smith et al., 2007). In pigs, early pregnancy is characterized by rapid morphological changes and development of conceptus and endometrium (Leiser and Kaufmann, 1994). Morphological changes of the uterus include VEGF-mediated development and remodeling of endometrial vasculature, and increased uterine vascular permeability, which is necessary for successful growth of the conceptus and establishment of pregnancy (Dantzer and Leiser, 1994; Keys and King, 1988; Keys et al., 1986; Laforest and King, 1992). VEGF from the conceptus could be important in implantation, possibly by inducing implantation site specific angiogenesis (Krussel et al., 2000).

In addition to the known angiogenetic effects of VEGF, circumstantial evidence suggests novel mechanisms by which VEGF regulate early embryo during peri-implantation. Recently, Hannan *et al* demonstrated that concentrations of VEGF in uterine fluids were less in infertile women as compared with fertile women and that addition of recombinant VEGF to cell culture conditions stimulated outgrowth of mouse blastocyst and adhesion of human endometrial epithelial cells (Hannan et al., 2011). Though *in vitro* studies with human extravillous trophoblast (EVT) have provided contrary results, VEGF may influence proliferation or migration of extravillous trophoblast cells (Athanasopoulos et al., 1998; Clark et al., 1996; Lash et al., 1999; Shiraishi et al., 1996; Torry and Torry, 1997). Additionally, VEGF supplementation in the *in vitro* culture medium is known to improve the rate of blastocyst formation and to increase blastocyst cell number (Biswas et al., 2011; Einspanier et al., 2002). But knowledge on the role of the VEGF-receptor system and, especially their regulatory mechanisms at the maternal-conceptus interface is very limited in pigs. During the peri-implantation period, porcine embryonic transcripts for the VEGF-receptor system have been detected from the 1-cell to the blastocyst stage (Biswas et al., 2011). Since there is no angiogenesis occurring in the peri-implantation embryos, these findings suggest that VEGF may induce novel functions other than angiogenetic responses in blastocysts and conceptuses during the peri-implantation period.

VEGF is known to exist in the uterus of various mammals such as human, mouse, rat, ewe, rabbit and pig (Charnock-Jones et al., 1993; Cullinan-Bove and Koos,

1993; Greb et al., 1997; Reynolds et al., 1998; Winther et al., 1999). And, VEGF is secreted by a wide range of tissues and cells including glandular epithelia, luminal epithelia, stroma, glial, tumor, smooth muscle cells, as well as macrophages, keratinocytes and cells of ovarian cysts (Rousseau et al., 2000). In the present study, temporal- and cell specific expression of the VEGF-receptor system in the porcine endometrium on different stages of the estrous cycle and early pregnancy are demonstrated. Transcripts for VEGF and its two receptors were detectable in LE, GE, scattered cells within the stroma and vessel walls of cyclic or pregnant endometrium. And our results also show up-regulation of endometrial transcripts for the VEGF-receptor system during the peri-implantation period, when proliferation and migration of trophoblast cells allow for rapid elongation of the conceptus. Our results support previous findings of increased endometrial vessel permeability and blood flow between Days 12 and 13 of pregnancy (Keys et al., 1986). Spatial and temporal expression of the VEGF-receptor system is regulated by ovarian steroids such as progesterone and estrogen both *in vitro* and *in vivo* (Classen-Linke et al., 2000; Cullinan-Bove and Koos, 1993; Greb et al., 1997; Shifren et al., 1996; Sugino et al., 2002). For example, previous research with sheep found that estrogen stimulates production of VEGF by vascular smooth muscle cells (Reynolds et al., 1998). In addition, interleukin (IL)-1 α , IL-6 and several growth factors including insulin-like growth factor (IGF), fibroblast growth factor (FGF), transforming growth factors (TGFs), fibroblast growth factor 7 (FGF7) and platelet-derived growth factor (PDGF) induce VEGF expression (Stavri et al., 1995). In the present study, intense expression of the VEGF-receptor system in porcine trophoblast between Days 12 and 14 of

pregnancy were observed. Our results indicate that endometrial- and/or trophoderm receptors of pigs play essential roles in peri-implantation events, and that VEGF acts in autocrine and paracrine manner to stimulate growth and development of the conceptus and to prepare the uterus for implantation.

Although the importance of VEGF system in implantation events have been documented, the regulatory mechanisms of VEGF action in the porcine conceptus during the peri-implantation period are not well understood. The PI3K-AKT1 cell signaling pathway has emerged as a central component that controls cell growth and proliferation through transmitting signals arising from various mitogens and nutrients (Levine et al., 2006; Toyofuku et al., 2006; Wen et al., 2005). In the present study, VEGF stimulation induced rapid activation of AKT1 in pTr cells. The 70kDa ribosomal S6 kinase (p70RSK), one of the common downstream targets of PI3K-AKT1 and mTOR pathways, was also activated by VEGF stimulation in pTr cells. Various mitogens and growth factors activate p70RSK protein and then the activated p70RSK transduces the signal via phosphorylation of downstream targets (Avruch et al., 2001). The primary downstream target of p70RSK is the 40S ribosomal protein S6 (RPS6), which is a major regulatory component of the protein synthetic machinery in mammalian cells (Dufner and Thomas, 1999; Peterson and Schreiber, 1998). The increase in translation of specific transcripts is a typical response to mitogen stimulation. In this study, VEGF also induced increases in phosphorylation of RPS6 proteins in pTr cells. And, VEGF activated phosphorylation of eIF4-binding proteins (4EBP1) by mTOR. Activation of the mTOR leads to phosphorylation of

4EBP1, resulting in its dissociation from eIF4E which stimulates mRNA translation. Furthermore, as shown in Figure 5-5 and Figure 5-6, pharmacological inhibitors of both PI3K (LY294002) and mTOR (rapamycin) abolished VEGF-induced proliferation and migration of pTr cells, indicating a central role of these cell signaling pathways in these processes. Taken together, these results propose that VEGF induces activation of PI3K-AKT1-mTOR cell signaling pathway which ultimately stimulates protein synthesis required for proliferation and migration of pTr cells.

Results of the present study further demonstrated that the MAPK cascade is involved in VEGF-induced proliferation and migration of pTr cells. The MAPK pathway has been implicated in regulation of various cellular processes in response to diverse stimuli including growth factors in a number of model systems (Klemke et al., 1997; Seger and Krebs, 1995). Among subfamilies of MAPKs, ERK1/2 and P38 MAPK pathways have been widely studied and established as major cascades in differentiation processes, including embryonic and placental development (Fernandez-Serra et al., 2004b; Wang et al., 2004a). In the present study, VEGF induced a rapid increase in phosphorylation of ERK1/2 proteins in pTr cells. Also, as shown in Figure 5-5 and Figure 5-6, pharmacological inhibitors of both ERK1/2 MAPK (U0126) and P38 MAPK activity (SB203580) abolished VEGF-induced proliferation and migration of pTr cells. Taken together, these results indicate that VEGF influences porcine conceptus development by simultaneously stimulating both the PI3K-AKT1 and the MAPK cell signaling cascades during early pregnancy.

Given the involvement of both PI3K-AKT1 and ERK1/2 MAPK pathways in proliferation and migration of pTr cells, possible cross-talk between PI3K-AKT1 and ERK1/2 MAPK cascades were examined. In the present study, we found that MAPK inhibitor (U0126) inhibited effects of VEGF on phosphorylation of ERK1/2 proteins as well as VEGF-induced proliferation and migration of pTr cells, but there was no significant effect on VEGF-induced activation of AKT1. The PI3K inhibitor (LY294002) inhibited VEGF-stimulated phosphorylation of AKT1 proteins as well as VEGF-induced proliferation and migration of pTr cells; however, stimulatory effects of VEGF on phosphorylation of ERK1/2 were also abolished by LY294002. Taken together, these results suggest that the ERK1/2 MAPK cell signaling pathway is regulated by PI3K pathway that regulates proliferation and migration of pTr cells in response to VEGF.

In conclusion, present results propose that VEGF from endometria and/or conceptuses regulates proliferation and migration of porcine conceptuses in a paracrine and/or autocrine manner and that PI3K-AKT1-mTOR and MAPK signaling pathways are involved in VEGF-induced signal transduction during the peri-implantation period. Further, these VEGF-stimulated pathways appear to exhibit cross-talk and be involved in mRNA translation and protein synthesis processes in early porcine trophectoderm cells. Results of the present study provide new insights into the mechanisms by which VEGF regulates growth and development of the porcine conceptus during the peri-implantation period of pregnancy.

CHAPTER 6

**Proliferation-Stimulating Effect of Colony
Stimulating Factor 2 on Porcine
Trophectoderm Cells is Mediated by
Activation of Phosphatidylinositol 3-Kinase
and Extracellular Signal-Regulated Kinase
1/2 Mitogen-Activated Protein Kinase**

1. Abstract

Colony-stimulating factor 2 (CSF2), also known as granulocyte macrophage colony-stimulating factor, facilitates mammalian embryonic development and implantation. However, biological functions and regulatory mechanisms of action of porcine endometrial CSF2 in peri-implantation events have not been elucidated. The aim of present study was to determine changes in cellular activities induced by CSFs and to access CSF2-induced intracellular signaling in porcine primary trophoctoderm (pTr) cells. Differences in expression of *CSF2* mRNA in endometrium from cyclic and pregnant gilts were evaluated. Endometrial *CSF2* mRNA expression increases during the peri-implantation period, Days 10 to 14 of pregnancy, as compared to the estrous cycle. pTr cells obtained in Day 12 of pregnancy were cultured in the presence or absence of CSF2 (20 ng/ml) and LY294002 (20 μ M), U0126 (20 μ M), rapamycin (20 nM), and SB203580 (20 μ M). CSF2 in pTr cell culture medium at 20 ng/ml significantly induced phosphorylation of AKT1, ERK1/2, MTOR, p70RSK and RPS6 protein, but not STAT3 protein. Also, the PI3K specific inhibitor (LY294002) abolished CSF2-induced increases in p-ERK1/2 and p-MTOR proteins, as well as CSF2-induced phosphorylation of AKT1. Changes in proliferation and migration of pTr cells in response to CSF2 were examined in dose- and time-response experiments. CSF2 significantly stimulated pTr cell proliferation and, U0126, rapamycin and LY294002 blocked this CSF2-induced proliferation of pTr cells. Collectively, during the peri-implantation phase of pregnancy in pigs, endometrial CSF2 stimulates proliferation of trophoctoderm by activation of the PI3K-and

ERK1/2 MAPK-dependent MTOR signal transduction cascades.

2. Introduction

In pigs, the peri-implantation period is when there are major morphological changes in the blastocyst as it transitions morphologically from spherical, to tubular and filamentous forms as a conceptus (embryo and its extra-embryonic membranes) which involves various cellular activities including increases in proliferation, migration, and gene expression by trophoblast cells, as well as extra-embryonic endoderm (Bazer et al., 2012b). And it is essential for the trophoblast to attach and adhere to the uterine luminal epithelium (LE) in preparation for establishment of an epitheliochorial type of placenta (Burghardt et al., 1997; Geisert et al., 1982b; Geisert and Yelich, 1997; Keys and King, 1990; Leiser and Kaufmann, 1994). For this process, the conceptus is dependent upon an astonishing amount of secretions from uterine LE and glandular epithelium (GE), that is known collectively as histotroph, which includes hormones, enzymes, nutrients, growth factors, cytokines and other factors (Carson et al., 2000; Gray et al., 2001a; Gray et al., 2001c; Lim et al., 2002; Schafer-Somi, 2003; Spencer and Bazer, 2004b; Spencer et al., 2007b). Deficiencies in histotroph-mediated local communication at the maternal-conceptus interface leads to a majority of conceptus mortality and poor outcomes of pregnancy (Bazer, 1975; Stroband and Van der Lende, 1990).

One key factor, colony-stimulating factor 2 (CSF2), is a cytokine considered essential for the survival, proliferation and differentiation of blood cells such as granulocyte and macrophages (Gasson, 1991; Rapoport et al., 1992;

Robertson et al., 1994). However, CSF2 is also proving to be intimately associated with several diverse aspects of pregnancy physiology including cell-cell adhesion and implantation, and fetal-placental growth and differentiation (Robertson, 2007). Knockout of the CSF2 gene in mice can have subtle effects on early embryonic development and maintenance of pregnancy. For example, mice deficient in CSF2 have blastocysts with reduced numbers of cells which is linked to impaired placental structure and increased mortality of early conceptuses (Pollard, 1997; Robertson et al., 2001).

During the period corresponding to fertilization and the peri-implantation period of pregnancy, CSF2 is expressed primarily by uterine LE and GE in humans and other mammalian species including sheep, cow, and pigs (Crainie et al., 1990; de Moraes et al., 1999; Imakawa et al., 1993; Kanzaki et al., 1991; O'Leary et al., 2004; Robertson et al., 1992; Zhao and Chegini, 1994). Through targeting cells of the pre-implantation embryo, CSF2 promotes blastocyst formation and subsequent development, and increases the number of cells in blastocysts in human, mouse, rat, cow and sheep (Hardy and Spanos, 2002; Robertson, 2007; Sjoblom et al., 1999). Supplementation of *in vitro* culture medium with exogenous CSF2 has a beneficial effect on development of the pre-implantation blastocyst in various species (Hardy and Spanos, 2002; Robertson, 2007; Robertson et al., 2001).

The effects CSF2 are mediated via heterodimeric receptor complexes comprising an α - and a β subunit. The α -subunit of the CSF2 receptor, also known as

GM-R α , binds only CSF2 with low affinity, while the β -subunit is common for interleukin (IL)-5 and IL-3 receptors and converts the low affinity interaction to high affinity binding of ligand (Miyajima et al., 1993). Non-lymphohematopoietic cells such as endothelial cells and placental trophoblast cells exhibit biological responsiveness to CSF2 independent of the β -subunit of the CSF2 receptor (Baldwin, 1992; Baldwin et al., 1991). In women and mice, expression of GM-R α is readily detectable at the time of fertilization of the oocyte and subsequent stages of blastocyst development when it is expressed in both trophoctoderm and inner cell mass (Robertson et al., 2001; Sjoblom et al., 2002). The intracellular signaling mediated by the CSF2 receptor has not been studied in porcine conceptus trophoctoderm, but experiments using other cell types have described CSF2 cell signaling. The CSF2 receptor transduces signals mainly through the JAK-STAT, MAPK and PI3K dependent pathways to elicit changes in target cell gene expression (Hayashida et al., 1990; Martinez-Moczygemba and Huston, 2003).

There is evidence that CSF2 promotes proliferation of bovine trophoctoderm cells prior to and during the peri-implantation period of pregnancy (Michael et al., 2006). Also, during the peri-implantation period, time-dependent secretions from trophoctoderm, including estrogens, interferons and PGE₂, stimulate expression of CSF2 by the uterine epithelia (Michael et al., 2006; Robertson, 2007). Based on this evidence, porcine CSF2 appears promising as a factor that stimulates conceptus development. However, little is known about CSF2-mediated intracellular signaling pathways in porcine trophoctoderm cells and how it stimulates development

of the peri-implantation conceptus. Therefore, present study provides evidence that porcine CSF2 is a factor stimulatory to conceptus development during the peri-implantation period of pregnancy through activation of key cell signaling mechanisms. This study was performed to determine: 1) the temporal expression of *CSF* mRNA in porcine endometrium during the estrous cycle and early pregnancy; 2) effects of CSF2 on transactivation of intracellular signaling pathways in porcine trophoctoderm cells; and 3) functional effects of CSF2 on proliferation of pTr cells.

3. Materials and Methods

Experimental Animals and Animal Care

Sexually mature gilts of similar age, weight, and genetic background were observed daily for estrus (Day 0) and exhibited at least two estrous cycles of normal duration (18-21 days) before being used in this study. All experimental and surgical procedures were in compliance with the Guide for Care and Use of Agricultural Animals in Teaching and Research and approved by the Institutional Animal Care and Use Committee of Texas A&M University.

Experimental Design and Tissue Collection

Gilts were assigned randomly to either cyclic or pregnant status. Those in the pregnant group were bred when detected in estrus and 12 and 24 h later. Gilts were ovariectomized on either Day 9, 12, or 15 of the estrous cycle or on Day 9, 10, 12, 13, 14, 15 or 20 of pregnancy (n = 3-4 pigs per day per status). For confirmation of pregnancy prior to implantation, the lumen of each uterine horn was flushed with 20 ml of physiological saline and examined for the presence of morphologically normal conceptuses. Uteri from cyclic and pregnant gilts were processed to obtain several sections (~0.5 cm) from the entire uterine wall in the middle of each uterine horn. The tissue was fixed in fresh 4% paraformaldehyde in PBS (pH 7.2) and embed the tissue in Paraplast-Plus (Oxford Laboratory, St. Louis, MO, USA).

Cell culture

Mononuclear porcine trophectoderm (pTr) cells from Day 12 pig conceptuses were cultured and used in the present *in vitro* studies as described previously (Ka et al., 2001). For experiments, monolayer cultures of pTr cells were grown in culture medium to 80% confluence in 100-mm tissue culture dishes. Cells were serum starved for 24 h, and then treated with recombinant porcine CSF2 (20 ng/ml; R&D Systems, Inc., Minneapolis, MN, USA) for 0, 5, 15, 30, 60 or 120 min. Based on preliminary dose-response experiments, 20 ng/ml (1.38 nM) CSF2 was selected for use in all experiments in the present study. This design was replicated in three independent experiments.

RNA Isolation

Total cellular RNA was isolated from endometrium from cyclic and pregnant gilts using Trizol reagent (Invitrogen, Carlsbad, CA, USA) and purified using an RNeasy Mini Kit (Qiagen, Hilden, Germany) according to the manufacturer's recommendations. The quantity and quality of total RNA was determined by spectrometry and denaturing agarose gel electrophoresis, respectively.

Quantitative PCR Analysis

Specific primers for porcine *CSF2* (forward: 5'- TGT TGG CCA AGC ACT ATG AG -3'; reverse: 5'- CAA AGG GGA TGG TGA AAA GA -3') were designed from sequences in the GenBank data base using Primer 3 (ver.4.0.0). All primers were synthesized by Bioneer Inc. (Daejeon, Korea). Gene expression levels were measured using SYBR[®] Green (Sigma, St. Louis, MO, USA) and a StepOnePlus[™] Real-Time PCR System (Applied Biosystems, Foster City, CA, USA). The PCR conditions were 95°C for 3 min, followed by 40 cycles at 95°C for 20 sec, 64°C for 40 sec, and 72°C for 1 min using a melting curve program (increasing the temperature from 55°C to 95°C at 0.5°C per 10 sec) and continuous fluorescence measurements. Sequence-specific products were identified by generating a melting curve in which the C_T value represented the cycle number at which a fluorescent signal was significantly greater than background, and relative gene expression was quantified using the $2^{-\Delta\Delta C_T}$ method. The glyceraldehydes-3-phosphate dehydrogenase (*GAPDH*) gene was used as the endogenous control to standardize the amount of RNA in each reaction.

Western Blot Analyses

Concentrations of protein in whole-cell extracts were determined using the Bradford protein assay (Bio-Rad, Hercules, CA, USA) with bovine serum albumin (BSA) as the standard. Proteins were denatured, separated using SDS-PAGE and transferred to nitrocellulose. Blots were developed using enhanced chemiluminescence detection (SuperSignal West Pico; Pierce, Rockford, IL, USA)

and quantified by measuring the intensity of light emitted from correctly sized bands under ultraviolet light using a ChemiDoc EQ system and Quantity One software (Bio-Rad, Hercules, CA, USA). Immunoreactive proteins were detected using rabbit anti-mouse polyclonal antibodies against p-AKT1 and AKT1 at a 1:1000 dilution and 10% SDS/PAGE gel; rabbit anti-human polyclonal antibodies against p-MTOR and rabbit anti-human monoclonal antibodies against MTOR at a 1:1000 dilution and 8% SDS/PAGE gel; rabbit anti-human polyclonal antibodies against p-p70RSK and p70RSK at a 1:1000 dilution and 10% SDS/PAGE gel; rabbit anti-human polyclonal p-ERK1/2 MAPK and rabbit anti-human monoclonal ERK1/2 MAPK IgG, each at a 1:1000 dilution, and 12% SDS/PAGE gel. As a loading control, mouse anti- α -tubulin (TUBA) was used to normalize results from detection of proteins by western blotting. All antibodies were from Cell Signaling Technology (Danvers, MA, USA). Multiple exposures of each western blot were performed to ensure linearity of chemiluminescent signals.

Proliferation assay

Proliferation assays were conducted using Cell Proliferation ELISA, BrdU kit (Roche, Indianapolis, IN, USA) according to the manufacturer's recommendations. Briefly, pTr cells were seeded in a 96-well microplate (tissue culture grade, flat bottom), and then incubated for 24 h in serum-free DMEM/F-12. Cells were then treated with recombinant porcine CSF2 protein and various treatments in a final volume of 100 μ l/well. After 24 h of incubation, 10 μ M BrdU was added to the cell

culture and the cells incubated for an additional 24 h at 37°C. After labeling cells with BrdU, the fixed cells were incubated with anti-BrdU-POD working solution for 90 min. The anti-BrdU-POD binds to BrdU incorporated into newly synthesized cellular DNA and these immune complexes were detected by the reaction to TMB (tetramethyl-benzidine) substrate solution. The absorbance values of the reaction product were quantified by measuring the absorbance at 370 nm using an ELISA reader (Bio-Rad, Seoul, Korea).

Migration assay

The pTr cells (50,000 cells per 100 μ l serum and insulin-free DMEM) were seeded on 8- μ m pore Transwell inserts (Corning Costar no. 3422; Corning, Inc., Corning, NY, USA). Cells were then treated with recombinant porcine CSF2 protein (0, 0.1, 1, 20 and 100 ng/ml) (n = 3 wells per treatment). After 12 h, cells on the upper side of the inserts were removed with a cotton swab. For evaluation of cells that migrated onto the lower surface, inserts were fixed in 50% ethanol for 5 min. The transwell membranes were then removed, placed on a glass slide with the side containing cells facing up, overlaid with prolong antifade mounting reagent with 4',6-diamidino-2-phenylindole, and overlaid with a coverslip (Invitrogen-Molecular Probes, Eugene, OR, USA). Migrated cells were counted systematically in five non-overlapping locations, which covered approximately 70% of the insert membrane growth area, using a Zeiss confocal microscope LSM710 (Carl Zeiss, Jena, German) fitted with a digital microscope camera AxioCam using Zen 2009 software. The

entire experiment was repeated at least three times.

Statistical Analyses

All quantitative data were subjected to least squares ANOVA using the General Linear Model procedures of the Statistical Analysis System (SAS Institute Inc., Cary, NC, USA). Western blot data were corrected for differences in sample loading using the TUBA data as a covariate. All tests of significance were performed using the appropriate error terms according to the expectation of the mean squares for error. A *P* value less than or equal to 0.05 was considered significant. Data are presented as least-square means (LSMs) with SEs.

3. Results

Temporal expression of CSF2 mRNA in porcine endometrium during the estrous cycle and pregnancy

Uterine *CSF2* mRNA levels in cyclic and pregnant pigs were determined by quantitative RT-PCR analysis (Figure 6-1). No significant differences were found in *CSF2* transcripts due to day of the estrous cycle (day, $P > 0.05$), but expression of *CSF2* mRNA increased between Days 10 and 14 of pregnancy ($P < 0.001$) and then declined to Day 20 of pregnancy. Expression of *CSF2* on Days 9 ($P > 0.05$), 12 ($P < 0.01$) and 15 ($P < 0.01$) of pregnancy tend to higher than on the same days of the estrous cycle. These results demonstrate that endometrial expression of *CSF2* is up-regulated during peri-implantation period of pregnancy when it is likely involved in peri-implantation events associated with conceptus development.

CSF2 stimulates proliferation of pTr cells and activates AKT1, ERK1/2, MTOR, p70RSK and RPS6 phosphorylation

CSF2 stimulated phosphorylation of AKT1 and ERK1/2 proteins in a dose-dependent manner (Figure 6-2A). Under the same specific culture conditions, effects of different concentrations of *CSF2* (0, 0.1, 1, 20, 100 ng/ml) on proliferation and migration of pTr cells were determined (Figure 6-2B and 6-2C). *CSF2* at 20 ng/ml or 100 ng/ml increased pTr cell proliferation by approximately 158% and 159%,

respectively ($P < 0.05$). On the other hand, there are no significant effects of CSF2 on pTr cell migration. Based on results from our dose-dependent experiments, CSF2 was used at 20 ng/ml in experiments to determine cell signaling pathways involved in pTr cell proliferation. As compared to basal values, CSF2 stimulated a rapid 3.2-fold ($P < 0.01$) increase in phosphorylated AKT1 (p-AKT1) within 15 min post-treatment which then gradually decreased to basal levels at 120 min (Figure 6-2D). Within 30 min after CSF2 treatment, phosphorylated ERK1/2 MAPK (p-ERK1/2 MAPK) increased 6.6-fold ($P < 0.001$), and then gradually decreased to 120 min, but remained higher ($P < 0.001$) than basal levels (Figure 6-2E). CSF2 also increased the abundance of phosphorylated MTOR (p-MTOR), p70RSK (p-p70RSK) and RPS6 (p-RPS6) in a time-dependent manner by 3.4-, 5.5- and 3.3-fold ($P < 0.001$), respectively, at 30 min post-treatment with only p-RPS6 returning to basal levels by 120 min (Figure 6-2F, 6-2G and 6-2H). On the other hand, there was no significant effect ($P > 0.05$) of CSF2 on abundance of phosphorylated STAT3 (p-STAT3) protein in pTr cells (Figure 6-2I).

CSF2 activates PI3K- and ERK1/2 MAPK-dependent MTOR signal transduction pathways in pTr cells

Effects of CSFs on PI3K-AKT1 and ERK1/2 MAPK cell signal transduction in pTr cells were investigated using pharmacological inhibitors of PI3K (20 μ M LY294002) and ERK1/2 MAPK activity (20 μ M U0126). Serum starved pTr cells were incubated with either LY294002 (20 μ M) or U0126 (20 μ M) 1 h prior to treatment with CSF2 (20 ng/ml). CSF2-induced phosphorylation of AKT1 was

inhibited completely by the PI3K inhibitor ($P < 0.001$), while U0126 did not affect the abundance of CSF2-induced p-AKT1 protein ($P > 0.05$) (Figure 6-3A). CSF2-induced increases in phospho-ERK1/2 were blocked by both U0126 ($P < 0.001$) and LY294002 ($P < 0.001$) (Figure 6-3B). Also, CSF2-induced phospho-MTOR proteins were less abundant ($P < 0.001$) in pTr cells treated with both U0126 ($P < 0.001$) and LY294002 ($P < 0.001$) (Figure 6-3C). These results suggest that PI3K is upstream of the ERK1/2 MAPK pathway and that MTOR is a common downstream target of these parallel cell signaling pathways induced by CSF2 in pTr cells.

CSF2 induced stimulation of pTr cell proliferation is mediated via the PI3K-MTOR and ERK1/2 MAPK cell signaling pathways

To confirm whether PI3K-AKT1 and ERK1/2 MAPK signal transduction pathways are involved in CSF2-induced stimulation of pTr cell proliferation, cell proliferation assays were conducted in the presence or absence of CSF2 (20 ng/ml), U0126 and LY294002. As shown in Figure 6-4, CSF2 increased pTr cell proliferation by approximately 139% ($P < 0.01$). However, pretreatment with either U0126 ($P < 0.001$) or LY294002 ($P < 0.01$) inhibited CSF2-induced proliferation of pTr cells as compared to effects of CSF2 alone. Pharmacological inhibitors of FRAP/mTOR activity (rapamycin) also reduced effects of CSF2 on proliferation of pTr cells ($P < 0.001$). To examine involvement of other intracellular messengers, a pharmacological inhibitor of P38 MAPK (SB203580) was used to find that it did not inhibit proliferation of pTr cells in response to CSF2 ($P > 0.05$). These results suggest that

activation of PI3K-AKT1-MTOR and ERK1/2 MAPK signaling pathways play a central role in stimulation of pTr cell proliferation in response to uterine-derived CSF2 during the peri-implantation period of pregnancy.

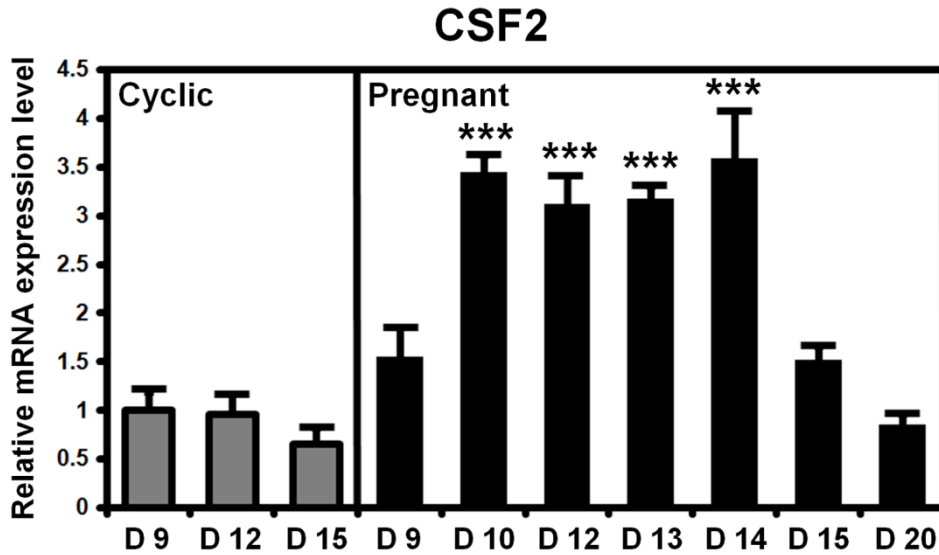


Figure 6-1. Relative quantification of *CSF2* mRNAs in porcine endometrium during the estrous cycle and pregnancy. Expression levels of endometrial *CSF2* mRNA were not affected by day of the estrous cycle, but effects of day of pregnancy on expression of *CSF2* mRNA were significant (day, $P < 0.01$). Endometrial *CSF2* mRNA expression increased between Day 10 and Day 14 of pregnancy. The asterisks denote statistically significant differences (** $P < 0.01$).

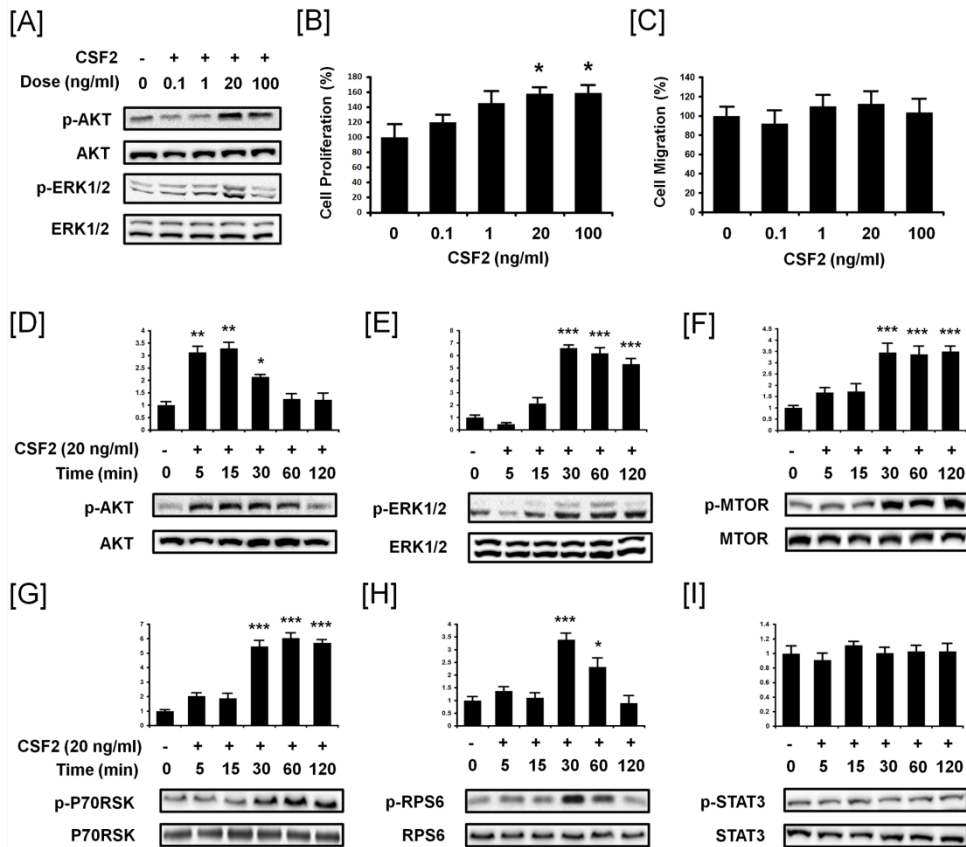


Figure 6-2. CSF2 increases the abundance of phosphorylated AKT1, ERK1/2, MTOR, p70RSK and RPS6 proteins and stimulates proliferation of pTr cells. [A] Western blot analyses showing dose-dependent effects of CSF2 to increase the abundance of p-AKT1 and p-ERK1/2 proteins in pTr cells *in vitro*. Tubulin-alpha (TUBA) was detected as a total protein control. [B] The effect of CSF2 (0, 0.1, 1, 20 and 100 ng/ml) on pTr cell proliferation. [C] The effect of CSF2 (0, 0.1, 1, 20 and 100 ng/ml) on pTr cell migration. [D-I] Detection of phosphorylated- and total AKT1, ERK1/2, MTOR, p70RSK, RPS6 and STAT3 proteins between 0 and 120 min after treatment of pTr cells with CSF2. Blots were imaged to calculate the normalized

values presented in the *graph* by measurements of abundance of phosphorylated proteins relative to total protein. The asterisks denote statistically significant differences ($***P < 0.001$, $**P < 0.01$ and $*P < 0.05$).

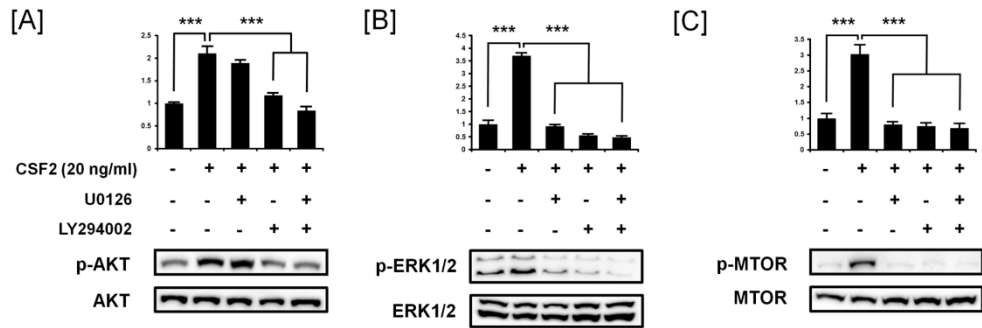


Figure 6-3. Inhibition of CSF2-induced AKT1 and ERK1/2 phosphorylation in pTr cells. [A] The effects of the PI3K inhibitor (LY294002) and MAPK inhibitor (U0126) on CSF2-induced p-AKT1 proteins. [B] The effects of the LY294002 and U0126 on CSF2-induced p-ERK1/2 proteins. [C] The effects of the LY294002 and U0126 on CSF2-induced p-MTOR proteins. Serum starved pTr cells were incubated with 20 μ M LY294002 or 20 μ M U0126 for 1 h and then stimulated with CSF2 for 30 min. Blots were imaged to calculate the normalized values presented in the *graph* by measurements of levels phosphorylated proteins relative to total proteins. The asterisk denotes statistically significant differences ($***P < 0.001$).

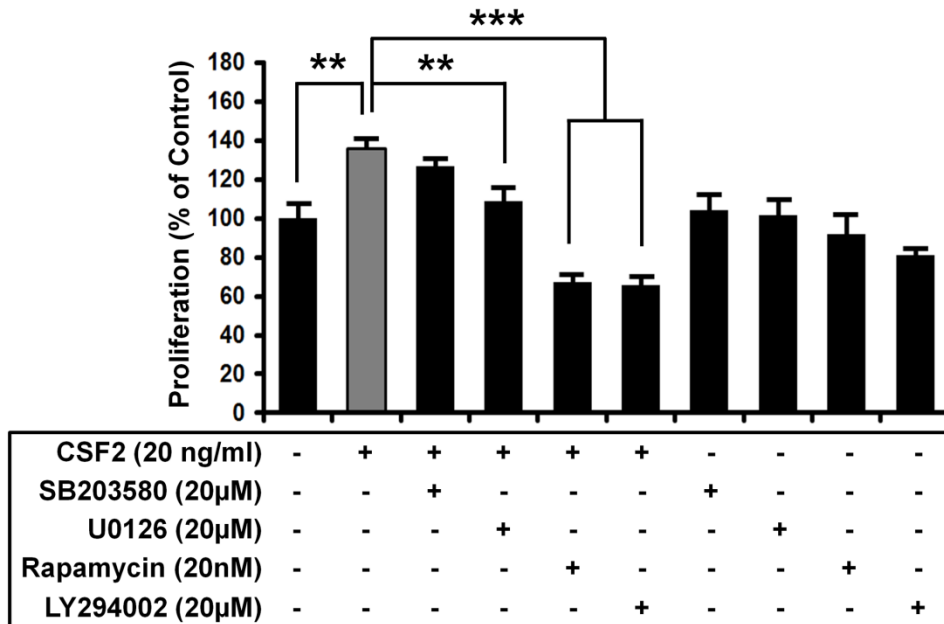


Figure 6-4. CSF2 stimulates proliferation of pTr cells through PI3K-MTOR and ERK1/2 MAPK pathways. The pTr cells seeded in a 96-well microplate were treated with recombinant CSF2 (20 ng/ml), SB203580 (20 μM), U0126 (20 μM), rapamycin (20 nM), LY294002 (20 μM), or their combination for 24 h in serum-free medium. After labeling of cells with BrdU for 24 h, cell numbers were determined by measuring the absorbance values of the reaction product. Data are expressed as a percentage relative to non-treated control pTr cells (100%). CSF2 stimulated ($P < 0.01$) pTr cell proliferation and, U0126 (20 μM), rapamycin (20 nM) and LY294002 (20 μM) blocked ($P < 0.001$ or $P < 0.01$) this CSF2-induced effect. However, there was no significant inhibitory effect of CSF2 by the inhibitor of P38 MAPK activity (SB203580). The asterisks denote a significant effect of CSF2 treatment ($***P < 0.001$ and $**P < 0.01$).

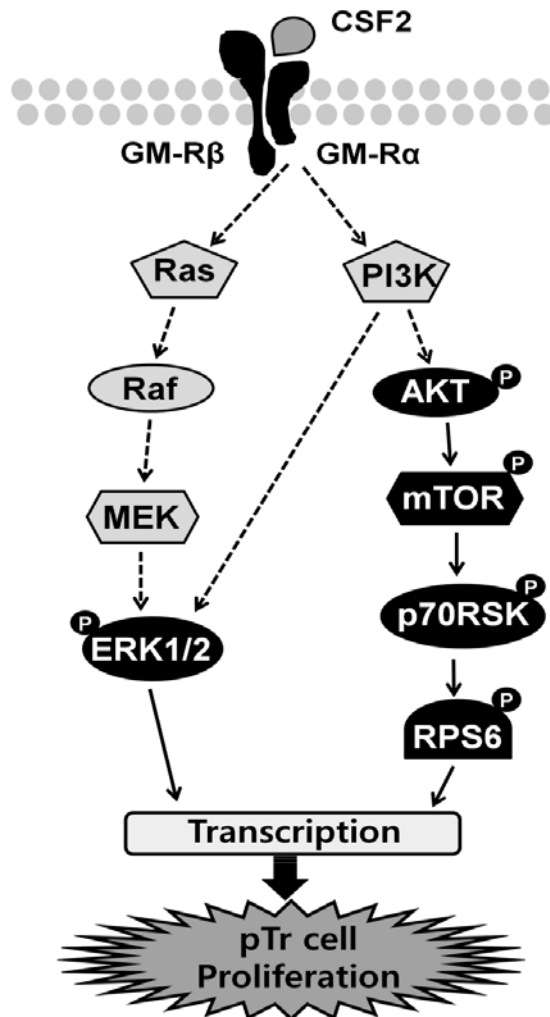


Figure 6-5. Schematic illustrating the current working hypothesis on CSF2-induced PI3K-AKT1 or ERK1/2 MAPK-P790RSK signaling pathways responsible for pTr cell proliferation.

5. Discussion

Results of the present study indicate a key role for CSF2 in stimulating proliferation of pTr cells via the PI3K-AKT1-dependent ERK1/2 MAPK cell signaling cascade (see Figure 6-5). This novel finding supports our hypothesis that during the peri-implantation period of pregnancy in pigs, CSF2 from uterine endometrium stimulates growth and development of the conceptus. Establishment of molecular crosstalk between mother and conceptus is most important for establishment and maintenance of pregnancy in the pig because survival and development of the conceptus depends on histotroph in the uterine lumen for nutrients, growth factors and cytokines (Geisert et al., 1982b; Gray et al., 2001c; Guillomot, 1995). CSF2 is implicated as an embryotrophic factor underpinning embryogenesis and implantation in most mammalian species.

There is emerging evidence that CSF2 improves the developmental rate of *in vitro* cultured embryos by increasing cell numbers in blastocysts (Diaz-Cueto and Gerton, 2001; Hardy and Spanos, 2002). Human embryos cultured with CSF2 reached the blastocyst stage earlier and had greater numbers of cell, which correlated with successful establishment of pregnancy after human IVF and embryo transfer (Sjoblom et al., 1999; Spandorfer et al., 1998). Studies of CSF2 null mice demonstrated that they have fewer cell numbers in the inner cell mass at the blastocyst stage (Robertson et al., 2001). Also, addition of CSF to embryo culture medium rescued deficiencies in placental structure and fetal growth, and also improved postnatal development of

mouse pups (Robertson et al., 2001; Sjoblom et al., 2005). Effects of CSF2 to stimulate *in vitro* development of embryos have also been reported for bovine and ovine embryos (de Moraes and Hansen, 1997; Imakawa et al., 1993). Growth and survival of bovine and ovine conceptuses *in vitro* was also promoted by CSF2 (Emond et al., 2000; Emond et al., 1998; Fortin et al., 1997).

The embryotrophic effects of CSF2 are likely to be more profound in pigs which experience high rates of embryonic mortality, and highly variable rates in conceptus development and implantation (Sjoblom et al., 1999). During the peri-implantation period of pregnancy, porcine conceptuses elongate rapidly and trophoctoderm then attaches to uterine LE which is especially important to ensure that pig conceptuses maximize contact with uterine endometrial surface for the efficient exchange of nutrients and gases (Bazer et al., 2011; Burghardt et al., 1997; Geisert et al., 1982b; Geisert and Yelich, 1997; Keys and King, 1990; Leiser and Kaufmann, 1994; Song et al., 2011a; Stroband and Van der Lende, 1990). Despite the requirement for histotrophic to induce active cell proliferation and differentiation during this period, previous studies with pigs have focused mainly on effects of CSF2 on development during the cleavage stages of embryonic development and not the peri-implantation phase when histotroph can have dramatic effects on conceptus development and survival (O'Leary et al., 2004). Therefore, the present study addressed the unresolved issue of effects of CSF2 on conceptuses during the peri-implantation period of pregnancy.

Throughout pregnancy, *CSF2* mRNA is expressed in the uterine endometrium, especially uterine LE and GE in species such as human, mouse, cow and sheep (Emond et al., 2004; Giacomini et al., 1995; Imakawa et al., 1993; Robertson et al., 1992; Zhao and Chegini, 1999). In the human and mouse, *CSF2* synthesis remains high for the first few days following fertilization in response to estrogen, and then declines at the time of implantation of the blastocyst when the uterus is under the influence of progesterone (Robertson et al., 1996; Tremellen et al., 1998). But, little information is available on temporal variations in expression of *CSF2* in the uterus during early pregnancy and the estrus cycle. In the present study, temporal changes in expression of the *CSF2* mRNA in the porcine endometrium on different days of the estrous cycle and early pregnancy are demonstrated. Our result revealed that *CSF2* mRNA expression significantly increases between Days 10 and 14 of pregnancy, and that expression levels on Days 12 and 15 of pregnancy are higher than those on the same days of the estrous cycle. This expression pattern is likely related to stimulatory effects of conceptus-derived estrogens during the peri-implantation phase of pregnancy. As well as increased secretion of *CSF2* in response to estrogen, expression of *CSF2* in cows is also stimulated by both conceptus derived-interferon tau (IFNT) and PGE₂ before and after the attachment phase of implantation (Emond et al., 2000; Emond et al., 1998; Emond et al., 2004; Fortin et al., 1997; Michael et al., 2006). Similarly, in sheep, uterine-derived *CSF2* has been reported to stimulate secretion of IFNT by ovine trophoblast and enhance uterine support for conceptus development during the period of pregnancy establishment (Imakawa et al., 1993). Results of the present study indicate that *CSF2* plays an essential role in peri-

implantation events via supporting the development and survival of the porcine conceptus and this may include stimulation of secretion of numerous factors from trophoderm including interferon delta.

In the present study, CSF2-induced cell signaling cascades in pTr cells responsible for cell proliferation were investigated. Although numerous studies have shown that CSF2 receptors are expressed in early embryos, knowledge of downstream signaling cascades triggered by CSF2 in developing embryos is limited. In other cell types, CSF2 activates several cell signaling pathways, including the PI3K-AKT, JAK-STAT and MAPK cascades via interaction with the β subunit of the CSF2 receptor (Tortorella et al., 2006). In the present study, time-dependent increases in phosphorylation of AKT1, ERK1/2, MTOR and p70RSK were detected in CSF2 treated pTr cells. The MTOR-RPS6K cell signaling pathway plays central roles in various cellular activities such as cell proliferation, differentiation, and protein synthesis (Gingras et al., 2004). Recently, it was reported that several amino acids including arginine, leucine, and glutamine stimulate pTr cell proliferation through activation of the MTOR-RP6K-RPS6 signaling pathway (Kim et al., 2013). In response to CSF2, the activated PI3K-MTOR-p70RSK cascades likely transduces signaling through downstream pathways such as RPS6K-RPS6-EIF4EBP1, leading to mRNA translation and protein synthesis required for cell proliferation and growth (Dufner and Thomas, 1999; Peterson and Schreiber, 1998). ERK1/2 MAPK has been implicated as a major participant in proliferation and differentiation processes, including embryonic and placental development in a number of model systems

(Fernandez-Serra et al., 2004b; Klemke et al., 1997; Seger and Krebs, 1995; Wang et al., 2004a). Along with the RTK-MAPK pathway, the JAK-STAT cell signaling pathway often mediates effects of numerous cytokines which influence migration, proliferation and differentiation of trophoblast cells (Fitzgerald et al., 2005a). Furthermore, CSF2 can stimulate the JAK-STAT signaling pathway through tyrosine phosphorylation of STAT3 that is indispensable for embryogenesis and invasion of human transformed trophoblast cells (Fitzgerald et al., 2005a; Fitzgerald et al., 2005b; Takeda et al., 1997). However, in the present study, there was no significant effect of CSF2 on phosphorylated STAT3 proteins in pTr cells. Taken together, our results suggest that activation of both PI3K-AKT1-MTOR and ERK1/2 MAPK cell signaling cascades are induced simultaneously by CSF2 in pTr cells.

Also, the ERK1/2 MAPK specific inhibitor (U0126) inhibited CSF2-induced activation of ERK1/2 and MTOR, but had no significant effect on AKT1 activation. However, the PI3K specific inhibitor (LY294002) inhibited CSF2-induced phosphorylation of ERK1/2 and MTOR as well as CSF2-induced phosphorylation of AKT1. These results indicate that ERK1/2 MAPK cell signaling is activated by the PI3K-AKT1 pathway in response to CSF2 and that MTOR protein is a common downstream target for phosphorylation and for cross-talk between these two cell signaling cascades. Furthermore, pharmacological inhibitors of ERK1/2, PI3K and FRAP/mTOR activity (rapamycin) abolished CSF2-induced pTr cell proliferation. But, there was no significant effect of inhibiting P38 MAPK activity (SB203580) on effects of CSF2-induced proliferation of pTr cells. Taken together, these results

suggest that CSF2 has stimulatory effects on proliferation of pTr cells that are mediated via activation of PI3K- and ERK1/2 dependent MTOR cell signaling pathways. CSF2 deficient mice exhibit reduced placental development due to reduced proliferation of mononuclear trophoblast cells (Robertson et al., 1999). This CSF2-induced proliferation of mononuclear trophoblast cells is likely accompanied by enhanced glucose uptake and/or anti-apoptotic processes (Behr et al., 2005; Robertson et al., 2001). When mouse embryos are exposed to stressors, CSF2 is likely to exert protective effects against cytotoxic mechanisms, with increased expression of anti-apoptotic factors such as Bcl-2 (Behr et al., 2005; Clark et al., 1994; Karagenc et al., 2005; Robertson et al., 2001).

In conclusion, endometrial CSF2 stimulates proliferation of porcine conceptus trophectoderm in a paracrine manner during the peri-implantation period. This beneficial event occurs via PI3K-dependent MTOR and MAPK signal transduction cascades. Results of the current study provide important insights into CSF2-induced regulatory mechanisms for successful development and implantation of the porcine conceptus, and, this could assist in improving survival of conceptuses during the peri-implantation period of pregnancy.

CHAPTER 7

AHCYL1 Is Mediated by Estrogen-Induced ERK1/2 MAPK Cell Signaling and MicroRNA Regulation to Effect Functional Aspects of the Avian Oviduct

1. Abstract

S-adenosylhomocysteine hydrolase-like protein 1 (AHCYL1), also known as IP₃ receptor-binding protein released with IP₃ (IRBIT), regulates IP₃-induced Ca²⁺ release into the cytoplasm of cells. AHCYL1 is a critical regulator of early developmental stages in zebrafish, but little is known about the function of AHCYL1 or hormonal regulation of expression of the *AHCYL1* gene in avian species. Therefore, we investigated differential expression profiles of the *AHCYL1* gene in various adult organs and in oviducts from estrogen-treated chickens. Chicken *AHCYL1* encodes for a protein of 540 amino acids that is highly conserved and has considerable homology to mammalian AHCYL1 proteins (>94% identity). *AHCYL1* mRNA was expressed abundantly in various organs of chickens. Further, the synthetic estrogen agonist induced *AHCYL1* mRNA and protein predominantly in luminal and glandular epithelial cells of the chick oviduct. In addition, estrogen activated AHCYL1 through the ERK1/2 signal transduction cascade and that activated expression of AHCYL1 regulated genes affecting oviduct development in chicks as well as calcium release in epithelial cells of the oviduct. Also the microRNAs, *miR-124a*, *miR-1669*, *miR-1710* and *miR-1782*, influenced *AHCYL1* expression via its 3'-UTR which suggests that post-transcriptional regulation influences *AHCYL1* expression in the chick oviduct. In conclusion, these results indicate that *AHCYL1* is a novel estrogen-stimulated gene expressed in epithelial cells of the chicken oviduct that likely affects growth, development and calcium metabolism of the mature oviduct of hens via an estrogen-mediated ERK1/2 MAPK cell signaling pathway.

2. Introduction

S-adenosylhomocysteine hydrolase-like protein 1 (AHCYL1) is a member of AHCY family of proteins involved in metabolism of S-adenosyl-L-homocysteine (Cooper et al., 2006). AHCYL1 consists of 540 amino acid residues and has a domain homologous to AHCY in the C-terminal region and multiple potential phosphorylation sites in the N-terminal region (Ando et al., 2003). Unlike AHCY that catalyzes a reversible reaction for S-adenosylhomocysteine hydrolysis (Bujnicki et al., 2003; De La Haba and Cantoni, 1959), AHCYL1 does not have hydrolase activity for adenosylhomocysteine due to the substitution of important amino acids in the critical enzymatically active site (Dekker et al., 2002; Gomi et al., 2008) although it has an AHCY-like domain in the C-terminal domain (Cooper et al., 2006). However, AHCYL1 plays important role in the inositol phospholipid (IP) signaling pathway by interacting with the inositol 1,4,5-trisphosphate (IP₃) receptor, which is an intracellular Ca²⁺ release channel located on the endoplasmic reticulum (Ando et al., 2006; Ando et al., 2003; Berridge, 1993; Berridge et al., 2000; Devogelaere et al., 2006; Gomi et al., 2008). Therefore, AHCYL1 influences the IP₃-induced Ca²⁺ signaling cascade essential for numerous cellular and physiological processes such as organ development, fertilization, and cell death (Ando et al., 2009; Berridge et al., 2000; Streb et al., 1983). Recently, Cooper and co-workers identified two zebrafish AHCYL1 orthologs and found that the function of AHCYL1 is different from AHCY and that it plays a key role in zebrafish embryogenesis in response to IP₃ receptor function for release of intracellular calcium (Cooper et al., 2006). Although AHCYL1

is highly conserved among various species, little is known about its expression and functional roles in chickens or any other avian species.

In mammals, the oviduct undergoes diverse cellular and molecular changes in response to sex steroids during the estrous/menstrual cycle and peri-implantation period as these actions are pivotal to establishing an optimal microenvironment from gamete transport and embryonic development (Buhi et al., 1997). Of these steroid hormones, estrogen is the primary female sex hormone that controls a number of biological events including cell proliferation and differentiation, protection against apoptosis, and diabetes (Hewitt et al., 2005; Louet et al., 2004). To investigate mechanisms of action of sex steroids, their biological effects and signal transduction cascades, the chicken oviduct is an established model due to its responsiveness to steroid hormones (Dougherty and Sanders, 2005). The chicken oviduct is a highly differentiated linear organ with compartments that undergo structural, cellular and biochemical changes in response to sex hormones during egg formation and oviposition (Chousalkar and Roberts, 2008). The oviduct of egg-laying hens consists of the infundibulum, magnum, isthmus, and shell gland essential for fertilization, production of egg-white proteins, formation of the soft shell membrane, and formation of the outer egg shell, respectively. In the chicken oviduct, estrogen induces both cell proliferation and differentiation, as well as anti-apoptotic effects on cells (Monroe et al., 2002; Monroe et al., 2000). In particular, estrogen stimulates formation of oviductal tubular glands and differentiation of epithelial cells into goblet and ciliated cells (Palmiter and Wrenn, 1971b). In addition, estrogen regulates the mechanism for

Ca²⁺ release necessary for formation of the egg shell in the shell gland of the chicken oviduct (Bar, 2009; Hincke et al., 2010).

We used differential gene profiling data from the chicken oviduct to identify the avian homolog of the human *AHCYL1* transcript and found it to be highly expressed in chicks treated with the synthetic estrogen agonist diethylstilbestrol (DES) (Song et al., 2011b). There is little known about the expression or function of *AHCYL1* in most species, except for humans and zebrafish (Ando et al., 2003; Cooper et al., 2006; Dekker et al., 2002). Therefore, the objectives of this study were to: 1) compare the primary sequences of chicken *AHCYL1* with those of selected mammalian species; 2) determine tissue- and cell-specific expression of *AHCYL1* gene in various organs of the mature chicken; 3) determine whether estrogen regulates expression of *AHCYL1* mRNA and protein during development of the chick oviduct; 4) determine whether *AHCYL1* regulates calcium release and expression of genes related to development of the chicken oviduct through an estrogen-induced MAPK signaling pathway(s); and 5) investigate post-transcriptional regulation of *AHCYL1* expression in the chicken oviduct. Results of this study provide novel insights into the *AHCYL1* gene with respect to its sequence, tissue specific expression and hormonal regulation of its expression during development of the chicken oviduct.

3. Materials and Methods

Experimental Animals and Animal Care

The experimental use of chickens for this study was approved by the Institute of Laboratory Animal Resources, Seoul National University (SNU-070823-5). White Leghorn (WL) hens, roosters, and chicks were subjected to standard management practices at the University Animal Farm, Seoul National University, Korea. All chickens were exposed to a light regimen of 15 h light and 9 h dark with *ad libitum* access to feed and water.

Tissue Samples

Following euthanasia of the WL hens and roosters, tissue samples were collected from brain, heart, liver, kidney, muscle, small intestine, gizzard, ovary, oviduct and testis of 1- to 2- year-old males (n = 5) and females (n = 5). The collected samples were frozen or fixed in 4% paraformaldehyde for further analyses. Frozen tissue samples were cut into 5- to 7- mm pieces, frozen in liquid nitrogen vapor, and stored at -80°C. The other samples were cut into 10 mm pieces and fixed in fresh 4% paraformaldehyde in PBS (pH 7.4). After 24 h, fixed tissues were changed to 70% ethanol for 24 h and then dehydrated and embedded in Paraplast-Plus (Leica Microsystems, Wetzlar, Germany). Paraffin-embedded tissues were sectioned at 5 µm.

Diethylstilbestrol (DES) Treatment and Oviduct Retrieval

Female chicks were identified by PCR analysis using W chromosome-specific primer sets (Lee et al., 2009). Treatment with DES and recovery of the oviduct were performed as reported previously (Sanders and McKnight, 1988; Seo et al., 2009). Briefly, a 15mg DES pellet was implanted subcutaneously in the abdominal region of 1-week-old female chicks for 10 days. The DES pellet was removed for 10 days, and a 30mg dose was administered for 10 additional days. Five 37-day-old chicks in each group were euthanized using 60%–70% carbon dioxide. Subsets of these samples were frozen or fixed in 4% paraformaldehyde for further analyses. Paraffin-embedded tissues were sectioned at 5 μ m.

RNA Isolation

Total cellular RNA was isolated from frozen tissues using Trizol reagent (Invitrogen, Carlsbad, CA) according to the manufacturer's recommendations. The quantity and quality of total RNA was determined by spectrometry and denaturing agarose gel electrophoresis, respectively.

Sequence Analysis

For pair-wise comparisons and multiple sequence alignment, the amino acid sequences encoded by *AHCYL1* genes from each species were aligned using

Geneious Pro Version 5.04 (Drummond et al., 2010) with default penalties for gap and the protein weight matrix of BLOSUM (Blocks Substitution Matrix). A phylogenetic tree was constructed using the neighbor-joining method (Saitou and Nei, 1987) of the Geneious Pro Version 5.04 (Drummond et al., 2010). To determine the confidence level for each internal node on the phylogenetic tree, 1,000 nonparametric bootstrap replications were used (Felsenstein, 1985).

Semiquantitative RT-PCR Analysis

The expression level of *AHCYLI* mRNA in various organs from chickens, including the oviduct, was assessed using semi-quantitative RT-PCR as described previously (Song et al., 2007b). The cDNA was synthesized from total cellular RNA (2 ug) using random hexamer (Invitrogen, Carlsbad, CA) and oligo (dT) primers and AccuPower® RT PreMix (Bioneer, Daejeon, Korea). The cDNA was diluted (1:10) in sterile water before use in PCR. For *AHCYLI*, the sense primer (5'-TTT GGA GGG AAG CAA GTG GC-3') and antisense primer (5'-GCT CAA TCA GAG CCA GAG CC-3') amplified a 481-bp product. For *GAPDH* (housekeeping gene; glyceraldehyde 3-phosphate dehydrogenase), the sense primer (5'-TGC CAA CCC CCA ATG TCT CTG TTG -3') and antisense primer (5'- TCC TTG GAT GCC ATG TGG ACC AT -3') amplified a 301-bp product. The primers, PCR amplification and verification of their sequences were conducted as described previously (Song et al., 2007b). PCR amplification was conducted using approximately 60 ng cDNA as follows: 1) 95°C for 3 min; 2) 95°C for 20 sec, 60°C for 40 sec, and 72°C for 1 min for 35 cycles

(*AHCYLI*) and 30 cycles (*GAPDH*); and 3) 72°C for 5 min. The amount of DNA present was quantified by measuring the intensity of light emitted from correctly sized bands under UV light using a Gel Doc™ XR+ system with Image Lab™ software (Bio-Rad).

Quantitative PCR Analysis

Total RNA was extracted from each oviduct of untreated and DES-treated chicks using TRIzol (Invitrogen) and purified using an RNeasy Mini Kit (Qiagen). Complementary DNA was synthesized using AccuPower® RT PreMix (Bioneer, Daejeon, Korea). Gene expression levels were measured using SYBR® Green (Sigma, St. Louis, MO, USA) and a StepOnePlus™ Real-Time PCR System (Applied Biosystems, Foster City, CA, USA). The PCR conditions were 95°C for 3 min, followed by 40 cycles at 95°C for 20 sec, 64°C for 40 sec, and 72°C for 1 min using a melting curve program (increasing the temperature from 55°C to 95°C at 0.5°C per 10 sec) and continuous fluorescence measurements. Sequence-specific products were identified by generating a melting curve in which the C_T value represented the cycle number at which a fluorescent signal was significantly greater than background, and relative gene expression was quantified using the 2^{-ΔΔCT} method (Livak and Schmittgen, 2001). For the control, the relative quantification of gene expression was normalized to the C_T value of the control oviduct.

In Situ Hybridization Analysis

For hybridization probes, PCR products were generated from cDNA with the primers used for RT-PCR analysis. The products were gel-extracted and cloned into pGEM-T vector (Promega). After verification of the sequences, plasmids containing gene sequences were amplified with T7- and SP6-specific primers (T7:5'-TGT AAT ACG ACT CAC TAT AGG G-3'; SP6:5'-CTA TTT AGG TGA CAC TAT AGA AT-3') then digoxigenin (DIG)-labeled RNA probes were transcribed using a DIG RNA labeling kit (Roche Applied Science, Indianapolis, IN). The signal was visualized by exposure to a solution containing 0.4 mM 5-bromo-4-chloro-3-indolyl phosphate, 0.4 mM nitroblue tetrazolium, and 2 mM levamisole (Sigma).

Immunohistochemistry

Immunocytochemical localization of AHCYL1 protein in the chicken oviduct was performed as described previously (Song et al., 2006) using an anti-human AHCYL1 monoclonal antibody (catalog number: ab56761; abcam, Cambridge, UK) at a final dilution of 1:500 (1 µg/ml). Antigen retrieval was performed using the boiling citrate method as described previously (Song et al., 2006). Negative controls included substitution of the primary antibody with purified non-immune mouse IgG at the same final concentration.

Western Blot Analyses

Chicken oviduct cells were isolated and cultured with minor modifications as we described previously (Jung et al., 2011). Cells were grown in DMEM-F12 containing 10% charcoal-stripped FBS until they were 80% confluent and starved in serum free medium for 24 h before DES treatment. The protein content was determined using the Bradford protein assay (Bio-Rad, Hercules, CA) with bovine serum albumin (BSA) as the standard. Proteins were denatured, separated using 10% SDS-PAGE and transferred to nitrocellulose. Blots were developed using enhanced chemiluminescence detection (SuperSignal West Pico, Pierce, Rockford, IL) and quantified by measuring the intensity of light emitted from correctly sized bands under ultraviolet light using a ChemiDoc EQ system and Quantity One software (Bio-Rad, Hercules, CA). Immunoreactive AHCYL1 and phosphorylated ERK1/2 protein was detected using an anti-human AHCYL1 monoclonal antibody (catalog number: ab56761; abcam, Cambridge, UK) at a final dilution 1:500 and anti-mouse phospho-ERK1/2 monoclonal IgG (catalog number: sc-7383; Santa Cruz, CA) at a final dilution 1:1000, respectively. As a loading control, western blotting with mouse anti-beta actin IgG (catalog number: sc-47778; Santa Cruz, CA) or anti-rabbit total ERK1/2 polyclonal IgG (catalog number: 9102; Cell signaling Technology) was performed.

Immunofluorescence Microscopy

Oviduct cells obtained from laying hens were examined for AHCYL1 protein expression patterns by immunofluorescence microscopy as described

previously (Lim et al., 2011b). Briefly, oviduct cells were cultured to 80% confluency in charcoal-stripped FBS to remove sex steroids, starved and then treated with 2 μ g/ml DES and 10 μ M U0126 (ERK1/2 inhibitor) for 24 h. Each type of cell was seeded onto Lab-Tek chamber slide (Nalge Nunc International, Rochester, NY). After 24h, cells were fixed with -20°C methanol and immunofluorescence staining was performed using an anti-human AHCYL1 monoclonal antibody (catalog number: ab56761; abcam, Cambridge, UK). Cells were then incubated with Alexa Fluor 488 rabbit anti-mouse IgG secondary antibody (A21204, Invitrogen). Slides were overlaid with DAPI before images were captured using a Zeiss confocal microscope LSM710 (Carl Zeiss) fitted with a digital microscope camera AxioCam using Zen 2009 software.

Target-specific siRNAs for AHCYL1 Knockdown

For messenger RNA sequences of chicken AHCYL1 (NM_001030913.1), three potential small interfering RNA target sites were determined using the Invitrogen design program. The most effective target sequence (GTG AGA AGC AGC AAA CCA A) was screened out and synthesized. Silencer Negative Control 1 siRNA (Ambion, Austin, TX), with no homology to any known gene, was used as a negative control. Down-regulation of AHCYL1 expression was confirmed by quantitative PCR and Western blotting analyses. The information on primers used for q-PCR is described in Table 2.

Transfection

Chicken oviduct cells were treated with specific *AHCYL1* siRNA or controls that included naïve treatment (no siRNA or Lipofectamine 2000) and sham treatment (Lipofectamine 2000 only). Transfection of siRNA was according to the manufacturer's procedure. To analyze the effect of DES on chicken oviduct cells, DES was added to the culture medium 48 h post-transfection and the incubation continued for either 6 or 24 h. Using red fluorescein-labeled control siRNA duplexes (Invitrogen), we estimated that more than 95% of the cells were transfected.

MicroRNA Target Validation Assay

The 3'-UTR of *AHCYL1* was cloned and confirmed by sequencing. The 3'-UTR was subcloned between the eGFP gene and the bovine growth hormone (bGH) poly-A tail in pcDNA3eGFP (Clontech, Mountain View, CA) to generate the eGFP-miRNA target 3'-UTR (pcDNA-eGFP-3'UTR) fusion constructs. For the dual fluorescence reporter assay, the fusion constructs containing the *DsRed* gene and either *miR-124a*, *miR-1602*, *miR-1612*, *miR-1669*, *miR-1710* or *miR-1782* were designed to be co-expressed under control of the CMV promoter (pcDNA-DsRed-miRNA). The pcDNA-eGFP-3'UTR and pcDNA-DsRed-miRNA (4µg) were co-transfected into 293FT cells using the calcium phosphate method. When the DsRed-miRNA is expressed and binds to the target site of the 3'-UTR downstream of the GFP transcript, green fluorescence intensity decreases due to degradation of the GFP

transcript. At 48 h post-transfection, dual fluorescence was detected by fluorescence microscopy and calculated by FACSCalibur flow cytometry (BD Biosciences). For flow cytometry, the cells were fixed in 4% paraformaldehyde and analyzed using FlowJo software (Tree Star Inc., Ashland, OR).

Calcium Release Assay

Chicken intact or AHCYL1 siRNA knockdown oviduct cells were treated with various concentrations of DES for 24 h and the supernatant was used to evaluate the release of calcium using Calcium Assay kit (Cayman Chemical, Ann Arbor, MI) according to the manufacturer's instructions. The 100 μ l working detection reagent was added to 10 μ l supernatant and gently mixed, incubated at room temperature for 5 min. Calcium concentration was quantified using a microplate reader with a 595 nm absorbance and compared to a calcium standard curve.

Statistical Analyses

Differences in the variance between control and DES-treated oviducts were analyzed using the *F* test, and differences between means were detected using the Student's *t* test. The probability value of $P < 0.05$ was considered statistically significant. Excel (Microsoft, Redmond, WA, USA) was used for statistical analyses.

4. Results

Sequence comparison, pair-wise alignment and phylogenetic tree analysis of AHCYL1

The chicken *AHCYL1* gene spanned 10.3 kb on chromosome 26. The gene consists of 16 exons and the mRNA has 3,445 bp encoding a protein with 540 amino acid residues. The primary sequence of chicken *AHCYL1* was compared to those of six mammals and the zebrafish. Chicken *AHCYL1* protein contained an NAD(P)-binding motif required for catalysis of S-adenosyl-L-homocysteine into adenosine and homocysteine as for mammalian *AHCYL1*s. This verified that *AHCYL1* has a different function from *AHCY* because *AHCYL1* lacks several binding sites for S-adenosyl-L-homocysteine, irrespective of the conserved cysteines required for a tight globular structure of *AHCY* and NAD^+ binding motifs (Cooper et al., 2006). In pair-wise comparisons of chicken *AHCYL1* proteins with seven other vertebrates, chicken *AHCYL1* protein has high homology to mammalian *AHCYL1* proteins (91-98%, Table 7-1). The phylogenetic tree was constructed using the neighbor-joining method. The human and orangutan *AHCYL1* genes clustered together and formed a larger cluster with mice and cattle, and an even larger cluster with sister groups was detected for dog and zebrafish. However, chicken *AHCYL1* is in a separate branch, but closer to rat than to other mammalian species. These results indicate that chicken *AHCYL1* diverged from mammalian *AHCYL1* at very early stage in its evolution.

AHCYL1 mRNA expression in various organs from chickens

Tissue specific expression of *AHCYL1* mRNA in brain, heart, liver, kidney, muscle, gizzard, small intestine, ovary, oviduct and testis of 1- to 2- year-old males and females was determined by RT-PCR. High levels of expression of *AHCYL1* mRNA were detected in kidney and testis from male, and liver and oviduct from female chickens (Figures 7-1A and 7-1B), and lower expression in liver, gizzard and small intestine from males and kidney and gizzard from females. However, expression of *AHCYL1* mRNA was not detected in other organs analyzed regardless of sex. Based on differential gene profiling data of the chicken oviduct, the avian homolog of the human *AHCYL1* transcript is highly expressed in the oviduct of chicks treated with DES (Song et al., 2011b). Since little is known about expression and function of *AHCYL1* in the oviduct of any species (Ando et al., 2003; Cooper et al., 2006; Dekker et al., 2002), this study focused on its expression in the chicken oviduct.

Localization of chicken AHCYL1 mRNA and protein in chicken oviduct

In situ hybridization analysis was used to determine cell-specific localization of *AHCYL1* mRNA in the chicken oviduct. The oviduct of egg-laying hens includes the infundibulum (site of fertilization), magnum (production of components of egg-white), isthmus (formation of the shell membrane), and shell gland (formation of the egg shell). As illustrated in Figure 7-1C, *AHCYL1* mRNA was most abundant in the luminal epithelium (LE) of the infundibulum and shell gland,

and it was also expressed at lower abundance in glandular epithelium (GE) and LE of the magnum and isthmus, and GE of the infundibulum and shell gland. Little or no mRNA was detected in stromal cells, blood vessels, immune cells or myometrium of the oviduct. Results of immunohistochemical analysis (Figure 7-1D) were consistent with results from *in situ* hybridization analyses. The AHCYL1 protein was abundant in LE of all segments of the oviduct, but less abundant in GE of magnum, isthmus and shell gland. The nonspecific mouse IgG, used as a negative control, did not detect AHCYL1 protein in any segment of the oviduct.

Effects of DES on AHCYL1 mRNA and protein expression in the chicken oviduct

Cell-specific expression of *AHCYL1* in the oviductal segments of mature hens suggested regulation by estrogen during development of the chick oviduct. We reported that exogenous DES affects growth, development and differentiation of the chick oviduct and discovered candidate genes and pathways regulating oviduct development (Song et al., 2011c). Therefore, we examined the effects of DES on *AHCYL1* expression in the chick oviduct. As shown in Figures 7-2A and 7-2B, semi-quantitative RT-PCR analysis indicated that DES increased *AHCYL1* mRNA in all segments of the 37-day-old chick oviduct. Further results from quantitative PCR revealed that DES induced a 3.3-fold increase ($P < 0.01$) in oviductal *AHCYL1* mRNA as compared to 37-day-old chicks that were not treated with DES (Figure 7-2C). In addition, DES stimulated 2.3-, 3.4-, 2.6- and 4.3-fold increases ($P < 0.01$) in *AHCYL1* mRNA in the infundibulum, magnum, isthmus, and shell gland, respectively (Figure

7-2D). *In situ* hybridization analyses revealed that *AHCYL1* mRNA is expressed specifically in superficial GE in close proximity to LE in all segments of the oviduct of chicks treated with DES (Figure 7-2E). *AHCYL1* mRNA is also expressed at lower abundance in LE of oviducts from untreated chicks. Consistent with results from *in situ* hybridization analyses, immunoreactive *AHCYL1* protein was detected predominantly in superficial GE of magnum and isthmus, and to a lesser extent in GE of shell glands of oviducts treated with DES and LE of oviducts from untreated chicks (Figure 7-2F).

DES activates ERK1/2 signal transduction in chicken oviduct cells

Epithelial cells from the chicken oviduct were isolated and cultured in the presence or absence of DES and subjected to protein extraction. Based on results from our preliminary experiments, we focused on MAPK signaling cascades, especially, the extracellular-signal regulated kinase1/2 (ERK1/2) signaling pathway. Based on dose–response experiments (Figure 7-3A), DES was used at 2 µg/ml in all experiments to determine cell signaling pathways mediating effects of DES on activation of ERK1/2 proteins. Western blot analyses of whole oviduct cell extracts with antibody to phosphorylated target proteins indicated that DES increased phospho-ERK1/2 (p-ERK1/2) 15.7-fold ($P < 0.01$) over basal levels within 5 min and this effect was maintained to 30 min (Figure 7-3B). In addition, the same dose of DES increased *AHCYL1* protein approximately 3-fold within 2 h and further stimulated it 6.3-fold over 24 h. Next, we examined effects of an ERK1/2 inhibitor (U0126) on the ability of

DES to increase synthesis of AHCYL1 protein (Figure 7-3C). As illustrated in Figure 7-3D, 1 to 10 μ M U0126 decreased the abundance of AHCYL1 protein in response to DES treatment. To verify these results, we performed immunofluorescence analyses and compared expression patterns of AHCYL1 protein in chick oviduct cells cultured in the presence or absence of DES or presence of DES with U0126 (Figure 7-3E). Immunoreactive AHCYL1 protein was most abundant in the cytoplasm of chicken oviduct epithelial cells treated with DES, but detectable at lower abundance in the cytoplasm of cells receiving no treatment or DES treatment with U0126. Furthermore, DES stimulated calcium release from epithelia cell of the magnum of the chicken oviduct in a dose-dependent manner (Figure 7-3F). However, calcium release was reduced in these cells when cultured in the presence of both DES and U0126 as compared to DES alone (Figure 7-3G).

AHCYL1 knockdown and expression of genes related to oviduct development in response to estrogen

The constitutive expression of AHCYL1 after transfection was not significantly different in chicken oviduct epithelial cells at 0.5, 1, 10, 25 and 50 nM of AHCYL1-specific siRNA. However, AHCYL1 protein expression was inhibited 25.3% at 48 h post-transfection with AHCYL1 siRNA at 100 nM (Figures 7-4A and 7-4B). Therefore, we investigated whether DES affects levels of AHCYL1 expression in chick oviduct cells transfected with AHCYL1 siRNA for 48 h and then treated with 2 μ g/ml DES for 0, 6 or 24 h. Cell transfected with AHCYL1-specific siRNA had less

AHCYL1 compared to sham-treated cells ($p < 0.001$) and cells transfected with control siRNA ($p < 0.001$) at each time point (Figure 7-4C). Sham and control siRNA cells treated with DES for 6 and 24 h had a greater increase in AHCYL1 protein compared to sham and control siRNA cells not treated (0 h) with DES ($p < 0.05$). To examine expression of genes related to chicken oviduct development and major egg white proteins in response to estrogen, we examined expression of *cathepsin B* (*CTSB*), *CTSC*, *CTSS*, *ERBB receptor feedback inhibitor 1* (*ERRF1*), *pleiotrophin* (*PTN*), *gallinacin 11* (*GAL11*), *ovalbumin*, *lysozyme* (*LYZ*) and *LYZ2* using quantitative PCR analyses. As illustrated in Figure 7-4D to 7-4F, the expression levels for *CTSB*, *CTSC*, *CTSS*, *ERRF1*, *PTN*, *ovalbumin* and *LYZ2* mRNAs were decreased significantly by AHCYL1 knockdown as compared to naïve, sham and control siRNA treatments: *CTSB* to 0.49- ($p < 0.001$), *CTSC* to 0.51- ($p < 0.001$), *CTSS* to 0.46- ($p < 0.001$), *ERRF1* to 0.22- ($p < 0.001$), *PTN* to 0.41- ($p < 0.001$), *ovalbumin* to 0.61- ($p < 0.05$) and *LYZ2* to 0.31-fold ($p < 0.01$). However, the expression of *GAL11* and *LYZ* mRNAs increased significantly in response to AHCYL1 knockdown: *GAL11* to 1.64- ($p < 0.05$) and *LYZ* to 2.88-fold ($p < 0.001$). In addition, calcium release was reduced significantly in response to AHCYL1 knockdown as compared to control or control siRNA treated cells (Figure 7-4G). Moreover, immunoreactive AHCYL1 protein was less abundant in the cytoplasm of the chicken oviduct cells receiving DES treatment and AHCYL1 siRNA transfection as compared to treatment with DES and the control siRNA (Figure 7-4H).

Post-transcriptional action of miRNAs on AHCYL1

Expression of *AHCYL1* may be regulated at the post-transcriptional level by microRNAs (miRNAs); therefore, we performed a miRNA target validation assay. Analysis of potential miRNA binding sites within the 3'-UTR of the *AHCYL1* gene using the miRNA target prediction database (miRDB; <http://mirdb.org/miRDB/>) revealed six putative binding sites for *miR-124a*, *miR-1602*, *miR-1612*, *miR-1669*, *miR-1710* and *miR-1782* (Figure 7-5A). Therefore, we determined whether these miRNAs influenced *AHCYL1* expression via its 3'-UTR. A fragment of the *AHCYL1* 3'-UTR harboring binding sites for the miRNAs were cloned in downstream of the green fluorescent protein (GFP) reading frame, thereby creating a fluorescent reporter for function of the 3'-UTR region (Figure 7-5B). After co-transfection of eGFP-*AHCYL1* 3'-UTR and DsRed-miRNA, the intensity of GFP expression and percentage of GFP-expressing cells were analyzed by fluorescence microscopy and FACS. As illustrated in Figures 7-5C and 7-5D, in the presence of *miR-124a*, *miR-1669*, *miR-1710*, *miR-1782*, the intensity and percentage of GFP-expressing cells (27.7% in control vs. 14.2% in *miR-124a*, 17.1% in *miR-1669*, 19.4% in the *miR-1782* and 23.2% in *miR-1710*) were decreased. However, in the presence of *miR-1602* and *miR-1612*, there was no significant decrease in green fluorescence compared to the control (data not shown). Further results from quantitative PCR revealed that DES induced a 3.38- and 3.18-fold increase ($P < 0.01$) in expression of *miR-1710* and *-1782*, respectively, in the oviduct as compared to control chicks (Figure 7-5E). However, expression of *miR-124a* and *miR-1669* was decreased in DES-treated oviducts ($P < 0.05$). These results indicate that *miR-124a*, *miR-1669*, *miR-1710* and *miR-1782*, influence

AHCYL1 expression *in vitro* via its 3'-UTR which suggests that pos-transcriptional events regulate or influence *AHCYL1* expression in the chick oviduct.

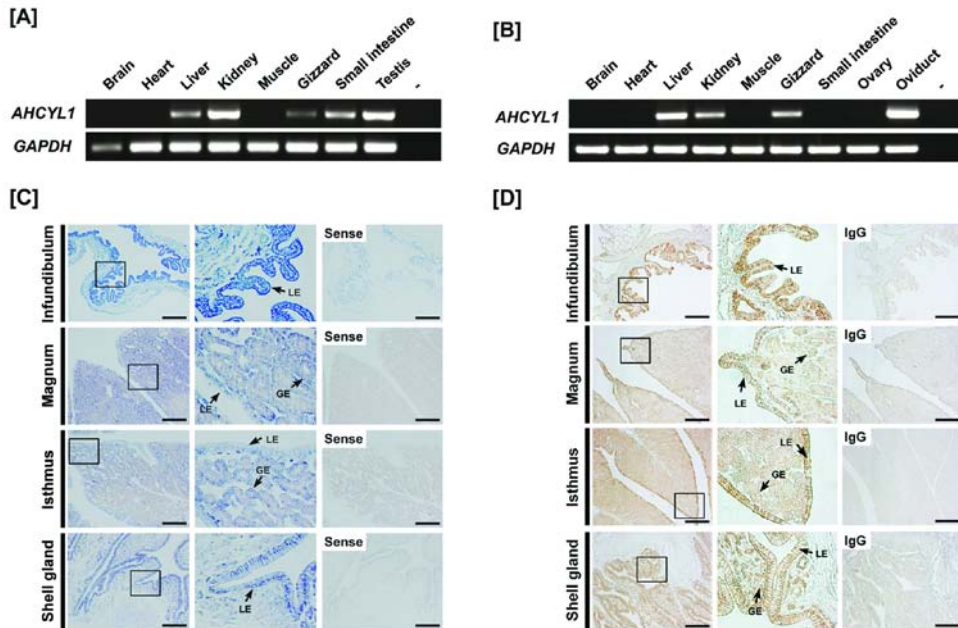


Figure 7-1. Expression of *AHCYL1* in chickens. [A and B] Expression of *AHCYL1* in various organs of male and female of chickens. Results of RT-PCR analysis using cDNA templates from different organs of male [A] and female [B] chickens with chicken *AHCYL1* and chicken *GAPDH*-specific primers. [C] *In situ* hybridization analyses of *AHCYL1* mRNAs in the chicken oviduct. Cross-sections of the four components of the chicken oviduct (infundibulum, magnum, isthmus and shell gland) were hybridized with antisense or sense chicken *AHCYL1* cRNA probes. [D] Immunoreactive *AHCYL1* protein in the chicken oviduct. For the IgG control, normal mouse IgG was substituted for the primary antibody. Sections were not counterstained. Legend: LE, luminal epithelium; GE, glandular epithelium; *Scale bar* represents 100 μm .

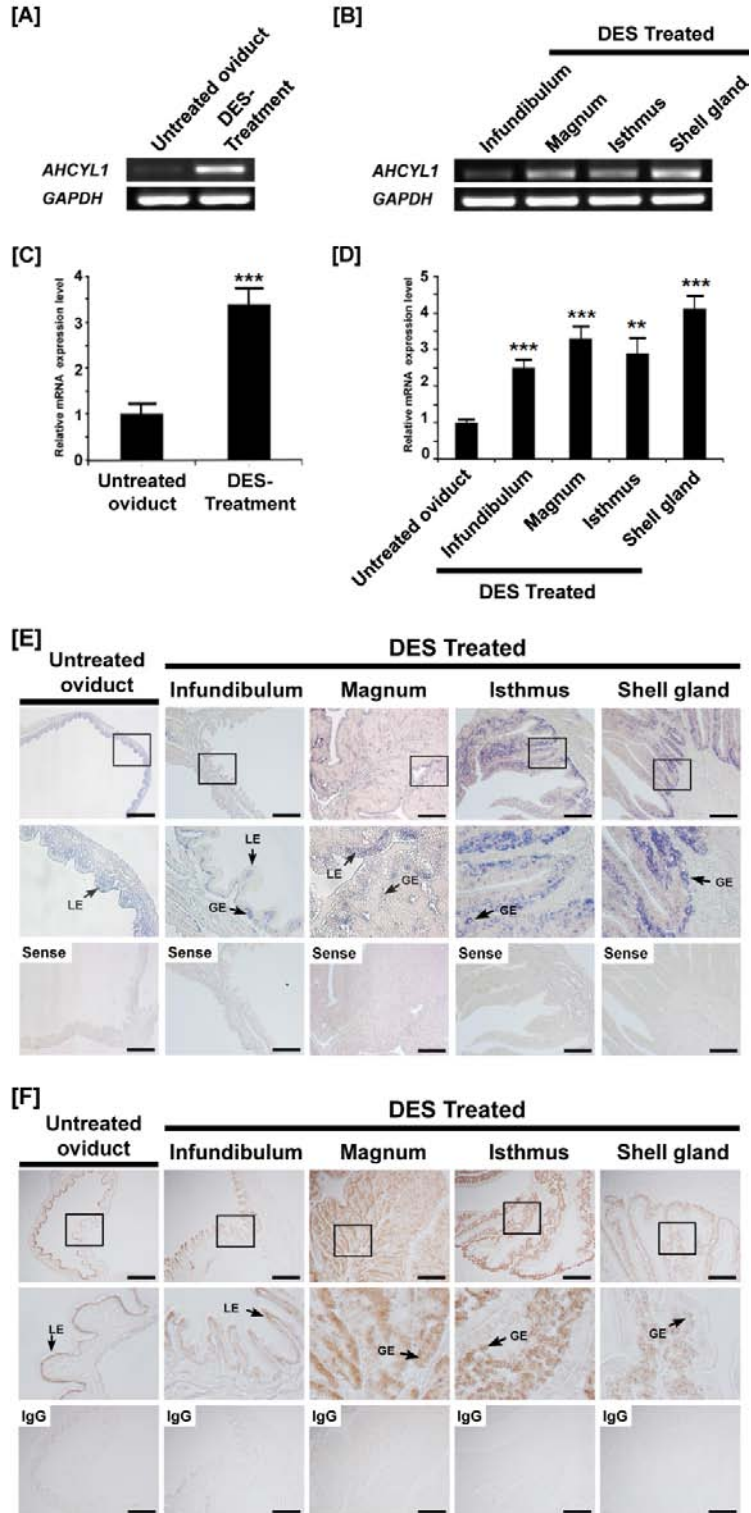


Figure 7-2. Effect of DES on tissue specific expression of chicken *AHCYL1*. Both RT-PCR [A and B] and q-PCR [C and D] analyses were performed using cDNA templates from DES-treated and control chicken oviducts. These experiments were conducted in triplicate and normalized to control *GAPDH* expression. [E] *In situ* hybridization analyses revealed cell-specific expression of *AHCYL1* mRNA in oviducts of DES-treated and untreated chicks. Cross-sections of the four segments of chicken oviduct (infundibulum, magnum, isthmus, and shell gland) treated with DES or vehicle were hybridized with antisense or sense chicken *AHCYL1* cRNA probes. [F] Immunoreactive *AHCYL1* protein in oviducts of DES-treated and untreated chicks. For the IgG control, normal goat IgG was substituted for the primary antibody. Sections were not counterstained. Legend: Untreated oviduct, non-treated whole oviduct; DES Treatment, DES treated whole oviduct; LE, luminal epithelium; GE, glandular epithelium; *Scale bar* represents 100 μm . The asterisks denote statistically significant differences (** $P < 0.01$ and *** $P < 0.001$).

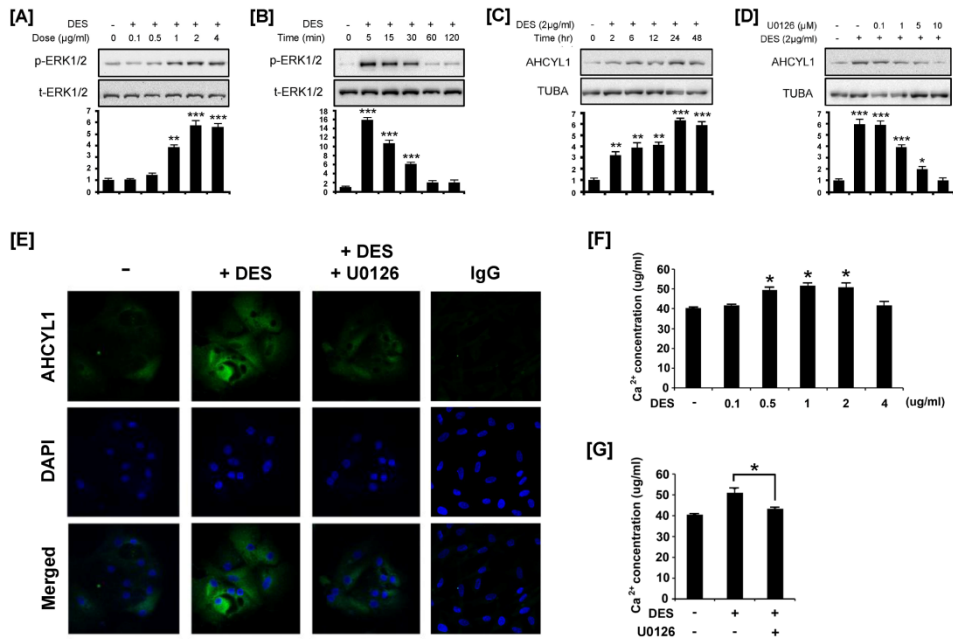


Figure 7-3. DES-induced phosphorylation of ERK1/2, stimulation of AHCYL1 and calcium release in chicken oviduct epithelial cells. [A and B] Dose-dependent and time-dependent expression of phosphorylated ERK1/2 in DES-treated chicken oviduct epithelial cells. Blots were imaged to calculate normalized values presented in graphs (bottom) by measurements of levels of phosphorylated protein relative to total protein. [C] In the DES-treated (2 μg/ml) and non-treated chicken oviduct cells, AHCYL1 protein levels were investigated to determine time-dependent effects of DES. [D] In chicken oviduct cells treated with DES (2 μg/ml) or both DES and an ERK1/2 inhibitor (U0126) for 24h, according to the result of a preliminary study to optimize time-dependent treatment effects, AHCYL1 protein decreased due to effects of U0126. In [C and D], blots were imaged to calculate the normalized values presented in graphs (bottom) for relative abundance of AHCYL1 protein and alpha-

tubulin (TUBA) protein. [E] Immunofluorescence microscopy detected AHCYL1 protein in chicken oviduct epithelial cells treated with DES or both DES and an ERK1/2 inhibitor. AHCYL1 protein was barely detectable in untreated, as well as DES- and ERK1/2 inhibitor-treated cells, but abundant in cytoplasm of DES-treated oviduct epithelial cells. Cell nuclei were stained with DAPI (blue). All images were captured at 40X objective magnification. [F and G] Cells were grown in media with various concentration of DES for 24 h or both DES and an ERK1/2 inhibitor. Then, calcium concentration from the cells was measured. The asterisk denotes a significant effect ($***P < 0.001$, $**P < 0.01$ and $*P < 0.05$).

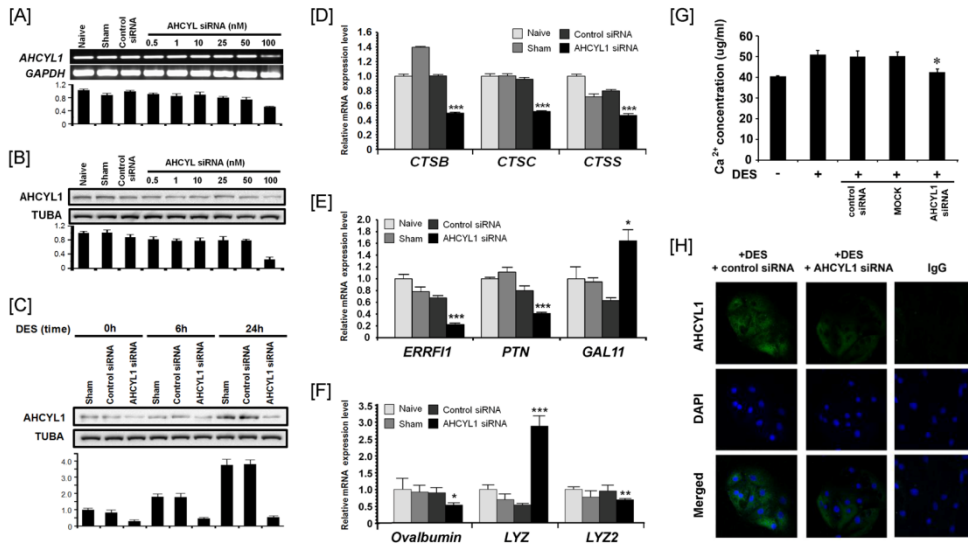


Figure 7-4. AHCYL1 knockdown decreased expression of genes associated with oviduct development and production of egg white proteins. [A] In the control group (naïve, sham and control siRNA treatment) and AHCYL1 silencing group (dose-dependent manner), *AHCYL1* mRNA levels were quantified by RT-PCR and quantitative RT-PCR analyses. [B] In the control group (naïve, sham and control siRNA treatment) and AHCYL1 silencing group (dose-dependent), immunoreactive AHCYL1 protein was quantified by western blotting. [C] The effects of DES treatment (time-dependent manner) on control cells and cells in which AHCYL1 was silenced is shown in Panels D to F. Total RNA isolated from chicken oviduct epithelial cells treated with AHCYL1 siRNA (100 nM) affected expression of *CTSB*, *CTSC*, *CTSS*, *ERRFI1*, *PTN*, *GAL11*, *ovalbumin*, *LYZ* and *LYZ2* mRNAs as determined using quantitative RT-PCR analyses. Legend: *CTSB*, cathepsin B; *CTSC*, cathepsin C; *CTSS*, cathepsin S; *ERRFI1*, ERBB receptor feedback inhibitor 1; *PTN*, pleiotrophin,

GAL11; gallinacin 11, LYZ; lysozyme. [G] Cells were grown in medium with the absence and presence of DES with siRNAs and then changes in amount of calcium released from the cells was measured. [H] Immunofluorescence microscopy detected AHCYL1 protein in chicken oviduct epithelial cells treated with DES with siRNAs. Cell nuclei were stained with DAPI (blue). All images were captured at 40X objective magnification. The asterisks denote statistically significant differences ($***P < 0.001$, $**P < 0.01$ and $*P < 0.05$).

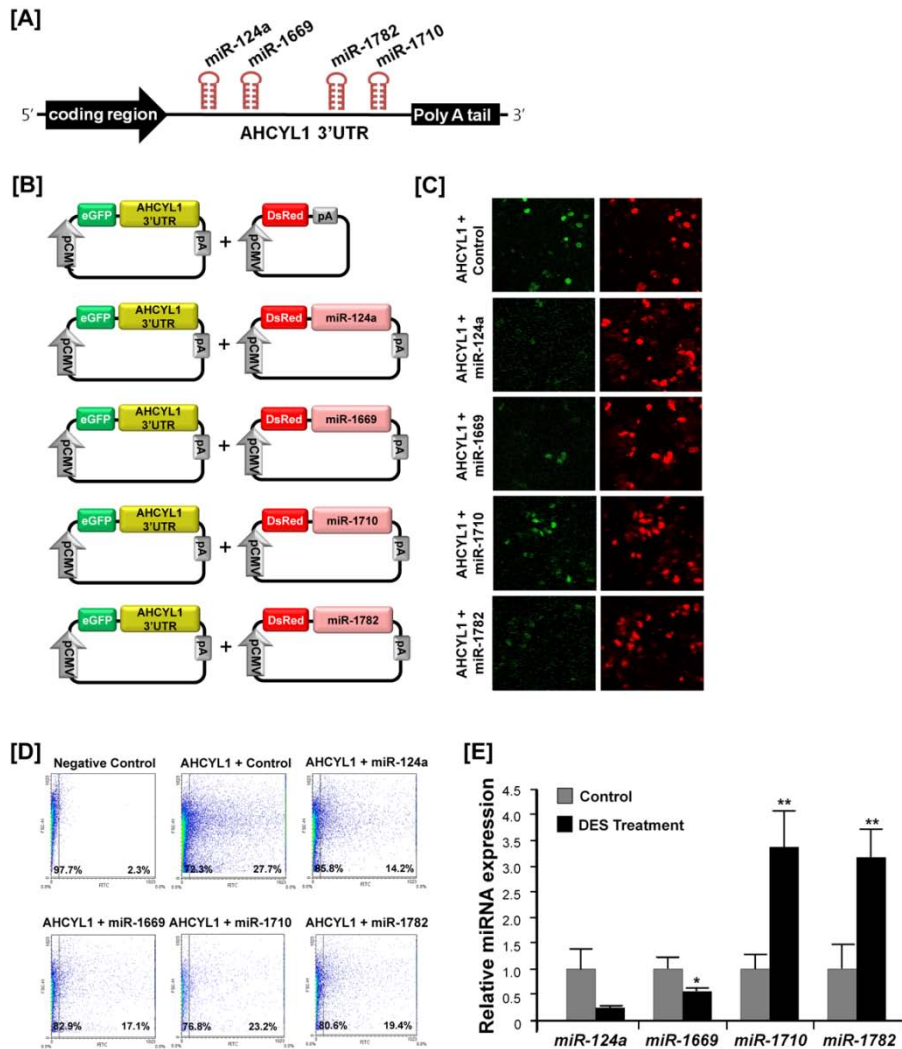


Figure 7-5. *In vitro* target assay of miR-124a, miR-1602, miR-1612, miR-1669, miR-1710 and miR-1782 on AHCYL1 transcript. [A] Diagram of miR-124a, miR-1669, miR-1710 and miR-1782 binding sites in AHCYL1 3'-UTR. [B] Expression vector maps for eGFP with AHCYL1 3'UTR and Ds-Red with each miRNA. The 3'-UTR of the AHCYL1 transcript was subcloned between the eGFP gene and the polyA tail to generate the fusion construct of the GFP transcript following the miRNA target

3'-UTR (pcDNA-eGFP-3'UTR) (upper panel) and miRNA expression vector was designed to co-express DsRed and each miRNA (pcDNA-DsRed-miRNA) (lower panel). [C and D] After co-transfection of pcDNA-eGFP-3'UTR for the *AHCYL1* transcript and pcDNA-DsRed-miRNA for the *miR-124a*, *miR-1669*, *miR-1710* and *miR-1782*, the fluorescence signals of GFP and DsRed were detected using FACS [C] and fluorescent microscopy [D]. [E] q-PCR analyses were performed using cDNA templates from DES-treated and untreated chicken oviducts (mean \pm SEM). These experiments were conducted in triplicate and normalized to control U6 snRNA expression. The asterisks denote statistically significant differences (** $P < 0.01$ and * $P < 0.05$).

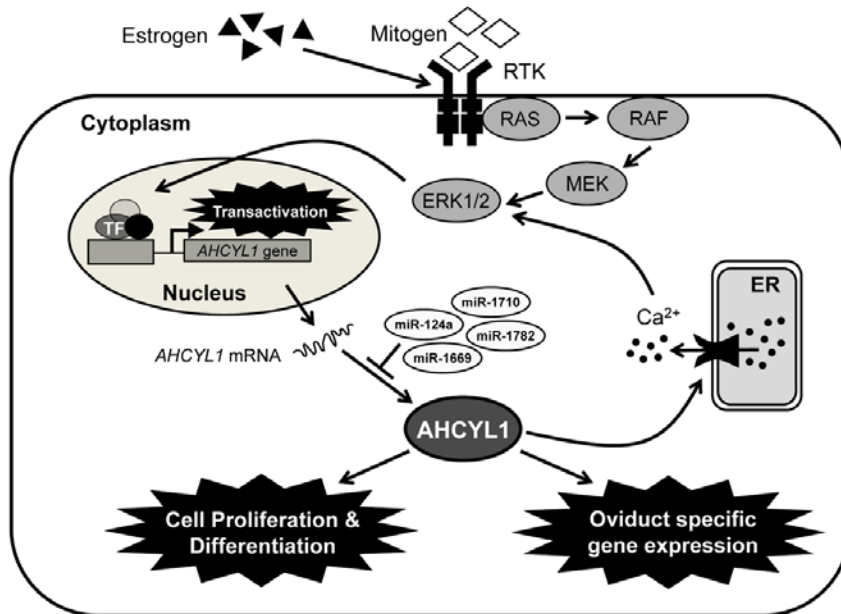


Figure 7-6. Schematic illustrating the current working hypothesis on estrogen-induced ERK1/2 MAPK signaling cascades in chicken oviduct cells. Evidence from the present study indicates that estrogen stimulates the classical estrogen- and alternative ERK1/2 MAPK signaling pathways. Legend: RTK, receptor tyrosine kinase; RAS, synaptic Ras-GTPase-activating protein; RAF (also known as MAPK3), mitogen-activated protein kinase (MAPK) kinase kinase; MEK (also known as MAPK2), MAPK kinase; ERK1/2, extracellular signal-regulated kinase; ERE, estrogen response element; ER, endoplasmic reticulum.

Table 7-1. Pairwise comparison of AHCYL1 proteins between chicken, mammalian and fish species.

Species	Symbol	Identity (%)
Chicken (<i>Gallus gallus</i>)	AHCYL1	-
vs. Human (<i>Homo sapiens</i>)	AHCYL1	96.3
vs. Orangutan (<i>Pongo abelii</i>)	AHCYL1	96
vs. Mouse (<i>Mus musculus</i>)	Ahcy11	96.3
vs. Rat (<i>Rattus norvegicus</i>)	Ahcy11	94
vs. Cattle (<i>Bos taurus</i>)	AHCYL1	97.8
vs. Dog (<i>Canis lupus familiaris</i>)	AHCYL1	98
vs. Zebrafish (<i>Danio rerio</i>)	ahcy11	91

Table 7-2. Primers used for quantitative RT-PCR.

Gene	Sequence (5' →3'):	GenBank	Product
	Forward and Reverse	Accession No.	Size (bp)
<i>AHCYL1</i>	GCCATTCCAACACGGAGAT	NM_001030913.1	179
	GATAGAGAGGACAAAGGTGGG		
<i>CTSB</i>	CTGGAGAAATGTGAATGGCG	NM_205371.1	157
	CTGGGGACTGAAGACTGGCT		
<i>CTSC</i>	GCACTACGGCATCACATCCT	XM_417207.2	151
	AACCTGCTCCCCTGACACAT		
<i>CTSS</i>	TGCCACGTGCTCCAAGTATG	NM_001031345.1	173
	CGTGGTTCACCTCCTGTGTG		
<i>ERRFI1</i>	AGGAGAGGAGGAGAGTATGG	XP_417525.2	125
	CTGGAACACAGAAGCAGAAC		
<i>PTN</i>	CCCTGCTGAACCCAGTGATA	XM_416358.2	174
	AAAATGCCCCCATCCTCTC		
<i>GAPDH</i>	CAGAACATCATCCCAGCGTC	NM_204305	133
	GGCAGGTCAGGTCAACAACA		

5. Discussion

Results of the present study are novel as they provide the first comparisons among chicken and mammalian *AHCYL1* genes with respect to structure, phylogenetic evolution, tissue specific expression of *AHCYL1* mRNA and protein, and regulation of expression by estrogen in an ERK1/2-dependent cell signaling cascade. Our results also indicate that *AHCYL1* is post-transcriptionally regulated by several miRNAs and knockdown of *AHCYL1* results in down-regulation of genes critical to development of the chick oviduct in response to estrogen in chicks. These results support our hypothesis that *AHCYL1* is required for growth, development and functional aspects of the mature oviduct of hens in response to estrogen during their reproductive cycle.

We reported that differential gene profiling data of the chick oviduct showed that the avian homolog of human *S-adenosylhomocysteine hydrolase like protein 1* (*AHCYL1*) transcript is highly expressed in chicks treated with DES (Song et al., 2011c). *AHCYL1* regulates numerous important cellular processes, especially Ca^{2+} -dependent processes, by modulating concentrations of Ca^{2+} in cytoplasm of cells (Ando et al., 2009; Streb et al., 1983). However, little is known about expression and function of *AHCYL1* in the oviduct of any species (Ando et al., 2003; Cooper et al., 2006; Dekker et al., 2002) although *AHCYL1* has potential role(s) in many important biological events such as development, fertilization, gene expression, secretion and cell death (Ando et al., 2009; Berridge et al., 2000; Streb et al., 1983).

In the present study, we found that the chicken *AHCYL1* gene consists of 16 exons encoding 540 amino acid residues and that it has high homology (greater than 90%) to mammalian *AHCYL1* proteins (Table 7-1). In addition, expression of *AHCYL1* mRNA in kidney, liver, testis, oviduct, and to a lesser extent, in gizzard and small intestine of chickens was found. However, expression was not detected in other organs analyzed in either sex. Furthermore, as illustrated in Figures 7-1C and 7-1D, *AHCYL1* mRNA and protein were most abundant in the LE of the infundibulum and shell gland, and at lower abundance in GE and LE of the magnum and isthmus, and GE of the infundibulum and shell gland of the oviduct. These results indicate that cell- and tissue-specific expression of *AHCYL1* may be associated with functional mechanism(s) of chicken oviduct functions including calcium metabolism for formation of the egg shell and oviposition (egg laying).

Generally, the biological actions of estrogen are mediated by its cognate nuclear receptors, estrogen receptors alpha (ESR1) and beta (ESR2) which activate and recruit a variety of transcription factors with estrogen response elements to the 5' upstream region of target genes (Dougherty and Sanders, 2005; Hewitt et al., 2005). Indeed, several steroid hormones, including estrogen, are involved in many physiological and developmental events requiring modification of cell-type and tissue-specific gene expression (Dougherty and Sanders, 2005; Okada et al., 2005). Although various animal models have been used to investigate developmental and hormonal mechanism of oviduct growth, development and differentiation, the most well studied

and informative model is the chick oviduct (Dougherty and Sanders, 2005). During development of the chicken oviduct, estrogen stimulates proliferation and cytodifferentiation of epithelial cells to tubular gland cells and expression of oviduct-specific genes (Palmiter and Wrenn, 1971a; Socher and Omalley, 1973). In particular, the differentiated tubular gland cells of the magnum synthesize and secrete the egg-white proteins including ovalbumin, lysozyme, ovotransferrin, ovomucoid and avidin during egg formation (Kohler et al., 1968). Indeed, the magnum is the most estrogen-responsive segment of the chicken oviduct. The administration of exogenous estrogen to neonatal chicks stimulates an 8-fold increase in wet weight of the magnum within three days (Munro and Kosin, 1943). Consistent with these results, we reported that exogenous DES affects growth, development and differentiation of the chicken oviduct (Seo et al., 2009) and discovered candidate genes and pathways regulating oviduct development in chickens (Song et al., 2011c). In the present study, as illustrated in Figure 7-2, DES treatment increased *AHCYL1* mRNA and protein in LE of the infundibulum and magnum, and GE of the isthmus and shell gland of the chick oviduct. These results strongly support our hypothesis that estrogen-mediated *AHCYL1* gene expression plays a crucial role(s) in growth, differentiation and function of the chicken oviduct.

Results of the current study revealed that estrogen stimulates activation of ERK1/2 phosphorylation, expression of *AHCYL1*, and calcium release by oviduct cells of chicks. Mitogen-activated protein kinases (MAPKs) are highly conserved in most organisms and respond to various extracellular stimuli such as mitogens, heat

shock, stress and cytokines (Widmann et al., 1999). Among the three well-characterized subfamilies of MAPKs, the ERK1/2 MAPK pathway plays important roles in growth and differentiation processes of female reproductive organs during early pregnancy, including embryonic and placental development (Daoud et al., 2005a; Fernandez-Serra et al., 2004a; Kim et al., 2008; Wang et al., 2004b). However, little is known about the ERK1/2 MAPK signal cascade in growth, development and differentiation of female reproductive tract such as oviduct and uterus. In the present study, DES induced a rapid increase in phosphorylation of ERK1/2 MAPK by 5 min and this effect was maintained to 30 min before declining by 60 min (Figure 7-3). In addition, the same dose of DES increased AHCYL1 protein 3-fold within 2 h and 6.3-fold by 24 h and induced calcium release in a dose-dependent manner. Meanwhile, treatment of chicken oviduct epithelial cells with both an ERK1/2 inhibitor (U0126) and DES decreased AHCYL1 protein in the cytoplasm of those cells and inhibited calcium release despite DES treatment. These results strongly suggest that estrogen influences development and differentiation of the chick oviduct by activating AHCYL1 and calcium release in an ERK1/2 MAPK-dependent manner.

RNA interference methods such as the siRNA-mediated recognition of homologous target mRNA molecule have been used successfully in biological research to examine effects of silencing target genes (Krueger et al., 2007). In this study, we determined that AHCYL1 knockdown decreases expression of several genes associated with oviduct development and differentiation including several members of the cathepsin (CTS) family of lysosomal proteases. CTSs degrade

extracellular matrix (ECM) molecules including collagens, laminin, fibronectin and proteoglycans and they are also involved in catabolism of intracellular proteins and processing of pro-hormones. In addition, the CTSs regulate intracellular protein metabolism (Turk et al., 2001), bone resorption (Saftig et al., 1998) and antigen presentation (Shi et al., 1999), as well as cell transformation, differentiation, motility, and adhesion (Obermajer et al., 2008). In the present study, the expression of *cathepin B (CTSB)*, *CTSC*, and *CTSS* mRNAs was significantly decreased by AHCYL1 knockdown compared to naïve, sham and control siRNA treatments (Figure 7-4D). Furthermore, the expression of *ERBB receptor feedback inhibitor 1 (ERRF1)*, *pleiotrophin (PTN)*, *gallinacin II (GALII)*, *ovalbumin*, *lysozyme (LYZ)* and *LYZ2* mRNAs, which are estrogen-induced genes or genes for egg white proteins expressed in the oviduct epithelial cells of the chicken were also significantly affected by AHCYL1 knockdown. These results suggest that estrogen-induced AHCYL1 regulates downstream genes for oviduct growth/remodeling and maintenance of oviduct function during the reproductive cycle of chickens.

MicroRNAs (miRNAs), as post-transcriptional regulators, play essential roles in a wide variety of biological processes including vertebrate growth, development and differentiation (Bartel, 2009). In the current study, we performed a miRNA target validation assay, based on the hypothesis that *AHCYL1* expression is regulated at the post-transcriptional level by miRNAs. As illustrated in Figure 7-5, co-transfection of eGFP-*AHCYL1* 3'-UTR and DsRed-miRNA decreased the percentage of GFP-positive cells and GFP fluorescence density in *miR-124a*, *miR-1669*, *miR-*

1710 and *miR-1782* transfected cells, but not in cell transfected with *miR-1602* and *miR-1612* when compared to control cells. However, as illustrated in Figure 7-5E, the *in vivo* DES-mediated decrease in *miR-124a* and *miR-1669* supports this hypothesis, whereas the DES mediated increase in *miR-1710* and *miR-1782* is inconsistent with the *in vitro* data. These results indicate that *miR-1710* and *miR-1782* may act indirectly or regulate expression of other DES-regulated genes *in vivo*. Correctively, these four miRNAs influence *AHCYL1* expression *in vitro* its 3'-UTR which suggests that post-transcriptional regulation influences *AHCYL1* expression in the chick oviduct. In addition, we propose that, of these four miRNAs, *miR-124a* and *miR-1669* are closely related to the regulatory pathways of oviduct development and differentiation in chickens; however, this requires further investigation.

Based on the collective results from the present studies, we propose a model (Figure 7-6) in which estrogen activates receptor tyrosine kinase (RTK) and phosphorylated RTK activates RAS-RAF-MEK to stimulate the ERK1/2 signal transduction cascade to effect expression of genes affecting growth- and/or development of the chick oviduct and to stimulate oviduct-specific genes for the production of egg white proteins and calcium release during egg formation. In conclusion, results of the present study provide important insights into the mechanism by which *AHCYL1* regulates growth, development and functional aspects of the mature oviduct of hens in response to estrogen-mediated ERK1/2 MAPK cell signaling during their reproductive cycle.

CHAPTER 8

Paradoxical Expression of AHCYL1 Affecting Ovarian Carcinogenesis between Chickens and Women

1. Abstract

We investigated *S*-adenosylhomocysteine hydrolase-like protein 1 (*AHCYL1*) gene expression in human epithelial ovarian cancer (EOC) using the chicken, which is the most relevant animal model. Ovarian cancer was detected in 10 of 136 laying hens (7.4%). Results of the present study indicated that *AHCYL1* mRNA and protein are most abundant in the glandular epithelium of adenocarcinoma of cancerous, but not normal ovaries of hens. In addition, bisulfite sequencing to examine methylation patterns in the promoter region of the *AHCYL1* gene revealed that 30-38% of the three CpG sites were demethylated in ovarian cancer cells as compared to normal ovarian cells. Furthermore, in human ovarian cancer cells such as OVCAR-3, *AHCYL1* protein was predominantly in the nucleus and had a similar expression pattern to that in chicken ovarian cancer cells. Thereafter, we examined the prognostic value of *AHCYL1* expression in patients with EOC using multivariate linear logistic regression and Cox' proportional hazard analyses. In 109 human patients with EOC, 14 (12.8%), 41 (37.6%) and 54 (49.6%) patients showed weak, moderate and strong expression of *AHCYL1* protein, respectively. However, intermediate or high expression of *AHCYL1* protein was a favorable factor for overall responses (adjusted odds ratio, 7.23; 95% confidence interval, 1.36-38.39), and for progression-free survival (PFS; adjusted hazard ratio, 0.20; 95% confidence interval, 0.07-0.55). From these results we conclude that *AHCYL1* expression is associated with ovarian carcinogenesis as an oncogene in chickens, whereas it plays the role of tumor suppressor in human EOC suggesting a paradoxical function of *AHCYL1* in ovarian

carcinogenesis.

2. Introduction

Although maximal cytoreduction and various types of chemotherapeutic agents have contributed to improve clinical outcomes in patients with epithelial ovarian cancer (EOC), advanced-stage disease, poor differentiation and chemoresistance still lead to a poor prognosis (Suh et al., 2010). In particular, more than two-thirds of patients with EOC are diagnosed with advanced-stage disease due to lack of specific symptoms, no effective screening methods, and treatment methods that fail to prolong their survival with only 25% of patients having a 5-year survival rate (Heintz et al., 2003; Heintz et al., 2006). Thus, recent strategies are being investigated to overcome the limitation in terms of both targeted molecular therapy (Banerjee and Kaye, 2011), and novel biomarkers for early diagnosis and prediction of prognosis (Dutta et al., 2010).

For developing biomarkers for EOC, the laying hen is the only animal that spontaneously develops tumors from ovarian surface epithelium in contrast to the artificial nature of the induced tumors in rodent models (Barua et al., 2009; Stammer et al., 2008; Vanderhyden et al., 2003). Recently, we have shown that SERPINB3 detected during ovarian carcinogenesis in the chicken model may be a prognostic factor for patients with EOC (unpublished data). In the current study, we investigated whether *S*-adenosylhomocysteine hydrolase-like protein 1 (AHCYL1), another protein detected in ovarian carcinogenesis of the chicken model, could serve as a novel biomarker for human EOC.

AHCYL1 consists of an N-terminal hydrophilic domain (106 amino acids) and a C-terminal domain (424 amino acids), which is homologous with 51% protein identity to the methylation pathway enzyme, *AHCYL* (Dekker et al., 2002). It is the evolutionarily conserved and ubiquitously expressed enzyme that catalyzes the reversible hydrolysis of *S*-adenosyl-*L*-homocysteine, a byproduct of the *S*-adenosyl-*L*-homomethionine-dependent methyltransferase reaction, into adenosine and homocysteine (Turner et al., 2000). Furthermore, AHCYL1 acts like an inositol 1,4,5-triphosphate receptor (IP₃R)-binding protein (termed IP₃R-binding protein released with inositol 1,4,5-triphosphate, or IRBIT) by competitively inhibiting the interaction of IP₃ with IP₃R (Ando et al., 2006; Ando et al., 2003). As a result, AHCYL1 regulates IP₃-induced Ca²⁺ signaling which plays crucial roles in numerous cellular processes including gene expression and cell death (Berridge et al., 2000).

Recently, we have shown regulation of AHCYL1 mRNA and protein expression by estrogen in a tissue and cell-specific manner in chickens (unpublished data). However, there is little known about expression or function of AHCYL1 in ovarian carcinogenesis. Thus, we compared the distribution and localization of AHCYL1 between normal and cancerous ovaries of chickens, and then AHCYL1 expression among normal and cancer cells of their ovaries, human EOC cell lines (OVCAR-3 and SKOV-3) and a human ovarian teratocarcinoma cell line (PA-1). Finally, we investigated the prognostic value of AHCYL1 expression in patients with EOC.

3. Materials and Methods

Experimental Animals and Animal Care

Approval for the experimental use of chickens was obtained from the Institute of Laboratory Animal Resources, Seoul National University (SNU-070823-5). White Leghorn (WL) chickens were managed according to approved standards for operation of the University Animal Farm, Seoul National University, Korea for reproduction and embryo manipulation procedures, as well as standard operating protocols in our laboratory. All chickens had free access to feed and water for *ad libitum* consumption.

Tissue Samples in the Chicken Model

A total 136 mature hens (88 over 36 months and 48 over 24 months of age), which had stopped laying eggs, were euthanized for collection of cancerous ovarian tissues. We obtained cancerous ovarian tissues from 10 hens and normal ovarian tissues from 10 egg-laying hens of age. We evaluated tumor stage of 10 hens with cancerous ovaries according to characteristics features of chicken ovarian cancer (Barua et al., 2009; Lim et al., 2011b). Three hens had stage III disease because ovarian tumor cells had metastasized to the gastrointestinal (GI) tract and liver surface with profuse ascites in the abdominal cavity. Five hens had tumor cells spread to distant organs including liver parenchyma, lung, GI tract and oviduct with profuse

ascites, indicating stage IV disease. Two hens had stage I disease as tumors were limited to their ovaries. Subsets of these samples were fixed in 4% paraformaldehyde for further analyses. After 24 h, fixed tissues were changed to 70% ethanol for 24 h and then dehydrated and embedded in Paraplast-Plus (Leica Microsystems, Wetzlar, Germany). Paraffin-embedded tissues were sectioned at 5 μm and stained with hematoxylin and eosin (Figure 8-7). Epithelial ovarian cancers in chickens were classified based on the cellular subtypes and patterns of cellular differentiation with reference to ovarian malignant tumor types in humans (Barua et al., 2009).

RNA Isolation

Total cellular RNA was isolated from frozen tissues using Trizol reagent (Invitrogen, Carlsbad, CA) according to the manufacturer's recommendations. The quantity and quality of total RNA was determined by spectrometry and denaturing agarose gel electrophoresis, respectively.

Semi-quantitative RT-PCR Analysis

The expression of *AHCYLI* mRNA in normal and cancerous ovaries of chickens was investigated using semi-quantitative RT-PCR as previously described (Song et al., 2007b). Briefly, complementary DNA was synthesized from 2 μg total cellular RNA using random hexamer (Invotrogen, Carlsbad, CA) and oligo (dT) primers and AccuPower[®] RT Premix (Bioneer, Daejeon, Korea). After PCR, equal

amounts of reaction product were analyzed using a 1% agarose gel, and PCR products were visualized using ethidium bromide staining. The amount of DNA present was quantified by measuring the intensity of light emitted from correctly sized bands under ultraviolet light using a Gel Doc™ XR+ system with Image Lab™ software (Bio-Rad).

Quantitative RT-PCR Analysis

Gene expression levels were measured using SYBR® Green (Sigma, St. Louis, MO, USA) and a StepOnePlus™ Real-Time PCR System (Applied Biosystems, Foster City, CA, USA). The *GAPDH* gene was analyzed simultaneously as a control and used for normalization to account for variation in loading. Each target gene and *GAPDH* were analyzed in triplicate. ROX dye (Invitrogen) was used as a negative control for the fluorescence measurements. Sequence-specific products were identified by generating a melting curve in which the C_T value represented the cycle number at which a fluorescent signal was statistically greater than background, and relative gene expression was quantified using the $2^{-\Delta\Delta C_T}$ method (Livak and Schmittgen, 2001). For the control, the relative quantification of gene expression was normalized to the C_T value for the control oviduct.

In Situ Hybridization Analysis

For *in situ* hybridization probes, PCR products were generated and gel-

extracted, and then cloned into the pGEM-T vector (Promega, Madison, WI) as described previously (Lim et al., 2011a). After verification of the sequences, plasmids containing the correct gene sequences were amplified with T7- and SP6-specific primers, and then digoxigenin (DIG)-labeled RNA probes were transcribed using a DIG RNA labeling kit (Roche Applied Science, Indianapolis, IN). After hybridization and blocking, the sections were incubated overnight with sheep anti-DIG antibody conjugated to alkaline phosphatase (Roche Applied Science, Indianapolis, IN). The signal was visualized by exposure to a solution containing 0.4 mM 5-bromo-4-chloro-3-indolyl phosphate, 0.4 mM nitroblue tetrazolium and 2 mM levamisole (Sigma).

Cell culture

Three human ovarian epithelial cancer cell lines and two chicken primary ovarian cell lines were used in this study. Human ovarian cancer cell lines (OVCAR-3, SKOV-3, and PA-1) were obtained from the American Type Culture Collection (ATCC, Manassas, VA) and cultured according to supplier's directions. In addition, three different primary ovarian surface epithelial cell lines from three normal and cancerous chickens, respectively, were isolated and cultured as previously described (Giles et al., 2006; Shepherd et al., 2006) with some modifications. The purity of these cell cultures was confirmed based on their by expression of cytokeratin (epithelial cells) or vimentin (mesenchymal cells) proteins (Giles et al., 2006).

Western Blot Analyses

Ovarian cancer cells and normal ovarian cells obtained from hens were rinsed with cold PBS and lysed by homogenization for 5 min in ice cold lysis buffer. Proteins were denatured, separated using 10% SDS-PAGE and transferred to nitrocellulose. Blots were developed using enhanced chemiluminescence detection (SuperSignal West Pico, Pierce, Rockford, IL) and quantified by measuring the intensity of light emitted from correctly sized bands under ultraviolet light using the ChemiDoc EQ system and Quantity One software (Bio-Rad, Hercules, CA). Immunoreactive AHCYL1 protein was detected using an anti-human AHCYL1 monoclonal antibody (catalog number: ab56761; abcam, Cambridge, UK) at a final dilution 1:1000. As a loading control, western blotting with mouse anti-beta actin IgG (Catalog number sc-47778; Santa Cruz Biotechnology Inc.) was performed.

Immunofluorescence Microscopy for Detecting AHCYL1 Activation

Each type of cell was seeded onto Lab-Tek chamber slides (Nalge Nunc International, Rochester, NY). After 24 h, cells were fixed with -20°C methanol and immunofluorescence staining was performed using an anti-human AHCYL1 monoclonal antibody (Abcam plc, Cambridge, UK). Cells were then incubated with Alexa Fluor 488 rabbit anti-goat IgG secondary antibody (A21222, Invitrogen). Slides were overlaid with DAPI before images were captured using a Zeiss confocal microscope LSM710 (Carl Zeiss) fitted with a digital microscope camera AxioCam and Zen 2009 software.

Prediction of Transcription Factor-Binding cis-Elements

The presence of transcription factor-binding *cis*-elements within the AHCYL1 promoter region was predicted using a bioinformatics tool for orthologous sequences (TFSEARCH ver. 1.3; <http://www.cbrc.jp/research/db/TFSEARCH.html>).

Bisulfite Sequencing

DNA samples were prepared using an AccuPrep Genomic DNA Extraction Kit (Bioneer) and converted using MethylEasyTMXceed (Human Genetic Signatures, North Ryde, NSW, Australia) according to the manufacturer's instructions. For amplifying the converted DNA, PCRs were performed and the PCR products were cloned into the pGEM-T easy vector (Promega, Madison, WI) and sequenced using an ABI Prism 3730 XL DNA Analyzer (Applied Biosystems, Foster City, CA).

Human Study Population

Clinico-pathologic data were extracted from a database of patients with EOC between June 2003 and March 2009. The current study was approved by the Institutional Review of Board of Seoul National University's Bundang Hospital. The inclusion criteria were as follows: patients diagnosed with EOC; those treated with maximum cytoreductive surgery followed by adjuvant taxanes- and platinum-based

chemotherapy if indicated; those showing Eastern Cooperative Oncology Group (ECOG) performance status of 0-2; and those without underlying disease affecting prognosis.

Optimal cytoreduction was defined as a residual tumor ≤ 1 cm while suboptimal cytoreduction was defined as a residual tumor > 1 cm in maximal diameter. All patients except those with the International Federation of Gynecology and Obstetrics (FIGO) stage IA or IB with grade 1 or 2 disease received adjuvant chemotherapy using paclitaxel (175 mg/m^2)/carboplatin (AUC 5.0) or paclitaxel (175 mg/m^2)/cisplatin (75 mg/m^2) for 1 or 2 weeks after surgery, and the chemotherapy was repeated every 3 weeks for 6 cycles.

Tumor response was evaluated by the Response Evaluation Criteria in Solid Tumors (RECIST) and serum CA-125 levels using a radioimmunoassay kit (Fujirebio Diagnostics, Malvern, PA, USA) (Kim et al., 2010; Panici et al., 2005). A complete response (CR) to treatment was defined as the disappearance of all measurable disease for at least 4 weeks and normalization of serum CA-125 levels at the end of therapy. A partial response (PR) was defined as a 30 % reduction in the product of the transverse diameters of each measurable lesion for at least 4 weeks or a complete response without normalization of serum CA-125 levels. Overall response (OR) was defined as the disease state with CR or PR. Progression-free survival (PFS) was defined as the time elapsed from the date of completion of primary adjuvant chemotherapy to the date of clinically proven resumption of growth of the tumor.

Overall survival (OS) was calculated from the date of staging laparotomy to the date of cancer-related death or the end of the study.

Immunohistochemistry

The localization of AHCYL1 protein in normal and cancerous ovaries of hens was evaluated by immunohistochemistry (IHC) using an anti-human AHCYL1 monoclonal antibody at a final dilution of 1:500 (2 µg/ml) (Abcam plc, Cambridge, UK). Antigen retrieval was performed using the boiling citrate method as described previously (Song et al., 2006). A histological section of ovarian cancer tissue was used as a positive control, whereas negative controls included normal ovarian tissue or cancerous ovarian tissue where the primary antibody was substituted with purified non-immune mouse IgG at the same final concentration.

For IHC of human ovarian cancer tissues, representative core tissue sections (2 mm in diameter) were taken from paraffin blocks and arranged in new tissue microarray (TMA) blocks using trephine apparatus (Superbiochips Laboratories, Seoul, Korea). In cases with variable histological features, the most representative area was selected for TMA construction. The IHC staining of human TMA samples was performed using similar methods for the laying hen model. Human normal ovarian tissues were used as a positive control because they showed strong expression of AHCYL1. On the other hand, we used EOC tissues treated with purified non-immune mouse IgG at the same final concentration as a negative control due to no or

weak expression of AHCYL1. The results of IHC were assessed semi-quantitatively by one pathologist unaware of clinico-pathologic status of the patient. Since nuclear staining was detected in both normal and cancerous ovarian tissues, expression of AHCYL1 was classified as weak (1+), moderate (2+) or strong (3+) based on staining intensity in tumor cells.

Statistical Analysis

For investigating AHCYL1 expression associated with ovarian carcinogenesis in the laying hen model and evaluating its prognostic value in patients with EOC, we used analysis of variance, Chi-square and Student's t-tests, Kaplan-Meier method with the log-rank test, logistic regression and Cox's proportional hazard analyses to determine odds ratio (OR), hazard ratio (HR), and 95% confidence interval (CI). Statistical analyses were performed using SPSS software (Version 19.0; SPSS Inc., Chicago, IL, USA). A probability value of $p < 0.05$ was considered statistically significant.

4. Results

Increased expression of AHCYL1 in normal and cancerous ovaries of chicken

In previous studies, morphological and immunohistochemical analyses compared normal and cancerous ovaries from hens (Ahn et al., 2010; Barua et al., 2009; Lim et al., 2011b). The morphological characteristics of cancerous ovaries included more solid shapes with surface tumor lesions and numerous small regressed follicles as compared to normal ovaries that contained several pre-ovulatory follicles that were hierarchically arranged for ovulation. Histological analysis between normal and cancerous ovaries revealed that cancerous ovaries had mostly gland-like structures in the compact stromal cell compartment with a few small follicles, whereas normal ovaries contained many small well-developed follicles surrounded by connective tissue. These results were consistent with those reported previously (Ansenberger et al., 2009; Barua et al., 2009; Hales et al., 2008; Urick and Johnson, 2006; Zhuge et al., 2009). Based on the results and our recent finding that AHCYL1 is involved in growth and development of the chicken oviduct via an estrogen-mediated ERK1/2 MAPK signaling pathway, we hypothesized that the expression pattern of the *AHCYL1* gene may differ between normal and cancerous tissues from chicken ovaries. Expression of *AHCYL1* mRNA in normal and cancerous ovaries was performed using RT-PCR analysis. *AHCYL1* mRNA expression was predominantly found in cancerous ovaries with little or no expression in normal ovaries (Figure 8-1A). Quantitative RT-PCR analysis showed a 2.3-fold increase of *AHCYL1* mRNA in cancerous ovaries (*P*

< 0.01), when compared to normal ovaries (Figure 8-1B). These results indicate that AHCYL1 may be a useful biomarker for chicken ovarian cancer as it is up-regulated during development of ovarian cancer.

Localization of AHCYL1 mRNA and protein in normal and cancerous ovarian tissues

To examine cell-specific expression of *AHCYL1* mRNA and protein in normal and cancerous ovaries from hens, we performed *in situ* hybridization and immunohistochemical analyses. *AHCYL1* mRNA was predominantly and abundantly expressed in glandular epithelium of cancerous ovaries, but not in luminal epithelium, stroma or blood vessels (Figure 8-2A). Consistent with this result, immunohistochemistry revealed that AHCYL1 protein was localized predominantly in glandular epithelium of cancerous ovaries, but not in any other cell types of the same tissues (Figure 8-2B). However, AHCYL1 protein was detectable at very low abundance around developing follicles and glandular epithelium of normal ovaries. In the negative control, mouse IgG failed to detect a signal. These results indicate that AHCYL1 is expressed specifically in the glandular epithelium of the adenocarcinoma of cancerous ovaries of hens.

Detection of AHCYL1 protein in cultured chicken ovarian carcinoma cells

To assess the quantity and intracellular localization of AHCYL1 protein in

epithelia of cancerous ovaries, we performed Western blotting and immunofluorescence analyses to compare expression patterns of AHCYL1 protein between normal and cancerous ovaries from hens. As illustrated in Figure 8-3A, immunoreactive AHCYL1 was abundant only in cancerous ovarian cells with little or no detectable AHCYL1 in normal ovarian cells. In addition, immunofluorescence microscopy revealed that AHCYL1 protein was most abundant in nuclei of chicken ovarian cancer cells, but detectable only at a lower level in the cytoplasm of normal ovarian epithelial cells (Figure 8-3B). These findings and our preliminary results indicate that AHCYL1 may play an important role in an unknown signaling cascade(s) essential for ovarian carcinogenesis.

Comparison of CpG methylation status in the 5' promoter region upstream of the start site for the AHCYL1 gene between normal and cancerous ovarian cells in hens

The effect of CpG demethylation in the 5' promoter region upstream of a gene is to increase transcriptional activity. Moreover, CpG methylation is closely associated with the development of cancers. Therefore, we investigated methylation patterns in the promoter region of the *AHCYL1* gene in normal and cancerous ovarian epithelia. Both normal and cancerous ovarian epithelial cells were extracted and cultured *in vitro* as previously reported (Giles et al., 2004; Lim et al., 2011b; Murdoch et al., 2005). Bisulfite sequencing results revealed CpG sites at -2,721, -2,799, -2,835 and -2,844 base pairs from the transcriptional start site that maintained methylated and unmethylated status in both type of cells, respectively (Figure 8-4 and Table 8-1).

However, about 37.5, 30 and 33.3 percent of the CpG sites at -2,702, -2,808 and -2,724 were unmethylated in ovarian cancerous cells, compared with normal ovarian cells. These results suggest that the decreased CpG methylation status in the upstream region of *AHCYL1* gene may enhance transcription of the *AHCYL1* gene in chicken ovarian tumors.

Immunofluorescence detection of AHCYL1 protein in human immortalized ovarian carcinoma cells

To examine the existence and potential function of AHCYL1 in human ovarian cancer, we performed immunofluorescence analyses and compared expression patterns of AHCYL1 protein between chicken and human ovarian cancer cells. In this study, three human ovarian cancer cell lines (OVCAR-3, SKOV-3 and PA-1 cells) were prepared, cultured, fixed, and then subjected to immunofluorescent microscopy. Similar to localization of AHCYL1 in chicken ovarian cancerous cells, immunoreactive AHCYL1 protein was most abundant in the nucleus of human OVCAR-3 cells, whereas it was mainly detected in the cytoplasm of human SKOV-3 and PA-1 cells (Figure 8-5). These results suggest a functional role of AHCYL1 in the nucleus that may be involved in activation of transcriptional cascades or signaling pathways associated with cell proliferation and development or inhibition of apoptosis during epithelial ovarian carcinogenesis in humans.

Different Expression of AHCYL1 Affecting Overall Response and Progression-free

Survival in Patients with Ovarian Epithelial Cancer

Next we examine the functional role(s) of AHCYL1 in human ovarian epithelial cancer. We enrolled 109 patients with a median age of 52 years (range, 23-82 years) in the study. Among them, 38 (34.9%) were in FIGO stage I, 20 (18.3%) in stage II, and 51 (46.8%) in stage III of the disease. Tumor grade was G1 in 21 (19.3%), G2 in 41 (37.6%) and G3 in 47 patients (43.1%). Histologically, 62 tumors (57%) were diagnosed as serous carcinoma, 17 (15.6%) with mucinous carcinoma, 12 (11%) with clear cell carcinoma, 9 (8.3%) with endometrioid carcinoma, 4 (3.6%) with undifferentiated carcinoma, and 3 (2.7%) with endometrioid and clear cell carcinoma, and 2 (1.8%) with serous and clear cell carcinoma. The median time to follow-up was 69.2 months (range, 2-88 months).

Optimal cytoreduction was performed in 65 patients (59.6%), whereas 44 (40.4%) underwent suboptimal cytoreduction. Among all patients, 90 (82.6%) received adjuvant chemotherapy after surgery, of which 84 (93.3%) received paclitaxel/carboplatin while paclitaxel/cisplatin was administered to 6 (6.7%) patients. IHC analysis revealed that AHCYL1 protein was abundant in the nucleus of EOC cells, and 14 (12.8%), 41 (37.6%) and 54 patients (49.4%) had weak, moderate and strong expression of AHCYL1 protein, respectively (Figure 8- 6).

After treatment, 75 (68.8%) and 18 patients (16.5%) showed CR and PR, suggesting an OR rate of 85.3%. Intermediate or high expression of AHCYL1 protein

was more frequent in patients showing OR (n=85, 91.4%) than in those showing non-OR (n=10, 62.5%) ($P < 0.01$). Furthermore, intermediate or high expression of AHCYL1 protein was a favorable prognostic factor for OR after adjustment using clinic-pathologic factors (adjusted OR, 7.23; 95% CI, 1.36-38.39) (Table 8-2). Although there was no difference in OS based on the expression of AHCYL1 protein (mean value, 46.9 vs. 61.3 months, $P > 0.05$), intermediate or high expression of AHCYL1 protein was associated with longer PFS than weak expression (mean value, 33.8 vs. 46.7 months, $P < 0.01$). Moreover, intermediate or high expression of AHCYL1 protein was also a favorable prognostic factor for PFS (adjusted HR, 0.20; 95% CI, 0.07-0.55) (Table 8-3).

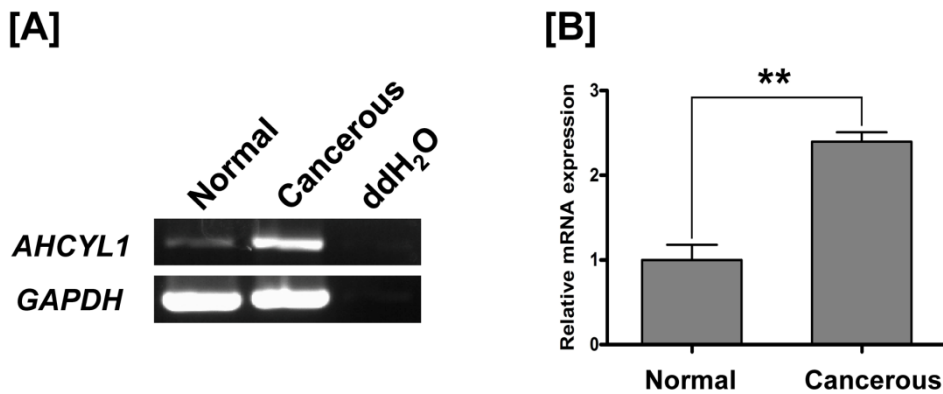


Figure 8-1. Expression and quantitation of *AHCYL1* mRNA in normal and cancerous ovaries from hens. [A] RT-PCR analyses were performed using mixed cDNA templates from normal (n=4) and cancerous (n=10) ovaries of chickens using chicken *AHCYL1* and *GAPDH*-specific primers. *AHCYL1* mRNA was predominantly found in cancerous ovaries with little or no expression in normal ovaries. [B] The quantitative PCR analyses indicated a 2.3-fold increase ($P < 0.01$) in *AHCYL1* mRNA in cancerous ovaries as compared to normal ovaries.

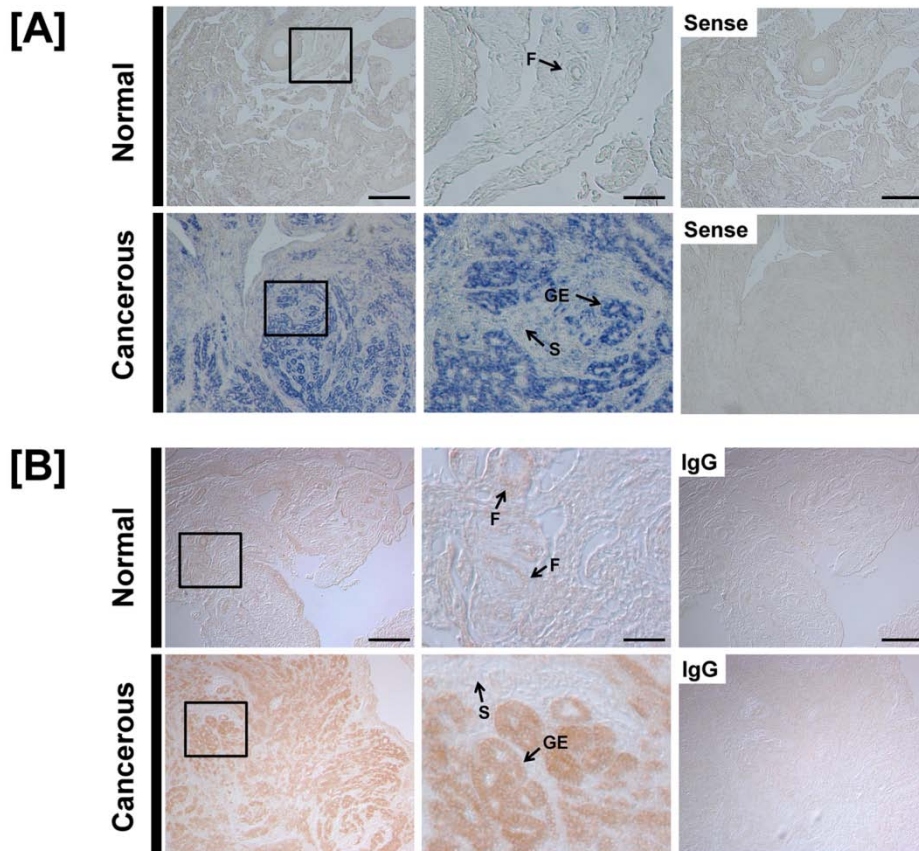


Figure 8-2. Expression of *AHCYL1* mRNA and protein is unique to glandular epithelium of cancerous ovaries from hens. [A] *In situ* hybridization analyses of *AHCYL1* mRNA. Cross-sections of normal and cancerous ovaries from chickens were hybridized with sense or anti-sense chicken *AHCYL1* cRNA probes. *AHCYL1* mRNA was predominantly and abundantly expressed in the glandular epithelium of cancerous ovaries, but not in luminal epithelium, stroma or blood vessels. [B] Immunohistochemical expression of *AHCYL1* protein. Immunoreactive *AHCYL1* protein was predominantly localized in glandular epithelium of cancerous ovaries, but not in any other cell types of the same tissues. However, *AHCYL1* protein was

detectable at very low abundance around developing follicles and glandular epithelium of normal ovaries. For a negative control, the primary antibody was substituted with purified non-immune mouse IgG. Legend: F, follicle; GE, glandular epithelium; S, stroma; *Scale bar* represents 200 μm (the first columnar panels and sense) or 50 μm (the second columnar panels).

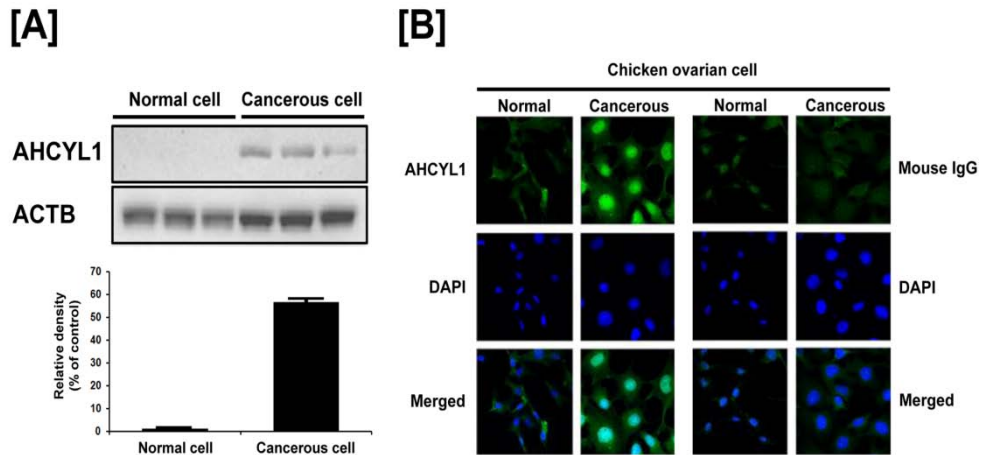


Figure 8-3. Differential expression of AHCYL1 protein in normal and cancerous ovarian cells from hens. [A] Western blotting for AHCYL1 protein from normal and ovarian cancer cell lines. Three different primary ovarian surface epithelial cell lines from three normal and cancerous chickens, respectively, were isolated and cultured with some modifications. Western blotting analyses detected a 57-fold increase ($P < 0.001$) in AHCYL1 protein in ovarian cancer cells as compared to normal ovarian cells. [B] Immunofluorescence microscopy for AHCYL1 protein in normal and ovarian cancer cell lines. Immunoreactive AHCYL1 protein was abundant in nuclei of chicken ovarian cancer cells, but detectable at lower levels in the cytoplasm of normal ovarian epithelial cells.

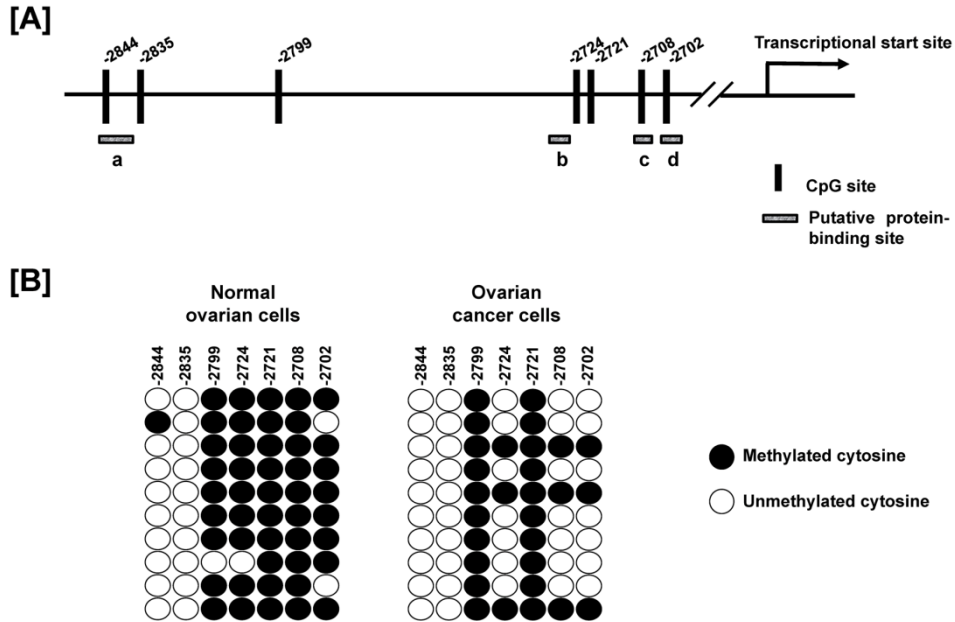


Figure 8-4. Bisulfite sequencing of CpG sites in 5' promoter upstream of the transcription start site for the *AHCYL1* gene. [A] Schematic of the seven CpG sites in the promoter region of the *AHCYL1* gene are indicated by the heavy black vertical lines. The numbers on the line indicate positions relative to the transcription start site. [B] The CpG methylation status in the upstream region of the *AHCYL1* gene was analyzed in normal ovarian cells and ovarian cancer cells of hens by bisulfate sequencing. Each circle indicates a CpG site in the primary sequence, and each line of circles represents analysis of a single cloned allele. Closed and open circles are methylated and unmethylated CpGs, respectively.

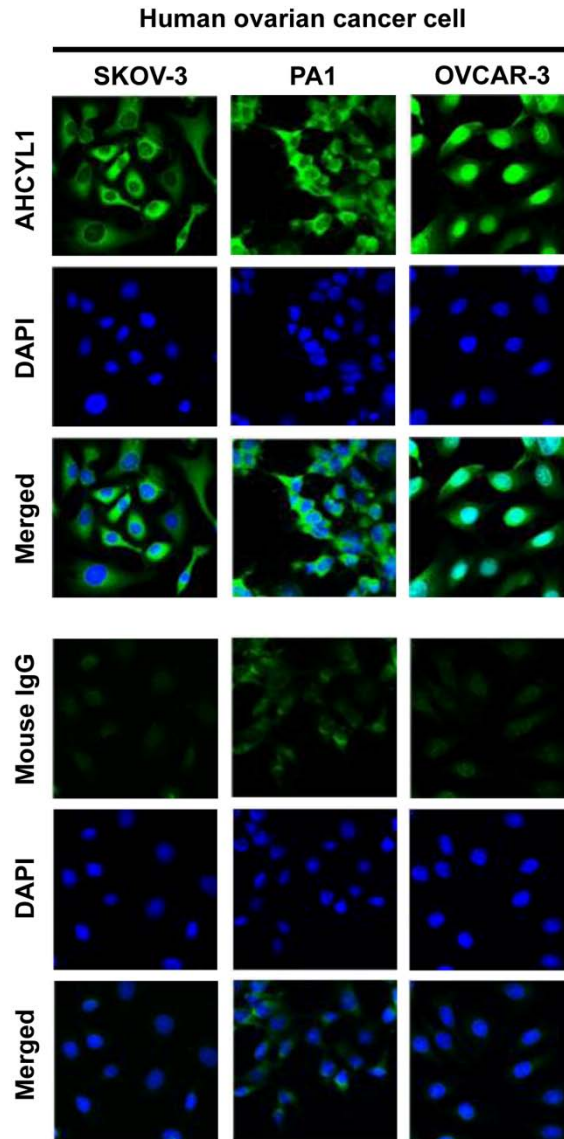


Figure 8-5. Differential localization of AHCYL1 protein in human immortalized ovarian carcinoma cells. Immunoreactive AHCYL1 protein was abundant in the nuclei of human OVCAR-3 cells, but cytoplasm of human SKOV-3 and PA-1 cells. Cell nuclei were stained with DAPI (blue). All images were captured at 40X objective magnification.

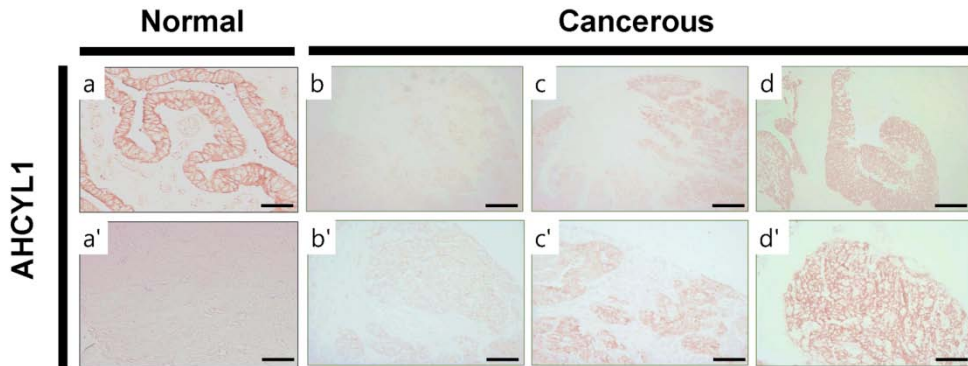


Figure 8-6. Immunohistochemical expression of AHCYL1 protein in normal and cancerous ovaries from women. Weak (b and b'), moderate (c and c') and strong (d and d') expression of AHCYL1 protein was detected in women with epithelial ovarian cancer. There was either no expression or very weak expression of AHCYL1 in cancerous ovaries, whereas AHCYL1 protein was readily detectable in normal ovaries (a and a'). The negative control was mouse IgG instead of primary antibody. *Scale bar* represents 200 μm (the first horizontal panels and IgG) or 50 μm (the second horizontal panels).

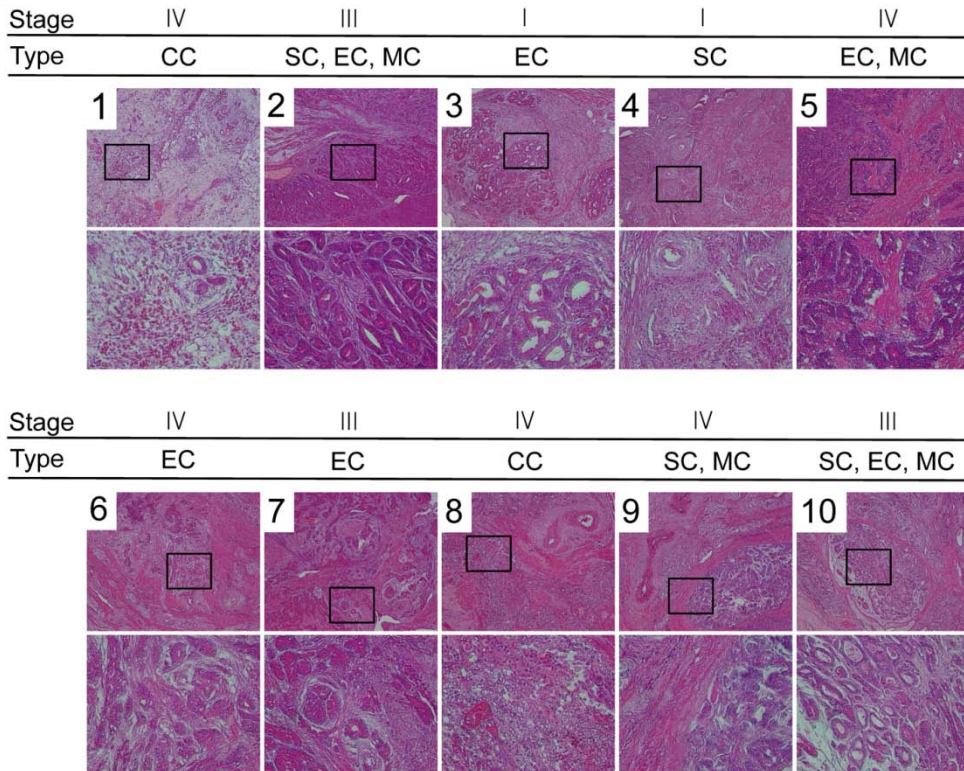


Figure 8-7. Histological types of chicken ovarian cancers used in this study.

Briefly, endometrioid carcinoma had many glands, serous carcinoma was a solid mass of cells with nuclear atypia, clear cell carcinoma showed vacuolated cells consisting of nuclear atypia and mucinous carcinoma was differentiated around the stromal region. Legend: 1, clear cell carcinoma; 2, endometrioid/serous carcinoma; 3, endometrioid carcinoma; 4, serous carcinoma; 5, endometrioid/mucinous carcinoma; 6, endometrioid carcinoma; 7, endometrioid carcinoma; 8, clear cell carcinoma; 9, serous/mucinous carcinoma; 10, endometrioid/serous carcinoma.

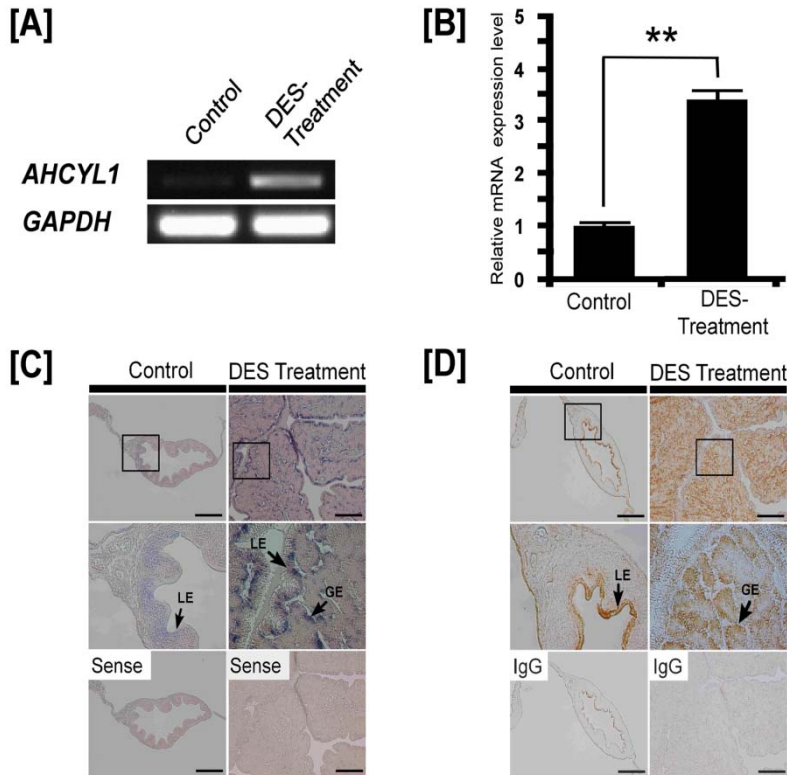


Figure 8-8. Effects of DES on *AHCYL1* mRNA and protein expression in the chicken oviduct. Both RT-PCR [A] and q-PCR [B] analyses were performed using cDNA templates from DES-treated and control chicken oviducts (mean \pm SEM; $P < 0.001$). As shown in Figures 8-2A, semi-quantitative RT-PCR analysis indicated that DES increased *AHCYL1* mRNA in the chick oviduct. Further results from quantitative PCR revealed that DES induced a 3.4-fold increase ($P < 0.01$) in oviductal *AHCYL1* mRNA as compared to control chicks (Figure 8-2B). These experiments were conducted in triplicate and normalized to control *GAPDH* expression. [C] *In situ* hybridization analyses determined cell-specific expression of *AHCYL1* mRNA in oviducts of DES-treated and control chicks. Cross-sections of the chicken oviduct

treated with DES or vehicle were hybridized with antisense or sense chicken AHCYL1 cRNA probes. [D] Immunoreactive AHCYL1 protein in oviducts of DES-treated and control chicks. For the IgG control, normal goat IgG was substituted for the primary antibody. Sections were not counterstained. Legend: LE, luminal epithelium; GE, glandular epithelium; Scale bar represents 100 μ m.

Table 8-1. Putative protein-binding sites within the upstream 5' promoter region of the *AHCYL1* gene.

Mark	Sequences	Position	Binding TF	Species
a	GGGCTGGG	-2838, -2845	AP-2	Human, Mouse, Rat, Chicken, Clawed frog
			AP-2alpha	Human, Mouse
			AP-2alphaA	Human
			AP-2alphaB	Human
b	GGGCA	-2725, -2729	ER-alpha	Human, Rat, Chicken, Clawed frog
			LF-A1	Human
			Sp1	Human, Mouse, Rat, Chicken, Rabbit, Pig
c	CCGA	-2706, -2709	RAF	Yeast
d	AGACGG	-2699, -2704	SIF	Human, Mouse, Rat

Table 8-2. Multivariate linear logistic regression analysis for factors affecting overall response.

Characteristics	Adjusted OR*	95% CI†	p value
Age ≥ 52 years	1.14	0.29-4.47	0.85
FIGO‡ stage I or II disease	0.61	0.13-2.79	0.53
Grade 1 or 2 disease	3.98	1.02-15.43	0.04
Serous adenocarcinoma	5.17	1.12-24.02	0.04
Adjuvant chemotherapy	1.32	0.21-8.28	0.77
Optimal cytoreduction	11.87	2.35-60.02	<0.01
Intermediate or high expression of <i>AHCYL1</i>	7.23	1.36-38.39	0.02

*Odds ratio.

†Confidence interval.

‡International Federation of Gynecology and Obstetrics.

Table 8-3. Multivariate Cox’s proportional hazard analysis for factors affecting progression-free survival.

Characteristics	Adjusted HR [*]	95% CI [†]	p value
Age ≥ 52 years	1.37	0.75-2.50	0.31
FIGO [‡] stage I or II disease	0.73	0.32-1.64	0.44
Grade 1 or 2 disease	0.72	0.41-1.29	0.27
Serous adenocarcinoma	1.87	0.85-4.11	0.12
Adjuvant chemotherapy	1.48	0.54-4.04	0.44
Optimal cytoreduction	0.15	0.06-0.34	<0.01
Intermediate or high expression of <i>AHCYL1</i>	0.20	0.07-0.55	<0.01

*Hazard ratio.

†Confidence interval.

‡International Federation of Gynecology and Obstetrics.

5. Discussion

In the present study, we first demonstrated that expression of the *AHCYL1* gene increased only in glandular epithelia of cancerous ovaries compared to normal ovaries of hens. Our current results support our hypothesis that *AHCYL1* is a critical regulator of growth and development of epithelial-derived ovarian cancer in hens. Chickens are the most relevant animal model to identify biomarkers for patients with EOC because their incessant ovulation increases the possibility of gene mutations by genomic damage to the ovarian surface epithelium, which can lead to ovarian cancer (Murdoch et al., 2005). In addition, various biomarkers such as CA125, cytokeratin, EGFR, Lewis Y, and erbB-2 for human ovarian cancer are cross-reactive and expressed in chicken ovarian carcinoma cells, but not in normal ovaries (Anderson et al., 2010; Jackson et al., 2007; Johnson, 2009; Rodriguez-Burford et al., 2001). Furthermore, hens have similar tumor-related gene alterations such as p53, ras, HER-2/neu compared with those of women (Hakim et al., 2009). Indeed, we reported that serpin peptidase inhibitor, clade B, member 3 (*SERPINB3*) is associated with ovarian carcinogenesis in chickens and it can serve as a prognostic factor for platinum resistance and poor survival in patients with EOC (Kim et al., 2011).

Recently, we found tissue specific expression of *AHCYL1* mRNA and protein in the chicken oviduct to be regulated by estrogen in a tissue and cell-specific manner (Figure 8-8). However, the significance of chicken *AHCYL1* is poorly understood in ovarian cancer research. Therefore, we investigated expression of

AHCYL1 in normal and cancerous ovaries from hens. As illustrated in Figures 8-1, 8-2 and 8-3, *AHCYL1* mRNA and protein were predominantly found in cancerous ovaries, but there was little or no expression in normal ovaries. These results indicate that AHCYL1 is a potential biomarker that is up-regulated in the glandular epithelium of cancerous chicken ovaries and confirms that the chicken is an appropriate animal model for ovarian cancer research to identify and develop biomarkers for early diagnosis and application of therapeutics to treat the disease.

In the current study, our results demonstrated that AHCYL1 protein is abundant in nuclei glandular epithelial cells of cancerous ovaries as compared to normal ovaries. In addition, bisulfite sequencing results to examine methylation patterns in the promoter region of the *AHCYL1* gene revealed that approximately 30 to 38% of the three CpG sites are demethylated in ovarian cancerous cells, compared with normal ovarian cells. These findings suggest that AHCYL1 plays a role in tumor development and proliferation of ovarian epithelial cells and that it is associated with ovarian carcinogenesis through the activation of transcription factors and increased transcriptional activity via a partial demethylation of the 5' promoter region of the gene. In spite of the lack of evidence for a direct association between AHCYL1 expression and ovarian carcinogenesis, the *AHCYL1* gene is down-regulated in response to chemotherapeutic drugs based on comparative genomic hybridization in a human malignant melanoma cell line (Wittig et al., 2002).

Based on the previous reports and findings in the present study, we

hypothesize that *AHCYL1* contributes to the development and progression of EOC. However, the pattern of expression of *AHCYL1* was different among patients with EOC. When we considered the strongest expression of AHCYL1 protein in normal ovaries, it was less abundant than that in EOC. Although we expected high expression of AHCYL1 to be associated with poor prognosis in patients with EOC as found in a previous study, intermediate or high expression of AHCYL1 was found to be a favorable prognostic factor for OR (adjusted OR, 7.23; 95% CI, 1.36-38.39) and PFS (adjusted HR, 0.20; 95% CI, 0.07-0.55). Thus, *AHCYL1* is an oncogene for developing ovarian cancer in the chicken model, whereas it acts as a tumor suppressor gene in human EOC. Since the functional role of the *AHCYL1* gene in cancer has not been reported previously, we presumed that it has a paradoxical function of acting as an oncogene in one species and a tumor suppressor gene in another species. Our hypothesis can be supported by previous reports indicating that specific genes have different functions in carcinogenesis. For example, Notch acts paradoxically in various types of tumors. It is an oncogene leading to loss of cellular differentiation in pancreas, breast, cervical and renal cancers (Reedijk et al., 2005; Sjolund et al., 2008; Wang et al., 2006; Zagouras et al., 1995), but a tumor suppressor gene leading growth arrest in neuroendocrine and thyroid cancers (Kunnimalaiyaan and Chen, 2007; Kunnimalaiyaan et al., 2006). Furthermore, Mdm2 can act both as an oncogene and a tumor suppressor gene. Mdm2 increase cellular proliferation and tumor development by inactivating p53, but it can also reduce mutant p53 expression to act as a tumor suppressor (Manfredi, 2010). Thus, the current study suggests paradoxical functions of *AHCYL1* in ovarian carcinogenesis that is variable among species.

To the best of our best knowledge, results of the current study are the first to indicate expression of *AHCYLI* in ovarian carcinogenesis and to provide evidence for it having paradoxical functions based on results obtained in comparing its expression in hens and in women with EOC. Contrary to the association between *AHCYLI* expression and ovarian carcinogenesis in chickens, high level of expression of *AHCYLI* was a favorable prognostic factor for tumor response and survival in women with EOC. Thus, *AHCYLI* is likely an important target gene related to EOC that requires further evaluation to determine the functional mechanism whereby it affects carcinogenesis.

CHAPTER 9

Cell-Specific and Temporal Aspects of Gene Expression in the Chicken Oviduct at Different Stages of the Laying Cycle

1. Abstract

Egg formation and embryonic development occur as the yolk passes through the magnum, isthmus and shell gland of the oviduct before oviposition in hens. The present identified candidate genes associated with secretory function of the chicken oviduct after ovulation and to egg formation and oviposition. Hens (n=5 per time point) were sacrificed to recover the reproductive tract when the egg was in the magnum (3 h after ovulation) and the shell gland (20 h after ovulation). Total RNA was extracted from each segment of the oviducts and subjected to Affymetrix chicken GeneChip analysis. Quantitative PCR and *in situ* hybridization analyses of selected genes confirmed the validity of the gene expression patterns detected using the microarray analysis. In particular, *ACPI*, *CALBI*, *CYP26A1*, *PENK*, *RCAN1* and *SPPI* increased significantly in the shell gland between 3h and 20 h post-ovulation whereas only *RCNA1* increased significantly in the magnum between 3h and 20 h post-ovulation. Results of the high-throughput analysis revealed cell-specific and temporal changes in gene expression in the oviduct at 3h and 20 h post-ovulation in laying hens that provide novel insight into changes at the molecular and cellular levels of candidate genes-related to formation of the egg and oviposition.

2. Introduction

The female reproductive tract in chickens is a unilateral organ with one functional ovary and one oviduct. The chicken oviduct is a complex biological organ in which hormones harmoniously orchestrate biochemical and cellular changes during egg formation and passage of the yolk between ovulation and oviposition. It is well-known as an excellent research model for organ development, morphogenesis, and hormonal responsiveness (Dougherty and Sanders, 2005). The oviduct of mature egg-laying hens includes five functionally specific regions; infundibulum (site of fertilization), magnum (production of components of egg-white), isthmus (formation of the soft shell membrane), shell gland or uterus (formation of calcified egg shell) and vagina (oviposition or egg laying). The oviductal epithelial cells differentiate into various cell types including luminal epithelium (LE), tubular glands lined by epithelial cells (GE), goblet cells and ciliated cells in the magnum (Palmiter and Wrenn, 1971b). Of these, the GE of tubular glands synthesize and secrete large amounts of critical egg-white proteins such as ovalbumin, conalbumin, lysozyme, and ovomucoid (Kohler et al., 1968), and perhaps transport nutrients such as glucose and amino acids to be incorporated into the egg-white. During passage of the egg through the oviduct, several layers of the eggshell membranes surround the yolk and the white of an egg sequentially as it passes through the successive sectors of the oviduct (Lavelin et al., 2000). About 2 to 3 h after ovulation, the fertilized egg, with secretion of egg-white proteins including albumen from the magnum, translocates into the isthmus which secretes various components of the soft shell membranes such as keratin-like protein,

and types I, V and X collagens (Leach et al., 1981; Wang et al., 2002). The formation of the eggshell with most calcium deposition (approximately 5 to 6 g of calcium carbonate) is completed in the shell gland of the oviduct within 17 to 20 h after ovulation (Lavelin et al., 2000).

Based on the chicken genome database, high-throughput analyses using the chicken DNA microarray technique has provided valuable data to study genes expressed in specific tissues from chickens. For instance, two research groups recently reported differentially expressed transcripts in the shell gland of the oviducts when comparing poor versus superb layer strains, and immature versus mature hens, respectively (Dunn et al., 2009b; Yang et al., 2007). In the present study, we examined spatial and temporal changes in transcripts of the oviduct of laying hens at different stages of the laying cycle and identified genes for which there were significant changes in expression in the magnum and shell gland of the oviducts. Furthermore, we focused on six genes for which little is known in the chicken oviduct during the ovulation to oviposition cycle or have a potential to be involved in production of egg-white proteins and formation of an egg. Future studies will investigate regulation and functions of these six genes that are expressed in response to Luteinizing Hormone and/or sex steroids in the oviduct of laying hens during the laying cycle.

3. Materials and Methods

Experimental Animals and Animal Care

The experimental use of chickens for this study was approved by the Institute of Laboratory Animal Resources, Seoul National University (SNU-070823-5). White Leghorn (WL) chickens were subjected to standard management practices at the University Animal Farm, Seoul National University, Korea. The management, reproduction, and tissue collection procedures adhered to standard operating protocols of our laboratory. All chickens were exposed to a regimen of 15 h light and 9 h dark with *ad libitum* access to feed and water.

Tissue Samples

Hens (n=5 per time point) in each group (3 h and 20 h after ovulation) were euthanized using 60%–70% carbon dioxide. Portions of the magnum and the shell gland of oviducts from each hen at each time point were either: 1) removed and placed in Optimal Cutting Temperature (OCT) compound (Miles, Oneonta, NY), frozen in liquid nitrogen and stored at -80°C; 2) fixed in freshly prepared 4% paraformaldehyde in PBS (pH 7.4); or 3) frozen immediately in liquid nitrogen and stored at -80°C until analyzed. After 24 h, tissues fixed in 4% paraformaldehyde were changed to 70% ethanol for 24 h and then dehydrated and embedded in Paraplast-Plus

(Leica Microsystems, Wetzlar, Germany). Paraffin-embedded tissues were sectioned at 5 μm .

RNA Isolation

Total cellular RNA was isolated from frozen tissues using Trizol reagent (Invitrogen, Carlsbad, CA) according to manufacturer's recommendations. The quantity and quality of total RNA was determined by spectrometry and denaturing agarose gel electrophoresis, respectively.

Microarray Analysis

Microarray analysis was performed using Affymetrix GeneChip[®] Chicken Genome Arrays (Affymetrix, Santa Clara, CA, USA). Data were generated by SeoulBio Bioscience Corporation (Seoul, Korea) and dChip software was used for the analysis (Li and Wong, 2001). Total RNA was extracted from the magnum and shell gland from each of the five hens at each time point (3 h and 20 h post-ovulation) using TRIzol (Invitrogen, Carlsbad, CA, USA) and purified using an RNeasy Mini Kit (Qiagen, Valencia, CA, USA). All experiments were performed using three independent RNA pools from 10 hens (5 each at 3 h and at 20 h post-ovulation) and three microarray chips.

Quantitative RT-PCR Analysis

Total RNA was extracted from each segment of oviduct at each time point using TRIzol (Invitrogen) and purified using an RNeasy Mini Kit (Qiagen). Complementary DNA was synthesized using a Superscript[®] III First-Strand Synthesis System (Invitrogen). All experiments were performed in triplicate with the cDNA synthesized from individual samples from the hens (n=3 for each time point). Gene expression levels were measured using SYBR[®] Green (Biotium, Hayward, CA, USA) and a StepOnePlus[™] Real-Time PCR System (Applied Biosystems, Foster City, CA, USA). The glyceraldehyde 3-phosphate dehydrogenase (*GAPDH*) gene was analyzed simultaneously as a control and used for normalization of data as its expression is considered to be most stable among the house-keeping genes commonly used to account for variation among samples. Each target gene and *GAPDH* was analyzed in triplicate. Using the standard curve method, we determined expression of the examined genes using the standard curves and Ct values, and normalized them using *GAPDH* expression. The PCR conditions were 94°C for 3 min, followed by 40 cycles at 94°C for 20 sec, 60°C for 40 sec, and 72°C for 1 min using a melting curve program (increasing the temperature from 55°C to 95°C at 0.5°C per 10 sec) and continuous fluorescence measurement. ROX dye (Invitrogen) was used as a negative control for the fluorescence measurements. Sequence-specific products were identified by generating a melting curve in which the Ct value represented the cycle number at which a fluorescent signal was statistically greater than background, and relative gene expression was quantified using the $2^{-\Delta\Delta Ct}$ method (Livak and Schmittgen, 2001). For the control, the relative quantification of gene expression was

normalized to the Ct value for the control oviduct. Information on the primer sets is provided in Table 9-1.

In Situ Hybridization Analysis

For hybridization probes, PCR products were generated from cDNA with the primers used for RT-PCR analysis. The products were extracted from the gel and cloned into pGEM-T vector (Promega). After verification of the sequences, plasmids containing gene sequences were amplified with T7- and SP6-specific primers (T7:5'-TGT AAT ACG ACT CAC TAT AGG G-3'; SP6:5'-CTA TTT AGG TGA CAC TAT AGA AT-3'). Then digoxigenin (DIG)-labeled RNA probes were transcribed using a DIG RNA labeling kit (Roche Applied Science, Indianapolis, IN). Information on the probes is provided in Table 9-2. Tissues were collected and fixed in 4% paraformaldehyde, embedded in paraffin and sectioned at 5 µm on APES-treated (silanized) slides. The sections were then deparaffinized in xylene and rehydrated to diethylpyrocarbonate (DEPC)-treated water through a graded series of alcohol. The sections were treated with 1% Triton X-100 in PBS for 20 min and washed two times in DEPC-treated PBS. After washing in DEPC-treated PBS, the sections were digested using 5 µg/ml Proteinase K (Sigma) in TE buffer (100 mM Tris-HCl, 50 mM EDTA, pH 8.0) at 37°C. After post-fixation in 4% paraformaldehyde, sections were incubated twice for 5 min each in DEPC-treated PBS and incubated in TEA buffer (0.1M triethanolamine) containing 0.25% (v/v) acetic anhydride. The sections were incubated in a prehybridization mixture containing 50% formamide and 4X standard

saline citrate (SSC) for at least 10 min at room temperature. After prehybridization, the sections were incubated overnight in overnight at 42°C in a humidified chamber in a hybridization mixture containing 40% formamide, 4X SSC, 10% dextran sulfate sodium salt, 10mM DTT, 1 mg/ml yeast tRNA, 1mg/ml salmon sperm DNA, 0.02% Ficoll, 0.02% polyvinylpyrrolidone, 0.2mg/ml RNase-free bovine serum albumin and denatured DIG-labeled cRNA probe. After hybridization, sections were washed for 15 min in 2X SSC at 37°C, 15min in 1X SSC at 37°C, 30 min in NTE buffer (10mM Tris, 500mM NaCl and 1mM EDTA) at 37°C and 30 min in 0.1X SSC at 37°C. After blocking with a 2% normal sheep serum (Santa Cruz Biotechnology, Inc., Santa Cruz, CA), the sections were incubated overnight with sheep anti-DIG antibody conjugated to alkaline phosphatase (Roche, Indianapolis, IN). The signal was visualized following exposure to a solution containing 0.4 mM 5-bromo-4-chloro-3-indolyl phosphate, 0.4 mM nitroblue tetrazolium, and 2 mM levamisole (Sigma Chemical Co., St. Louis, MO).

Statistical Analyses

Data for quantitative PCR were subjected to analysis of variance (ANOVA) according to the general linear model (PROC-GLM) of the SAS program (SAS Institute, Cary, NC) to determine whether effects of time post-ovulation were significant. Data are presented as mean \pm SEM unless otherwise stated.

4. Results

Gene expression is altered in the oviduct at each time point after ovulation

Microarray analysis identified significant differences in various transcripts from magnum and shell gland of the oviduct at 3 h and 20 h after ovulation in chickens (Figure 9-1 and 9-2). A quantitative-PCR analysis was performed to validate the effects of each time point on selected genes from the microarray analyses, including acid phosphatase 1, tartrate resistant (*ACPI*), calbindin 1 (*CALBI*), retinoic acid degrading enzyme CYP26 (*CYP26A1*), proenkephalin (*PENK*), regulator of calcineurin 1 (*RCANI*) and secreted phosphoprotein 1 (*SPP1*) in each oviductal segment at 3 h and 20 h after ovulation. As illustrated in Figures 9-3 and 9-4, expression of *CALBI*, *CYP26A1*, *PENK* and *SPP1* mRNAs was not different ($P > 0.05$) between 3 h and 20 h in the magnum; however, *RCANI* mRNA levels increased 1.4-fold ($P < 0.001$) and *ACPI* mRNA levels decreased 0.6-fold ($P < 0.001$) in the magnum between 3 h and 20 h post-ovulation.

In the shell gland, expression of *ACPI*, *CALBI*, *CYP26A1*, *PENK*, *RCANI* and *SPP1* mRNAs increased 1.5- ($P < 0.001$), 9- ($P < 0.001$), 11- ($P < 0.001$), 26- ($P < 0.01$), 10- ($P < 0.001$) and 22-fold ($P < 0.05$) between 3 h and 20 h post-ovulation, respectively. The changes in expression levels of the five genes revealed by q-PCR analysis were consistent with changes detected by microarray analysis (Table 9-3).

The cell-specific localization of mRNAs of the selected genes in the magnum and shell gland of the oviduct was assessed by *in situ* hybridization analysis. Cell-specific differences in expression of the validated genes were observed within the magnum and shell gland of the chicken oviduct. *ACPI*, *CALBI*, *CYP26A1*, *PENK*, *RCANI* and *SPPI* expression levels were weak in the magnum of the oviduct at both 3 h and 20 h post-ovulation (Figures 9-5 and 9-7). However, as illustrated in Figures 9-6 and 9-8, all mRNAs were localized predominantly in the GE of the shell gland at 20 h after ovulation and, to a lesser extent, in GE of the magnum at 3 h post-ovulation. In addition, *CYP26A1* mRNA was abundant in GE of magnum at 3 h.

Functional categories of oviductal genes were altered significantly at 3 h and 20 h after ovulation

In the magnum and shell gland between 3 h and 20 h after ovulation, gene ontology analysis revealed genes enriched in and involved in physiological/developmental system, molecular and cellular function, and disease/disorder categories (Figure 9-2). In the physiological system development and function category, genes are associated with tissue development, connective tissue development, skeletal and muscular system development, embryonic development, cardiovascular system development, organismal survival/development and nervous system development (Figure 9-2A and 9-2D). In the category of molecular and cellular functions, genes that changed were related to cellular growth and proliferation, cell death, gene expression, cellular movement, protein synthesis, and post-

translational modification (Figure 9-2B and 9-2E). Furthermore, as illustrated in Figure 9-2C and 9-2F, many genes were also in the disease and disorders category: genetic disorder, cancer, neurological disease, skeletal and muscular disorders, reproductive system disease and gastrointestinal disease.

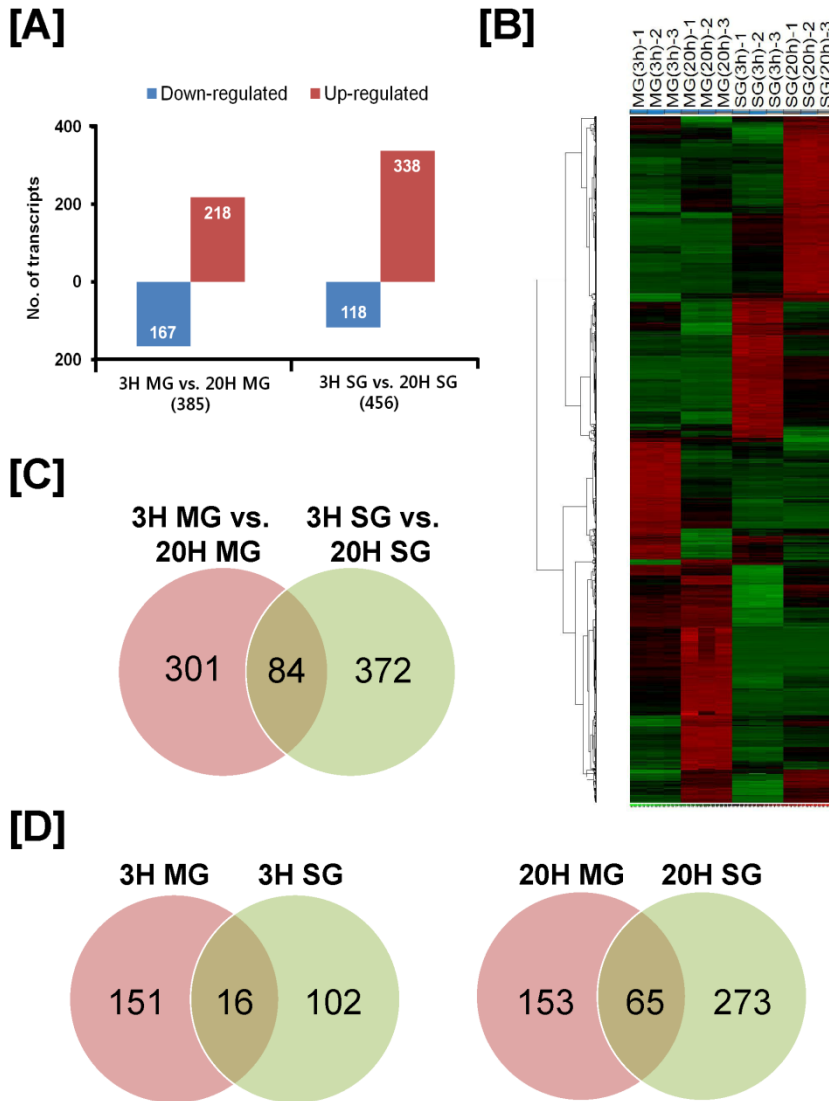


Figure 9-1. Identification of genes that changed significantly in the magnum and the shell gland of the oviduct during the egg laying cycle in hens. [A] The number of genes for which expression increased or decreased significantly in the magnum and the shell gland of the chicken oviducts between 3 h and 20 h after ovulation. [B] Clustering analysis of genes that changed significantly in the magnum and the shell

gland. [C and D] The relationship between genes that changed in expression in the magnum and shell gland between 3 h and 20 h post-ovulation [C] and in the magnum and shell gland at the same times post-ovulation. [D] The numbers displayed within the intersections of the circles indicate genes common to the two comparisons. Legend: MG, magnum; SG, shell gland.

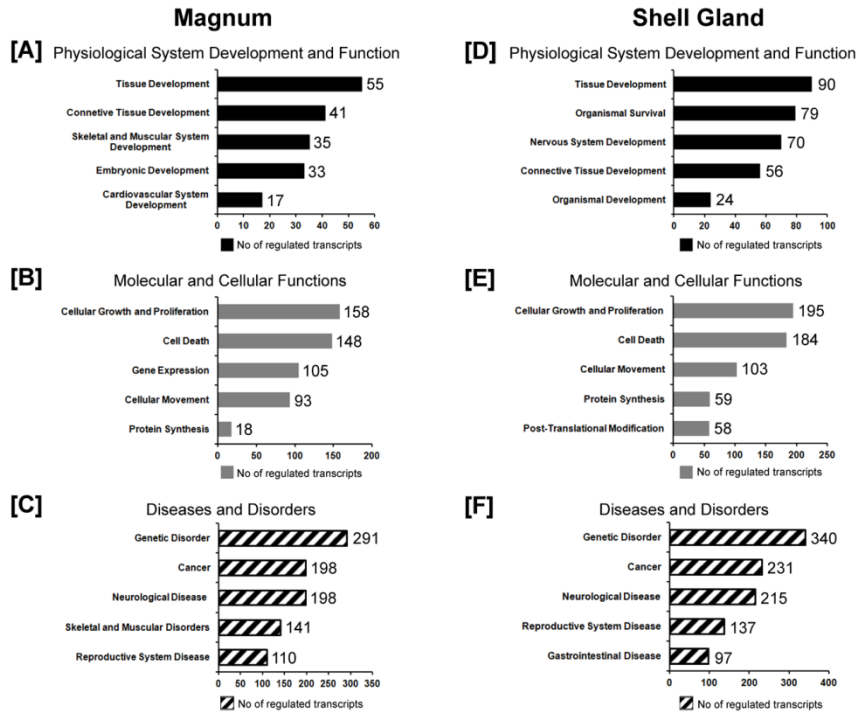


Figure 9-2. Functional categorization of the genes that changed in the magnum and shell gland during interval from ovulation to oviposition in laying hens. Gene expression patterns that changed in the magnum [A, B and C] and in the shell gland [D, E and F] are presented. Genes that changed significantly were annotated and assigned to various functional categories using Gene Ontology.

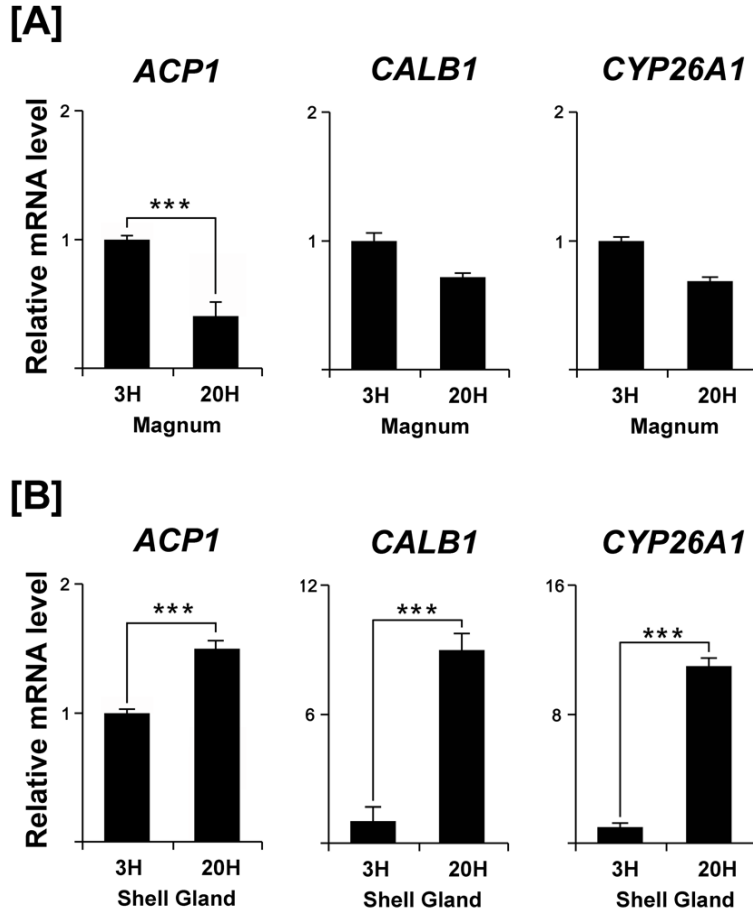


Figure 9-3. Comparison of relative expression of mRNAs for *ACP1*, *CALB1* and *CYP26A1* which changed significantly in the oviduct of hens during the egg laying cycle based on quantitative RT-PCR analyses. Expression of *ACP1* mRNA level decreased ($P < 0.001$) and *CALB1* and *CYP26A1* mRNA levels were not different ($P > 0.05$) between 3 h and 20 h in the magnum. In contrast, expression of those mRNAs increased in the shell gland between 3 h and 20 h post-ovulation ($P < 0.001$). Each bar represents the mean \pm SEM of three independent experiments. The asterisks denote effects that were significant ($***P < 0.001$).

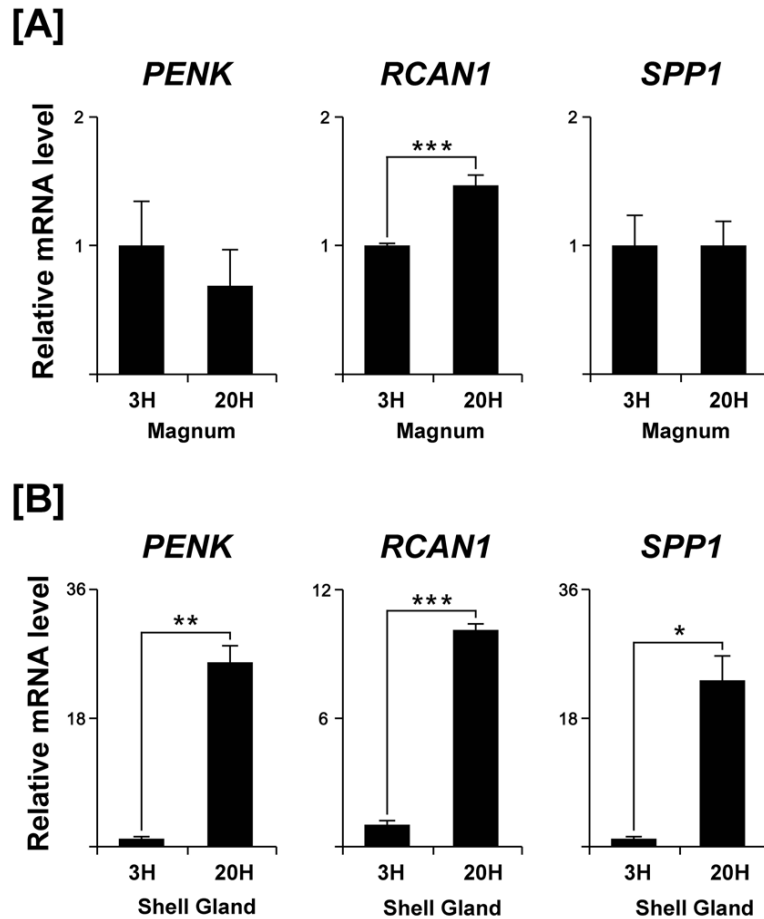


Figure 9-4. Comparison of relative expression of mRNAs for *PENK*, *RCAN1* and *SPP1* which changed significantly in the oviduct of hens during the egg laying cycle based on quantitative RT-PCR analyses. Expression of *PENK* and *SPP1* mRNAs was not different ($P > 0.05$), but expression of *RCAN1* mRNA increased ($P < 0.001$) between 3 h and 20 h in the magnum. In contrast, those mRNA levels increased in the shell gland at 20 h post-ovulation ($P < 0.05$ to $P < 0.001$). Each bar represents the mean \pm SEM of three independent experiments. The asterisks denote effects that were significant (** $P < 0.01$, *** $P < 0.001$, or * $P < 0.05$).

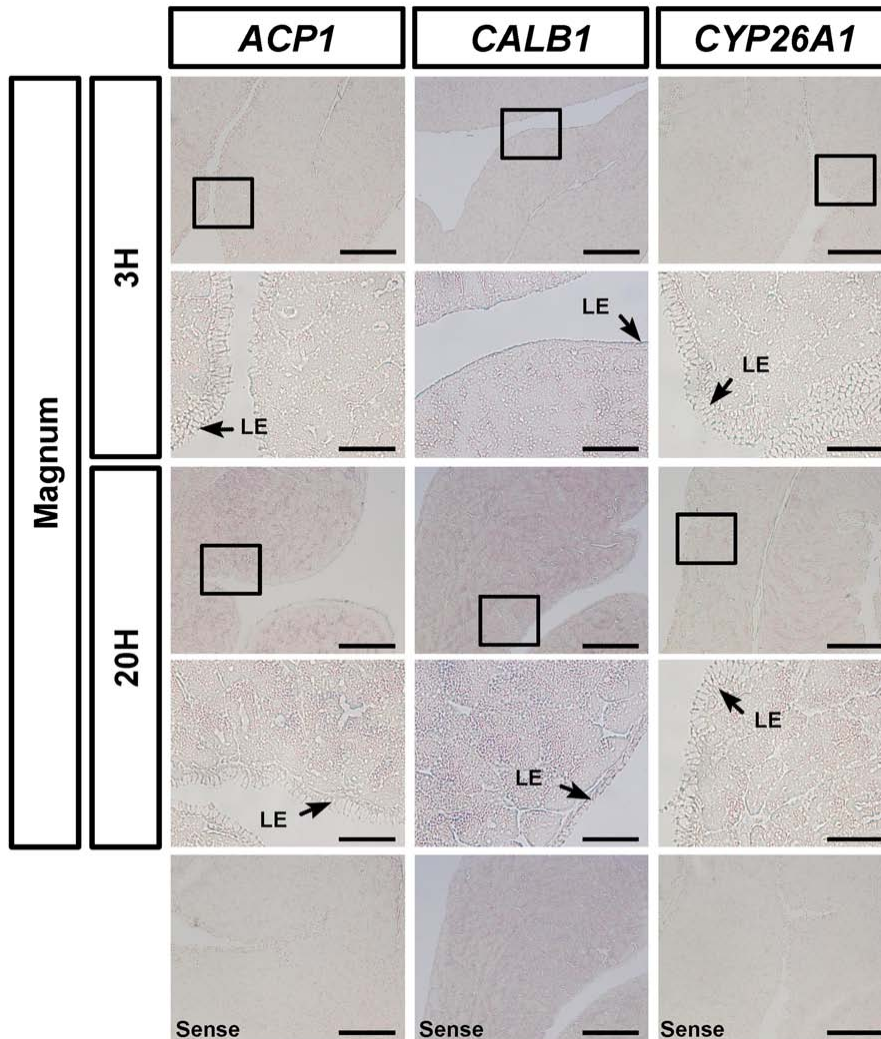


Figure 9-5. Cell-specific localization of mRNAs for *ACP1*, *CALB1* and *CYP26A1* in the magnum are presented for oviducts of hens at 3 h and 20 h post-ovulation. All mRNAs were expressed at very low abundance in GE of the magnum of the oviducts between 3h and 20 h after ovulation. Legend: LE, Luminal epithelium; GE, glandular epithelium. *Scale bar* represents 10 μm .

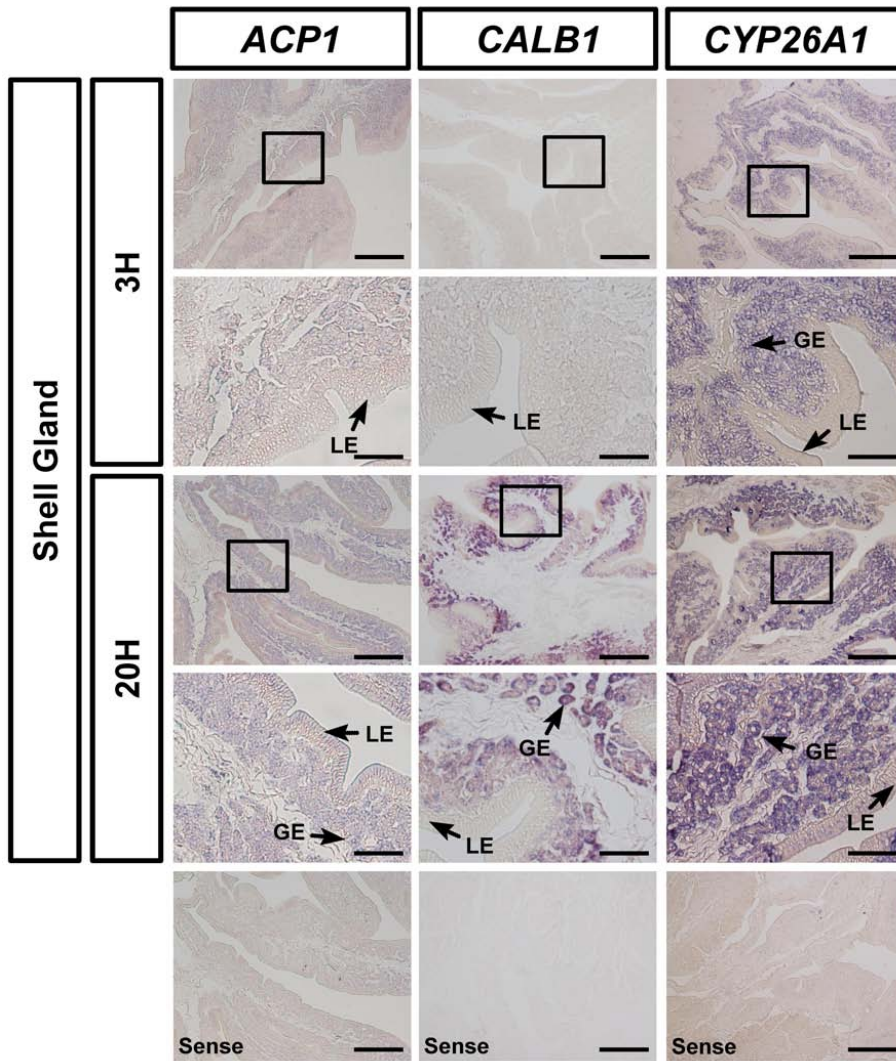


Figure 9-6. Cell-specific localization of mRNAs for *ACP1*, *CALB1* and *CYP26A1* in the shell gland of oviducts of hens are presented for 3 h and 20 h post-ovulation. All mRNAs were localized predominantly in the glandular epithelium (GE) of the shell gland at 20 h after ovulation. Interestingly, *CYP26A1* mRNA was also abundant in GE of the magnum at 3 h post-ovulation. Legend: LE, Luminal epithelium; GE, glandular epithelium. *Scale bar* represents 10 μ m.

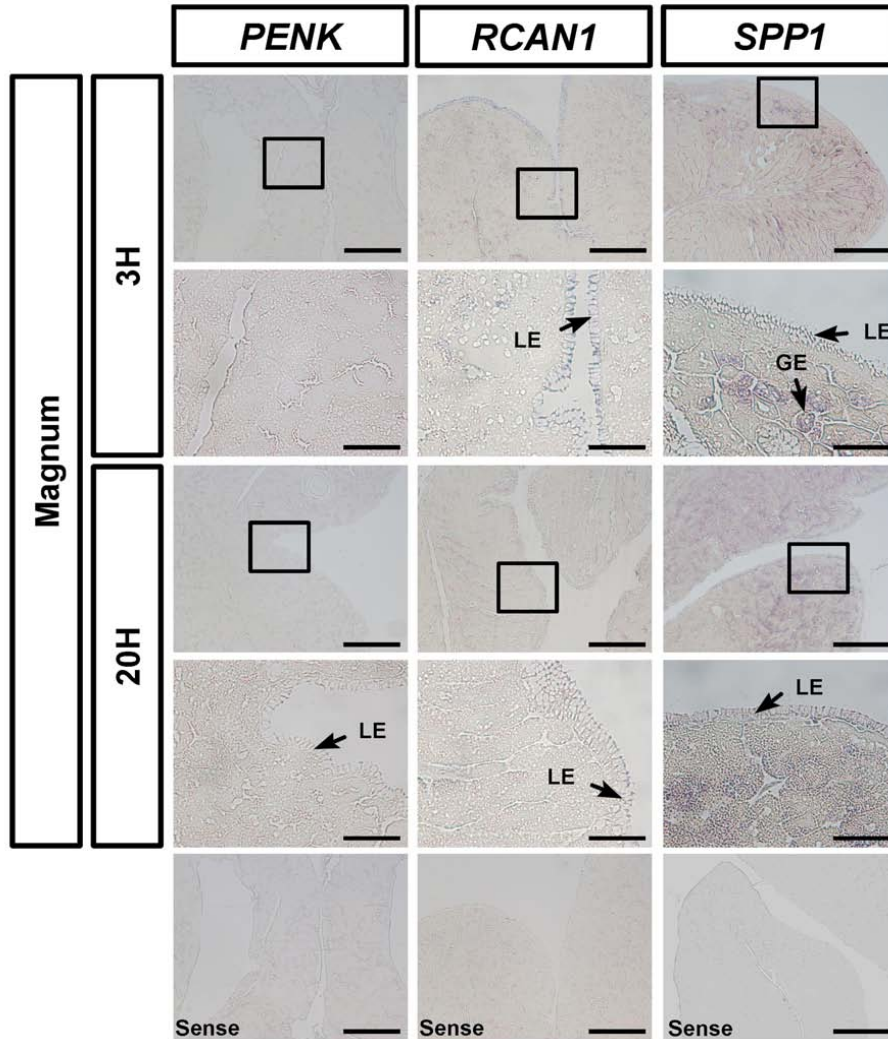


Figure 9-7. Cell-specific localization of mRNAs for *PENK*, *RCAN1* and *SPP1* in the magnum are presented for oviducts of hens at 3 h and 20 h post-ovulation. All mRNAs were expressed at very low abundance in GE of the magnum of the oviducts between 3h and 20 h after ovulation. Legend: LE, Luminal epithelium; GE, glandular epithelium. *Scale bar* represents 10 μm .

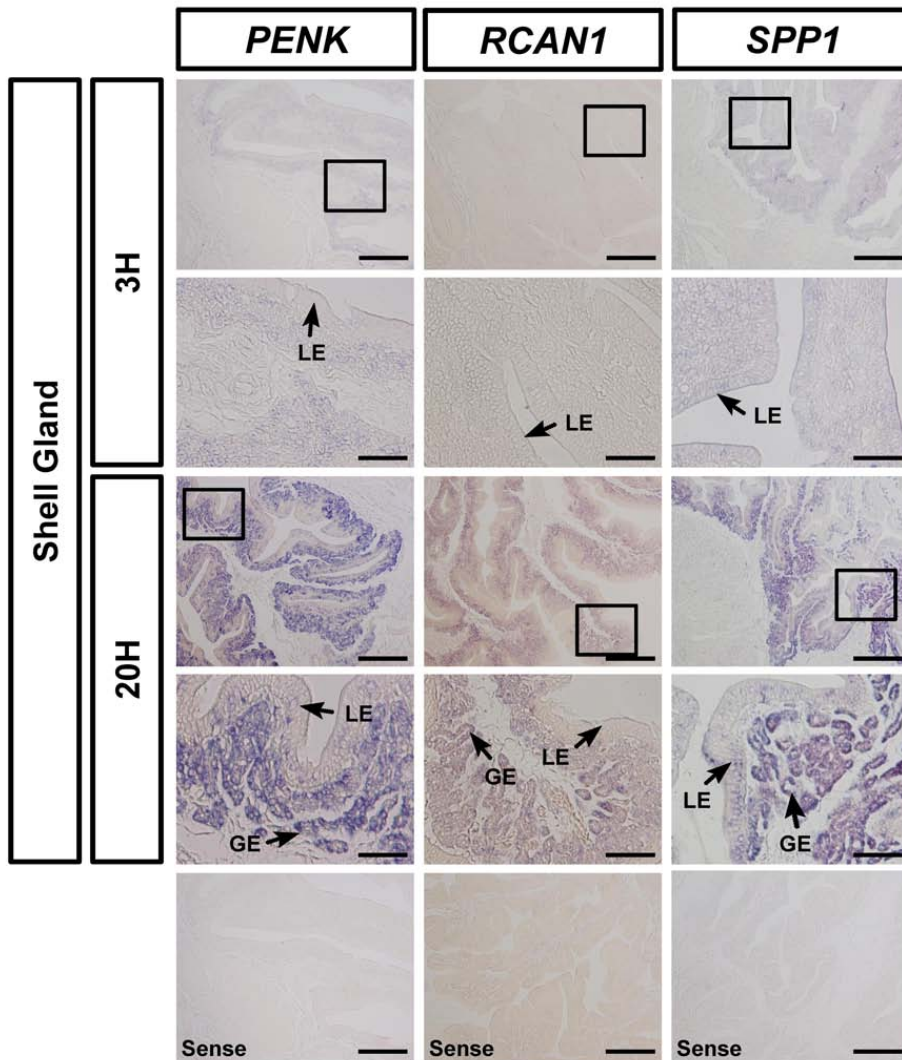


Figure 9-8. Cell-specific localization of mRNAs for *PENK*, *RCAN1* and *SPP1* in the shell gland of oviducts of hens are presented for 3 h and 20 h post-ovulation. All mRNAs were localized predominantly in the glandular epithelium (GE) of the shell gland at 20 h after ovulation. Legend: LE, Luminal epithelium; GE, glandular epithelium. *Scale bar* represents 10 μ m.

Table 9-1. Primers used for quantitative RT-PCR analysis

Gene	GenBank accession no.	Sequence (forward and reverse)
<i>CALB1</i>	NM_205513.1	TCAGCCTTGGTCTTGGCAT TGTGTGGAGTGGAAGTAAAGCC
<i>CYP26A1</i>	AF199462.1	GCCTTTCAGTGGGCTCTACC ACCCTGTGTGTGCTCCATCA
<i>PENK</i>	BX930983.1	GCTGGATGAGAACCATCTGC AGCCTCCGTACCTCTTAGCC
<i>RCAN1</i>	BU422433.1	CCTGGTCGCTCTCACATACG CTCCTGCCTCTCCACCTGTT
<i>SPPI</i>	NM_204535.4	AGGAGTTGCTGCTGGGATTG TGCCTGGATTTGCTCACTGG
<i>ACPI</i>	NM_001039291.1	TGTGCTCTTCGTTTGTCTGG TGAGGCTTCTCCAAAAATGC

Table 9-2. Primers used for generating probes for in situ hybridization analysis

Gene	GenBank accession no.	Sequence (forward and reverse)
<i>CALB1</i>	NM_205513.1	GGCCTGGTTCTTTTACTTTGC TCCTGCACTCCATAACATGC
<i>CYP26A1</i>	AF199462.1	GTTGATGGAGCACACACAGG GGTTGAACTCGTCCTTGTCG
<i>PENK</i>	BX930983.1	CTGCTTGCCAAGAAATACGG CAGAAGGGAGAATGGAATCG
<i>RCAN1</i>	BU422433.1	CTTCTTCCACGTCGTTTTCC TCAATCAAGCAGAACCAAGG
<i>SPPI</i>	NM_204535.4	GCTGACTTCTCCAGCACAGG CATCATCCACGGCCTCTTGG
<i>ACPI</i>	NM_001039291.1	TGTGCTCTTCGTTTGTCTGG TGAGGCTTCTCCAAAAATGC

Table 9-3. The fold-changes in expression of six genes (*ACPI*, *CALBI*, *CYP26A1*, *PENK*, *RCANI* and *SPPI*) detected using quantitative RT-PCR and microarray analyses

Gene	Fold-change in quantitative RT-PCR		Fold-change in microarray analyses	
	Magnum (3 h vs. 20 h)	Shell Gland (3 h vs. 20 h)	Magnum (3 h vs. 20 h)	Shell Gland (3 h vs. 20 h)
<i>CALBI</i>	N.S. [†]	8.76±1.33	N.S. [†]	45.74
<i>CYP26A1</i>	N.S. [†]	10.95±0.54	N.S. [†]	12.60
<i>PENK</i>	N.S. [†]	25.88±3.35	N.S. [†]	21.84
<i>RCANI</i>	1.47±0.07	10.08±0.21	N.S. [†]	11.58
<i>SPPI</i>	N.S. [†]	22.13±6.79	N.S. [†]	70.53
<i>ACPI</i>	0.41±0.11	1.52±0.07	N.D. [§]	N.D. ^{§-}

[†]N.S. No significant difference was detected due to time post-ovulation.

[§]N.D. Not detected

The value for quantitative RT-PCR represents the mean ± SEM of three independent experiments.

5. Discussion

In the present study, our high-throughput analysis identified candidate genes that potentially regulate production and secretion of egg-white proteins, assembly of egg shell membranes and the formation of an egg during its passage through specific segments of the oviduct of chickens. Results of the present study revealed cell-specific and temporal differences in expression of selected candidate genes in the magnum and shell gland of the oviduct during the different stages of the ovulation to oviposition cycle of laying hens, and provide novel insights into changes at the molecular and cellular levels of candidate genes-related to formation of the egg and oviposition.

In the present study, q-PCR and *in situ* hybridization (ISH) analyses validated expression of selected genes at each time point in each tissue post-ovulation including *ACPI*, *CALBI*, *CYP26A1*, *PENK*, *RCAN1* and *SPPI*. These six candidate genes were chosen because they are related to egg formation or oviposition in chickens by regulating production and secretion of egg-white proteins, assembly of egg shell membranes and/or formation of the calcified egg shell. The temporal and cell-specific expression of these genes suggests that they are novel genes associated with changes in the egg-laying cycle and that they have important roles in the reproductive system of hens. *In situ* hybridization is widely used to determine temporal and cell-specific changes in expression of mRNAs in tissues; therefore, we compared the expression levels of specific mRNAs at 3 h and 20 h post-ovulation in

the oviduct of the hens. The results of ISH also provide a link between differential expression and function of selected genes and serve to validate overall results from the microarray analysis and q-PCR.

CALB1 is a Ca^{+2} -binding protein found at high concentrations in intestine and shell gland of birds (Corradino et al., 1968; Wasserman and Taylor, 1966). This protein contains four active Ca^{+2} -binding domains and two modified domains without Ca^{+2} -binding capacity, and acts as a Ca^{+2} buffer/sensor holding four molecules of Ca^{+2} in the EF-hands, which is a helix-loop-helix structural domain found in a large family of Ca^{+2} -binding proteins, of loops EF1, EF3, EF4 and EF5 (Kojetin et al., 2006). In chickens, a large amount of Ca^{+2} carbonate is deposited in the shell gland and transferred into the egg shell along with high concentrations of CALB1 during the period of egg shell formation (Corradino et al., 1968; Nys et al., 1989). In this study, *CALB1* mRNA increased about 9-fold ($P < 0.001$) in the shell gland at 20 h after ovulation (Figure 9-4). These results confirm a previous report that the concentration of *CALB1* mRNA in the shell gland of laying hens is low 4 h after ovulation and increases markedly 12 h and 18 h later when shell calcification takes place (Nys et al., 1989). In addition, a decline in egg shell density in aged hens is likely caused by a physiological deficiency in Ca^{+2} or by a defect in the hens' ability to alter CALB1 synthesis in response to the demand for Ca^{+2} (Bar et al., 1992a; Bar et al., 1992b). Results of the present study and previous reports indicate that CALB1 plays an essential role in calcification of the egg shell before oviposition.

The second gene of interest, *CYP26A1*, is a member of the cytochrome P450 superfamily of enzymes that regulate gene expression in both embryonic and adult tissues under tight control of cellular concentrations of retinoic acid which is an active metabolite of vitamin A essential to cell signaling cascades during the period of vertebrate development (Maden, 1998; Maden et al., 1998). It is also involved in the synthesis of biomaterials such as cholesterol, steroids and some lipids (White et al., 1997; White et al., 1998). Indeed, *Cyp26a1* null mice die just before parturition and exhibit many defects and disorders such as caudal regression, hindbrain patterning defects and vertebral malformations (Abu-Abed et al., 1998; Sakai et al., 2001). However, little is known about the expression and functional role of CYP26A1 in the chicken oviduct. In the present study, CYP26A1 expression was weak in the magnum after ovulation, but increased significantly in GE of the shell gland at 20 h after ovulation. These results suggest that the well-organized spatial and temporal expression patterns of retinoic acid-related enzymes provide combinatorial effects that mediate morphological remodeling of tissues during the egg-laying cycle.

Another gene of interest in the present study was proenkephalin (*PENK*). Neuropeptides are potent regulators of a variety of biological processes, including growth, development, reproduction, memory and behavior (Hook et al., 2008). Enkephalin is a member of opioid peptide family that includes endorphins and dynorphins that are translated from the *PENK* gene as Met-enkephalin and Leu-enkephalin, and bind to opioid receptors in the central nervous system (CNS) and in peripheral tissues (Noda et al., 1982). Indeed, enkephalins are detected in extra-CNS.

For example, human *PENK* mRNA has been detected in esophagus, gastrointestinal tract, pancreas, and gallbladder (Monstein et al., 2006) and chicken enkephalins have been detected in the lumbar spinal cord and thyroid C cells (Kameda et al., 2000; Maderdrut et al., 1986). In addition, endogenous enkephalins have been identified in female reproductive organs of several animal species such as ovaries, uterus, and follicular fluid of rats, hamsters, cows, pigs, rabbits and women (Jin et al., 1988; Kilpatrick et al., 1985; Li et al., 1991a; Li et al., 1991b; Petraglia et al., 1985). In the present study, we identified for the first time *PENK* mRNA in the chicken oviduct. *PENK* mRNA increased over 20-fold in the shell gland at 20 h after ovulation based on both microarray and q-PCR analyses and was abundant in the GE of the shell gland at 20 h post-ovulation. It may serve to reduce pain associated with oviposition; however, further studies are needed to assess the functional role(s) of the *PENK* gene in female reproductive organs.

We found that *RCANI* expression increased in the shell gland at 20 h after ovulation. Calcineurin, a calcium-dependent serine-threonine phosphatase, plays essential roles in many important biological events. Indeed, *RCANI* is a member of the *RCAN* family of genes previously known as mammalian DSCR1, MCIP1, Calcipressin1 and Adapt78 (Davies et al., 2007). In humans, the *RCANI* gene consists of seven exons on chromosome 21 known as the Down syndrome critical region and transcribes different alternatively spliced isoforms (Esteban et al., 2011; Fuentes et al., 1997). *RCAN1* is involved in various physiological and pathological procedures such as attenuation of carcinogenesis and angiogenesis, inhibition of cardiac hypertrophy,

mast cell function, and Alzheimer's disease (Davies et al., 2007; Ermak et al., 2001; Esteban et al., 2011; Minami et al., 2004; Rothermel et al., 2001) and it activates protein kinase A-mediated cAMP response element-binding protein (CREB) signaling through inhibition of calcineurin activity (Kim and Seo, 2011). Furthermore, calcineurin is activated in uteri of pregnant mice at term (Tabata et al., 2009). In the present study, *RCAN1* mRNA increased at 20 h post-ovulation in the shell gland suggesting that RCAN1 may play an important role in signal transduction of calcineurin and its regulator during egg formation and oviposition.

The fifth gene of interest, SPP1, also known as osteopontin, is a highly phosphorylated sialoprotein that is an essential component of most mineralized structures in biology such as bones, teeth and cartilage (Sodek et al., 2000). SPP1 was originally isolated from bones of rats (Oldberg et al., 1986) and the gene has seven exons on chromosome 4q13 in humans and chromosome 5 in mice. SPP1 has a polyaspartic acid sequence and a highly conserved RGD (Arg-Gly-Asp) motif (Butler, 1989; Sodek et al., 2000). In chickens, SPP1 is secreted by the shell gland of the oviduct of laying hens for egg shell calcification (Pines et al., 1995). Of particular note, chicken SPP1 has seven of nine consecutive residues of aspartic acid, an RGD integrin recognition motif and four recognition sequences for phosphorylation with the greatest similarity to mammalian SPP1 (Moore et al., 1991; Rafidi et al., 1994). In addition, chicken SPP1 is temporally associated with eggshell mineralization in a phosphorylation-dependent manner and physical distension of the shell gland with passage of the egg (Chien et al., 2009; Lavelin et al., 1998). However, unlike previous

reports (Arazi et al., 2009; Fernandez et al., 2003; Pines et al., 1995), we found abundant levels of *SPP1* mRNA in GE of the shell gland.

The sixth gene of interest was *ACP1*. Purple acid phosphatases (mammalian enzymes known as type 5 tartrate resistant acid phosphatases; ACP5) are a diverse group of binuclear metallohydrolases identified and characterized in plants, animals, fungi and a few bacteria (Flanagan et al., 2006). Their characteristic purple color is due to a tyrosine to ferric iron charge transfer transition (Antanaitis et al., 1983). Surprisingly, the *ACP5* gene is not present in the chicken genome. Rather, *ACP1* has the highest homology to mammalian ACP5 and belongs to the low molecular weight phosphotyrosine protein phosphatase family (Caldwell et al., 2005), but there are no reports on functional aspects of chicken ACP1. The secreted proteins of pig uterine GE are enriched in ACP5 (initially named uteroferrin) that exists as a heterodimer with one of the three ACP5-associated proteins (Bazer and Roberts, 1983). Porcine ACP5 transports iron from uterine GE across the placental areolae and into the fetal circulation where it is utilized in the formation of hemoglobin in erythrocytes of fetal pigs (Bazer and Roberts, 1983) and it is also a hematopoietic growth factor (Bazer et al., 1991). In humans with spondyloenchondrodysplasia and various autoimmune phenotypes, haplotype data and linkage analysis studies revealed biallelic mutations in the *ACP5* gene and loss of expressed ACP5 (Briggs et al., 2011). Since ACP5 can alter the phosphorylation status of *SPP1*, mutations in the *ACP5* gene appear to lead to hyperphosphorylated *SPP1* and increases in circulating levels of interferon alpha (IFNA) in individuals with spondyloenchondrodysplasia due to dysregulated bone mineralization,

as well as abnormal brain calcifications associated with neurologic symptoms (Behrens and Graham, 2011). It was further suggested that excessive intracellular hyperphosphorylated SPP1 leads to production of IFNA by plasmacytoid dendritic cells via toll-like receptor 9-mediated signaling that may lead to lupus-like autoimmunity through a variety of mechanisms (Behrens and Graham, 2011). Results of the present study are the first to indicate expression of avian ACP1 in both the magnum and shell gland of the chicken oviduct at 3 h and 20 h post-ovulation. The incorporation of both ACP1 and SPP1 into egg-white proteins may affect the degree of phosphorylation of SPP1 during development of bone during embryonic development prior to hatching. Also, the coordinate increase in ACP1 and SPP1 in the shell gland between 3 h and 20 h post-ovulation suggests that ACP1 could affect the phosphorylation status of SPP1 and calcification of the egg shell.

Collectively, results of the present microarray study represent part of a continuing effort to identify candidate genes that regulate events during the ovulation-oviposition cycle in the oviduct of laying hens. Moreover, the genes identified in this study point to the need for studies of mechanisms for egg formation and oviposition under complex regulation of steroid hormones and other hormones, growth factors and other regulatory molecules in laying hens. Further research is required to fully understand the roles and functions of these genes in the context of functional aspects of the avian female reproductive tract.

CHAPTER 10

Recrudescence Mechanism and Gene Expression Profile of the Reproductive Tracts in Chicken during the Molting Period

1. Abstract

The reproductive system of chickens undergoes dynamic morphological and functional tissue remodeling during the molting period. The present study identified global gene expression profiles following oviductal tissue regression and regeneration in laying hens in which molting were induced by feeding high levels of zinc in the diet. During the molting and recrudescence processes, progressive morphological and physiological changes included regression and re-growth of reproductive organs and fluctuations in concentrations of testosterone, progesterone, estradiol and corticosterone in blood. The cDNA microarray analysis of oviductal tissues revealed the biological significance of gene expression-based modulation in oviductal tissue during its remodeling. Based on the gene expression profiles, expression patterns of selected genes such as, *TF*, *ANGPTL3*, *p20K*, *PTN*, *AvBD11* and *SERPINB3* exhibited similar patterns in expression with gradual decreases during regression of the oviduct and sequential increases during resurrection of the functional oviduct. Also, *miR-1689** inhibited expression of *Sp1*, while *miR-17-3p*, *miR-22** and *miR-1764* inhibited expression of *STAT1*. Similarly, chicken *miR-1562* and *miR-138* reduced the expression of *ANGPTL3* and *p20K*, respectively. These results suggest that these differentially regulated genes are closely correlated with the molecular mechanism(s) for development and tissue remodeling of the avian female reproductive tract, and that miRNA-mediated regulation of key genes likely contributes to remodeling of the avian reproductive tract by controlling expression of those genes post-transcriptionally. The discovered global gene profiles provide new molecular candidates responsible for

regulating morphological and functional recrudescence of the avian reproductive tract, and provide novel insights into understanding the remodeling process at the genomic and epigenomic levels.

2. Introduction

The chicken has unique features for basic studies of developmental processes such as organogenesis, so it is an excellent animal model for studies of vertebrate developmental biology. Under natural condition, domestic laying hens start to lay eggs after reaching sexual maturity at about 5 months of age, and the laying hen then produces an egg on 90% or more of the days in her first year of laying eggs (Garlich et al., 1984). As the hen ages, the egg production rate progressively decreases and the hen naturally undergoes annual period of molting at the end of each laying cycle (Berry, 2003). Molting is a phenomenon that includes renewal of old feathers with new feathers and an associated complete remodeling of the reproductive system (Berry, 2003; Mrosovsky and Sherry, 1980). During this process, the reproductive organs undergo regression and rejuvenation, and then recovery in preparation for a new egg laying cycle (Berry, 2003). Artificially induced molting is an effective tool in commercial poultry farming for improving the rate of egg production and quality of eggs as it renews the hen's laying cycle (al-Batshan et al., 1994; Webster, 2003). The removal of feed has been used most frequently in commercial poultry farms to induced molting in hens; however, this practice has come under criticism of severe fasting from animal welfare advocacy groups (Ruszler, 1998). Furthermore, molting through feed withdrawal leads to greater susceptibility to salmonella infection than in the laying phase (Ariyadi et al., 2012; Holt et al., 1994). Therefore, several alternative methods without starvation have been developed. These include feeding diets deficient in an essential nutrient or modifying the diet by feeding low levels of

calcium or high levels of zinc (Alodan and Mashaly, 1999; Breeding et al., 1992; Damme et al., 1987; McCormick and Cunningham, 1984). Among these, the practice of feeding a diet high in zinc has received more attention as it is easy to practice and post-molt performance of laying hens is acceptable without increase in susceptibility to *S. enteritidis* (Moore et al., 2004; Park et al., 2004; Sundaresan et al., 2008).

The majority of previous studies investigating molting process and associated changes in the chicken oviduct have been comparative studies of physiological changes focused on phenomena only during the period of regression of the oviduct. Therefore, relatively little is known about mechanisms regulating remodeling of the oviduct after cessation of egg production during the molting process or recrudescence of the oviduct following the molting period. Moreover, little is known about genome-based mechanisms responsible for the regenerative ability of the reproductive tract in laying hens following molting and tissue remodeling. Therefore, the present study was designed to discover novel genes and pathways underlying molecular mechanism(s) for tissue remodeling of the oviduct of laying hens following a high zinc diet-induced molting period. A better appreciation of reproductive tissue remodeling is crucial to understanding the overall genetic and molecular mechanism(s) for both regression and regeneration of the avian female reproductive organs. Actually, most female reproductive organs undergo repetitive morphological changes according to programmed processes associated with menstrual and estrous cycles and molting process involving ovarian and reproductive tract tissues. For example, reproductive organs in women, especially uterine endometrium,

undergoes dynamic tissue remodeling during some 400 menstrual cycles between puberty and menopause (Jabbour et al., 2006; McLennan and Rydell, 1965). This repetitive phenotypic change is also accompanied by dramatic changes in gene expression profiles (Ponnampalam et al., 2004).

The aims of this study were to: 1) investigate the physiological changes and gene expression profiles in reproductive organs of laying hens during molting; 2) identify novel genes and their interactions related to reproductive tissue remodeling; and 3) determine epigenetic mechanisms affecting the reproductive tract of laying hens during regression, remodeling and recrudescence associated with the period of molting. Along with completion of sequencing of the chicken genome, many applications of chicken DNA microarrays have led to massive increase in the discovery of genes whose expression is stimulated by estrogen, differential genes expression in the oviduct between immature versus mature hens, and between 3 h versus 20 h post-ovulation (Dunn et al., 2009a; Jeong et al., 2012; Song et al., 2011b). In the present study, we induced molting and changes in oviductal status by feeding high levels of zinc in the diet and assessed its suitability for investigations of molecular mechanisms controlling pre-molting and post-molting processes. Using cDNA microarray analysis, we now report large-scale gene expression profiles for the oviducts of laying hens during the molting and recrudescence periods. We also determined spatio-temporal specific mRNA expression patterns and validated chicken microRNAs (miRNAs) regulating these genes post-transcriptionally. Our approach contributes to the development of novel insights into degeneration and regeneration

mechanisms of female reproductive organ at the molecular level.

3. Materials and Methods

Experimental Animals and Animal Care

The experimental use of chickens for this study was approved by the Institute of Laboratory Animal Resources, Seoul National University (SNU-070823-5). White Leghorn (WL) chickens were subjected to standard management practices at the University Animal Farm, Seoul National University, Korea. All chickens were exposed to a regimen of 15 h light and 9 h dark.

Molting and Recrudescence Induction

Molting of laying hens was induced as described previously that involves adding 20,000 ppm zinc to the diet to effectively reduce feed-intake and induces molting (Berry and Brake, 1985; Creger and Scott, 1977). Briefly, molting was induced by feeding hens in the zinc-fed group a diet containing high zinc (mixed 252 g zinc oxide per 10 kg feed to achieve a final concentration of 20,000 ppm of zinc). Laying hens in the molting group completely ceased egg production within 12 days after feeding the high zinc-diet. The 35 laying hens (47-week-old) were divided into two larger groups, including molting-progressing or post-molting-progressing group, and kept in individual cages. The molting group was divided into three subgroups based on the number of days of feeding the high zinc diet (normal feeding group, 6 days and 12 days after onset of zinc feeding). The recrudescence (post-molting) group

was divided into four subgroups based on the number of normal feeding days after complete cessation of egg laying and initiation of feeding a normal commercial diet: 20, 25, 30 or 35 days after onset of zinc feeding or 8, 13, 18 or 23 normal feeding days after cessation of egg production and removal from the high zinc diet.

Tissue and Blood Sample Collection

Hens (n=5 per time point) in each subgroup (0, 6, 12, 20, 25, 30 and 35 days after onset of zinc feeding) were bled and serum was obtained and stored at -80 °C until further use. After euthanizing the hens using 60%–70% carbon dioxide, the ovary and oviduct were removed and measured for length and weight at each assigned day. Oviduct weight was taken after removing the egg, if present, from the oviduct. Portions of the ovary, magnum, isthmus and shell gland of each oviduct from each hen at each time point were cut into 10- to 15-mm pieces and either: 1) frozen immediately in liquid nitrogen and stored at -80°C until analyzed; or 2) fixed in freshly prepared 4% paraformaldehyde in PBS (pH 7.4). After 24 h, tissues fixed in 4% paraformaldehyde were changed to 70% ethanol for 24 h and then dehydrated and embedded in Paraplast-Plus (Leica Microsystems, Wetzlar, Germany). Paraffin-embedded tissues were sectioned at 5 µm and stained with hematoxylin and eosin. Histomorphological changes of the stained tissue sections were evaluated using a microscope (Leica Microsystems, DM3000, Germany).

Estimation of Serum Hormones

Concentrations of testosterone, progesterone, estradiol and corticosterone in serum from individual hens during molting and the recrudescence processes were determined by EIA kits for testosterone (catalog number EA78; Oxford Biomedical Research, MI, USA), progesterone (catalog number EA74; Oxford Biomedical Research, MI, USA), estradiol (catalog number EA70; Oxford Biomedical Research, MI, USA) and corticosterone (catalog number EA66; Oxford Biomedical Research, MI, USA). Each sample was assayed in duplicate according to the manufacturer's directions. Briefly, arterial blood samples from each hen were centrifuged at 3000 g for 30 min at 4°C and plasma separated and incubated with diluted hormone conjugate for 1 h. Unbounded hormone was removed through a washing process and bound hormone conjugate was detected following the addition of substrate which generates an optimal color. Quantitative results were obtained by measuring and comparing the absorbance reading of the samples against the standards with a microplate reader (Bio-Rad, CA, USA) at 450 nm (for samples) or 650 nm (for standards), respectively.

RNA Isolation

Total RNA was isolated from frozen magnum tissues from each time point using Trizol reagent (Invitrogen, Carlsbad, CA) according to manufacturer's recommendations. The quantity and quality of total RNA was determined by spectrometry and denaturing agarose gel electrophoresis, respectively.

Microarray Analysis

Microarray analysis was performed using Affymetrix GeneChip® Chicken Genome Arrays (Affymetrix, Santa Clara, CA, USA) which contained 30,000 probes corresponding to known chicken genes. For microarray analysis, total RNAs were extracted from the magnum from each of the four hens at each time point (0, 6, 12, 20, 25, 30 and 35 days after onset of zinc feeding) and purified using an RNeasy Mini Kit (Qiagen, Valencia, CA, USA). Data were generated by InsilicoGen (Suwon, Korea) and dChip software was used for the analysis. All experiments were performed using four independent RNA pools from each of the four hens at each time point and three independent microarray chips. The signal intensity of each spot was calculated, and then differentially expressed genes were identified by the net intensity ratios between the two test groups. The student t-test p-values were used to compare intensities between the two groups. A p-value of 0.05 was used as threshold value for statistical significance. Next, pathway analysis was performed using Pathway Studio software to classify specific signaling pathways and gene regulation maps. Gene Ontology (GO) analysis was conducted to further clarify the functional roles of differentially expressed genes and classify them based on their functions in cellular processes using GeneSpring software (Silicon Genetics, Agilent Technologies, Palo Alto, CA).

Quantitative RT-PCR Analysis

Complementary DNA was synthesized using total RNA extracted from magnum and AccuPower® RT PreMix (Bioneer, Daejeon, Korea). Gene expression levels were measured using SYBR® Green (Sigma, St. Louis, MO, USA) and a StepOnePlus™ Real-Time PCR System (Applied Biosystems, Foster City, CA, USA). The *GAPDH* gene was simultaneously analyzed as a control and used for normalization for variation in loading. Each target gene and *GAPDH* was analyzed in triplicate. Using the standard curve method, we determined the level of expression of the examined genes using the standard curves and C_T values, and normalized them based on *GAPDH* expression. The PCR conditions were 95°C for 3 min, followed by 40 cycles at 95°C for 30 sec, 60°C for 30 sec, and 72°C for 30 sec using a melting curve program (increasing the temperature from 55°C to 95°C at a rate of 0.5°C per 10 sec) and continuous fluorescence measurement. ROX dye (Invitrogen) was used as a negative control for the fluorescence measurements. Sequence-specific products were identified by generating a melting curve in which the C_T value represented the cycle number at which a fluorescent signal was statistically greater than background, and relative gene expression was quantified using the $2^{-\Delta\Delta CT}$ method (Livak and Schmittgen, 2001). For the control, the relative quantification of gene expression was normalized to the C_T of the Day 0 magnum.

Detection of Apoptotic Cell Death

Embedded and sectioned tissues were deparaffinized in xylene and washed in 0.1 M PBS. For immunostaining, sections were then permeabilized in proteinase K,

and subjected to TUNEL (terminal deoxynucleotidyl transferase-mediated dUTP-fluorescein nick-end labeling) staining mixture using the In Situ Cell Death Detection kit, TMR red (Roche Diagnostics, Canada) for 1 h at 37°C. As negative controls, tissues were incubated only in the labeling solution instead of the TUNEL reaction mixture. For positive controls, tissues were treated with DNaseI for 10 min at room temperature to induce DNA strand breaks before TUNEL initiating labeling procedures. Fluorescence was detected using a confocal microscope LSM710 (Carl Zeiss) fitted with a digital microscope camera AxioCam using Zen 2009 software.

In Situ Hybridization Analysis

For hybridization probes, PCR products were generated from cDNA with the primers used for RT-PCR analysis. The products were gel-extracted and cloned into TOPO® vector (Invitrogen). After verification of the sequences, plasmids containing the correct gene sequences were amplified with T7- and SP6-specific primers (T7:5'-TGT AAT ACG ACT CAC TAT AGG G-3'; SP6:5'-CTA TTT AGG TGA CAC TAT AGA AT-3') then digoxigenin (DIG)-labeled RNA probes were transcribed using a DIG RNA labeling kit (Roche Applied Science, Indianapolis, IN). Tissues were collected and fixed in 4% paraformaldehyde, embedded in paraffin and sectioned at 5 µm on APES-treated (silanized) slides. The sections were then deparaffinized in xylene and rehydrated to diethylpyrocarbonate (DEPC)-treated water through a graded series of alcohol. The sections were treated with 1% Triton X-100 in PBS for 20 min and washed two times in DEPC-treated PBS. After washing in

DEPC-treated PBS, they were digested with 5 µg/ml proteinase K (Sigma) in TE buffer (100 mM Tris-HCl, 50 mM EDTA, pH 8.0) at 37°C. Paraffin-embedded tissue sections were incubated twice for 5 min each in DEPC-treated PBS and incubated in TEA buffer (0.1M triethanolamine) containing 0.25% (v/v) acetic anhydride. The sections were next incubated in a prehybridization mixture containing 50% formamide and 4X standard saline citrate (SSC) for at least 10 min at room temperature. After prehybridization, the sections were incubated with a hybridization mixture containing 40% formamide, 4X SSC, 10% dextran sulfate sodium salt, 10mM DTT, 1 mg/ml yeast tRNA, 1mg/ml salmon sperm DNA, 0.02% Ficoll, 0.02% polyvinylpyrrolidone, 0.2 mg/ml RNase-free bovine serum albumin and denatured DIG-labeled cRNA probe overnight at 42°C in a humidified chamber. After hybridization, sections were washed for 15 min in 2X SSC at 37°C, 15 min in 1X SSC at 37°C, 30 min in NTE buffer (10mM Tris, 500mM NaCl and 1mM EDTA) at 37°C and 30 min in 0.1X SSC at 37°C. After blocking with a 2% normal sheep serum (Santa Cruz Biotechnology, INC.), the sections were incubated overnight with sheep anti-DIG antibody conjugated to alkaline phosphatase (Roche). The signal was visualized by exposure to a solution containing 0.4 mM 5-bromo-4-chloro-3-indolyl phosphate, 0.4 mM nitroblue tetrazolium, and 2 mM levamisole (Sigma).

Immunohistochemistry

Immunohistochemical localization of cytokeratin, vimentin and PCNA protein in pre-molting and post-molting magnum from hens was performed as

described previously (Song et al., 2006) using an anti-mouse cytokeratin monoclonal antibody (catalog number MAB3412; Millipore, MA, USA) at a final dilution of 1:500 (2 μ g/ml), anti-mouse vimentin monoclonal antibody (catalog number CBL202; Millipore, MA, USA) at a final dilution of 1:100 (0.5 μ g/ml) and an anti-mouse PCNA monoclonal antibody (catalog number sc-56; Santa Cruz Biotechnology, CA, USA) at a final dilution of 1:1000 (1 μ g/ml). Antigen retrieval was performed using the boiling citrate method as described previously (Song et al., 2006). Negative controls included substitution of the primary antibody with purified non-immune mouse IgG at the same final concentration.

MicroRNA Target Validation Assay

The 3'-UTRs of *Sp1*, *STAT1*, *ANGPTL3* and *p20K* were cloned and confirmed by sequencing. Each 3'-UTR was subcloned between the eGFP gene and the bovine growth hormone poly-A tail in pcDNA3eGFP (Clontech, Mountain View, CA) to generate the eGFP-miRNA target 3'-UTR (pcDNA-eGFP-3'UTR) fusion constructs. For the dual fluorescence reporter assay, the fusion contained the *DsRed* gene and either *miR-1689** for *Sp1*; *miR-17-3p*, *miR-22** or *miR-1764* for *STAT1*; *miR-1562* for *ANGPTL3* and *miR-138* for *p20K* which were designed to be co-expressed under control of the CMV promoter (pcDNA-DsRed-miRNA). The pcDNA-eGFP-3'UTR and pcDNA-DsRed-miRNA (4 μ g) were co-transfected into 293FT cells using the calcium phosphate method. When the DsRed-miRNA is expressed and binds to the target site of the 3'-UTR downstream of the *GFP* transcript,

green fluorescence intensity decreases due to degradation of the *GFP* transcript. At 48 h post-transfection, dual fluorescence was detected by fluorescence microscopy and calculated by FACSCalibur flow cytometry (BD Biosciences). For flow cytometry, the cells were fixed in 4% paraformaldehyde and analyzed using FlowJo software (Tree Star Inc., Ashland, OR).

Statistical Analyses

Data for quantitative PCR were subjected to analysis of variance (ANOVA) according to the general linear model (PROC-GLM) of the SAS program (SAS Institute, Cary, NC) to determine whether differential gene expression during the molting and recrudescence periods were significant. Data are presented as mean \pm SEM unless otherwise stated.

4. Results

Morphological Changes during Induced Molting and Oviduct Recrudescence

We identified dramatic morphological changes in oviducts and ovaries at different days during the induced molting and recrudescence periods (Figure 10-1A). The regression of oviducts and ovarian follicles at day 6 and day 12 (high zinc feeding days) was followed by sequentially recrudescence by feeding a normal diet after complete cessation of egg production at day 12. In order to determine morphological changes during induced molting and recrudescence, we analyzed body weight, weight and length of the oviduct, and weight of the ovaries. The average body weight of hens fed the high zinc diet for 6 days and 12 days decreased as compared with body weights prior to being fed the high zinc diet, and body weights increased to day 35 or 23 days after cessation of feeding the high zinc diet (Figure 10-1B). Similarly, the weights and lengths of oviduct decreased progressively during the induced molting period (days 0 to 12) when egg laying ceased, and rapid growth of the oviduct occurred between days 12 and 35 of this study (Figure 10-1C and 10-1D). In the same manner, weights of the ovaries decreased significantly at day 12 as compared with hens on a control diet, and gradually increased during the recrudescence periods to that of normal ovaries (Figure 10-1E).

Endocrinological and Histological Changes during Induced Molting and Oviduct Recrudescence

We hypothesized that the morphological and functional changes during the molting period were closely related to alterations in the endocrine system. As we expected, concentrations of testosterone, progesterone, estradiol and corticosterone in serum decreased during the induced molting period (Figure 10-1F, 10-1G, 10-1H and 10-1I) and then increased during the recrudescence period (days 20 to 35). Histological analysis of the tissues revealed regression and remodeling of the ovaries and oviducts in hens undergoing molting or recrudescence that included: dramatic changes in size, involution and formation of tubular glands; regression and recrudescence of ovarian stroma; degeneration of epithelia and reductions in secretions in glands that were followed by gradual recovery during oviduct recrudescence (Figure 10-2).

Apoptotic Cell Deaths during Molting and Recrudescence

To detect apoptotic cell death at the single cell level in oviducts of molting or recrudescenced hens, we detected changes in DNA fragmentation generated by DNase activity in nuclei during apoptosis (Figure 10-3). DNA fragments were detected by labeling free 3'-OH termini. We found that most cells in the magnum were TUNEL (TdT-Mediated dUTP Nick End Labeling) positive starting day 6 and in a stable fashion until day 20. With return to a normal diet, the intensive staining gradually decreased during oviduct recrudescence (days 25 to 35).

Immunohistochemical Staining for Cytokeratin, Vimentin and Proliferating Cell

Nuclear Antigen (PCNA)

Regression and recrudescence of the oviduct was assessed by immunohistochemical analysis for markers of EMT (epithelial-to-mesenchymal transition) and proliferation, that is, cytokeratin (epithelial cell marker), vimentin (mesenchymal cell marker) and PCNA (proliferating cell marker) (Figure 10-4). Luminal epithelial cells and glandular epithelial cells had abundant amounts of cytokeratin on day 20. Vimentin expression was detected in the endometrial stroma and blood vessels. Extensive expression of vimentin, a mesenchymal cytoskeletal protein, was detected in cells of mesenchymal origin such as endothelial cells and arteries. On days 25 and 30, the relative frequency of PCNA-positive cells increased as compared with other days, and stained cells were detected in the basal region of the luminal and glandular epithelia and stromal cells. By 23 days after cessation of zinc feeding (day 35), the frequency of PCNA-positive cells decreased to that determined for the reproductive tract of laying hens prior to molting (day 0).

Altered Gene Expression Patterns during Induced Molting and Oviduct Recrudescence

Using affymetrix Genechip microarrays, we compared genome-wide gene expression patterns in the magnum of the oviduct between individual days (day 0 vs. day 6, day 6 vs. day 12, day 12 vs. day 20, day 20 vs. day 25, day 25 vs. day 30, and day 30 vs. day 35) (Figure 10-5). As illustrated in Figure 10-5A, clustering analysis of

significant genes identified associations of these changes in expression to sets of genes with similar profiles. We used a two-fold change as the experimental cut-off value that would imply significance based on Student's t-test p-values ($p < 0.05$). Of the all genes, 725 transcripts were up-regulated and 2182 transcripts were down-regulated more than two-fold at day 0 (normal feeding hens) as compared with day 6 (high zinc feeding hens for 6 days), 147 transcripts were up-regulated and 278 transcripts were down-regulated over two-fold at day 6 as compared with day 12 (high zinc feeding hens for 12 days), and 92 transcripts were up-regulated and 328 transcripts were down-regulated over two-fold at day 12 as compared with day 20 (normal feed for hens for 8 days after cessation of egg production). Furthermore, 339 transcripts were up-regulated and 292 transcripts were down-regulated at day 20 as compared with day 25 (normal feed for hens for 13 days after cessation of egg production), 104 transcripts were up-regulated and 58 transcripts were down-regulated at day 25 as compared with day 30 (normal feed for hens or 18 days after cessation of egg production), and 1331 transcripts were up-regulated and 319 transcripts were down-regulated at day 30 as compared with day 35 (normal feed for hens for 23 days after cessation of egg production) (Figure 10-5B). The continuously co-regulated genes are presented as Venn diagrams (Figure 10-5C).

Functional Categorization of Significantly Altered Genes during Induced Molting and Recrudescence of the Oviduct

We performed functional analysis of genes that were differentially

expressed during molting and the recrudescence processes based on their involvement in specific biological processes using the Gene Ontology annotations (Figure 10-6). From day 0 through day 35, differentially expressed genes were enriched with functional annotations relating to cellular processes such as apoptosis, cell proliferation and cell differentiation, and most categories were uniformly induced or repressed in their gene expression patterns. In the magnum, between days 0 and 6, days 6 and 12, and days 12 and 20, most genes relating to apoptosis, cell proliferation and cell differentiation were down-regulated. Otherwise, in the magnum between days 20 and 25, days 25 and 30, and days 30 and day 35, most genes relating to apoptosis, cell proliferation and cell differentiation were up-regulated.

Validation of Selected Genes

Changes in expression of mRNAs for nine selected genes in the magnum from hens fed a control diet (day 0), zinc fed hens (days 6 and 12) and recrudescence hens (days 20, 25, 30 and 35) were analyzed by quantitative RT-PCR analysis. As shown in figure 10-7, *Sp1* mRNA levels increased 2-fold ($p < 0.001$) on day 12 as compared to day 0 and then decreased from day 12 to day 35 (during recrudescence period). *STAT1* mRNA levels increased 1.8-fold (not significant) on day 12 as compare to day 0, and decreased to less than 35% of that on day 0 ($p < 0.05$) on day 35. In contrast, expression of *TF*, *ANGPTL3*, *p20K*, *PTN*, *GAL11* and *SERPINB3* mRNAs decreased to less than 0.008- ($p < 0.001$), 0.02- ($p < 0.001$), 0.08- ($p < 0.001$), 0.01- ($p < 0.001$), 0.04- ($p < 0.05$) and 0.02% ($p < 0.001$) of day 0 levels as compared

to values on day 12, and from days 12 to 35 (recrudescence period) expression of mRNAs for these genes increased. These mRNA expression patterns were consistent with results from the microarray analysis. The *RGS6* mRNA decreased less than 50% ($p < 0.05$) of that on day 0 at day 6, but was not different ($p > 0.05$) between days 0 and any other day in the magnum. The cell specific localization of these validated mRNAs was assessed in the magnum of hens at different days during induced molting and recrudescence by *in situ* hybridization analysis (Figure 10-8). As expected, *TF*, *ANGPTL3*, *p20K*, *RGS6*, *PTN*, *GAL11* and *SERPINB3* mRNAs were detected predominantly in glandular (GE) and luminal (LE) epithelia of the magnum on day 0, but expression of all of these mRNAs decreased to basal levels by day 12 before increasing from days 12 to 35 in GE and LE to that detected on day 0. *STAT1* expression was localized to LE at a very weak basal level. In contrast, *Sp1* expression was generally strong on all experimental days in GE and LE of the magnum.

Experimental Validation of miRNA-mRNA Target of Selected Genes

To determine the post-transcriptional regulation of selected genes by microRNA (miRNA), we performed miRNA target validation assays. The miRNA target prediction database (miRDB; <http://mirdb.org/miRDB/>) predicts potential miRNA binding sites on specific mRNA targets (Figure 10-9A, 10-10A, 10-11A and 10-12A). The 3'UTR of the target gene of interest was cloned in immediately downstream of the green fluorescent protein open reading frame sequence, and miRNAs for each specific mRNA target site was cloned in downstream of the red

fluorescent protein open reading frame sequence. The recombinant plasmids were co-transfected into 293FT cells, and for experimental control, just DsRed constructs that do not express the miRNA of interest are transfected into cells (Figure 10-9B, 10-10B, 10-11B and 10-12B). The percentage of GFP-expressing cells and total GFP intensities of multiple cells were measured using fluorescence microscopy and fluorescence activated cell sorting (FACS). The binding of a predicted miRNA to its specific target site on the 3'UTR reduces production of GFP thereby repressing GFP expression which can be measured and compared to a control. As illustrated in Figures 9C and 9D, *miR-1689** reduced the intensity of GFP signal (25.6±3.0% in control vs. 10.0±2.0% in *miR-1689**; $p < 0.01$) suggesting that chicken *miR-1689** interacted with the predicted binding site harbored within the 3'UTR of the *Sp1* gene. In the presence of *miR-17-3p*, *miR-22** and *miR-1764* which target the 3'UTR of *STAT1*, the intensities of GFP signals (21.3±3.4% in control vs. 6.0±3.1% in *miR-17-3p*; $p < 0.01$, 4.3±2.1% in *miR-22**; $p < 0.01$ and 4.4±2.6% in *miR-1764*; $p < 0.01$) were decreased, respectively (Figure 10-10C and 10-10D). Similarly, *miR-1562* targeting the 3'UTR of *ANGPTL3* 3'UTR and *miR-138* targeting the 3'UTR of *p20K* reduced the intensity of the GFP signal (25.9±3.2% in control vs. 5.6±1.3% in *miR-1562*; $p < 0.001$ and 35.7±3.1% in control vs. 4.5±1.0% in *miR-138*; $p < 0.001$), suggesting that chicken *miR-1562* and *miR-138* bind within the 3'UTR of *ANGPTL3* and *p20K* genes, respectively (Figure 10-11C, 10-11D, 10-12C and 10-12D).

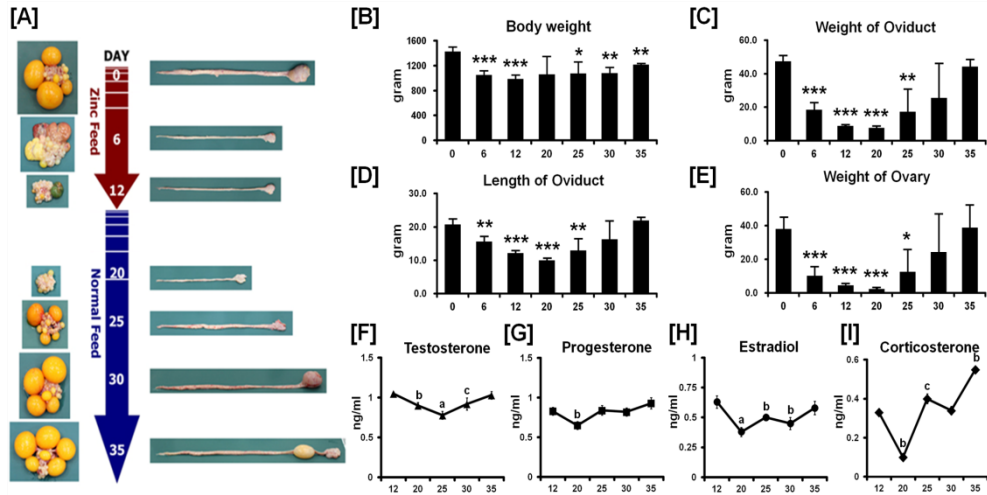


Figure 10-1. Establishment of an *in vivo* experimental model of degeneration and recrudescence of the chicken oviduct. [A] Experimental protocol. The numbers in the red arrows indicate high-zinc feeding days as hens gradually lost the function of the oviduct. The numbers in the blue arrows indicate days of feeding a normal commercial diet after complete cessation of egg production (day 12), and the hens begin to regain function of the oviduct. [B-E] Changes in body weight [B], oviduct weight [C], oviduct length [D] and ovarian weight [E] of hens at different days during the molting and recrudescence periods induced by feeding a high zinc diet followed by feeding a recrudescence normal commercial diet. The graphs show the mean of weights or lengths for each sample obtained on each day of the study (mean \pm SEM, $n=5$). The asterisks denote effects that were significant (***) $p < 0.001$, (**) $p < 0.01$, or (*) $p < 0.05$). [F-I] Profiles of concentrations of testosterone [F], progesterone [G], estradiol [H] and corticosterone [I] in serum from different days of the molting and recrudescence periods. Each bar is mean \pm S.E of three independent experiments.

Different alphabets above the lines indicate significant difference in the means (^a $p < 0.001$, ^b $p < 0.01$, or ^c $p < 0.05$).

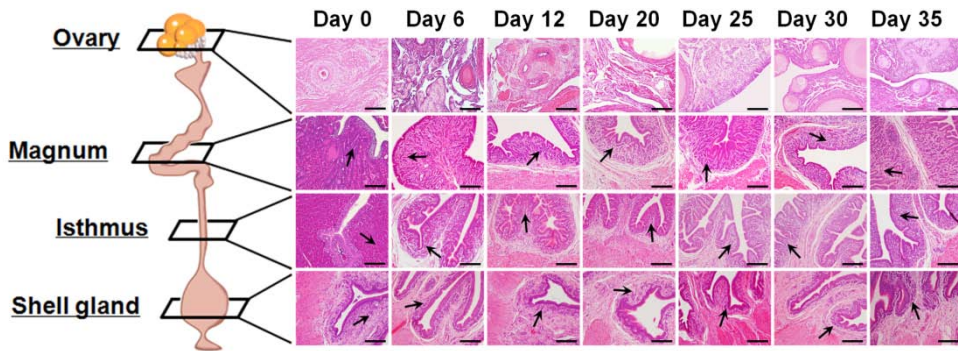


Figure 10-2. Histological evaluation of ovarian and oviductal tissues at different days of the molting and recrudescence periods. The tissues from the ovary, magnum, isthmus and shell gland were observed following staining with hematoxylin and eosin (H&E). Images were captured at 20X magnification. Arrow: Examples of tubular glands; *Scale bar* represents 100 μm .

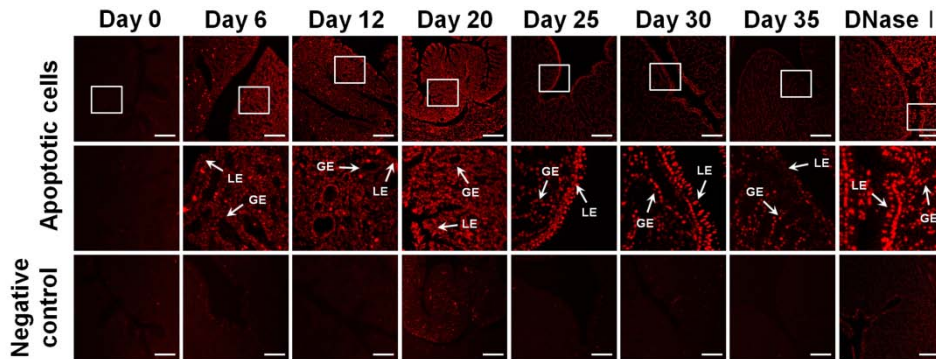


Figure 10-3. TUNEL (TdT-Mediated dUTP Nick End Labeling) stained cells in the magnum of hens fed a high zinc diet or a normal diet. Endogenous DNA fragmentation in nuclei of cells indicates programmed cell death. For positive controls, tissues were incubated with DNase I prior to labeling procedures. And for negative controls, tissues were incubated only in the label solution instead of TUNEL reaction mixture. Images were captured at 20X (top) and 40X (middle) magnification. Legend: LE, luminal epithelium; GE, glandular epithelium; *Scale bar* represents 50 μm .

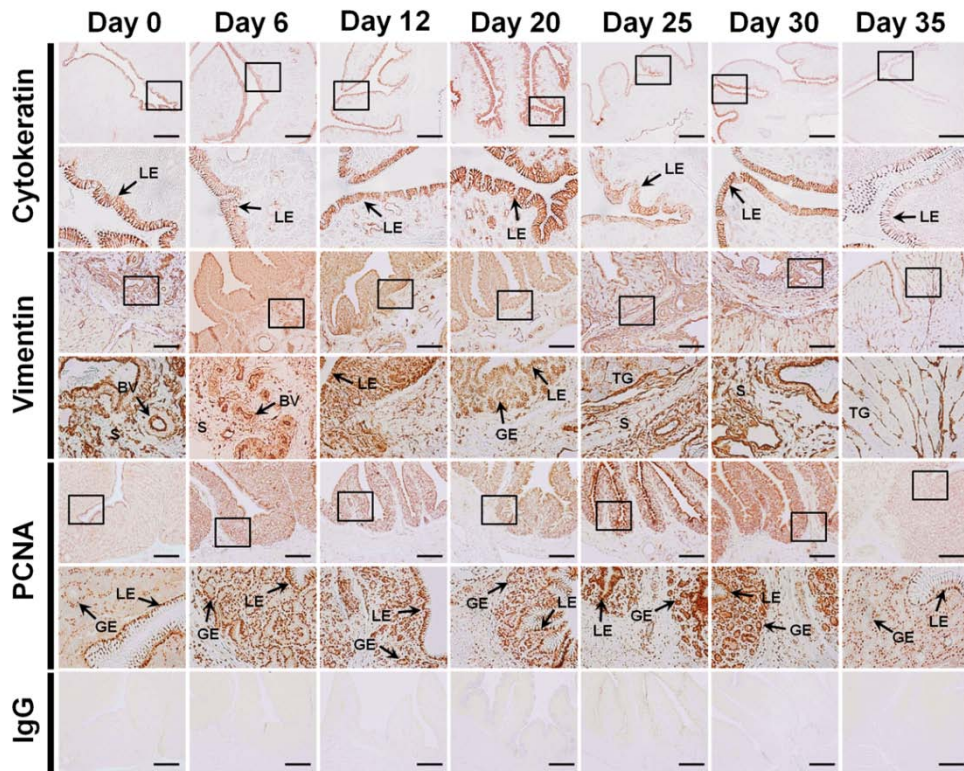


Figure 10-4. Immunohistochemical staining for detection of cytokeratin, vimentin and PCNA in cells of the magnum from each of the days during the molting and recrudescence processes. For negative controls, tissues were incubated with a nonspecific IgG. Legend: LE, luminal epithelium; GE, glandular epithelium; TG, tubular gland; S, stroma; *Scale bar* represents 100 μm .

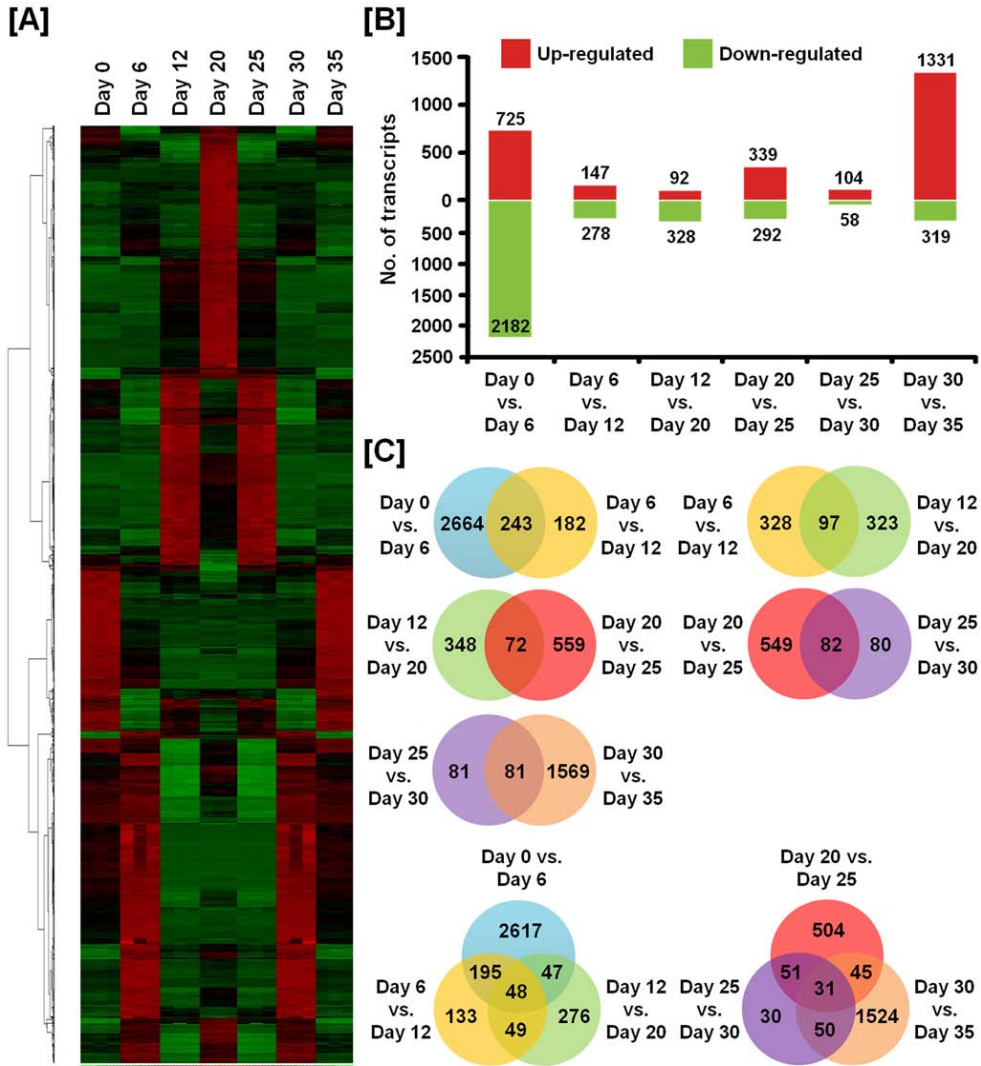


Figure 10-5. Identification of significant up- or down-regulated genes on each day during regression and regeneration of the oviduct. [A] Heat map of hierarchically clustered genes detected alterations in their expression across the time course of this study. [B] The number of transcripts for which expression increased or decreased significantly in the magnum on different days. Differentially expressed

genes were selected using two-sample comparison according to the following criteria: lower bound of 90% confidence interval of fold-change greater than 2.0 and an absolute value of difference between groups means greater than 100. [C] The numbers displayed within the intersections of the circles indicate the number of common genes in the two or three comparisons.

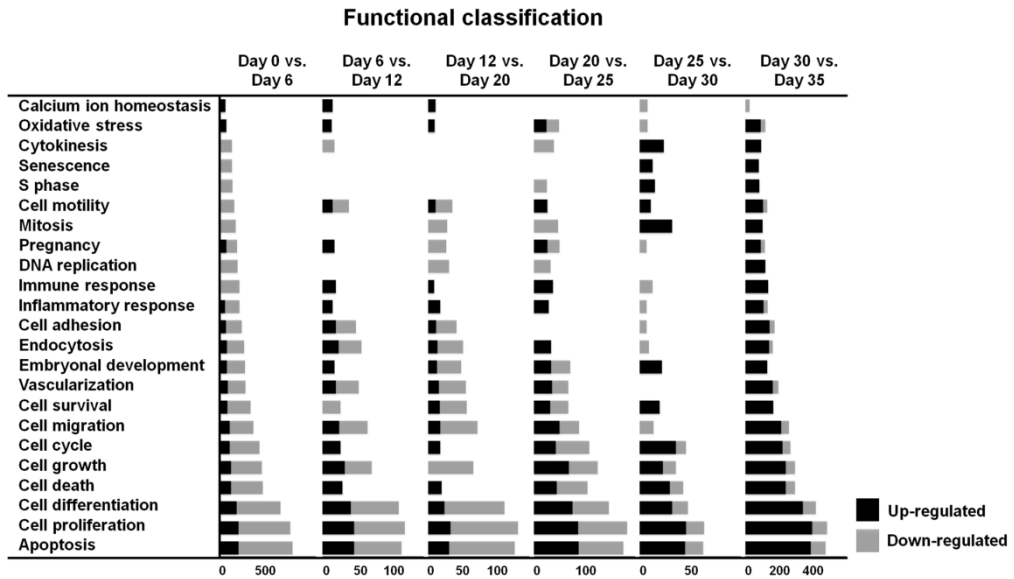


Figure 10-6. Functional categorization of differentially expressed genes found to be associated in the cellular and molecular functions. Genes that changed significantly were assigned to various functional annotations related to cellular processes based on Gene ontology annotation.

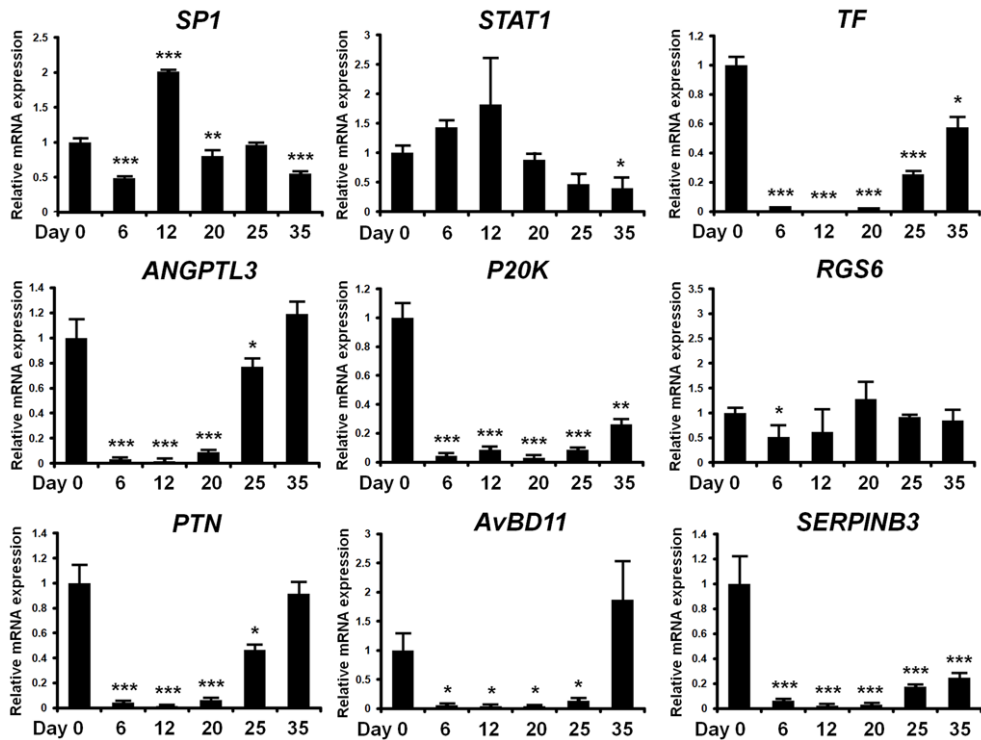


Figure 10-7. Validation of microarray gene expression data by quantitative RT-PCR analysis. Based on the microarray data, nine genes were selected and their expression pattern confirmed for each pooled RNA sample. All values were normalized to *GAPDH* housekeeping gene. Each bar is mean \pm SEM of three independent experiments. The asterisks denote effects that were significant (***) $p < 0.001$, ** $p < 0.01$, or * $p < 0.05$).

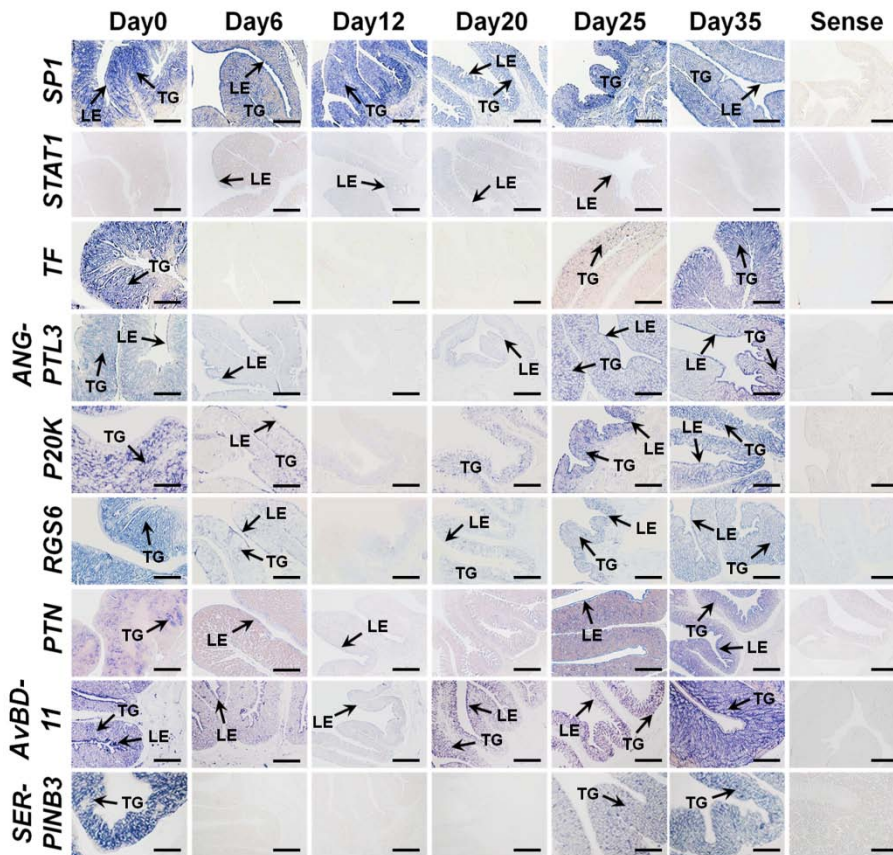


Figure 10-8. Cell-specific localization of mRNAs for selected genes for which expression changed significantly in the magnum of hens at different days during the pre- and post-molting periods. Expression of *TF*, *PTN*, *ANGPTL3*, *p20K*, *RGS6*, *GAL11* and *SERPINB3* mRNAs were very abundant in GE and LE of the magnum on Day 0 (normal diet), but expression of those mRNAs were very low at Day 12 (cessation of egg laying and regression of the oviduct). Then, from Days 12 to 35 (normal diet and regeneration of the oviduct), those mRNAs increased gradually in the GE and LE. Legend: TG, tubular gland; LE, luminal epithelium. *Scale bar* represents 100 μm .

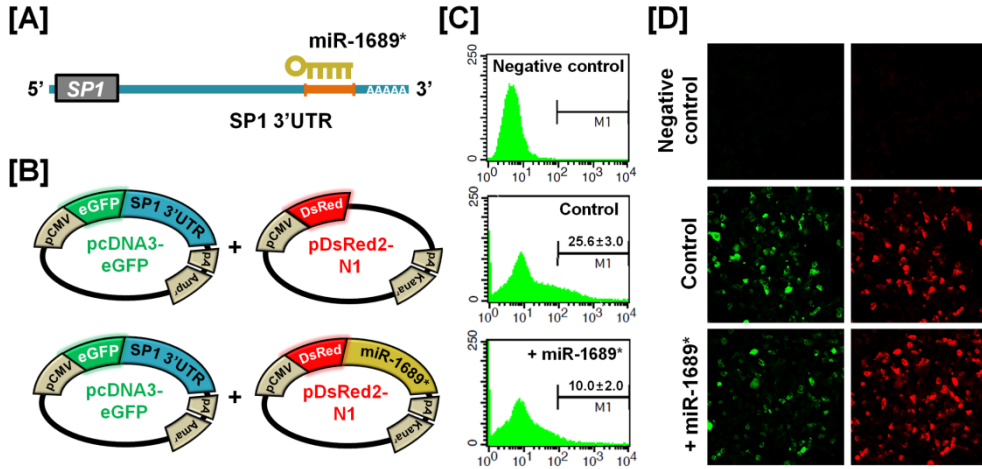


Figure 10-9. *In vitro* target assay for effects of the chicken *miR-1689** on expression of the *Sp1* transcript. [A] Diagram of *miR-1689** binding site in the 3'-UTR region of the *Sp1* transcript. [B] The maps of eGFP-*Sp1* 3'-UTR expressing and *DsRed*-*miR-1689** expressing vector. The *Sp1* 3'-UTR sequence was subcloned between the eGFP gene and the polyA tail, generating the fusion construct of the *GFP* transcript following the *Sp1* 3'-UTR (left panel). A miRNA expressing vector was designed to generate *DsRed* and *miR-1689** fused transcript or only *DsRed* transcript for the experimental control (right panel). [C and D] After co-transfection of pcDNA-eGFP-*Sp1* 3'-UTR and pcDNA-*DsRed*-*miR-1689** into 293FT cells, the fluorescence signals of GFP and *DsRed* were detected using FACS [C] and fluorescent microscopy [D]. In the panel C, gated event value from histogram statistics was used to find out statistical percentages of the positive events (GFP-expressing cells) and the numbers indicate mean \pm SEM of three independent experiments.

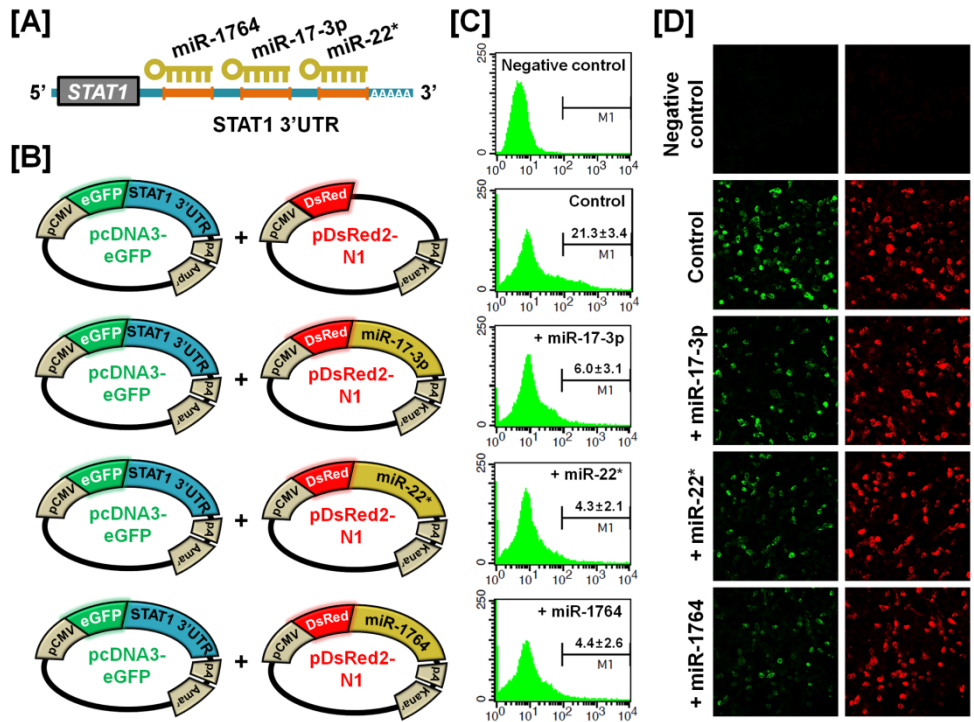


Figure 10-10. *In vitro* target assay for effects of chicken *miR-17-3p*, *miR-22 and *miR-1764* on expression of the *STAT1* transcript.** [A] Diagram of miRNAs binding sites in the 3'-UTR region of the *STAT1* transcript. [B] The maps of eGFP-*STAT1* 3'-UTR expressing and DsRed-each miRNA expressing vector. The *STAT1* 3'-UTR sequence was subcloned between the eGFP gene and the polyA tail, generating the fusion construct of the *GFP* transcript following the *STAT1* 3'-UTR (left panel). A miRNA expressing vector was designed to generate *DsRed* and each miRNA fused transcript or only *DsRed* transcript for the experimental control (right panel). [C and D] After co-transfection of pcDNA-eGFP-*STAT1* 3'-UTR and pcDNA-DsRed-each miRNA into 293FT cells, the fluorescence signals of GFP and DsRed were detected using FACS [C] and fluorescent microscopy [D]. In the panel C, gated event value

from histogram statistics was used to find out statistical percentages of the positive events (GFP-expressing cells) and the numbers indicate mean \pm SEM of three independent experiments.

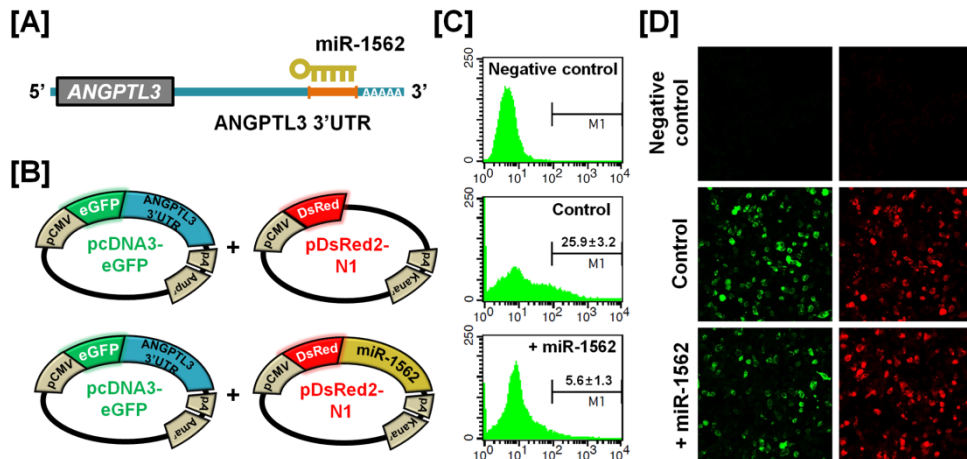


Figure 10-11. *In vitro* target assay for effects of the chicken *miR-1562* on expression of the *ANGPTL3* transcript. [A] Diagram of the miRNA binding site in the 3'-UTR region of the *ANGPTL3* transcript. [B] The maps of eGFP-*ANGPTL3* 3'-UTR expressing and DsRed-each miRNA expressing vector. The *ANGPTL3* 3'-UTR sequence was subcloned between the eGFP gene and the polyA tail, generating the fusion construct of the *GFP* transcript following the *ANGPTL3* 3'-UTR (left panel). A miRNA expressing vector was designed to generate *DsRed* and *miR-1562* fused transcript or only *DsRed* transcript for the experimental control (right panel). [C and D] After co-transfection of pcDNA-eGFP-*ANGPTL3* 3'-UTR and pcDNA-DsRed-miR-1562 into 293FT cells, the fluorescence signals of GFP and DsRed were detected using FACS [C] and fluorescent microscopy [D]. In the panel C, gated event value from histogram statistics was used to find out statistical percentages of the positive events (GFP-expressing cells) and the numbers indicate mean \pm SEM of three independent experiments.

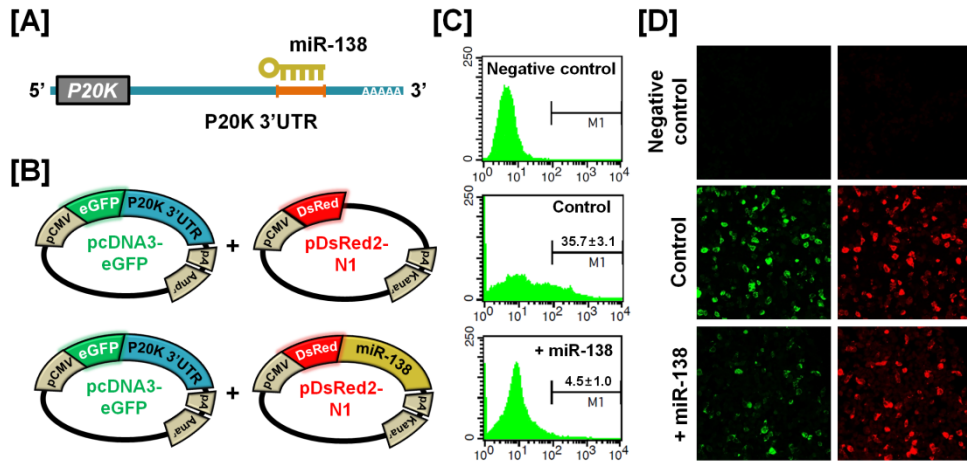


Figure 10-12. *In vitro* target assay for expression of the chicken *miR-138* on expression of the *p20K* transcript. [A] Diagram of miRNA binding site in the 3'-UTR region of the *p20K* transcript. [B] The maps of eGFP-*p20K* 3'-UTR expressing and DsRed-*miR-138* expressing vector. The *p20K* 3'-UTR sequence was subcloned between the eGFP gene and the polyA tail, generating the fusion construct of the *GFP* transcript following the *p20K* 3'-UTR (left panel). A miRNA expressing vector was designed to generate *DsRed* and *miR-138* fused transcript or only *DsRed* transcript for the experimental control (right panel). [C and D] After co-transfection of pcDNA-eGFP-*p20K* 3'-UTR and pcDNA-DsRed-*miR-138* into 293FT cells, the fluorescence signals of GFP and DsRed were detected using FACS [C] and fluorescent microscopy [D]. In the panel C, gated event value from histogram statistics was used to find out statistical percentages of the positive events (GFP-expressing cells) and the numbers indicate mean \pm SEM of three independent experiments.

5. Discussion

The molting process leads to dynamic changes in morphology, physiology and function of the reproductive tract of laying hens. In the present study, results from differential gene profiling identified global genes that potentially regulate oviductal regression and recrudescence during and following molting. Our results also revealed spatial and temporal expression of selected candidate genes in the magnum during tissue remodeling and post-transcriptional regulation of these genes by specific chicken miRNAs. These results support our hypothesis that complete recovery of the reproductive system following molting involves complex tissue remodeling that is reversible and involves specific changes in gene expression and molecular aspects.

In order to identify candidate genes that potentially regulate oviduct regression or tissue remodeling, we established the chicken *in vivo* model for induced molting and post-molting recrudescence (Figure 10-1). For induction of molting, we fed hens a diet enriched in zinc as previously reported (Berry and Brake, 1987; Scott JT, 1976; Sundaresan et al., 2008), which led to complete cessation of egg production within 12 days. After the complete cessation of egg production (day 12), molted hens were removed from the high zinc diets and they resumed egg production within 23 days, which is similar to results reported by Scott *et al.* (Scott JT, 1976; Shippee RL, 1979).

Along with changes in egg production, dramatic regression of oviduct and

ovary occurred in response to the high zinc diet, but this was followed by recrudescence after the hens were returned to a normal diet. Weights of the whole body and reproductive organs, as well as length of the oviduct were measured, all of which showed similar V-shaped patterns. The change in overall body weight is directly associated with in weights of liver, muscle, adipose tissue, and involution of reproductive tissues (Berry and Brake, 1985; Brake and Thaxton, 1979b). The extent of body loss during molting is a key factor for successful post-molting improvements in egg quality and egg production (Baker et al., 1981). The decreases and gains in ovarian and oviductal weights may be related to the overall rejuvenation of the hen associated with increases in metabolic processes of many tissues (Brake and Thaxton, 1979a; Park et al., 2004). The overall regeneration processes included recovery of atretic follicles, release of egg yolk materials and ovarian steroids, and increases in weights of reproductive tissues, as well as cellular and tissue morphology (Berry, 2003).

Previous studies have focused mainly on the period of regression of the oviduct, so the physiological mechanisms that regulate recrudescence processes are not understood to date. In the current study, however, changes in circulating concentrations of testosterone, progesterone, estradiol and corticosterone were determined in hens undergoing recrudescence (Figure 10-1F, 10-1G, 10-1H and 10-1I). Hoshino *et al* reported that concentrations of progesterone and estradiol decrease during molting due to low activities of enzymes for ovarian steroidogenesis (Hoshino et al., 1988). The decrease in selected ovarian steroids leads to apoptosis in the oviduct

and regression of the ovary during molting in hens (Monroe et al., 2002). During the recrudescence period, luteinizing hormone and follicle stimulating hormone levels increase, which stimulates ovarian development and their secretion of estradiol and progesterone to stimulate growth of the oviduct. Circulating levels of testosterone and corticosterone are transiently greater in hens during molting than in normal laying hens, and they decline as the molting progresses and increases with resumption of egg laying (Berry, 2003; Hoshino et al., 1988). In the present study, corticosterone levels increased upon return to the normal diet, which is considered to be associated with changes in activity of the hypothalamic-pituitary-adrenal (HPA) axis following replenishment of energy reserves in the body (Williams et al., 1985). And, although the function of testosterone in the recrudescence process is obscure, the increase in testosterone may influence oviductal regeneration, as well as thermoregulation.

Histomorphological changes in the magnum size, tubular glands and ovarian stroma during tissue regression and regeneration were dramatic (Figure 10-2). Regression of the reproductive organs during induced molting is achieved through apoptotic processes (Heryanto et al., 1997b). We observed that induction of molting by feeding a high zinc diet caused apoptotic cell death in all cell types of the magnum (Figure 3). Zinc is an endogenous regulator of apoptosis via involvement in several complex processes such as the alterations in caspase activity, and regulation of cytokine expression and hormone levels (Kondoh et al., 2002; Sundaresan et al., 2008). We also observed cytokeratin-, vimentin-, and PCNA-positive cells in the magnum of hens undergoing oviductal regression and recrudescence (Figure 10-4).

Epithelial-to-mesenchymal transition (EMT) endows cells with migratory and invasive properties, and plays an important role in developmental processes including tissue repair and differentiation (Thiery et al., 2009). Previously, Heryanto *et al* suggested that the tubular glands were generated by the invasion and cytodifferentiation of the mucosal epithelium and old glandular cells were replaced with newly derived GE during oviductal tissue remodeling (Heryanto et al., 1997a; Pageaux et al., 1986). Our results suggest that up-regulation of cytokeratin is a defining factor for initiation of regeneration and plays a significant role in initial tissue remodeling of the reproductive tract. And the relative high frequency of PCNA-positive cells in the developing magnum between days 25 and 30 suggests active proliferation during the gradual recrudescence of reproductive organs. We assume that proliferation of oviductal cells between days 25 and 30 is likely induced by ovarian steroids following resumption of ovarian steroidogenesis. These morphological and physiological findings of the present study indicate that the laying hen undergoing molting and recovery from molting is a highly efficient animal model for research on regression and recrudescence of the mammalian reproductive system.

Using cDNA microarray analysis of tissues from this *in vivo* model, we identified a large number of genes that are differentially regulated in the magnum portion which undergoes the most dramatic changes during reproductive tissue remodeling (Figure 10-5). Interestingly, we observed expression of about 20 genes including *transferrin (TF)*, *angiopoietin-like 3 (ANGPTL3)*, *p20K*, *regulator of G-protein signaling 6 (RGS6)*, *pleiotrophin (PTN)*, *avian beta-defensin11 (AvBD11)* and

SERPINB3 that decreased gradually during molting and increased following regeneration of the oviduct. And, through pathway analysis, these genes are considered to be commonly regulated by *Sp1* and *STAT1*. The expression levels of mRNAs for nine interrelated genes during oviductal remodeling were analyzed to validate results from the cDNA microarray analysis. Sp1 is a ubiquitous transcription factor expressed in diverse cell types and believed to bind to GC/GT-boxes on promoters and other regulatory sequences of genes (Dyana and Tjian, 1983a, b). It has diverse functions via synergistically activating or repressing transcription of genes involved in various biological processes (Abdelrahim et al., 2002; Desjardins and Hay, 1993; Feng et al., 2000; Kavurma and Khachigian, 2003; Kavurma et al., 2001; Lagger et al., 2003; Leggett et al., 1995; Mastrangelo et al., 1991; Olofsson et al., 2007; Sherr and Roberts, 1999; Su et al., 1991; Yuan et al., 2007). STAT1, similar to Sp1, is a latent ubiquitous transcription factor that regulates expression of a wide range of downstream genes in response to cytokines and growth factors (Ihle and Kerr, 1995; Schindler and Darnell, 1995). STAT1 translocate to the nucleus and bind to conserved enhancer elements that lead to transcriptional activation of immediate early response genes (Heim et al., 1995). Although *Sp1* and *STAT1* are expressed ubiquitously, the expression of those genes changes according to developmental stages or cell type implying specific roles in developmental processes (Saffer et al., 1991). The important phenotypic changes during oviductal regression and recrudescence would appear to result from a finely balanced transcriptional response by several transcription factors including Sp1 and STAT1.

The third gene of interest, *TF*, encodes for an iron-binding protein that absorbs dietary iron from the gut and transports it throughout the body (Ponka et al., 1998). In chickens, this gene is synthesized by both liver cells and oviduct cells, and stimulated by estrogen or dietary iron deficiency (Chen and Bissell, 1987; Lee et al., 1978; Silphaduang et al., 2006). The expression of this gene increased during oviduct regeneration indicating that it might be affected by changes in gross metabolic rates. It is well known that iron is essential for various metabolic processes including DNA synthesis, oxygen transport and the electron transport system in a wide range of tissues. Dramatic tissue remodeling involving degeneration and regeneration of female reproductive organs is necessarily coupled with angiogenic processes. *ANGPTL3* has features common to angiopoietins that play important roles during angiogenesis as vascular endothelial cell-specific growth factors (Conklin et al., 1999; Geva and Jaffe, 2000; Musunuru et al., 2010). In the present study, there was a remarkable increase of *ANGPTL3* mRNA during oviductal recrudescence which implies a requirement for re-growth of the vascular network in developing tissue. The fifth gene of interest, p20K, encodes for a small protein cloned from chicken embryo fibroblasts, and its transcription is induced in the growth arrested phase of the cell cycle such as serum-deprivation and contact-inhibition (Mao et al., 1993). RGS6, a member of regulator of G protein signaling (RGS) proteins, negatively regulates G protein signaling by activating the GTPase activity (Berman and Gilman, 1998; De Vries et al., 2000). Although the precise physiological roles of p20K and RGS6 are unknown, they are linked to cellular stress responses and possess abilities to induce cell cycle arrest and apoptosis (Berman et al., 2004; Liu and Fisher, 2004; Maity et al.,

2011).

Results from our previous studies indicate that *PTN*, *AvBD11* and *SERPINB3* are estrogen-stimulated genes during development of the chicken oviduct (Lee et al., 2012; Lim et al., 2012a; Lim et al., 2013). *PTN*, also known as heparin binding growth factor 8 (HBGF-8), is a developmentally regulated growth factor which is widely distributed in various tissues (Milner et al., 1989; Muramatsu, 2002). In chickens, it especially plays important roles in differentiation and morphogenesis of the embryo by promoting cell growth and migration (Li et al., 1990; Muramatsu, 2002; Raulais et al., 1991; Vigny et al., 1989). *AvBD11*, a component of egg-white proteins, is an antimicrobial peptide that plays a role in innate immunity (Ganz, 2003; Klotman and Chang, 2006; Xiao et al., 2004). We reported that *AvBD11* may influence oviduct development and protect the chicken embryo from pathogenic microorganisms (Herve-Grepinet et al., 2010; Song et al., 2011b). *SERPINB3* was first identified in squamous cell carcinoma of the human uterus and, in chickens, it plays a crucial role in formation of egg yolk and egg white (D'Alessandro et al., 2010; Kato and Torigoe, 1977). Complicated actions of estrogen in various biological processes affect physiological changes through diverse regulatory cascades by trans-activating transcription factors and inducing expression of various target genes. Because estrogen produced by the ovary may orchestrate the expression of *PTN*, *AvBD11* and *SERPINB3*, temporal patterns of expression of these genes during molting and oviduct recrudescence may be closely related to changes in estrogen levels following withdrawal and restart of ovarian steroidogenesis. Taken together, tissue-specific and

developmentally regulated expression of these nine genes indicates that they have regulatory functions during reproductive tissue remodeling and development of the oviduct in chickens.

For dramatic phenotypic changes in the reproductive tract of female chickens (see Figure 10-1), microRNA (miRNA)-mediated posttranscriptional regulation of genes can effect changes in expression of related genes at the cellular level (Carletti and Christenson, 2009). To further investigate the possible involvement of miRNA-mediated posttranscriptional regulation during regeneration of the chicken oviduct, we performed screening to identify potential miRNAs targeting *Sp1*, *STAT1*, *ANGPTL3* and *p20K* transcripts. As shown in Figures 10-9, 10-10, 10-11, and 10-12, specific chicken miRNAs reduced expression of *Sp1*, *STAT1*, *ANGPTL3* and *p20K*, respectively. Similarly, we previously demonstrated inhibitory effects of chicken miRNAs on *PTN*, *AvBD11* and *SERPINB3* gene expression (Lee et al., 2012; Lim et al., 2013; Lim et al., 2012b). These results indicate that specific chicken miRNAs interact with transcripts for at least these seven genes that determine oviduct development and remodeling, and regulate their expression post-transcriptionally during remodeling of reproductive organs. Emerging evidence gathered from animal models suggest that microRNAs are expressed within the female reproductive tract in various animals. And post-transcriptional regulation of genes through miRNAs is essential to regulate cellular pathways for proper development and function of the organs. Even though miRNA-mediated gene regulation plays an important role in the synthesis of all proteins that are necessary for the rapid phenotypic changes occurring

in the female reproductive tract, much less is known about it in oviductal tissue regression or re-growth. Also the identity and functional analysis of individual miRNA expressed in the reproductive tract of chicken, and the identification of their specific mRNA targets are just now beginning. Although the significance of this regulation by these chicken miRNAs remains to be determined in more detail, present results might be helpful to elucidate the regulation mechanism of suggested miRNAs in oviductal regression and remodeling processes. And also it will provide new research approaches and insight into how post-transcriptional regulation by miRNAs enhances reproductive efficiency or development of reproductive organs.

In summary, global gene expression profiles from our present microarray study using a well-established *in vivo* model for molting and regeneration of chicken oviductal tissue identified new molecular candidates regulating this process. Our findings also revealed the biological significance of genetic and miRNA-mediated epigenetic regulation in morphological- and functional recrudescence of the reproductive tract in chickens. These findings provide new clues for further studies to determine regulatory roles of novel developmentally related genes and molecular mechanism for reproductive tissue remodeling in chickens.

CHAPTER 11

Conclusion

The establishment of a synchronized dialog between mother and conceptus is indispensable for successful implantation and the maintenance of pregnancy in mammals. During the peri-implantation period, the survival and development of the conceptus ultimately depend on receiving a sufficient supply of histotroph that locally provides mediators such as growth factors and cytokines. This study has presented evidence that four factors, EGF, IGF-I, VEGF, and CSF2, stimulate proliferation and/or migration of pTr cells. Our results also indicate that these factors activate various intracellular signaling pathways including the PI3K-AKT1 and ERK1/2 MAPK signaling cascades in pTr cells. These novel findings support our hypothesis that during the peri-implantation period of pregnancy in pigs, these four factors derived from uterine endometrial tissues and/or from the conceptus play pivotal roles in implantation events by regulating the development of the porcine conceptus, and that appropriate amounts of these factors are critical for implantation events during early pregnancy.

In pigs, most oocytes undergo fertilization, which initiates development. However, 20-30 % of conceptuses are lost between Days 12 and 30 of pregnancy, and the most critical period occurs when the conceptus undergoes dramatic morphological changes, leading to high prenatal mortality and low reproductive efficacy (Geisert et al., 1982a; Pope et al., 1990). These findings suggest that not only early embryonic development but also the peri-implantation period is a critical phase of conceptus viability and pregnancy establishment in the pig. During early pregnancy, rapid morphological changes and conceptus survival rely on a reciprocal conceptus-uterine

crosstalk that is mediated by nutrients, growth factors, and cytokines (Geisert et al., 1982b). Deficiencies in these factors lead to a failure of implantation and placentation and developmental abnormalities. Evidence from studies conducted using the uterine gland knockout sheep model emphasizes that uterine glands and their secretions are crucial for early conceptus survival, development, implantation and placentation during the early pregnancy. However, understanding of the mediators of the maternal-conceptus interface and their function in the implantation process remains far from complete.

The conceptus-uterine dialog is especially critical in pigs, in which non-invasive epitheliochorial implantation occurs and involves a prolonged pre-implantation phase. Porcine conceptuses must receive a sufficient supply of histotroph and maximize the area of contact with the uterine endometrial surface to exchange histotroph and gases. Consequently, using pigs is advantageous when elucidating the intercellular communication mechanisms at maternal-conceptus interspaces, and it also circumvents the restrictions placed on direct analysis of embryo-uterine interactions in human implantation.

EGF, IGF-I, VEGF, and CSF2 present in the uterine cavity are implicated as promising embryotrophic factors that underpin embryogenesis and regulate implantation in various mammalian species. However, the precise functions of these factors in the porcine trophoctoderm and the details of the intracellular signaling cascades involved remain undefined. The spatiotemporal expression patterns of these

four factors were determined in this study. The EGF, IGF-I, VEGF, and CSF2 system components were expressed at higher levels during peri-implantation development than during the estrous cycle, and the increase in expression coincided temporally with the dramatic elongation of blastocysts and the secretion of estrogens by the trophoblast. The use of *in situ* hybridization and/or immunohistochemical analysis also confirmed the presence of these factors and/or their receptors in the uterine endometrium and/or the trophoctoderm around the time of conceptus elongation. These results suggest paracrine and/or autocrine roles of the selected factors in conceptus development and trophoblastic elongation.

The potential cellular signaling pathways that are activated by EGF, IGF-I, VEGF, and CSF2, which are differentially expressed during the peri-implantation period, were also evaluated. Our studies showed that all four factors activated PI3K-AKT and MAPK signaling pathways in pTr cells cultured *in vitro*. Furthermore, the IGF-I, VEGF, and CSF2-stimulated pathways appeared to trigger cross-talk between the PI3K- and ERK1/2 MAPK signaling pathways, which differentially activate common downstream targets associated with mRNA translation and protein synthesis, such as mTOR, p70RSK, p90RSK, RPS6, and/or 4EBP1. By contrast, in EGF-stimulated signaling, the PI3K and ERK1/2 MPAK signaling pathways appeared to function independently and probably act on distinct downstream targets in pTr cells.

Interestingly, the EGFR knockdown study provides evidence supporting a role of EGF in regulating the *mRNA* expression of implantation-related genes such as

IFND and *TGFβ-1* during the peri-implantation period. However, additional studies are required to clarify the precise correlation between EGF, IFND and TGFβ-1. The four factors studied here also exhibited stimulatory effects on proliferation and/or migration of *in vitro* cultured pTr cells, but these effects were abolished upon inhibition of PI3K-, ERK1/2 MAPK-, P38 MAPK-, and MTOR signaling pathways, indicating that these factors coordinately regulate multiple cell signaling pathways that are critical to cell proliferation and migration and gene-expression changes in trophoblast cells during early pregnancy in pigs.

Collectively, the four separate approaches presented in this study bring novel insight into the mechanisms by which EGF, IGF-I, VEGF and CSF2 in the uterine trophoblast regulate the conceptus trophoblastic properties and activate intracellular signaling during the peri-implantation period of pregnancy. Our results reveal that the four uterine growth factors stimulate the proliferation and/or migration of pTr cells and that these effects are regulated in a coordinated manner by the PI3K-AKT and ERK1/2 MAPK signaling cascades during early pregnancy (Figure 11-1).

Further investigation is required to elucidate more precisely the roles and signaling mechanisms of the selected factors in regulating the development and function of the endometrium and conceptuses during early pregnancy in pigs. Our study did not determine whether these maternally and/or fetally derived growth factors also affect the maternal endometrium. The results described herein showing the concurrent expression of the growth factors and their receptor in maternal endometrial

cells suggests that autocrine signaling occurs. Therefore, future research could examine the functional mechanisms and the signaling pathways by which the selected growth factors induce structural- and functional changes in uterine endometria.

Another key unresolved question is the nature of the endogenous growth-factor systems' response to other molecules. This study has demonstrated only the independent actions of each growth-factor system in pTr cells, but future research will determine the combined actions of these factors and the correlation between these factors and other molecules at the maternal-conceptus interface. The growth factors studied here form a subset of a range of factors at the maternal-conceptus interface that together determine the integrated bioavailability and responsiveness in cells. Among these other molecules, maternal steroids are considered to be key regulators of the expression and bioactivity of growth factor systems; moreover, the pTr cells derived from Day 12 blastocysts are a natural source of estrogen and growth factors. Thus, elucidating how circulating hormones and/or other histotroph components affect the expression, secretion, and functions of these growth factor-receptor systems will be useful. Furthermore, the differential expression of the growth factor-receptor systems in pTr cells and the degree to which the growth factors bind to their receptors during the peri-implantation period should also be determined. Melding the independent- and combined actions of these growth factors will allow a broad and comprehensive understanding of the complex autocrine, paracrine, and juxtacrine interactions that occur in the uterine microenvironment.

Although certain questions remain to be resolved, the results of this study and future studies will enable detailed and comprehensive understanding of the physiological models of conceptus development and the conceptus-maternal interaction mediated by growth factors in mammalian species. An enhanced understanding of this mechanism could also be of clinical relevance; unraveling the nature of this mechanism may help identify new strategies to improve embryo culture conditions and alleviate early embryonic losses and implantation failure, and thus ensure improved reproductive health in humans and economically critical livestock.

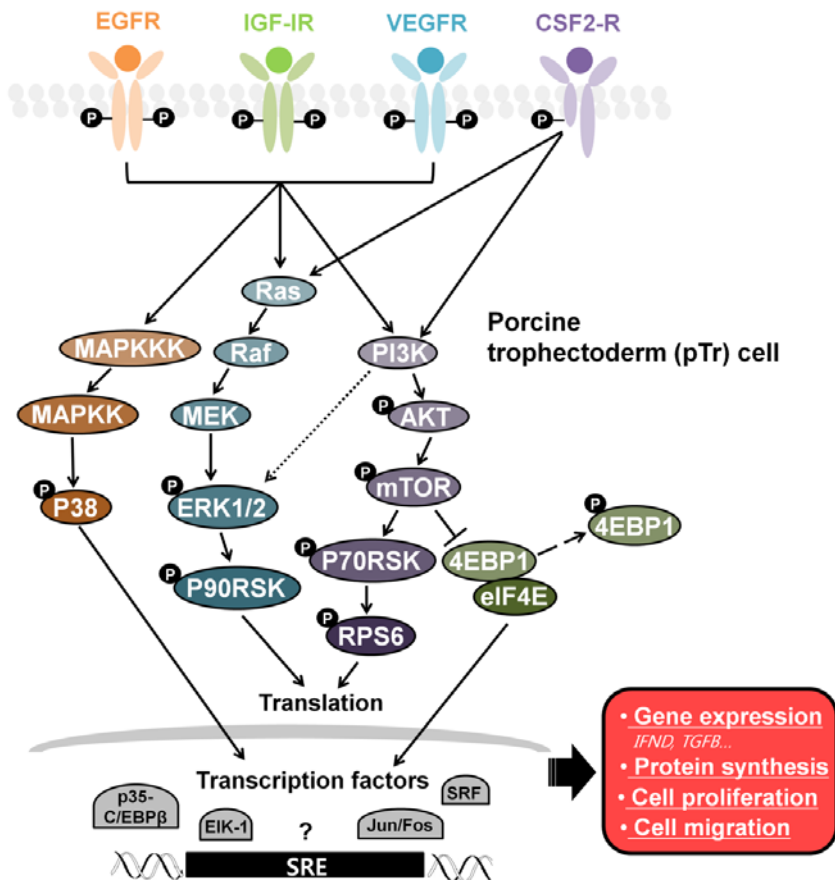


Figure 11-1. A schematic illustration of the mechanisms by which the selected growth factors affect various intracellular signaling cascades responsible for the cellular activities of pTr cells during the peri-implantation period. Endometrium- and/or trophoblast-derived factors commonly induce the phosphorylation of MTOR-RPS6 through the PI3K-AKT1 signaling pathway. The ERK1/2 and P38 MAPK signaling cascades act in parallel to transduce the signals from EGF, IGF-I, and VEGF. These activated signaling pathways are likely involved in regulating gene expression and protein synthesis in the case of growth- and/or development-related genes that affect the proliferation and migration of the porcine trophoblast.

REFERENCES

- Abdelrahim, M., Samudio, I., Smith, R., 3rd, Burghardt, R., and Safe, S. (2002). Small inhibitory RNA duplexes for Sp1 mRNA block basal and estrogen-induced gene expression and cell cycle progression in MCF-7 breast cancer cells. *J Biol Chem* **277**, 28815-22.
- Abu-Abed, S. S., Beckett, B. R., Chiba, H., Chithalen, J. V., Jones, G., Metzger, D., Chambon, P., and Petkovich, M. (1998). Mouse P450RAI (CYP26) expression and retinoic acid-inducible retinoic acid metabolism in F9 cells are regulated by retinoic acid receptor gamma and retinoid X receptor alpha. *J Biol Chem* **273**, 2409-15.
- Aflalo, E. D., Sod-Moriah, U. A., Potashnik, G., and Har-Vardi, I. (2007). EGF increases expression and activity of PAs in preimplantation rat embryos and their implantation rate. *Reprod Biol Endocrinol* **5**, 4.
- Ahn, S. E., Choi, J. W., Rengaraj, D., Seo, H. W., Lim, W., Han, J. Y., and Song, G. (2010). Increased expression of cysteine cathepsins in ovarian tissue from chickens with ovarian cancer. *Reprod Biol Endocrinol* **8**, 100.
- al-Batshan, H. A., Scheideler, S. E., Black, B. L., Garlich, J. D., and Anderson, K. E. (1994). Duodenal calcium uptake, femur ash, and eggshell quality decline with age and increase following molt. *Poult Sci* **73**, 1590-6.
- Allison Gray, C., Bartol, F. F., Taylor, K. M., Wiley, A. A., Ramsey, W. S., Ott, T. L., Bazer, F. W., and Spencer, T. E. (2000). Ovine uterine gland knock-out model: effects of gland ablation on the estrous cycle. *Biol Reprod* **62**, 448-56.
- Alodan, M. A., and Mashaly, M. M. (1999). Effect of induced molting in laying hens on production and immune parameters. *Poult Sci* **78**, 171-7.
- Anderson, G. L., McIntosh, M., Wu, L., Barnett, M., Goodman, G., Thorpe, J. D., Bergan, L., Thornquist, M. D., Scholler, N., Kim, N., O'Briant, K., Drescher, C., and Urban, N. (2010). Assessing lead time of selected ovarian cancer biomarkers: a nested case-control study. *J Natl Cancer Inst* **102**, 26-38.
- Ando, H., Mizutani, A., Kiefer, H., Tsuzurugi, D., Michikawa, T., and Mikoshiba, K. (2006). IRBIT suppresses IP3 receptor activity by competing with IP3 for the common binding site on the IP3 receptor. *Mol Cell* **22**, 795-806.
- Ando, H., Mizutani, A., Matsu-ura, T., and Mikoshiba, K. (2003). IRBIT, a novel inositol 1,4,5-trisphosphate (IP3) receptor-

binding protein, is released from the IP₃ receptor upon IP₃ binding to the receptor. *J Biol Chem* **278**, 10602-12.

Ando, H., Mizutani, A., and Mikoshiba, K. (2009). An IRBIT homologue lacks binding activity to inositol 1,4,5-trisphosphate receptor due to the unique N-terminal appendage. *J Neurochem* **109**, 539-50.

Anegon, I., Cuturi, M. C., Godard, A., Moreau, M., Terqui, M., Martinat-Butte, F., and Soullou, J. P. (1994). Presence of leukaemia inhibitory factor and interleukin 6 in porcine uterine secretions prior to conceptus attachment. *Cytokine* **6**, 493-9.

Ansenberger, K., Zhuge, Y., Lagman, J. A., Richards, C., Barua, A., Bahr, J. M., and Hales, D. B. (2009). E-cadherin expression in ovarian cancer in the laying hen, *Gallus domesticus*, compared to human ovarian cancer. *Gynecol Oncol* **113**, 362-9.

Antanaitis, B. C., Aisen, P., and Lilienthal, H. R. (1983). Physical characterization of two-iron uteroferrin. Evidence for a spin-coupled binuclear iron cluster. *J Biol Chem* **258**, 3166-72.

Aplin, J. D., and Kimber, S. J. (2004). Trophoblast-uterine interactions at implantation. *Reprod Biol Endocrinol* **2**, 48.

Arazi, H., Yoselewitz, I., Malka, Y., Kelner, Y., Genin, O., and Pines, M. (2009). Osteopontin and calbindin gene expression in the eggshell gland as related to eggshell abnormalities. *Poult Sci* **88**, 647-53.

Ariyadi, B., Isobe, N., and Yoshimura, Y. (2012). Differences in the mucosal surface barrier formed by mucin in the lower oviductal segments between laying and molting hens. *Poult Sci* **91**, 1173-8.

Ashworth, M. D., Ross, J. W., Stein, D. R., Allen, D. T., Spicer, L. J., and Geisert, R. D. (2005). Endocrine disruption of uterine insulin-like growth factor expression in the pregnant gilt. *Reproduction* **130**, 545-51.

Athanassiades, A., Hamilton, G. S., and Lala, P. K. (1998). Vascular endothelial growth factor stimulates proliferation but not migration or invasiveness in human extravillous trophoblast. *Biol Reprod* **59**, 643-54.

Avruch, J., Belham, C., Weng, Q., Hara, K., and Yonezawa, K. (2001). The p70 S6 kinase integrates nutrient and growth signals to control translational capacity. *Prog Mol Subcell Biol* **26**, 115-54.

Baker, M., Brake, J., and Mcdaniel, G. R. (1981). The Relationship between Body-Weight Loss during a Forced Molt and Post-Molt Reproductive-Performance of Caged Layers. *Poultry Science* **60**, 1594-1594.

Baldwin, G. C. (1992). The biology of granulocyte-macrophage colony-stimulating factor: effects on hematopoietic and

nonhematopoietic cells. *Dev Biol* **151**, 352-67.

Baldwin, G. C., Golde, D. W., Widhopf, G. F., Economou, J., and Gasson, J. C. (1991). Identification and characterization of a low-affinity granulocyte-macrophage colony-stimulating factor receptor on primary and cultured human melanoma cells. *Blood* **78**, 609-15.

Banerjee, S., and Kaye, S. (2011). The role of targeted therapy in ovarian cancer. *Eur J Cancer* **47 Suppl 3**, S116-30.

Bar, A. (2009). Differential Regulation of Calbindin in the Calcium-Transporting Organs of Birds with High Calcium Requirements. *Journal of Poultry Science* **46**, 267-285.

Bar, A., Striem, S., Vax, E., Talpaz, H., and Hurwitz, S. (1992a). Regulation of calbindin mRNA and calbindin turnover in intestine and shell gland of the chicken. *Am J Physiol* **262**, R800-5.

Bar, A., Vax, E., and Striem, S. (1992b). Relationships between calbindin (Mr 28,000) and calcium transport by the eggshell gland. *Comp Biochem Physiol Comp Physiol* **101**, 845-8.

Barber, K. J., Franklyn, J. A., McCabe, C. J., Khanim, F. L., Bulmer, J. N., Whitley, G. S., and Kilby, M. D. (2005). The in vitro effects of triiodothyronine on epidermal growth factor-induced trophoblast function. *J Clin Endocrinol Metab* **90**, 1655-61.

Bartel, D. P. (2009). MicroRNAs: target recognition and regulatory functions. *Cell* **136**, 215-33.

Barua, A., Bitterman, P., Abramowicz, J. S., Dirks, A. L., Bahr, J. M., Hales, D. B., Bradaric, M. J., Edassery, S. L., Rotmensh, J., and Luborsky, J. L. (2009). Histopathology of ovarian tumors in laying hens: a preclinical model of human ovarian cancer. *Int J Gynecol Cancer* **19**, 531-9.

Bass, K. E., Morrish, D., Roth, I., Bhardwaj, D., Taylor, R., Zhou, Y., and Fisher, S. J. (1994). Human cytotrophoblast invasion is up-regulated by epidermal growth factor: evidence that paracrine factors modify this process. *Dev Biol* **164**, 550-61.

Bazer, F. W. (1975). Uterine protein secretions: Relationship to development of the conceptus. *J Anim Sci* **41**, 1376-82.

Bazer, F. W., Kim, J., Song, G., Ka, H., Tekwe, C. D., and Wu, G. (2012a). Select nutrients, progesterone, and interferon tau affect conceptus metabolism and development. *Ann N Y Acad Sci* **1271**, 88-96.

Bazer, F. W., and Roberts, R. M. (1983). Biochemical aspects of conceptus--endometrial interactions. *J Exp Zool* **228**, 373-83.

- Bazer, F. W., Song, G., Kim, J., Dunlap, K. A., Satterfield, M. C., Johnson, G. A., Burghardt, R. C., and Wu, G. (2012b). Uterine biology in pigs and sheep. *J Anim Sci Biotechnol* **3**, 23.
- Bazer, F. W., Spencer, T. E., Johnson, G. A., and Burghardt, R. C. (2011). Uterine receptivity to implantation of blastocysts in mammals. *Front Biosci (Schol Ed)* **3**, 745-67.
- Bazer, F. W., Spencer, T. E., Johnson, G. A., Burghardt, R. C., and Wu, G. (2009). Comparative aspects of implantation. *Reproduction* **138**, 195-209.
- Bazer, F. W., and Thatcher, W. W. (1977). Theory of maternal recognition of pregnancy in swine based on estrogen controlled endocrine versus exocrine secretion of prostaglandin F₂alpha by the uterine endometrium. *Prostaglandins* **14**, 397-400.
- Bazer, F. W., Vallet, J. L., Roberts, R. M., Sharp, D. C., and Thatcher, W. W. (1986). Role of conceptus secretory products in establishment of pregnancy. *J Reprod Fertil* **76**, 841-50.
- Bazer, F. W., Worthington-White, D., Fliss, M. F., and Gross, S. (1991). Uteroferrin: a progesterone-induced hematopoietic growth factor of uterine origin. *Exp Hematol* **19**, 910-5.
- Bazer, F. W., Wu, G., Spencer, T. E., Johnson, G. A., Burghardt, R. C., and Bayless, K. (2010). Novel pathways for implantation and establishment and maintenance of pregnancy in mammals. *Mol Hum Reprod* **16**, 135-52.
- Behr, B., Mooney, S., Wen, Y., Polan, M. L., and Wang, H. (2005). Preliminary experience with low concentration of granulocyte-macrophage colony-stimulating factor: a potential regulator in preimplantation mouse embryo development and apoptosis. *J Assist Reprod Genet* **22**, 25-32.
- Behrens, T. W., and Graham, R. R. (2011). TRAPing a new gene for autoimmunity. *Nat Genet* **43**, 90-1.
- Berman, D. M., and Gilman, A. G. (1998). Mammalian RGS proteins: barbarians at the gate. *J Biol Chem* **273**, 1269-72.
- Berman, D. M., Wang, Y., Liu, Z., Dong, Q., Burke, L. A., Liotta, L. A., Fisher, R., and Wu, X. (2004). A functional polymorphism in RGS6 modulates the risk of bladder cancer. *Cancer Res* **64**, 6820-6.
- Berridge, M. J. (1993). Inositol trisphosphate and calcium signalling. *Nature* **361**, 315-25.
- Berridge, M. J., Lipp, P., and Bootman, M. D. (2000). The versatility and universality of calcium signalling. *Nat Rev Mol Cell*

Biol **1**, 11-21.

Berry, W. D. (2003). The physiology of induced molting. *Poult Sci* **82**, 971-80.

Berry, W. D., and Brake, J. (1985). Comparison of Parameters Associated with Molt Induced by Fasting, Zinc, and Low Dietary-Sodium in Caged Layers. *Poultry Science* **64**, 2027-2036.

Berry, W. D., and Brake, J. (1987). Postmolt performance of laying hens molted by high dietary zinc, low dietary sodium, and fasting: egg production and eggshell quality. *Poult Sci* **66**, 218-26.

Biadasiewicz, K., Sonderegger, S., Haslinger, P., Haider, S., Saleh, L., Fiala, C., Pollheimer, J., and Knofler, M. (2011). Transcription factor AP-2alpha promotes EGF-dependent invasion of human trophoblast. *Endocrinology* **152**, 1458-69.

Binoux, M. (1995). The IGF system in metabolism regulation. *Diabete Metab* **21**, 330-7.

Biswas, D., Jung, E. M., Jeung, E. B., and Hyun, S. H. (2011). Effects of vascular endothelial growth factor on porcine preimplantation embryos produced by in vitro fertilization and somatic cell nuclear transfer. *Theriogenology* **75**, 256-67.

Brake, J., and Thaxton, P. (1979a). Physiological changes in caged layers during a forced molt. 1. Body temperature and selected blood constituents. *Poult Sci* **58**, 699-706.

Brake, J., and Thaxton, P. (1979b). Physiological changes in caged layers during a forced molt. 2. Gross changes in organs. *Poult Sci* **58**, 707-16.

Breeding, S. W., Brake, J., Garlich, J. D., and Johnson, A. L. (1992). Molt induced by dietary zinc in a low-calcium diet. *Poult Sci* **71**, 168-80.

Briggs, T. A., Rice, G. I., Daly, S., Urquhart, J., Gornall, H., Bader-Meunier, B., Baskar, K., Baskar, S., Baudouin, V., Beresford, M. W., Black, G. C., Dearman, R. J., de Zegher, F., Foster, E. S., Frances, C., Hayman, A. R., Hilton, E., Job-Deslandre, C., Kulkarni, M., Le Merrer, M., Linglart, A., Lovell, S. C., Maurer, K., Musset, L., Navarro, V., Picard, C., Puel, A., Rieux-Laucat, F., Roifman, C. M., Scholl-Burgi, S., Smith, N., Szykiewicz, M., Wiedeman, A., Wouters, C., Zeef, L. A., Casanova, J. L., Elkon, K. B., Janckila, A., Lebon, P., and Crow, Y. J. (2011). Tartrate-resistant acid phosphatase deficiency causes a bone dysplasia with autoimmunity and a type I interferon expression signature. *Nat Genet* **43**, 127-31.

- Brigstock, D. R., Kim, G. Y., Steffen, C. L., Liu, A., Vegunta, R. K., and Ismail, N. H. (1996). High molecular mass forms of epidermal growth factor in pig uterine secretions. *J Reprod Fertil* **108**, 313-20.
- Buhi, W. C., Alvarez, I. M., and Kouba, A. J. (1997). Oviductal regulation of fertilization and early embryonic development. *J Reprod Fertil Suppl* **52**, 285-300.
- Bujnicki, J. M., Prigge, S. T., Caridha, D., and Chiang, P. K. (2003). Structure, evolution, and inhibitor interaction of S-adenosyl-L-homocysteine hydrolase from *Plasmodium falciparum*. *Proteins* **52**, 624-32.
- Burghardt, R. C., Bowen, J. A., Newton, G. R., and Bazer, F. W. (1997). Extracellular matrix and the implantation cascade in pigs. *J Reprod Fertil Suppl* **52**, 151-64.
- Burton, G. J., Jauniaux, E., and Charnock-Jones, D. S. (2007). Human early placental development: potential roles of the endometrial glands. *Placenta* **28 Suppl A**, S64-9.
- Butler, W. T. (1989). The nature and significance of osteopontin. *Connect Tissue Res* **23**, 123-36.
- Caldwell, R. B., Kierzek, A. M., Arakawa, H., Bezzubov, Y., Zaim, J., Fiedler, P., Kutter, S., Blagodatski, A., Kostovska, D., Koter, M., Plachy, J., Carninci, P., Hayashizaki, Y., and Buerstedde, J. M. (2005). Full-length cDNAs from chicken bursal lymphocytes to facilitate gene function analysis. *Genome Biol* **6**, R6.
- Carletti, M. Z., and Christenson, L. K. (2009). MicroRNA in the ovary and female reproductive tract. *J Anim Sci* **87**, E29-38.
- Carmeliet, P., Ferreira, V., Breier, G., Pollefeyt, S., Kieckens, L., Gertsenstein, M., Fahrig, M., Vandenhoeck, A., Harpal, K., Eberhardt, C., Declercq, C., Pawling, J., Moons, L., Collen, D., Risau, W., and Nagy, A. (1996). Abnormal blood vessel development and lethality in embryos lacking a single VEGF allele. *Nature* **380**, 435-9.
- Carpenter, G., and Cohen, S. (1990). Epidermal growth factor. *J Biol Chem* **265**, 7709-12.
- Carson, D. D., Bagchi, I., Dey, S. K., Enders, A. C., Fazleabas, A. T., Lessey, B. A., and Yoshinaga, K. (2000). Embryo implantation. *Dev Biol* **223**, 217-37.
- Cartwright, J. E., Tse, W. K., and Whitley, G. S. (2002). Hepatocyte growth factor induced human trophoblast motility involves phosphatidylinositol-3-kinase, mitogen-activated protein kinase, and inducible nitric oxide synthase. *Exp Cell Res* **279**, 219-26.

- Cencic, A., Guillomot, M., Koren, S., and La Bonnardiére, C. (2003). Trophoblastic interferons: do they modulate uterine cellular markers at the time of conceptus attachment in the pig? *Placenta* **24**, 862-9.
- Charnock-Jones, D. S., Sharkey, A. M., Rajput-Williams, J., Burch, D., Schofield, J. P., Fountain, S. A., Boocock, C. A., and Smith, S. K. (1993). Identification and localization of alternately spliced mRNAs for vascular endothelial growth factor in human uterus and estrogen regulation in endometrial carcinoma cell lines. *Biol Reprod* **48**, 1120-8.
- Chegini, N., Rao, C. V., Wakim, N., and Sanfilippo, J. (1986). Binding of 125I-epidermal growth factor in human uterus. *Cell Tissue Res* **246**, 543-8.
- Chen, L. H., and Bissell, M. J. (1987). Transferrin mRNA level in the mouse mammary gland is regulated by pregnancy and extracellular matrix. *J Biol Chem* **262**, 17247-50.
- Chien, Y. C., Hincke, M. T., and McKee, M. D. (2009). Avian eggshell structure and osteopontin. *Cells Tissues Organs* **189**, 38-43.
- Choi, I., Simmen, R. C., and Simmen, F. A. (1996). Molecular cloning of cytochrome P450 aromatase complementary deoxyribonucleic acid from periimplantation porcine and equine blastocysts identifies multiple novel 5'-untranslated exons expressed in embryos, endometrium, and placenta. *Endocrinology* **137**, 1457-67.
- Chousalkar, K. K., and Roberts, J. R. (2008). Ultrastructural changes in the oviduct of the laying hen during the laying cycle. *Cell Tissue Res* **332**, 349-58.
- Clark, D. A., Chaouat, G., Mogil, R., and Wegmann, T. G. (1994). Prevention of spontaneous abortion in DBA/2-mated CBA/J mice by GM-CSF involves CD8+ T cell-dependent suppression of natural effector cell cytotoxicity against trophoblast target cells. *Cell Immunol* **154**, 143-52.
- Clark, D. E., Smith, S. K., Sharkey, A. M., and Charnock-Jones, D. S. (1996). Localization of VEGF and expression of its receptors flt and KDR in human placenta throughout pregnancy. *Hum Reprod* **11**, 1090-8.
- Classen-Linke, I., Alfer, J., Krusche, C. A., Chwalisz, K., Rath, W., and Beier, H. M. (2000). Progesterins, progesterone receptor modulators, and progesterone antagonists change VEGF release of endometrial cells in culture. *Steroids* **65**, 763-71.

- Clemmons, D. R. (1989). Structural and functional analysis of insulin-like growth factors. *Br Med Bull* **45**, 465-80.
- Cohen, M., and Bischof, P. (2007). Factors regulating trophoblast invasion. *Gynecol Obstet Invest* **64**, 126-30.
- Conklin, D., Gilbertson, D., Taft, D. W., Maurer, M. F., Whitmore, T. E., Smith, D. L., Walker, K. M., Chen, L. H., Wattler, S., Nehls, M., and Lewis, K. B. (1999). Identification of a mammalian angiopoietin-related protein expressed specifically in liver. *Genomics* **62**, 477-82.
- Cooper, B. J., Key, B., Carter, A., Angel, N. Z., Hart, D. N., and Kato, M. (2006). Suppression and overexpression of adenosylhomocysteine hydrolase-like protein 1 (AHCYL1) influences zebrafish embryo development: a possible role for AHCYL1 in inositol phospholipid signaling. *J Biol Chem* **281**, 22471-84.
- Corradino, R. A., Wasserman, R. H., Pubols, M. H., and Chang, S. I. (1968). Vitamin D3 induction of a calcium-binding protein in the uterus of the laying hen. *Arch Biochem Biophys* **125**, 378-80.
- Crainie, M., Guilbert, L., and Wegmann, T. G. (1990). Expression of novel cytokine transcripts in the murine placenta. *Biol Reprod* **43**, 999-1005.
- Creger, C. R., and Scott, J. T. (1977). Dietary Zinc as an Effective Resting Agent for Laying Hen. *Poultry Science* **56**, 1706-1706.
- Cullinan-Bove, K., and Koos, R. D. (1993). Vascular endothelial growth factor/vascular permeability factor expression in the rat uterus: rapid stimulation by estrogen correlates with estrogen-induced increases in uterine capillary permeability and growth. *Endocrinology* **133**, 829-37.
- D'Alessandro, A., Righetti, P. G., Fasoli, E., and Zolla, L. (2010). The egg white and yolk interactomes as gleaned from extensive proteomic data. *J Proteomics* **73**, 1028-42.
- Damme, K., Pirchner, F., Willeke, H., and Eichinger, H. (1987). Fasting metabolic rate in hens. I. Effects of body weight, feather loss, and activity. *Poult Sci* **66**, 881-90.
- Dantzer, V. (1985). Electron microscopy of the initial stages of placentation in the pig. *Anat Embryol (Berl)* **172**, 281-93.
- Dantzer, V., and Leiser, R. (1994). Initial vascularisation in the pig placenta: I. Demonstration of nonglandular areas by

histology and corrosion casts. *Anat Rec* **238**, 177-90.

Daoud, G., Amyot, M., Rassart, E., Masse, A., Simoneau, L., and Lafond, J. (2005a). ERK1/2 and p38 regulate trophoblasts differentiation in human term placenta. *The Journal of physiology* **566**, 409-23.

Daoud, G., Amyot, M., Rassart, E., Masse, A., Simoneau, L., and Lafond, J. (2005b). ERK1/2 and p38 regulate trophoblasts differentiation in human term placenta. *J Physiol* **566**, 409-23.

Das, S. K., Chakraborty, I., Wang, J., Dey, S. K., and Hoffman, L. H. (1997). Expression of vascular endothelial growth factor (VEGF) and VEGF-receptor messenger ribonucleic acids in the peri-implantation rabbit uterus. *Biol Reprod* **56**, 1390-9.

Das, S. K., Tsukamura, H., Paria, B. C., Andrews, G. K., and Dey, S. K. (1994). Differential expression of epidermal growth factor receptor (EGF-R) gene and regulation of EGF-R bioactivity by progesterone and estrogen in the adult mouse uterus. *Endocrinology* **134**, 971-81.

Davies, K. J., Ermak, G., Rothermel, B. A., Pritchard, M., Heitman, J., Ahn, J., Henrique-Silva, F., Crawford, D., Canaider, S., Strippoli, P., Carinci, P., Min, K. T., Fox, D. S., Cunningham, K. W., Bassel-Duby, R., Olson, E. N., Zhang, Z., Williams, R. S., Gerber, H. P., Perez-Riba, M., Seo, H., Cao, X., Klee, C. B., Redondo, J. M., Maltais, L. J., Bruford, E. A., Povey, S., Molkentin, J. D., McKeon, F. D., Duh, E. J., Crabtree, G. R., Cyert, M. S., de la Luna, S., and Estivill, X. (2007). Renaming the DSCR1/Adapt78 gene family as RCAN: regulators of calcineurin. *FASEB J* **21**, 3023-8.

De La Haba, G., and Cantoni, G. L. (1959). The enzymatic synthesis of S-adenosyl-L-homocysteine from adenosine and homocysteine. *J Biol Chem* **234**, 603-8.

de Moraes, A. A., and Hansen, P. J. (1997). Granulocyte-macrophage colony-stimulating factor promotes development of in vitro produced bovine embryos. *Biol Reprod* **57**, 1060-5.

de Moraes, A. A., Paula-Lopes, F. F., Chegini, N., and Hansen, P. J. (1999). Localization of granulocyte-macrophage colony-stimulating factor in the bovine reproductive tract. *J Reprod Immunol* **42**, 135-45.

De Vries, L., Zheng, B., Fischer, T., Elenko, E., and Farquhar, M. G. (2000). The regulator of G protein signaling family. *Annu Rev Pharmacol Toxicol* **40**, 235-71.

- DeChiara, T. M., Efstratiadis, A., and Robertson, E. J. (1990). A growth-deficiency phenotype in heterozygous mice carrying an insulin-like growth factor II gene disrupted by targeting. *Nature* **345**, 78-80.
- Dekker, J. W., Budhia, S., Angel, N. Z., Cooper, B. J., Clark, G. J., Hart, D. N., and Kato, M. (2002). Identification of an S-adenosylhomocysteine hydrolase-like transcript induced during dendritic cell differentiation. *Immunogenetics* **53**, 993-1001.
- Denley, A., Cosgrove, L. J., Booker, G. W., Wallace, J. C., and Forbes, B. E. (2005). Molecular interactions of the IGF system. *Cytokine Growth Factor Rev* **16**, 421-39.
- Desjardins, E., and Hay, N. (1993). Repeated Ct Elements Bound by Zinc-Finger Proteins Control the Absolute and Relative Activities of the 2 Principal Human C-Myc Promoters. *Molecular and Cellular Biology* **13**, 5710-5724.
- Devogelaere, B., Nadif Kasri, N., Derua, R., Waelkens, E., Callewaert, G., Missiaen, L., Parys, J. B., and De Smedt, H. (2006). Binding of IRBIT to the IP3 receptor: determinants and functional effects. *Biochem Biophys Res Commun* **343**, 49-56.
- Diaz-Cueto, L., and Gerton, G. L. (2001). The influence of growth factors on the development of preimplantation mammalian embryos. *Arch Med Res* **32**, 619-26.
- Dougherty, D. C., and Sanders, M. M. (2005). Estrogen action: revitalization of the chick oviduct model. *Trends Endocrinol Metab* **16**, 414-9.
- Drummond, A. J., Ashton, B., Buxton, S., Cheung, M., Cooper, A., Heled, J., Kearse, M., Mior, R., Stones-Havas, S., Sturrock, S., Thierer, T., and Wilson, A. (2010). Geneious v5.04, Available from <http://www.geneious.com>.
- Dufner, A., and Thomas, G. (1999). Ribosomal S6 kinase signaling and the control of translation. *Exp Cell Res* **253**, 100-9.
- Dunn, I. C., Wilson, P. W., Lu, Z., Bain, M. M., Crossan, C. L., Talbot, R. T., and Waddington, D. (2009a). New hypotheses on the function of the avian shell gland derived from microarray analysis comparing tissue from juvenile and sexually mature hens. *Gen Comp Endocrinol* **163**, 225-32.
- Dunn, I. C., Wilson, P. W., Lu, Z., Bain, M. M., Crossan, C. L., Talbot, R. T., and Waddington, D. (2009b). New hypotheses on the function of the avian shell gland derived from microarray analysis comparing tissue from juvenile and sexually mature hens. *General and Comparative Endocrinology* **163**, 225-232.

- Dupont, J., and Holzenberger, M. (2003). Biology of insulin-like growth factors in development. *Birth Defects Res C Embryo Today* **69**, 257-71.
- Dutta, S., Wang, F. Q., Phalen, A., and Fishman, D. A. (2010). Biomarkers for ovarian cancer detection and therapy. *Cancer Biol Ther* **9**, 668-77.
- Dynan, W. S., and Tjian, R. (1983a). Isolation of Transcription Factors That Discriminate between Different Promoters Recognized by Rna Polymerase-Ii. *Cell* **32**, 669-680.
- Dynan, W. S., and Tjian, R. (1983b). The Promoter-Specific Transcription Factor-Sp1 Binds to Upstream Sequences in the Sv40 Early Promoter. *Cell* **35**, 79-87.
- Dziuk, P. J. (1968). Effect of number of embryos and uterine space on embryo survival in the pig. *J Anim Sci* **27**, 673-6.
- Einspanier, R., Schonfelder, M., Muller, K., Stojkovic, M., Kosmann, M., Wolf, E., and Schams, D. (2002). Expression of the vascular endothelial growth factor and its receptors and effects of VEGF during in vitro maturation of bovine cumulus-oocyte complexes (COC). *Mol Reprod Dev* **62**, 29-36.
- Emond, V., Asselin, E., Fortier, M. A., Murphy, B. D., and Lambert, R. D. (2000). Interferon-tau stimulates granulocyte-macrophage colony-stimulating factor gene expression in bovine lymphocytes and endometrial stromal cells. *Biol Reprod* **62**, 1728-37.
- Emond, V., Fortier, M. A., Murphy, B. D., and Lambert, R. D. (1998). Prostaglandin E2 regulates both interleukin-2 and granulocyte-macrophage colony-stimulating factor gene expression in bovine lymphocytes. *Biol Reprod* **58**, 143-51.
- Emond, V., MacLaren, L. A., Kimmins, S., Arosh, J. A., Fortier, M. A., and Lambert, R. D. (2004). Expression of cyclooxygenase-2 and granulocyte-macrophage colony-stimulating factor in the endometrial epithelium of the cow is up-regulated during early pregnancy and in response to intrauterine infusions of interferon-tau. *Biol Reprod* **70**, 54-64.
- Ermak, G., Morgan, T. E., and Davies, K. J. (2001). Chronic overexpression of the calcineurin inhibitory gene DSCR1 (Adapt78) is associated with Alzheimer's disease. *J Biol Chem* **276**, 38787-94.
- Esteban, V., Mendez-Barbero, N., Jimenez-Borreguero, L. J., Roque, M., Novensa, L., Garcia-Redondo, A. B., Salaices, M., Vila, L., Arbones, M. L., Campanero, M. R., and Redondo, J. M. (2011). Regulator of calcineurin 1 mediates pathological vascular wall

remodeling. *J Exp Med* **208**, 2125-39.

Estrada, J. L., Jones, E. E., Johnson, B. H., and Petters, R. M. (1991). Effect of insulin-like growth factor-I on protein synthesis in porcine embryonic discs cultured in vitro. *J Reprod Fertil* **93**, 53-61.

Fazleabas, A. T., Kim, J. J., and Strakova, Z. (2004). Implantation: embryonic signals and the modulation of the uterine environment--a review. *Placenta* **25 Suppl A**, S26-31.

Felsenstein, J. (1985). Confidence-Limits on Phylogenies - an Approach Using the Bootstrap. *Evolution* **39**, 783-791.

Feng, X. H., Lin, X., and Derynck, R. (2000). Smad2, Smad3 and Smad4 cooperate with Sp1 to induce p15(Ink4B) transcription in response to TGF-beta. *EMBO J* **19**, 5178-93.

Fernandez-Serra, M., Consales, C., Livigni, A., and Amone, M. I. (2004a). Role of the ERK-mediated signaling pathway in mesenchyme formation and differentiation in the sea urchin embryo. *Developmental biology* **268**, 384-402.

Fernandez-Serra, M., Consales, C., Livigni, A., and Amone, M. I. (2004b). Role of the ERK-mediated signaling pathway in mesenchyme formation and differentiation in the sea urchin embryo. *Dev Biol* **268**, 384-402.

Fernandez, M. S., Escobar, C., Lavelin, I., Pines, M., and Arias, J. L. (2003). Localization of osteopontin in oviduct tissue and eggshell during different stages of the avian egg laying cycle. *J Struct Biol* **143**, 171-80.

Ferrara, N., Carver-Moore, K., Chen, H., Dowd, M., Lu, L., O'Shea, K. S., Powell-Braxton, L., Hillan, K. J., and Moore, M. W. (1996). Heterozygous embryonic lethality induced by targeted inactivation of the VEGF gene. *Nature* **380**, 439-42.

Ferrara, N., Gerber, H. P., and LeCouter, J. (2003). The biology of VEGF and its receptors. *Nat Med* **9**, 669-76.

Finn, C. A., and Martin, L. (1974). The control of implantation. *J Reprod Fertil* **39**, 195-206.

Fischer, H. E., Bazer, F. W., and Fields, M. J. (1985). Steroid metabolism by endometrial and conceptus tissues during early pregnancy and pseudopregnancy in gilts. *J Reprod Fertil* **75**, 69-78.

Fitzgerald, J. S., Busch, S., Wengenmayer, T., Foerster, K., de la Motte, T., Poehlmann, T. G., and Markert, U. R. (2005a). Signal transduction in trophoblast invasion. *Chem Immunol Allergy* **88**, 181-99.

Fitzgerald, J. S., Tsareva, S. A., Poehlmann, T. G., Berod, L., Meissner, A., Corvinus, F. M., Wiederanders, B., Pfitzner, E.,

Markert, U. R., and Friedrich, K. (2005b). Leukemia inhibitory factor triggers activation of signal transducer and activator of transcription 3, proliferation, invasiveness, and altered protease expression in choriocarcinoma cells. *Int J Biochem Cell Biol* **37**, 2284-96.

Flanagan, J. U., Cassady, A. I., Schenk, G., Guddat, L. W., and Hume, D. A. (2006). Identification and molecular modeling of a novel, plant-like, human purple acid phosphatase. *Gene* **377**, 12-20.

Fong, G. H., Rossant, J., Gertsenstein, M., and Breitman, M. L. (1995). Role of the Flt-1 receptor tyrosine kinase in regulating the assembly of vascular endothelium. *Nature* **376**, 66-70.

Ford, S. P., and Christenson, L. K. (1991). Direct effects of oestradiol-17 beta and prostaglandin E-2 in protecting pig corpora lutea from a luteolytic dose of prostaglandin F-2 alpha. *J Reprod Fertil* **93**, 203-9.

Ford, S. P., and Christenson, R. K. (1979). Blood flow to uteri of sows during the estrous cycle and early pregnancy: local effect of the conceptus on the uterine blood supply. *Biol Reprod* **21**, 617-24.

Fortin, M., Ouellette, M. J., and Lambert, R. D. (1997). TGF-beta 2 and PGE2 in rabbit blastocoelic fluid can modulate GM-CSF production by human lymphocytes. *Am J Reprod Immunol* **38**, 129-39.

Frank, M., Bazer, F. W., Thatcher, W. W., and Wilcox, C. J. (1977). A study of prostaglandin F2alpha as the luteolysin in swine: III effects of estradiol valerate on prostaglandin F, progestins, estrone and estradiol concentrations in the utero-ovarian vein of nonpregnant gilts. *Prostaglandins* **14**, 1183-96.

Fuentes, J. J., Pritchard, M. A., and Estivill, X. (1997). Genomic organization, alternative splicing, and expression patterns of the DSCR1 (Down syndrome candidate region 1) gene. *Genomics* **44**, 358-61.

Ganz, T. (2003). Defensins: antimicrobial peptides of innate immunity. *Nat Rev Immunol* **3**, 710-20.

Gardner, H. G., and Kaye, P. L. (1991). Insulin increases cell numbers and morphological development in mouse pre-implantation embryos in vitro. *Reprod Fertil Dev* **3**, 79-91.

Garlich, J., Brake, J., Parkhurst, C. R., Thaxton, J. P., and Morgan, G. W. (1984). Physiological profile of caged layers during one production year, molt, and postmolt: egg production, egg shell quality, liver, femur, and blood parameters. *Poult Sci* **63**, 339-43.

Garlow, J. E., Ka, H., Johnson, G. A., Burghardt, R. C., Jaeger, L. A., and Bazer, F. W. (2002). Analysis of osteopontin at the

maternal-placental interface in pigs. *Biol Reprod* **66**, 718-25.

Gasson, J. C. (1991). Molecular physiology of granulocyte-macrophage colony-stimulating factor. *Blood* **77**, 1131-45.

Geisert, R. D., Brookbank, J. W., Roberts, R. M., and Bazer, F. W. (1982a). Establishment of pregnancy in the pig: II. Cellular remodeling of the porcine blastocyst during elongation on day 12 of pregnancy. *Biol Reprod* **27**, 941-55.

Geisert, R. D., Chamberlain, C. S., Vonnahme, K. A., Malayer, J. R., and Spicer, L. J. (2001). Possible role of kallikrein in proteolysis of insulin-like growth factor binding proteins during the oestrous cycle and early pregnancy in pigs. *Reproduction* **121**, 719-28.

Geisert, R. D., Lee, C. Y., Simmen, F. A., Zavy, M. T., Fliss, A. E., Bazer, F. W., and Simmen, R. C. (1991). Expression of messenger RNAs encoding insulin-like growth factor-I, -II, and insulin-like growth factor binding protein-2 in bovine endometrium during the estrous cycle and early pregnancy. *Biol Reprod* **45**, 975-83.

Geisert, R. D., Pratt, T. N., Bazer, F. W., Mayes, J. S., and Watson, G. H. (1994). Immunocytochemical localization and changes in endometrial progesterin receptor protein during the porcine oestrous cycle and early pregnancy. *Reprod Fertil Dev* **6**, 749-60.

Geisert, R. D., Renegar, R. H., Thatcher, W. W., Roberts, R. M., and Bazer, F. W. (1982b). Establishment of pregnancy in the pig: I. Interrelationships between preimplantation development of the pig blastocyst and uterine endometrial secretions. *Biol Reprod* **27**, 925-39.

Geisert, R. D., Thatcher, W. W., Roberts, R. M., and Bazer, F. W. (1982c). Establishment of pregnancy in the pig: III. Endometrial secretory response to estradiol valerate administered on day 11 of the estrous cycle. *Biol Reprod* **27**, 957-65.

Geisert, R. D., and Yelich, J. V. (1997). Regulation of conceptus development and attachment in pigs. *J Reprod Fertil Suppl* **52**, 133-49.

Geisert, R. D., Zavy, M. T., Moffatt, R. J., Blair, R. M., and Yellin, T. (1990). Embryonic steroids and the establishment of pregnancy in pigs. *J Reprod Fertil Suppl* **40**, 293-305.

Geva, E., and Jaffe, R. B. (2000). Role of angiopoietins in reproductive tract angiogenesis. *Obstet Gynecol Surv* **55**, 511-9.

Giacomini, G., Tabibzadeh, S. S., Satyaswaroop, P. G., Bonsi, L., Vitale, L., Bagnara, G. P., Strippoli, P., and Jasonni, V. M. (1995). Epithelial cells are the major source of biologically active granulocyte macrophage colony-stimulating factor in human

endometrium. *Hum Reprod* **10**, 3259-63.

Giles, J. R., Olson, L. M., and Johnson, P. A. (2006). Characterization of ovarian surface epithelial cells from the hen: a unique model for ovarian cancer. *Exp Biol Med (Maywood)* **231**, 1718-25.

Giles, J. R., Shivaprasad, H. L., and Johnson, P. A. (2004). Ovarian tumor expression of an oviductal protein in the hen: a model for human serous ovarian adenocarcinoma. *Gynecol Oncol* **95**, 530-3.

Gingras, A. C., Raught, B., and Sonenberg, N. (2004). mTOR signaling to translation. *Curr Top Microbiol Immunol* **279**, 169-97.

Gleeson, L. M., Chakraborty, C., McKinnon, T., and Lala, P. K. (2001). Insulin-like growth factor-binding protein 1 stimulates human trophoblast migration by signaling through alpha 5 beta 1 integrin via mitogen-activated protein Kinase pathway. *J Clin Endocrinol Metab* **86**, 2484-93.

Gluckman, P. D. (1986). The role of pituitary hormones, growth factors and insulin in the regulation of fetal growth. *Oxf Rev Reprod Biol* **8**, 1-60.

Gomi, T., Takusagawa, F., Nishizawa, M., Agussalim, B., Usui, I., Sugiyama, E., Taki, H., Shinoda, K., Hounoki, H., Miwa, T., Tobe, K., Kobayashi, M., Ishimoto, T., Ogawa, H., and Mori, H. (2008). Cloning, bacterial expression, and unique structure of adenosylhomocysteine hydrolase-like protein 1, or inositol 1,4,5-triphosphate receptor-binding protein from mouse kidney. *Biochim Biophys Acta* **1784**, 1786-94.

Gray, C. A., Bartol, F. F., Tarleton, B. J., Wiley, A. A., Johnson, G. A., Bazer, F. W., and Spencer, T. E. (2001a). Developmental biology of uterine glands. *Biol Reprod* **65**, 1311-23.

Gray, C. A., Bazer, F. W., and Spencer, T. E. (2001b). Effects of neonatal progestin exposure on female reproductive tract structure and function in the adult ewe. *Biol Reprod* **64**, 797-804.

Gray, C. A., Burghardt, R. C., Johnson, G. A., Bazer, F. W., and Spencer, T. E. (2002). Evidence that absence of endometrial gland secretions in uterine gland knockout ewes compromises conceptus survival and elongation. *Reproduction* **124**, 289-300.

Gray, C. A., Taylor, K. M., Ramsey, W. S., Hill, J. R., Bazer, F. W., Bartol, F. F., and Spencer, T. E. (2001c). Endometrial glands are required for preimplantation conceptus elongation and survival. *Biol Reprod* **64**, 1608-13.

- Greb, R. R., Heikinheimo, O., Williams, R. F., Hodgen, G. D., and Goodman, A. L. (1997). Vascular endothelial growth factor in primate endometrium is regulated by oestrogen-receptor and progesterone-receptor ligands in vivo. *Hum Reprod* **12**, 1280-92.
- Green, M. L., Blaeser, L. L., Simmen, F. A., and Simmen, R. C. (1996). Molecular cloning of spermidine/spermine N1-acetyltransferase from the periimplantation porcine uterus by messenger ribonucleic acid differential display: temporal and conceptus-modulated gene expression. *Endocrinology* **137**, 5447-55.
- Green, M. L., Simmen, R. C., and Simmen, F. A. (1995). Developmental regulation of steroidogenic enzyme gene expression in the periimplantation porcine conceptus: a paracrine role for insulin-like growth factor-I. *Endocrinology* **136**, 3961-70.
- Guan, Z., Buckman, S. Y., Miller, B. W., Springer, L. D., and Morrison, A. R. (1998). Interleukin-1beta-induced cyclooxygenase-2 expression requires activation of both c-Jun NH2-terminal kinase and p38 MAPK signal pathways in rat renal mesangial cells. *J Biol Chem* **273**, 28670-6.
- Guillomot, M. (1995). Cellular interactions during implantation in domestic ruminants. *J Reprod Fertil Suppl* **49**, 39-51.
- Gupta, A., Bazer, F. W., and Jaeger, L. A. (1996). Differential expression of beta transforming growth factors (TGF beta 1, TGF beta 2, and TGF beta 3) and their receptors (type I and type II) in peri-implantation porcine conceptuses. *Biol Reprod* **55**, 796-802.
- Gupta, A., Ing, N. H., Bazer, F. W., Bustamante, L. S., and Jaeger, L. A. (1998). Beta transforming growth factors (TGFs) at the porcine conceptus-maternal interface. Part I: expression of TGFbeta1, TGFbeta2, and TGFbeta3 messenger ribonucleic acids. *Biol Reprod* **59**, 905-10.
- Haase, I., Evans, R., Pofahl, R., and Watt, F. M. (2003). Regulation of keratinocyte shape, migration and wound epithelialization by IGF-1- and EGF-dependent signalling pathways. *J Cell Sci* **116**, 3227-38.
- Hakim, A. A., Barry, C. P., Barnes, H. J., Anderson, K. E., Petite, J., Whitaker, R., Lancaster, J. M., Wenham, R. M., Carver, D. K., Turbov, J., Berchuck, A., Kopelovich, L., and Rodriguez, G. C. (2009). Ovarian adenocarcinomas in the laying hen and women share similar alterations in p53, ras, and HER-2/neu. *Cancer Prev Res (Phila)* **2**, 114-21.
- Halder, J. B., Zhao, X., Soker, S., Paria, B. C., Klagsbrun, M., Das, S. K., and Dey, S. K. (2000). Differential expression of VEGF isoforms and VEGF(164)-specific receptor neuropilin-1 in the mouse uterus suggests a role for VEGF(164) in vascular

permeability and angiogenesis during implantation. *Genesis* **26**, 213-24.

Hales, D. B., Zhuge, Y., Lagman, J. A., Ansenberger, K., Mahon, C., Barua, A., Luborsky, J. L., and Bahr, J. M. (2008).

Cyclooxygenases expression and distribution in the normal ovary and their role in ovarian cancer in the domestic hen (*Gallus domesticus*).

Endocrine **33**, 235-44.

Hammond, M. G., Oh, S. T., Anners, J., Surrey, E. S., and Halme, J. (1993). The effect of growth factors on the proliferation of

human endometrial stromal cells in culture. *Am J Obstet Gynecol* **168**, 1131-6; discussion 1136-8.

Han, V. K., and Carter, A. M. (2000). Spatial and temporal patterns of expression of messenger RNA for insulin-like growth

factors and their binding proteins in the placenta of man and laboratory animals. *Placenta* **21**, 289-305.

Hannan, N. J., Paiva, P., Meehan, K. L., Rombauts, L. J., Gardner, D. K., and Salamonsen, L. A. (2011). Analysis of fertility-

related soluble mediators in human uterine fluid identifies VEGF as a key regulator of embryo implantation. *Endocrinology* **152**, 4948-56.

Hardy, K., and Spanos, S. (2002). Growth factor expression and function in the human and mouse preimplantation embryo. *J*

Endocrinol **172**, 221-36.

Hartt, L. S., Carling, S. J., Joyce, M. M., Johnson, G. A., Vanderwall, D. K., and Ott, T. L. (2005). Temporal and spatial

associations of oestrogen receptor alpha and progesterone receptor in the endometrium of cyclic and early pregnant mares. *Reproduction*

130, 241-50.

Harvey, M. B., and Kaye, P. L. (1988). Insulin stimulates protein synthesis in compacted mouse embryos. *Endocrinology* **122**,

1182-4.

Harvey, M. B., and Kaye, P. L. (1990). Insulin increases the cell number of the inner cell mass and stimulates morphological

development of mouse blastocysts in vitro. *Development* **110**, 963-7.

Harvey, M. B., and Kaye, P. L. (1991). Mouse blastocysts respond metabolically to short-term stimulation by insulin and IGF-1

through the insulin receptor. *Mol Reprod Dev* **29**, 253-8.

Harvey, M. B., and Kaye, P. L. (1992a). IGF-2 stimulates growth and metabolism of early mouse embryos. *Mech Dev* **38**, 169-

73.

Harvey, M. B., and Kaye, P. L. (1992b). Insulin-like growth factor-1 stimulates growth of mouse preimplantation embryos in vitro. *Mol Reprod Dev* **31**, 195-9.

Harvey, M. B., and Kaye, P. L. (1992c). Mediation of the actions of insulin and insulin-like growth factor-1 on preimplantation mouse embryos in vitro. *Mol Reprod Dev* **33**, 270-5.

Hayashida, K., Kitamura, T., Gorman, D. M., Arai, K., Yokota, T., and Miyajima, A. (1990). Molecular cloning of a second subunit of the receptor for human granulocyte-macrophage colony-stimulating factor (GM-CSF): reconstitution of a high-affinity GM-CSF receptor. *Proc Natl Acad Sci U S A* **87**, 9655-9.

Heim, M. H., Kerr, I. M., Stark, G. R., and Darnell, J. E., Jr. (1995). Contribution of STAT SH2 groups to specific interferon signaling by the Jak-STAT pathway. *Science* **267**, 1347-9.

Heintz, A. P., Odicino, F., Maisonneuve, P., Beller, U., Benedet, J. L., Creasman, W. T., Ngan, H. Y., and Pecorelli, S. (2003). Carcinoma of the ovary. *Int J Gynaecol Obstet* **83 Suppl 1**, 135-66.

Heintz, A. P., Odicino, F., Maisonneuve, P., Quinn, M. A., Benedet, J. L., Creasman, W. T., Ngan, H. Y., Pecorelli, S., and Beller, U. (2006). Carcinoma of the ovary. FIGO 26th Annual Report on the Results of Treatment in Gynecological Cancer. *Int J Gynaecol Obstet* **95 Suppl 1**, S161-92.

Henic, E., Sixt, M., Hansson, S., Hoyer-Hansen, G., and Casslen, B. (2006). EGF-stimulated migration in ovarian cancer cells is associated with decreased internalization, increased surface expression, and increased shedding of the urokinase plasminogen activator receptor. *Gynecol Oncol* **101**, 28-39.

Henricks, D. M., Guthrie, H. D., and Handlin, D. L. (1972). Plasma estrogen, progesterone and luteinizing hormone levels during the estrous cycle in pigs. *Biol Reprod* **6**, 210-8.

Herbst, R. S. (2004). Review of epidermal growth factor receptor biology. *Int J Radiat Oncol Biol Phys* **59**, 21-6.

Herve-Grepinet, V., Rehault-Godbert, S., Labas, V., Magallon, T., Derache, C., Lavergne, M., Gautron, J., Lalmanach, A. C., and Nys, Y. (2010). Purification and characterization of avian beta-defensin 11, an antimicrobial peptide of the hen egg. *Antimicrob Agents Chemother* **54**, 4401-9.

Heryanto, B., Yoshimura, Y., and Tamura, T. (1997a). Cell proliferation in the process of oviducal tissue remodeling during induced molting in hens. *Poult Sci* **76**, 1580-6.

Heryanto, B., Yoshimura, Y., Tamura, T., and Okamoto, T. (1997b). Involvement of apoptosis and lysosomal hydrolase activity in the oviducal regression during induced molting in chickens: a cytochemical study for end labeling of fragmented DNA and acid phosphatase. *Poult Sci* **76**, 67-72.

Hewitt, S. C., Harrell, J. C., and Korach, K. S. (2005). Lessons in estrogen biology from knockout and transgenic animals. *Annu Rev Physiol* **67**, 285-308.

Heyner, S., Smith, R. M., and Schultz, G. A. (1989). Temporally regulated expression of insulin and insulin-like growth factors and their receptors in early mammalian development. *Bioessays* **11**, 171-6.

Hincke, M. T., Nys, Y., and Gautron, J. (2010). The Role of Matrix Proteins in Eggshell Formation. *Journal of Poultry Science* **47**, 208-219.

Hofig, A., Simmen, F. A., Bazer, F. W., and Simmen, R. C. (1991). Effects of insulin-like growth factor-I on aromatase cytochrome P450 activity and oestradiol biosynthesis in preimplantation porcine conceptuses in vitro. *J Endocrinol* **130**, 245-50.

Hofmann, G. E., and Anderson, T. L. (1990). Immunohistochemical localization of epidermal growth factor receptor during implantation in the rabbit. *Am J Obstet Gynecol* **162**, 837-41.

Holt, P. S., Buhr, R. J., Cunningham, D. L., and Porter, R. E., Jr. (1994). Effect of two different molting procedures on a Salmonella enteritidis infection. *Poult Sci* **73**, 1267-75.

Hook, V., Funkelstein, L., Lu, D., Bark, S., Wegrzyn, J., and Hwang, S. R. (2008). Proteases for processing proneuropeptides into peptide neurotransmitters and hormones. *Annu Rev Pharmacol Toxicol* **48**, 393-423.

Hoshino, S., Suzuki, M., Kakegawa, T., Imai, K., Wakita, M., Kobayashi, Y., and Yamada, Y. (1988). Changes in plasma thyroid hormones, luteinizing hormone (LH), estradiol, progesterone and corticosterone of laying hens during a forced molt. *Comp Biochem Physiol A Comp Physiol* **90**, 355-9.

Houck, K. A., Ferrara, N., Winer, J., Cachianes, G., Li, B., and Leung, D. W. (1991). The vascular endothelial growth factor

family: identification of a fourth molecular species and characterization of alternative splicing of RNA. *Mol Endocrinol* **5**, 1806-14.

Hynes, R. O. (1992). Integrins: versatility, modulation, and signaling in cell adhesion. *Cell* **69**, 11-25.

Ihle, J. N., and Kerr, I. M. (1995). Jaks and Stats in signaling by the cytokine receptor superfamily. *Trends Genet* **11**, 69-74.

Imakawa, K., Helmer, S. D., Nephew, K. P., Meka, C. S., and Christenson, R. K. (1993). A novel role for GM-CSF: enhancement of pregnancy specific interferon production, ovine trophoblast protein-1. *Endocrinology* **132**, 1869-71.

Irwin, J. C., Suen, L. F., Martina, N. A., Mark, S. P., and Giudice, L. C. (1999). Role of the IGF system in trophoblast invasion and pre-eclampsia. *Hum Reprod* **14 Suppl 2**, 90-6.

Jabbour, H. N., Kelly, R. W., Fraser, H. M., and Critchley, H. O. (2006). Endocrine regulation of menstruation. *Endocr Rev* **27**, 17-46.

Jackson, E., Anderson, K., Ashwell, C., Petite, J., and Mozdziak, P. E. (2007). CA125 expression in spontaneous ovarian adenocarcinomas from laying hens. *Gynecol Oncol* **104**, 192-8.

Jaeger, L. A., Johnson, G. A., Ka, H., Garlow, J. G., Burghardt, R. C., Spencer, T. E., and Bazer, F. W. (2001). Functional analysis of autocrine and paracrine signalling at the uterine-conceptus interface in pigs. *Reprod Suppl* **58**, 191-207.

Jeong, W., Lim, W., Kim, J., Ahn, S. E., Lee, H. C., Jeong, J. W., Han, J. Y., Song, G., and Bazer, F. W. (2012). Cell-specific and temporal aspects of gene expression in the chicken oviduct at different stages of the laying cycle. *Biol Reprod* **86**, 172.

Jin, D. F., Muffly, K. E., Okulicz, W. C., and Kilpatrick, D. L. (1988). Estrous cycle- and pregnancy-related differences in expression of the proenkephalin and proopiomelanocortin genes in the ovary and uterus. *Endocrinology* **122**, 1466-71.

Jingjing, L., Xue, Y., Agarwal, N., and Roque, R. S. (1999). Human Muller cells express VEGF183, a novel spliced variant of vascular endothelial growth factor. *Invest Ophthalmol Vis Sci* **40**, 752-9.

Johnson, K. A. (2009). The standard of perfection: thoughts about the laying hen model of ovarian cancer. *Cancer Prev Res (Phila)* **2**, 97-9.

Jones, J. I., and Clemmons, D. R. (1995). Insulin-like growth factors and their binding proteins: biological actions. *Endocr Rev* **16**, 3-34.

Joslin, E. J., Opresko, L. K., Wells, A., Wiley, H. S., and Lauffenburger, D. A. (2007). EGF-receptor-mediated mammary epithelial cell migration is driven by sustained ERK signaling from autocrine stimulation. *J Cell Sci* **120**, 3688-99.

Jung, J. G., Park, T. S., Kim, J. N., Han, B. K., Lee, S. D., Song, G., and Han, J. Y. (2011). Characterization and Application of Oviductal Epithelial Cells In Vitro in Gallus domesticus. *Biology of reproduction* **85**, 798-807.

Ka, H., Jaeger, L. A., Johnson, G. A., Spencer, T. E., and Bazer, F. W. (2001). Keratinocyte growth factor is up-regulated by estrogen in the porcine uterine endometrium and functions in trophectoderm cell proliferation and differentiation. *Endocrinology* **142**, 2303-10.

Ka, H., Spencer, T. E., Johnson, G. A., and Bazer, F. W. (2000). Keratinocyte growth factor: expression by endometrial epithelia of the porcine uterus. *Biol Reprod* **62**, 1772-8.

Kameda, Y., Miura, M., and Ohno, S. (2000). Expression and development of the proenkephalin mRNA in the C cells of chicken ultimobranchial glands. *Brain Res* **852**, 453-62.

Kane, M. T., Morgan, P. M., and Coonan, C. (1997). Peptide growth factors and preimplantation development. *Hum Reprod Update* **3**, 137-57.

Kanzaki, H., Crainie, M., Lin, H., Yui, J., Guilbert, L. J., Mori, T., and Wegmann, T. G. (1991). The in situ expression of granulocyte-macrophage colony-stimulating factor (GM-CSF) mRNA at the maternal-fetal interface. *Growth Factors* **5**, 69-74.

Karagenc, L., Lane, M., and Gardner, D. K. (2005). Granulocyte-macrophage colony-stimulating factor stimulates mouse blastocyst inner cell mass development only when media lack human serum albumin. *Reprod Biomed Online* **10**, 511-8.

Kato, H., and Torigoe, T. (1977). Radioimmunoassay for tumor antigen of human cervical squamous cell carcinoma. *Cancer* **40**, 1621-8.

Kavurma, M. M., and Khachigian, L. M. (2003). Sp1 inhibits proliferation and induces apoptosis in vascular smooth muscle cells by repressing p21(WAF1/Cip1) transcription and cyclin D1-Cdk4-p21(WAF1/Cip1) complex formation. *Journal of Biological Chemistry* **278**, 32537-32543.

Kavurma, M. M., Santiago, F. S., Bonfoco, E., and Khachigian, L. M. (2001). Sp1 phosphorylation regulates apoptosis via

extracellular FasL-Fas engagement. *Journal of Biological Chemistry* **276**, 4964-4971.

Kaye, P. L., Bell, K. L., Beebe, L. F., Dungleison, G. F., Gardner, H. G., and Harvey, M. B. (1992). Insulin and the insulin-like growth factors (IGFs) in preimplantation development. *Reprod Fertil Dev* **4**, 373-86.

Kennedy, T. G., Brown, K. D., and Vaughan, T. J. (1994). Expression of the genes for the epidermal growth factor receptor and its ligands in porcine oviduct and endometrium. *Biol Reprod* **50**, 751-6.

Keys, J. L., and King, G. J. (1988). Morphological evidence for increased uterine vascular permeability at the time of embryonic attachment in the pig. *Biol Reprod* **39**, 473-87.

Keys, J. L., and King, G. J. (1990). Microscopic examination of porcine conceptus-maternal interface between days 10 and 19 of pregnancy. *Am J Anat* **188**, 221-38.

Keys, J. L., King, G. J., and Kennedy, T. G. (1986). Increased uterine vascular permeability at the time of embryonic attachment in the pig. *Biol Reprod* **34**, 405-11.

Kilpatrick, D. L., Howells, R. D., Noe, M., Bailey, L. C., and Udenfriend, S. (1985). Expression of preproenkephalin-like mRNA and its peptide products in mammalian testis and ovary. *Proc Natl Acad Sci U S A* **82**, 7467-9.

Kim, H. S., Lim, W., Kim, Y. B., Kim, M. A., Park, Y. S., Park, N. H., Bazer, F. W., Song, Y. S., Han, J. Y., and Song, G. (2011). SERPINB3 in the chicken model of ovarian cancer: a novel biomarker for predicting platinum resistance and survival in patients with epithelial ovarian cancer. *The 97th Annual Congress of Korean Society of Obstetrics and Gynecology*, Seoul, Republic of Korea.

Kim, H. S., Park, N. H., Kang, S., Seo, S. S., Chung, H. H., Kim, J. W., Song, Y. S., and Kang, S. B. (2010). Comparison of the efficacy between topotecan- and belotecan-, a new camptothecin analog, based chemotherapies for recurrent epithelial ovarian cancer: a single institutional experience. *J Obstet Gynaecol Res* **36**, 86-93.

Kim, J., Song, G., Gao, H., Farmer, J. L., Satterfield, M. C., Burghardt, R. C., Wu, G., Johnson, G. A., Spencer, T. E., and Bazer, F. W. (2008). Insulin-like growth factor II activates phosphatidylinositol 3-kinase-protooncogenic protein kinase 1 and mitogen-activated protein kinase cell Signaling pathways, and stimulates migration of ovine trophectoderm cells. *Endocrinology* **149**, 3085-94.

Kim, J., Song, G., Wu, G., Gao, H., Johnson, G. A., and Bazer, F. W. (2013). Arginine, leucine, and glutamine stimulate

proliferation of porcine trophoblast cells through the MTOR-RPS6K-RPS6-EIF4EBP1 signal transduction pathway. *Biol Reprod* **88**, 113.

Kim, J. G., Vallet, J. L., and Christenson, R. K. (2001). Characterization of uterine epidermal growth factor during early pregnancy in pigs. *Domest Anim Endocrinol* **20**, 253-65.

Kim, S. S., and Seo, S. R. (2011). The Regulator of Calcineurin 1 (RCAN1/DSCR1) Activates the cAMP Response Element-binding Protein (CREB) Pathway. *J Biol Chem* **286**, 37841-8.

Kim, Y. J., Lee, G. S., Hyun, S. H., Ka, H. H., Choi, K. C., Lee, C. K., and Jeung, E. B. (2009). Uterine expression of epidermal growth factor family during the course of pregnancy in pigs. *Reprod Domest Anim* **44**, 797-804.

Klemke, R. L., Cai, S., Giannini, A. L., Gallagher, P. J., de Lanerolle, P., and Cheresch, D. A. (1997). Regulation of cell motility by mitogen-activated protein kinase. *J Cell Biol* **137**, 481-92.

Klotman, M. E., and Chang, T. L. (2006). Defensins in innate antiviral immunity. *Nat Rev Immunol* **6**, 447-56.

Knofler, M. (2010). Critical growth factors and signalling pathways controlling human trophoblast invasion. *Int J Dev Biol* **54**, 269-80.

Ko, Y., Choi, I., Green, M. L., Simmen, F. A., and Simmen, R. C. (1994). Transient expression of the cytochrome P450 aromatase gene in elongating porcine blastocysts is correlated with uterine insulin-like growth factor levels during peri-implantation development. *Mol Reprod Dev* **37**, 1-11.

Ko, Y., Lee, C. Y., Ott, T. L., Davis, M. A., Simmen, R. C., Bazer, F. W., and Simmen, F. A. (1991). Insulin-like growth factors in sheep uterine fluids: concentrations and relationship to ovine trophoblast protein-1 production during early pregnancy. *Biol Reprod* **45**, 135-42.

Kohler, P. O., Grimley, P. M., and O'Malley, B. W. (1968). Protein synthesis: differential stimulation of cell-specific proteins in epithelial cells of chick oviduct. *Science* **160**, 86-7.

Kojetin, D. J., Venters, R. A., Kordys, D. R., Thompson, R. J., Kumar, R., and Cavanagh, J. (2006). Structure, binding interface and hydrophobic transitions of Ca²⁺-loaded calbindin-D(28K). *Nat Struct Mol Biol* **13**, 641-7.

- Kol, S., Kehat, I., and Adashi, E. Y. (2002). Ovarian interleukin-1-induced gene expression: privileged genes threshold theory. *Med Hypotheses* **58**, 6-8.
- Kondoh, M., Tasaki, E., Araragi, S., Takiguchi, M., Higashimoto, M., Watanabe, Y., and Sato, M. (2002). Requirement of caspase and p38MAPK activation in zinc-induced apoptosis in human leukemia HL-60 cells. *Eur J Biochem* **269**, 6204-11.
- Krueger, U., Bergauer, T., Kaufmann, B., Wolter, I., Pilk, S., Heider-Fabian, M., Kirch, S., Artz-Oppitz, C., Isselhorst, M., and Konrad, J. (2007). Insights into effective RNAi gained from large-scale siRNA validation screening. *Oligonucleotides* **17**, 237-50.
- Krusell, J., Behr, B., Hirchenhain, J., Wen, Y., Milki, A. A., Cupisti, S., Bielfeld, P., and Polan, M. L. (2000). Expression of vascular endothelial growth factor mRNA in human preimplantation embryos derived from tripronuclear zygotes. *Fertil Steril* **74**, 1220-6.
- Kunnimalaiyaan, M., and Chen, H. (2007). Tumor suppressor role of Notch-1 signaling in neuroendocrine tumors. *Oncologist* **12**, 535-42.
- Kunnimalaiyaan, M., Vaccaro, A. M., Ndiaye, M. A., and Chen, H. (2006). Overexpression of the NOTCH1 intracellular domain inhibits cell proliferation and alters the neuroendocrine phenotype of medullary thyroid cancer cells. *J Biol Chem* **281**, 39819-30.
- Laforest, J. P., and King, G. J. (1992). Structural and functional aspects of porcine endometrial capillaries on days 13 and 15 after oestrus or mating. *J Reprod Fertil* **94**, 269-77.
- Lagger, G., Doetzlhofer, A., Schuettengruber, B., Haidweger, E., Simboeck, E., Tischler, J., Chiocca, S., Suske, G., Rotheneder, H., Wintersberger, E., and Seiser, C. (2003). The tumor suppressor p53 and histone deacetylase 1 are antagonistic regulators of the cyclin-dependent kinase inhibitor p21/WAF1/CIP1 gene. *Mol Cell Biol* **23**, 2669-79.
- Lash, G. E., Cartwright, J. E., Whitley, G. S., Trew, A. J., and Baker, P. N. (1999). The effects of angiogenic growth factors on extravillous trophoblast invasion and motility. *Placenta* **20**, 661-7.
- Lathi, R. B., Hess, A. P., Tulac, S., Nayak, N. R., Conti, M., and Giudice, L. C. (2005). Dose-dependent insulin regulation of insulin-like growth factor binding protein-1 in human endometrial stromal cells is mediated by distinct signaling pathways. *J Clin Endocrinol Metab* **90**, 1599-606.
- Lavelin, I., Meiri, N., and Pines, M. (2000). New insight in eggshell formation. *Poult Sci* **79**, 1014-7.

- Lavelin, I., Yarden, N., Ben-Bassat, S., Bar, A., and Pines, M. (1998). Regulation of osteopontin gene expression during egg shell formation in the laying hen by mechanical strain. *Matrix Biol* **17**, 615-23.
- Lawson, R. A., Parr, R. A., and Cahill, L. P. (1983). Evidence for maternal control of blastocyst growth after asynchronous transfer of embryos to the uterus of the ewe. *J Reprod Fertil* **67**, 477-83.
- Leach, R. M., Jr., Rucker, R. B., and Van Dyke, G. P. (1981). Egg shell membrane protein: a nonelastin desmosine/isodesmosine-containing protein. *Arch Biochem Biophys* **207**, 353-9.
- Lee, D. C., McKnight, G. S., and Palmiter, R. D. (1978). The action of estrogen and progesterone on the expression of the transferrin gene. A comparison of the response in chick liver and oviduct. *J Biol Chem* **253**, 3494-503.
- Lee, J. Y., Jeong, W., Lim, W., Kim, J., Bazer, F. W., Han, J. Y., and Song, G. (2012). Chicken pleiotrophin: regulation of tissue specific expression by estrogen in the oviduct and distinct expression pattern in the ovarian carcinomas. *PLoS One* **7**, e34215.
- Lee, S. I., Lee, W. K., Shin, J. H., Han, B. K., Moon, S., Cho, S., Park, T., Kim, H., and Han, J. Y. (2009). Sexually dimorphic gene expression in the chick brain before gonadal differentiation. *Poult Sci* **88**, 1003-15.
- Lefevre, F., Guillomot, M., D'Andrea, S., Battagay, S., and La Bonnardiére, C. (1998). Interferon-delta: the first member of a novel type I interferon family. *Biochimie* **80**, 779-88.
- Leggett, R. W., Armstrong, S. A., Barry, D., and Mueller, C. R. (1995). Sp1 Is Phosphorylated and Its DNA-Binding Activity down-Regulated Upon Terminal Differentiation of the Liver. *Journal of Biological Chemistry* **270**, 25879-25884.
- Leiser, R., and Kaufmann, P. (1994). Placental structure: in a comparative aspect. *Exp Clin Endocrinol* **102**, 122-34.
- Lessey, B. A. (1995). Integrins and reproduction revisited. *Eur J Obstet Gynecol Reprod Biol* **62**, 264-5.
- Lessey, B. A., Killam, A. P., Metzger, D. A., Haney, A. F., Greene, G. L., and McCarty, K. S., Jr. (1988). Immunohistochemical analysis of human uterine estrogen and progesterone receptors throughout the menstrual cycle. *J Clin Endocrinol Metab* **67**, 334-40.
- Lessey, B. A., Yeh, I., Castelbaum, A. J., Fritz, M. A., Ilesanmi, A. O., Korzeniowski, P., Sun, J., and Chwalisz, K. (1996). Endometrial progesterone receptors and markers of uterine receptivity in the window of implantation. *Fertil Steril* **65**, 477-83.
- Letcher, R., Simmen, R. C., Bazer, F. W., and Simmen, F. A. (1989). Insulin-like growth factor-I expression during early

conceptus development in the pig. *Biol Reprod* **41**, 1143-51.

Levine, A. J., Feng, Z., Mak, T. W., You, H., and Jin, S. (2006). Coordination and communication between the p53 and IGF-1-AKT-TOR signal transduction pathways. *Genes Dev* **20**, 267-75.

Li, C., and Wong, W. H. (2001). Model-based analysis of oligonucleotide arrays: expression index computation and outlier detection. *Proc Natl Acad Sci U S A* **98**, 31-6.

Li, R. H., and Zhuang, L. Z. (1997). The effects of growth factors on human normal placental cytotrophoblast cell proliferation. *Hum Reprod* **12**, 830-4.

Li, W. I., Sung, L. C., and Bazer, F. W. (1991a). Immunoreactive methionine-enkephalin secretion by porcine uterus. *Endocrinology* **128**, 21-6.

Li, W. I., Wu, H. X., and Kumar, A. M. (1991b). Synthesis and secretion of immunoreactive methionine-enkephalin from rabbit reproductive tissues in vivo and in vitro. *Biol Reprod* **45**, 691-7.

Li, Y. S., Milner, P. G., Chauhan, A. K., Watson, M. A., Hoffman, R. M., Kodner, C. M., Milbrandt, J., and Deuel, T. F. (1990). Cloning and expression of a developmentally regulated protein that induces mitogenic and neurite outgrowth activity. *Science* **250**, 1690-4.

Lim, H., Song, H., Paria, B. C., Reese, J., Das, S. K., and Dey, S. K. (2002). Molecules in blastocyst implantation: uterine and embryonic perspectives. *Vitam Horm* **64**, 43-76.

Lim, W., Ahn, S. E., Jeong, W., Kim, J. H., Kim, J., Lim, C. H., Bazer, F. W., Han, J. Y., and Song, G. (2012a). Tissue specific expression and estrogen regulation of SERPINB3 in the chicken oviduct. *Gen Comp Endocrinol* **175**, 65-73.

Lim, W., Jeong, W., Kim, J., Yoshimura, Y., Bazer, F. W., Han, J. Y., and Song, G. (2013). Expression and regulation of beta-defensin 11 in the oviduct in response to estrogen and in ovarian tumors of chickens. *Mol Cell Endocrinol* **366**, 1-8.

Lim, W., Kim, H. S., Jeong, W., Ahn, S. E., Kim, J., Kim, Y. B., Kim, M. A., Kim, M. K., Chung, H. H., Song, Y. S., Bazer, F. W., Han, J. Y., and Song, G. (2012b). SERPINB3 in the chicken model of ovarian cancer: a prognostic factor for platinum resistance and survival in patients with epithelial ovarian cancer. *PLoS One* **7**, e49869.

Lim, W., Kim, J. H., Ahn, S. E., Jeong, W., Kim, J., Bazer, F. W., Han, J. Y., and Song, G. (2011a). Avian SERPINB11 Gene:

Characteristics, Tissue-Specific Expression, and Regulation of Expression by Estrogen. *Biol Reprod*.

Lim, W., Kim, J. H., Ahn, S. E., Jeong, W., Kim, J., Park, T. S., Jang, H. J., Lee, S. I., Bazer, F. W., Han, J. Y., and Song, G.

(2011b). Avian SERPINB11 Gene: A Marker for Ovarian Cancer in Chickens. *Experimental Biology and Medicine*, (in press).

Liu, Z., and Fisher, R. A. (2004). RGS6 interacts with DMAP1 and DNMT1 and inhibits DMAP1 transcriptional repressor activity. *J Biol Chem* **279**, 14120-8.

Livak, K. J., and Schmittgen, T. D. (2001). Analysis of relative gene expression data using real-time quantitative PCR and the 2(-Delta Delta C(T)) Method. *Methods* **25**, 402-8.

Llimargas, M., and Casanova, J. (1999). EGF signalling regulates cell invagination as well as cell migration during formation of tracheal system in *Drosophila*. *Dev Genes Evol* **209**, 174-9.

Louet, J. F., LeMay, C., and Mauvais-Jarvis, F. (2004). Antidiabetic actions of estrogen: insight from human and genetic mouse models. *Curr Atheroscler Rep* **6**, 180-5.

Maden, M. (1998). The role of retinoids in developmental mechanisms in embryos. *Subcell Biochem* **30**, 81-111.

Maden, M., Sonneveld, E., van der Saag, P. T., and Gale, E. (1998). The distribution of endogenous retinoic acid in the chick embryo: implications for developmental mechanisms. *Development* **125**, 4133-44.

Maderdrut, J. L., Merchenthaler, I., Sundberg, D. K., Okado, N., and Oppenheim, R. W. (1986). Distribution and development of proenkephalin-like immunoreactivity in the lumbar spinal cord of the chicken. *Brain Res* **377**, 29-40.

Maity, B., Yang, J., Huang, J., Askeland, R. W., Bera, S., and Fisher, R. A. (2011). Regulator of G protein signaling 6 (RGS6) induces apoptosis via a mitochondrial-dependent pathway not involving its GTPase-activating protein activity. *J Biol Chem* **286**, 1409-19.

Manfredi, J. J. (2010). The Mdm2-p53 relationship evolves: Mdm2 swings both ways as an oncogene and a tumor suppressor. *Genes Dev* **24**, 1580-9.

Mao, P. L., Beauchemin, M., and Bedard, P. A. (1993). Quiescence-dependent activation of the p20K promoter in growth-arrested chicken embryo fibroblasts. *J Biol Chem* **268**, 8131-9.

Martinez-Moczygomba, M., and Huston, D. P. (2003). Biology of common beta receptor-signaling cytokines: IL-3, IL-5, and

GM-CSF. *J Allergy Clin Immunol* **112**, 653-65; quiz 666.

Mastrangelo, I. A., Courey, A. J., Wall, J. S., Jackson, S. P., and Hough, P. V. C. (1991). DNA Looping and Sp1 Multimer Links - a Mechanism for Transcriptional Synergism and Enhancement. *Proceedings of the National Academy of Sciences of the United States of America* **88**, 5670-5674.

Mattson, B. A., Overstrom, E. W., and Albertini, D. F. (1990). Transitions in trophectoderm cellular shape and cytoskeletal organization in the elongating pig blastocyst. *Biol Reprod* **42**, 195-205.

Maulik, D., Frances Evans, J., and Ragolia, L. (2006). Fetal growth restriction: pathogenic mechanisms. *Clin Obstet Gynecol* **49**, 219-27.

McCormick, C. C., and Cunningham, D. L. (1984). High dietary zinc and fasting as methods of forced resting: a performance comparison. *Poult Sci* **63**, 1201-6.

McKinnon, T., Chakraborty, C., Gleeson, L. M., Chidiac, P., and Lala, P. K. (2001). Stimulation of human extravillous trophoblast migration by IGF-II is mediated by IGF type 2 receptor involving inhibitory G protein(s) and phosphorylation of MAPK. *J Clin Endocrinol Metab* **86**, 3665-74.

McLennan, C. E., and Rydell, A. H. (1965). Extent of endometrial shedding during normal menstruation. *Obstet Gynecol* **26**, 605-21.

Meikle, A., Sahlin, L., Ferraris, A., Masironi, B., Blanc, J. E., Rodriguez-Iraozqui, M., Rodriguez-Pinon, M., Kindahl, H., and Forsberg, M. (2001). Endometrial mRNA expression of oestrogen receptor alpha, progesterone receptor and insulin-like growth factor-I (IGF-I) throughout the bovine oestrous cycle. *Anim Reprod Sci* **68**, 45-56.

Michael, D. D., Wagner, S. K., Ocon, O. M., Talbot, N. C., Rooke, J. A., and Ealy, A. D. (2006). Granulocyte-macrophage colony-stimulating-factor increases interferon-tau protein secretion in bovine trophectoderm cells. *Am J Reprod Immunol* **56**, 63-7.

Miese-Looy, G., MJ, V. D. H., Edwards, A. K., Lamarre, J., and Tayade, C. (2012). Expression of insulin-like growth factor (IGF) family members in porcine pregnancy. *J Reprod Dev* **58**, 51-60.

Milner, P. G., Li, Y. S., Hoffman, R. M., Kodner, C. M., Siegel, N. R., and Deuel, T. F. (1989). A novel 17 kD heparin-binding

growth factor (HBGF-8) in bovine uterus: purification and N-terminal amino acid sequence. *Biochem Biophys Res Commun* **165**, 1096-103.

Minami, T., Horiuchi, K., Miura, M., Abid, M. R., Takabe, W., Noguchi, N., Kohro, T., Ge, X., Aburatani, H., Hamakubo, T., Kodama, T., and Aird, W. C. (2004). Vascular endothelial growth factor- and thrombin-induced termination factor, Down syndrome critical region-1, attenuates endothelial cell proliferation and angiogenesis. *J Biol Chem* **279**, 50537-54.

Miyajima, A., Mui, A. L., Ogorochi, T., and Sakamaki, K. (1993). Receptors for granulocyte-macrophage colony-stimulating factor, interleukin-3, and interleukin-5. *Blood* **82**, 1960-74.

Modric, T., Kowalski, A. A., Green, M. L., Simmen, R. C., and Simmen, F. A. (2000). Pregnancy-dependent expression of leukaemia inhibitory factor (LIF), LIF receptor-beta and interleukin-6 (IL-6) messenger ribonucleic acids in the porcine female reproductive tract. *Placenta* **21**, 345-53.

Monroe, D. G., Berger, R. R., and Sanders, M. M. (2002). Tissue-protective effects of estrogen involve regulation of caspase gene expression. *Mol Endocrinol* **16**, 1322-31.

Monroe, D. G., Jin, D. F., and Sanders, M. M. (2000). Estrogen opposes the apoptotic effects of bone morphogenetic protein 7 on tissue remodeling. *Mol Cell Biol* **20**, 4626-34.

Monstein, H. J., Grahn, N., and Ohlsson, B. (2006). Proenkephalin-A mRNA is widely expressed in tissues of the human gastrointestinal tract. *Eur Surg Res* **38**, 464-8.

Moore, M. A., Gotoh, Y., Rafidi, K., and Gerstenfeld, L. C. (1991). Characterization of a cDNA for chicken osteopontin: expression during bone development, osteoblast differentiation, and tissue distribution. *Biochemistry* **30**, 2501-8.

Moore, R. W., Park, S. Y., Kubena, L. F., Byrd, J. A., McReynolds, J. L., Burnham, M. R., Hume, M. E., Birkhold, S. G., Nisbet, D. J., and Ricke, S. C. (2004). Comparison of zinc acetate and propionate addition on gastrointestinal tract fermentation and susceptibility of laying hens to *Salmonella enteritidis* during forced molt. *Poult Sci* **83**, 1276-86.

Mrosovsky, N., and Sherry, D. F. (1980). Animal anorexias. *Science* **207**, 837-42.

Mukku, V. R., and Stancel, G. M. (1985). Regulation of epidermal growth factor receptor by estrogen. *J Biol Chem* **260**, 9820-4.

- Munro, S. S., and Kosin, T. L. (1943). Dramatic response of the chick oviduct to estrogen. *Poultry Science* **22** 330–331.
- Muramatsu, T. (2002). Midkine and pleiotrophin: two related proteins involved in development, survival, inflammation and tumorigenesis. *J Biochem* **132**, 359-71.
- Murdoch, W. J., Van Kirk, E. A., and Alexander, B. M. (2005). DNA damages in ovarian surface epithelial cells of ovulatory hens. *Exp Biol Med (Maywood)* **230**, 429-33.
- Musunuru, K., Pirruccello, J. P., Do, R., Peloso, G. M., Guiducci, C., Sougnez, C., Garimella, K. V., Fisher, S., Abreu, J., Barry, A. J., Fennell, T., Banks, E., Ambrogio, L., Cibulskis, K., Kemytsky, A., Gonzalez, E., Rudzicz, N., Engert, J. C., DePristo, M. A., Daly, M. J., Cohen, J. C., Hobbs, H. H., Altshuler, D., Schonfeld, G., Gabriel, S. B., Yue, P., and Kathiresan, S. (2010). Exome sequencing, ANGPTL3 mutations, and familial combined hypolipidemia. *N Engl J Med* **363**, 2220-7.
- Nara, B. S., Darmadja, D., and First, N. L. (1981). Effect of removal of follicles, corpora lutea or ovaries on maintenance of pregnancy in swine. *J Anim Sci* **52**, 794-801.
- Nelson, K. G., Takahashi, T., Bossert, N. L., Walmer, D. K., and McLachlan, J. A. (1991). Epidermal growth factor replaces estrogen in the stimulation of female genital-tract growth and differentiation. *Proc Natl Acad Sci U S A* **88**, 21-5.
- Noda, M., Teranishi, Y., Takahashi, H., Toyosato, M., Notake, M., Nakanishi, S., and Numa, S. (1982). Isolation and structural organization of the human preproenkephalin gene. *Nature* **297**, 431-4.
- Nys, Y., Mayel-Afshar, S., Bouillon, R., Van Baelen, H., and Lawson, D. E. (1989). Increases in calbindin D 28K mRNA in the uterus of the domestic fowl induced by sexual maturity and shell formation. *Gen Comp Endocrinol* **76**, 322-9.
- O'Leary, S., Jasper, M. J., Warnes, G. M., Armstrong, D. T., and Robertson, S. A. (2004). Seminal plasma regulates endometrial cytokine expression, leukocyte recruitment and embryo development in the pig. *Reproduction* **128**, 237-47.
- Obermajer, N., Jevnikar, Z., Doljak, B., and Kos, J. (2008). Role of cysteine cathepsins in matrix degradation and cell signalling. *Connect Tissue Res* **49**, 193-6.
- Okada, A., Sato, T., Ohta, Y., and Iguchi, T. (2005). Sex steroid hormone receptors in the developing female reproductive tract of laboratory rodents. *J Toxicol Sci* **30**, 75-89.

Oldberg, A., Franzen, A., and Heinegard, D. (1986). Cloning and sequence analysis of rat bone sialoprotein (osteopontin) cDNA reveals an Arg-Gly-Asp cell-binding sequence. *Proc Natl Acad Sci U S A* **83**, 8819-23.

Olofsson, B. A., Kelly, C. M., Kim, J., Hornsby, S. M., and Azizkhan-Clifford, J. (2007). Phosphorylation of Sp1 in response to DNA damage by ataxia telangiectasia-mutated kinase. *Molecular Cancer Research* **5**, 1319-1330.

Oxender, W. D., Hafs, H. D., and Ederton, L. A. (1972). Serum growth hormone, LH and prolactin in the pregnant cow. *J Anim Sci* **35**, 51-5.

Pageaux, J. F., Laugier, C., Pal, D., D'Almeida, M. A., Sandoz, D., and Pacheco, H. (1986). Magnum morphogenesis during the natural development of the quail oviduct: analysis of egg white proteins and progesterone receptor concentration. *Biol Reprod* **35**, 657-66.

Palmiter, R. D., and Wrenn, J. T. (1971a). Interaction of Estrogen and Progesterone in Chick Oviduct Development .3. Tubular Gland Cell Cytodifferentiation. *Journal of Cell Biology* **50**, 598-&.

Palmiter, R. D., and Wrenn, J. T. (1971b). Interaction of estrogen and progesterone in chick oviduct development. 3. Tubular gland cell cytodifferentiation. *J Cell Biol* **50**, 598-615.

Panici, P. B., Maggioni, A., Hacker, N., Landoni, F., Ackermann, S., Campagnutta, E., Tamussino, K., Winter, R., Pellegrino, A., Greggi, S., Angioli, R., Mancini, N., Scambia, G., Dell'Anna, T., Fossati, R., Floriani, I., Rossi, R. S., Grassi, R., Favalli, G., Raspagliesi, F., Giannarelli, D., Martella, L., and Mangioni, C. (2005). Systematic aortic and pelvic lymphadenectomy versus resection of bulky nodes only in optimally debulked advanced ovarian cancer: a randomized clinical trial. *J Natl Cancer Inst* **97**, 560-6.

Paria, B. C., Huet-Hudson, Y. M., and Dey, S. K. (1993). Blastocyst's state of activity determines the "window" of implantation in the receptive mouse uterus. *Proc Natl Acad Sci U S A* **90**, 10159-62.

Park, S. Y., Birkhold, S. G., Kubena, L. F., Nisbet, D. J., and Ricke, S. C. (2004). Effects of high zinc diets using zinc propionate on molt induction, organs, and postmolt egg production and quality in laying hens. *Poultry Science* **83**, 24-33.

Pedersen, P. H., Ness, G. O., Engebraaten, O., Bjerkvig, R., Lillehaug, J. R., and Laerum, O. D. (1994). Heterogeneous response to the growth factors [EGF, PDGF (bb), TGF-alpha, bFGF, IL-2] on glioma spheroid growth, migration and invasion. *Int J Cancer* **56**, 255-61.

- Perry, J. S. (1981). The mammalian fetal membranes. *J Reprod Fertil* **62**, 321-35.
- Perry, J. S., Heap, R. B., and Amoroso, E. C. (1973). Steroid hormone production by pig blastocysts. *Nature* **245**, 45-7.
- Perry, J. S., Heap, R. B., Burton, R. D., and Gadsby, J. E. (1976). Endocrinology of the blastocyst and its role in the establishment of pregnancy. *J Reprod Fertil Suppl*, 85-104.
- Persson, E., Sahlin, L., Masironi, B., Dantzer, V., Eriksson, H., and Rodriguez-Martinez, H. (1997). Insulin-like growth factor-I in the porcine endometrium and placenta: localization and concentration in relation to steroid influence during early pregnancy. *Anim Reprod Sci* **46**, 261-81.
- Peterson, R. T., and Schreiber, S. L. (1998). Translation control: connecting mitogens and the ribosome. *Curr Biol* **8**, R248-50.
- Petraglia, F., Segre, A., Facchinetti, F., Campanini, D., Ruspa, M., and Genazzani, A. R. (1985). Beta-endorphin and met-enkephalin in peritoneal and ovarian follicular fluids of fertile and postmenopausal women. *Fertil Steril* **44**, 615-21.
- Pharriss, B. B., Tillson, S. A., and Erickson, R. R. (1972). Prostaglandins in luteal function. *Recent Prog Horm Res* **28**, 51-89.
- Pines, M., Knopov, V., and Bar, A. (1995). Involvement of osteopontin in egg shell formation in the laying chicken. *Matrix Biol* **14**, 765-71.
- Polge, C., Rowson, L. E., and Chang, M. C. (1966). The effect of reducing the number of embryos during early stages of gestation on the maintenance of pregnancy in the pig. *J Reprod Fertil* **12**, 395-7.
- Pollard, J. W. (1997). Role of colony-stimulating factor-1 in reproduction and development. *Mol Reprod Dev* **46**, 54-60; discussion 60-1.
- Poltorak, Z., Cohen, T., Sivan, R., Kandelis, Y., Spira, G., Vlodavsky, I., Keshet, E., and Neufeld, G. (1997). VEGF145, a secreted vascular endothelial growth factor isoform that binds to extracellular matrix. *J Biol Chem* **272**, 7151-8.
- Ponka, P., Beaumont, C., and Richardson, D. R. (1998). Function and regulation of transferrin and ferritin. *Seminars in Hematology* **35**, 35-54.
- Ponnampalam, A. P., Weston, G. C., Trajstman, A. C., Susil, B., and Rogers, P. A. (2004). Molecular classification of human endometrial cycle stages by transcriptional profiling. *Mol Hum Reprod* **10**, 879-93.

- Pope, W. F. (1988). Uterine asynchrony: a cause of embryonic loss. *Biol Reprod* **39**, 999-1003.
- Pope, W. F., Lawyer, M. S., Nara, B. S., and First, N. L. (1986). Effect of asynchronous superinduction on embryo survival and range of blastocyst development in swine. *Biol Reprod* **35**, 133-7.
- Pope, W. F., Xie, S., Broermann, D. M., and Nephew, K. P. (1990). Causes and consequences of early embryonic diversity in pigs. *J Reprod Fertil Suppl* **40**, 251-60.
- Psychoyos, A. (1973). Hormonal control of ovoimplantation. *Vitam Horm* **31**, 201-56.
- Pusateri, A. E., Rothschild, M. F., Warner, C. M., and Ford, S. P. (1990). Changes in morphology, cell number, cell size and cellular estrogen content of individual littermate pig conceptuses on days 9 to 13 of gestation. *J Anim Sci* **68**, 3727-35.
- Qiu, Q., Yang, M., Tsang, B. K., and Gruslin, A. (2004a). Both mitogen-activated protein kinase and phosphatidylinositol 3-kinase signalling are required in epidermal growth factor-induced human trophoblast migration. *Mol Hum Reprod* **10**, 677-84.
- Qiu, Q., Yang, M., Tsang, B. K., and Gruslin, A. (2004b). EGF-induced trophoblast secretion of MMP-9 and TIMP-1 involves activation of both PI3K and MAPK signalling pathways. *Reproduction* **128**, 355-63.
- Rabbani, M. L., and Rogers, P. A. (2001). Role of vascular endothelial growth factor in endometrial vascular events before implantation in rats. *Reproduction* **122**, 85-90.
- Rafidi, K., Simkina, I., Johnson, E., Moore, M. A., and Gerstenfeld, L. C. (1994). Characterization of the chicken osteopontin-encoding gene. *Gene* **140**, 163-9.
- Rapoport, A. P., Abboud, C. N., and DiPersio, J. F. (1992). Granulocyte-macrophage colony-stimulating factor (GM-CSF) and granulocyte colony-stimulating factor (G-CSF): receptor biology, signal transduction, and neutrophil activation. *Blood Rev* **6**, 43-57.
- Raulais, D., Lagente-Chevallier, O., Guettet, C., Duprez, D., Courtois, Y., and Vigny, M. (1991). A new heparin binding protein regulated by retinoic acid from chick embryo. *Biochem Biophys Res Commun* **174**, 708-15.
- Rechler, M. M., and Nissley, S. P. (1985). The nature and regulation of the receptors for insulin-like growth factors. *Annu Rev Physiol* **47**, 425-42.
- Reedijk, M., Odorcic, S., Chang, L., Zhang, H., Miller, N., McCready, D. R., Lockwood, G., and Egan, S. E. (2005). High-level

coexpression of JAG1 and NOTCH1 is observed in human breast cancer and is associated with poor overall survival. *Cancer Res* **65**, 8530-7.

Reima, I., Lehtonen, E., Virtanen, I., and Flechon, J. E. (1993). The cytoskeleton and associated proteins during cleavage, compaction and blastocyst differentiation in the pig. *Differentiation* **54**, 35-45.

Reynolds, L. P., Kirsch, J. D., Kraft, K. C., and Redmer, D. A. (1998). Time-course of the uterine response to estradiol-17beta in ovariectomized ewes: expression of angiogenic factors. *Biol Reprod* **59**, 613-20.

Reynolds, L. P., and Redmer, D. A. (2001). Angiogenesis in the placenta. *Biol Reprod* **64**, 1033-40.

Reynolds, T. S., Stevenson, K. R., and Wathes, D. C. (1997). Pregnancy-specific alterations in the expression of the insulin-like growth factor system during early placental development in the ewe. *Endocrinology* **138**, 886-97.

Robertson, H. A., and King, G. J. (1974). Plasma concentrations of progesterone, oestrone, oestradiol-17beta and of oestrone sulphate in the pig at implantation, during pregnancy and at parturition. *J Reprod Fertil* **40**, 133-41.

Robertson, S. A. (2007). GM-CSF regulation of embryo development and pregnancy. *Cytokine Growth Factor Rev* **18**, 287-98.

Robertson, S. A., Mayrhofer, G., and Seamark, R. F. (1992). Uterine epithelial cells synthesize granulocyte-macrophage colony-stimulating factor and interleukin-6 in pregnant and nonpregnant mice. *Biol Reprod* **46**, 1069-79.

Robertson, S. A., Mayrhofer, G., and Seamark, R. F. (1996). Ovarian steroid hormones regulate granulocyte-macrophage colony-stimulating factor synthesis by uterine epithelial cells in the mouse. *Biol Reprod* **54**, 183-96.

Robertson, S. A., Roberts, C. T., Farr, K. L., Dunn, A. R., and Seamark, R. F. (1999). Fertility impairment in granulocyte-macrophage colony-stimulating factor-deficient mice. *Biol Reprod* **60**, 251-61.

Robertson, S. A., Seamark, R. F., Guilbert, L. J., and Wegmann, T. G. (1994). The role of cytokines in gestation. *Crit Rev Immunol* **14**, 239-92.

Robertson, S. A., Sjoblom, C., Jasper, M. J., Norman, R. J., and Seamark, R. F. (2001). Granulocyte-macrophage colony-stimulating factor promotes glucose transport and blastomere viability in murine preimplantation embryos. *Biol Reprod* **64**, 1206-15.

Robinson, C. J., and Stringer, S. E. (2001). The splice variants of vascular endothelial growth factor (VEGF) and their receptors.

J Cell Sci **114**, 853-65.

Robinson, R. S., Mann, G. E., Gadd, T. S., Lamming, G. E., and Wathes, D. C. (2000). The expression of the IGF system in the bovine uterus throughout the oestrous cycle and early pregnancy. *J Endocrinol* **165**, 231-43.

Rodriguez-Burford, C., Barnes, M. N., Berry, W., Partridge, E. E., and Grizzle, W. E. (2001). Immunohistochemical expression of molecular markers in an avian model: a potential model for preclinical evaluation of agents for ovarian cancer chemoprevention. *Gynecol Oncol* **81**, 373-9.

Ross, J. W., Malayer, J. R., Ritchey, J. W., and Geisert, R. D. (2003). Characterization of the interleukin-1beta system during porcine trophoblastic elongation and early placental attachment. *Biol Reprod* **69**, 1251-9.

Rothermel, B. A., McKinsey, T. A., Vega, R. B., Nicol, R. L., Mammen, P., Yang, J., Antos, C. L., Shelton, J. M., Bassel-Duby, R., Olson, E. N., and Williams, R. S. (2001). Myocyte-enriched calcineurin-interacting protein, MCIP1, inhibits cardiac hypertrophy in vivo. *Proc Natl Acad Sci U S A* **98**, 3328-33.

Rousseau, S., Houle, F., and Huot, J. (2000). Integrating the VEGF signals leading to actin-based motility in vascular endothelial cells. *Trends Cardiovasc Med* **10**, 321-7.

Ruszler, P. L. (1998). Health and husbandry considerations of induced molting. *Poult Sci* **77**, 1789-93.

Saffer, J. D., Jackson, S. P., and Annarella, M. B. (1991). Developmental Expression of Sp1 in the Mouse. *Molecular and Cellular Biology* **11**, 2189-2199.

Saftig, P., Hunziker, E., Wehmeyer, O., Jones, S., Boyde, A., Rommerskirch, W., Moritz, J. D., Schu, P., and von Figura, K. (1998). Impaired osteoclastic bone resorption leads to osteopetrosis in cathepsin-K-deficient mice. *Proc Natl Acad Sci U S A* **95**, 13453-8.

Sahlin, L., Rodriguez-Martinez, H., Stanchev, P., Dalin, A. M., Norstedt, G., and Eriksson, H. (1990). Regulation of the uterine expression of messenger ribonucleic acids encoding the oestrogen receptor and IGF-I peptides in the pig uterus. *Zentralbl Veterinarmed A* **37**, 795-800.

Saitou, N., and Nei, M. (1987). The neighbor-joining method: a new method for reconstructing phylogenetic trees. *Molecular Biology and Evolution* **4**, 406-25.

- Sakai, Y., Meno, C., Fujii, H., Nishino, J., Shiratori, H., Saijoh, Y., Rossant, J., and Hamada, H. (2001). The retinoic acid-inactivating enzyme CYP26 is essential for establishing an uneven distribution of retinoic acid along the antero-posterior axis within the mouse embryo. *Genes Dev* **15**, 213-25.
- Sanders, M. M., and McKnight, G. S. (1988). Positive and negative regulatory elements control the steroid-responsive ovalbumin promoter. *Biochemistry* **27**, 6550-7.
- Schafer-Somi, S. (2003). Cytokines during early pregnancy of mammals: a review. *Anim Reprod Sci* **75**, 73-94.
- Schindler, C., and Darnell, J. E., Jr. (1995). Transcriptional responses to polypeptide ligands: the JAK-STAT pathway. *Annu Rev Biochem* **64**, 621-51.
- Schrick, F. N., Surface, R. A., Pritchard, J. Y., Dailey, R. A., Townsend, E. C., and Inskeep, E. K. (1993). Ovarian structures during the estrous cycle and early pregnancy in ewes. *Biol Reprod* **49**, 1133-40.
- Schultz, G. A., and Heyner, S. (1993). Growth factors in preimplantation mammalian embryos. *Oxf Rev Reprod Biol* **15**, 43-81.
- Scott JT, C. C. (1976). The use of zinc as an effective molting agent in laying hens. *Poult Sci* **55**, 2089.
- Seger, R., and Krebs, E. G. (1995). The MAPK signaling cascade. *FASEB J* **9**, 726-35.
- Seo, H. W., Park, J. Y., Lee, H. C., Kim, D., Song, Y. S., Lim, J. M., Song, G., and Han, J. Y. (2009). Physiological Effects of Diethylstilbestrol Exposure on the Development of the Chicken Oviduct. *J Anim Sci & Technol* **51**, 485-492.
- Shepherd, T. G., Theriault, B. L., Campbell, E. J., and Nachtigal, M. W. (2006). Primary culture of ovarian surface epithelial cells and ascites-derived ovarian cancer cells from patients. *Nat Protoc* **1**, 2643-9.
- Sherr, C. J., and Roberts, J. M. (1999). CDK inhibitors: positive and negative regulators of G(1)-phase progression. *Genes & Development* **13**, 1501-1512.
- Shi, G. P., Villadangos, J. A., Dranoff, G., Small, C., Gu, L., Haley, K. J., Riese, R., Ploegh, H. L., and Chapman, H. A. (1999). Cathepsin S required for normal MHC class II peptide loading and germinal center development. *Immunity* **10**, 197-206.
- Shifren, J. L., Tseng, J. F., Zaloudek, C. J., Ryan, I. P., Meng, Y. G., Ferrara, N., Jaffe, R. B., and Taylor, R. N. (1996). Ovarian steroid regulation of vascular endothelial growth factor in the human endometrium: implications for angiogenesis during the menstrual

cycle and in the pathogenesis of endometriosis. *J Clin Endocrinol Metab* **81**, 3112-8.

Shippee RL, S. P., Koehn U, Lambert JL, Simmons RW (1979). High dietary zinc or magnesium as forced-resting agents for laying hens. *Poult Sci* **58**, 949-954.

Shiraishi, S., Nakagawa, K., Kinukawa, N., Nakano, H., and Sueishi, K. (1996). Immunohistochemical localization of vascular endothelial growth factor in the human placenta. *Placenta* **17**, 111-21.

Silphaduang, U., Hincke, M. T., Nys, Y., and Mine, Y. (2006). Antimicrobial proteins in chicken reproductive system. *Biochemical and Biophysical Research Communications* **340**, 648-655.

Simmen, F. A., and Simmen, R. C. (1991). Peptide growth factors and proto-oncogenes in mammalian conceptus development. *Biol Reprod* **44**, 1-5.

Simmen, F. A., Simmen, R. C., Geisert, R. D., Martinat-Butte, F., Bazer, F. W., and Terqui, M. (1992). Differential expression, during the estrous cycle and pre- and postimplantation conceptus development, of messenger ribonucleic acids encoding components of the pig uterine insulin-like growth factor system. *Endocrinology* **130**, 1547-56.

Simmen, R. C., Simmen, F. A., Hofig, A., Farmer, S. J., and Bazer, F. W. (1990). Hormonal regulation of insulin-like growth factor gene expression in pig uterus. *Endocrinology* **127**, 2166-74.

Sjoblom, C., Roberts, C. T., Wikland, M., and Robertson, S. A. (2005). Granulocyte-macrophage colony-stimulating factor alleviates adverse consequences of embryo culture on fetal growth trajectory and placental morphogenesis. *Endocrinology* **146**, 2142-53.

Sjoblom, C., Wikland, M., and Robertson, S. A. (1999). Granulocyte-macrophage colony-stimulating factor promotes human blastocyst development in vitro. *Hum Reprod* **14**, 3069-76.

Sjoblom, C., Wikland, M., and Robertson, S. A. (2002). Granulocyte-macrophage colony-stimulating factor (GM-CSF) acts independently of the beta common subunit of the GM-CSF receptor to prevent inner cell mass apoptosis in human embryos. *Biol Reprod* **67**, 1817-23.

Sjolund, J., Johansson, M., Manna, S., Norin, C., Pietras, A., Beckman, S., Nilsson, E., Ljungberg, B., and Axelson, H. (2008). Suppression of renal cell carcinoma growth by inhibition of Notch signaling in vitro and in vivo. *J Clin Invest* **118**, 217-28.

- Slayden, O. D., and Brenner, R. M. (2004). Hormonal regulation and localization of estrogen, progesterin and androgen receptors in the endometrium of nonhuman primates: effects of progesterone receptor antagonists. *Arch Histol Cytol* **67**, 393-409.
- Slowey, M. J., Verhage, H. G., and Fazleabas, A. T. (1994). Epidermal growth factor, transforming growth factor-alpha, and epidermal growth factor receptor localization in the baboon (*Papio anubis*) uterus during the menstrual cycle and early pregnancy. *J Soc Gynecol Investig* **1**, 277-84.
- Smith, G. C., Crossley, J. A., Aitken, D. A., Jenkins, N., Lyall, F., Cameron, A. D., Connor, J. M., and Dobbie, R. (2007). Circulating angiogenic factors in early pregnancy and the risk of preeclampsia, intrauterine growth restriction, spontaneous preterm birth, and stillbirth. *Obstet Gynecol* **109**, 1316-24.
- Smith, K., LeJeune, S., Harris, A. H., and Rees, M. C. (1991). Epidermal growth factor receptor in human uterine tissues. *Hum Reprod* **6**, 619-22.
- Socher, S. H., and Omalley, B. W. (1973). Estrogen-Mediated Cell-Proliferation during Chick Oviduct Development and Its Modulation by Progesterone. *Developmental Biology* **30**, 411-417.
- Sodek, J., Ganss, B., and McKee, M. D. (2000). Osteopontin. *Crit Rev Oral Biol Med* **11**, 279-303.
- Song, G., Bazer, F. W., and Spencer, T. E. (2007a). Differential expression of cathepsins and cystatin C in ovine uteroplacental tissues. *Placenta* **28**, 1091-8.
- Song, G., Bazer, F. W., and Spencer, T. E. (2007b). Pregnancy and interferon tau regulate RSAD2 and IFIH1 expression in the ovine uterus. *Reproduction* **133**, 285-95.
- Song, G., Fleming, J. A., Kim, J., Spencer, T. E., and Bazer, F. W. (2011a). Pregnancy and interferon tau regulate DDX58 and PLSCR1 in the ovine uterus during the peri-implantation period. *Reproduction* **141**, 127-38.
- Song, G., Seo, H. W., Choi, J. W., Rengaraj, D., Kim, T. M., Lee, B. R., Kim, Y. M., Yun, T. W., Jeong, J. W., and Han, J. Y. (2011b). Discovery of candidate genes and pathways regulating oviduct development in chickens. *Biol Reprod* **85**, 306-14.
- Song, G., Seo, H. W., Choi, J. W., Rengaraj, D., Kim, T. M., Lee, B. R., Kim, Y. M., Yun, T. W., Jeong, J. W., and Han, J. Y. (2011c). Discovery of Candidate Genes and Pathways Regulating Oviduct Development in Chickens. *Biol. Reprod* (**in press**).

- Song, G., Spencer, T. E., and Bazer, F. W. (2006). Progesterone and interferon-tau regulate cystatin C in the endometrium. *Endocrinology* **147**, 3478-83.
- Spandorfer, S. D., Barmat, L. I., Liu, H. C., Mele, C., Veeck, L., and Rosenwaks, Z. (1998). Granulocyte macrophage-colony stimulating factor production by autologous endometrial co-culture is associated with outcome for in vitro fertilization patients with a history of multiple implantation failures. *Am J Reprod Immunol* **40**, 377-81.
- Spencer, T. E., and Bazer, F. W. (1995). Temporal and spatial alterations in uterine estrogen receptor and progesterone receptor gene expression during the estrous cycle and early pregnancy in the ewe. *Biol Reprod* **53**, 1527-43.
- Spencer, T. E., and Bazer, F. W. (2004a). Conceptus signals for establishment and maintenance of pregnancy. *Reprod Biol Endocrinol* **2**, 49.
- Spencer, T. E., and Bazer, F. W. (2004b). Uterine and placental factors regulating conceptus growth in domestic animals. *J Anim Sci* **82 E-Suppl**, E4-13.
- Spencer, T. E., Johnson, G. A., Bazer, F. W., and Burghardt, R. C. (2007a). Fetal-maternal interactions during the establishment of pregnancy in ruminants. *Soc Reprod Fertil Suppl* **64**, 379-96.
- Spencer, T. E., Johnson, G. A., Bazer, F. W., Burghardt, R. C., and Palmarini, M. (2007b). Pregnancy recognition and conceptus implantation in domestic ruminants: roles of progesterone, interferons and endogenous retroviruses. *Reprod Fertil Dev* **19**, 65-78.
- Squires, M. S., Hudson, E. A., Howells, L., Sale, S., Houghton, C. E., Jones, J. L., Fox, L. H., Dickens, M., Prigent, S. A., and Manson, M. M. (2003). Relevance of mitogen activated protein kinase (MAPK) and phosphatidylinositol-3-kinase/protein kinase B (PI3K/PKB) pathways to induction of apoptosis by curcumin in breast cells. *Biochem Pharmacol* **65**, 361-76.
- Stammer, K., Edassery, S. L., Barua, A., Bitterman, P., Bahr, J. M., Hales, D. B., and Luborsky, J. L. (2008). Selenium-Binding Protein 1 expression in ovaries and ovarian tumors in the laying hen, a spontaneous model of human ovarian cancer. *Gynecol Oncol* **109**, 115-21.
- Stavri, G. T., Hong, Y., Zachary, I. C., Breier, G., Baskerville, P. A., Yla-Herttuala, S., Risau, W., Martin, J. F., and Erusalimsky, J. D. (1995). Hypoxia and platelet-derived growth factor-BB synergistically upregulate the expression of vascular endothelial growth

factor in vascular smooth muscle cells. *FEBS Lett* **358**, 311-5.

Stewart, C. L., and Cullinan, E. B. (1997). Preimplantation development of the mammalian embryo and its regulation by growth factors. *Dev Genet* **21**, 91-101.

Streb, H., Irvine, R. F., Berridge, M. J., and Schulz, I. (1983). Release of Ca²⁺ from a nonmitochondrial intracellular store in pancreatic acinar cells by inositol-1,4,5-trisphosphate. *Nature* **306**, 67-9.

Stroband, H. W., and Van der Lende, T. (1990). Embryonic and uterine development during early pregnancy in pigs. *J Reprod Fertil Suppl* **40**, 261-77.

Su, W., Jackson, S., Tjian, R., and Echols, H. (1991). DNA Looping between Sites for Transcriptional Activation - Self-Association of DNA-Bound Sp1. *Genes & Development* **5**, 820-826.

Stugno, N., Kashida, S., Karube-Harada, A., Takiguchi, S., and Kato, H. (2002). Expression of vascular endothelial growth factor (VEGF) and its receptors in human endometrium throughout the menstrual cycle and in early pregnancy. *Reproduction* **123**, 379-87.

Suh, D. H., Kim, J. W., Kim, K., and Kang, S. B. (2010). Major clinical research advances in gynecologic cancer in 2010. *J Gynecol Oncol* **21**, 209-18.

Sundaresan, N. R., Anish, D., Sastry, K. V., Saxena, V. K., Nagarajan, K., Subramani, J., Leo, M. D., Shit, N., Mohan, J., Saxena, M., and Ahmed, K. A. (2008). High doses of dietary zinc induce cytokines, chemokines, and apoptosis in reproductive tissues during regression. *Cell Tissue Res* **332**, 543-54.

Surveyor, G. A., Gendler, S. J., Pemberton, L., Das, S. K., Chakraborty, I., Julian, J., Pimental, R. A., Wegner, C. C., Dey, S. K., and Carson, D. D. (1995). Expression and steroid hormonal control of Muc-1 in the mouse uterus. *Endocrinology* **136**, 3639-47.

Tabata, C., Ogita, K., Sato, K., Nakamura, H., Qing, Z., Negoro, H., Kumasawa, K., Temma-Asano, K., Tsutsui, T., Nishimori, K., and Kimura, T. (2009). Calcineurin/NFAT pathway: a novel regulator of parturition. *Am J Reprod Immunol* **62**, 44-50.

Takeda, K., Noguchi, K., Shi, W., Tanaka, T., Matsumoto, M., Yoshida, N., Kishimoto, T., and Akira, S. (1997). Targeted disruption of the mouse Stat3 gene leads to early embryonic lethality. *Proc Natl Acad Sci U S A* **94**, 3801-4.

Telford, N. A., Watson, A. J., and Schultz, G. A. (1990). Transition from maternal to embryonic control in early mammalian

development: a comparison of several species. *Mol Reprod Dev* **26**, 90-100.

Thiery, J. P., Acloque, H., Huang, R. Y., and Nieto, M. A. (2009). Epithelial-mesenchymal transitions in development and disease. *Cell* **139**, 871-90.

Thomas, C. Y., Chouinard, M., Cox, M., Parsons, S., Stallings-Mann, M., Garcia, R., Jove, R., and Wharen, R. (2003). Spontaneous activation and signaling by overexpressed epidermal growth factor receptors in glioblastoma cells. *Int J Cancer* **104**, 19-27.

Tomanek, M., Kopecny, V., and Kanka, J. (1989). Genome reactivation in developing early pig embryos: an ultrastructural and autoradiographic analysis. *Anat Embryol (Berl)* **180**, 309-16.

Torry, D. S., and Torry, R. J. (1997). Angiogenesis and the expression of vascular endothelial growth factor in endometrium and placenta. *Am J Reprod Immunol* **37**, 21-9.

Tortorella, C., Simone, O., Piazzolla, G., Stella, I., Cappiello, V., and Antonaci, S. (2006). Role of phosphoinositide 3-kinase and extracellular signal-regulated kinase pathways in granulocyte macrophage-colony-stimulating factor failure to delay fas-induced neutrophil apoptosis in elderly humans. *J Gerontol A Biol Sci Med Sci* **61**, 1111-8.

Toyofuku, A., Hara, T., Taguchi, T., Katsura, Y., Ohama, K., and Kudo, Y. (2006). Cyclic and characteristic expression of phosphorylated Akt in human endometrium and decidual cells in vivo and in vitro. *Hum Reprod* **21**, 1122-8.

Tranguch, S., Daikoku, T., Guo, Y., Wang, H., and Dey, S. K. (2005). Molecular complexity in establishing uterine receptivity and implantation. *Cell Mol Life Sci* **62**, 1964-73.

Tremellen, K. P., Seamark, R. F., and Robertson, S. A. (1998). Seminal transforming growth factor beta1 stimulates granulocyte-macrophage colony-stimulating factor production and inflammatory cell recruitment in the murine uterus. *Biol Reprod* **58**, 1217-25.

Tuo, W., Harney, J. P., and Bazer, F. W. (1995). Colony-stimulating factor-1 in conceptus and uterine tissues in pigs. *Biol Reprod* **53**, 133-42.

Tuo, W., Harney, J. P., and Bazer, F. W. (1996). Developmentally regulated expression of interleukin-1 beta by peri-implantation conceptuses in swine. *J Reprod Immunol* **31**, 185-98.

Turk, V., Turk, B., and Turk, D. (2001). Lysosomal cysteine proteases: facts and opportunities. *EMBO J* **20**, 4629-33.

- Turner, M. A., Yang, X., Yin, D., Kuczera, K., Borchardt, R. T., and Howell, P. L. (2000). Structure and function of S-adenosylhomocysteine hydrolase. *Cell Biochem Biophys* **33**, 101-25.
- Urick, M. E., and Johnson, P. A. (2006). Cyclooxygenase 1 and 2 mRNA and protein expression in the Gallus domesticus model of ovarian cancer. *Gynecol Oncol* **103**, 673-8.
- Vanderhyden, B. C., Shaw, T. J., and Ethier, J. F. (2003). Animal models of ovarian cancer. *Reprod Biol Endocrinol* **1**, 67.
- Vaughan, T. J., James, P. S., Pascall, J. C., and Brown, K. D. (1992a). Expression of the genes for TGF alpha, EGF and the EGF receptor during early pig development. *Development* **116**, 663-9.
- Vaughan, T. J., Littlewood, C. J., Pascall, J. C., and Brown, K. D. (1992b). Epidermal growth factor concentrations in pig tissues and body fluids measured using a homologous radioimmunoassay. *J Endocrinol* **135**, 77-83.
- Vigny, M., Raulais, D., Puzenat, N., Duprez, D., Hartmann, M. P., Jeanny, J. C., and Courtois, Y. (1989). Identification of a new heparin-binding protein localized within chick basement membranes. *Eur J Biochem* **186**, 733-40.
- Waltenberger, J., Claesson-Welsh, L., Siegbahn, A., Shibuya, M., and Heldin, C. H. (1994). Different signal transduction properties of KDR and Flt1, two receptors for vascular endothelial growth factor. *J Biol Chem* **269**, 26988-95.
- Wang, H., and Dey, S. K. (2006). Roadmap to embryo implantation: clues from mouse models. *Nat Rev Genet* **7**, 185-99.
- Wang, X., Ford, B. C., Praul, C. A., and Leach, R. M., Jr. (2002). Collagen X expression in oviduct tissue during the different stages of the egg laying cycle. *Poult Sci* **81**, 805-8.
- Wang, Y., Wang, F., Sun, T., Trostinskaia, A., Wygle, D., Puscheck, E., and Rappolee, D. A. (2004a). Entire mitogen activated protein kinase (MAPK) pathway is present in preimplantation mouse embryos. *Dev Dyn* **231**, 72-87.
- Wang, Y., Wang, F., Sun, T., Trostinskaia, A., Wygle, D., Puscheck, E., and Rappolee, D. A. (2004b). Entire mitogen activated protein kinase (MAPK) pathway is present in preimplantation mouse embryos. *Developmental dynamics : an official publication of the American Association of Anatomists* **231**, 72-87.
- Wang, Z., Zhang, Y., Li, Y., Banerjee, S., Liao, J., and Sarkar, F. H. (2006). Down-regulation of Notch-1 contributes to cell growth inhibition and apoptosis in pancreatic cancer cells. *Mol Cancer Ther* **5**, 483-93.

- Wasserman, R. H., and Taylor, A. N. (1966). Vitamin d3-induced calcium-binding protein in chick intestinal mucosa. *Science* **152**, 791-3.
- Wathes, D. C., Reynolds, T. S., Robinson, R. S., and Stevenson, K. R. (1998). Role of the insulin-like growth factor system in uterine function and placental development in ruminants. *J Dairy Sci* **81**, 1778-89.
- Watson, A. J., Hogan, A., Hahnel, A., Wiemer, K. E., and Schultz, G. A. (1992). Expression of growth factor ligand and receptor genes in the preimplantation bovine embryo. *Mol Reprod Dev* **31**, 87-95.
- Watson, A. J., Westhusin, M. E., and Winger, Q. A. (1999). IGF paracrine and autocrine interactions between conceptus and oviduct. *J Reprod Fertil Suppl* **54**, 303-15.
- Webster, A. B. (2003). Physiology and behavior of the hen during induced molt. *Poult Sci* **82**, 992-1002.
- Welter, H., Wollenhaupt, K., Tiemann, U., and Einspanier, R. (2003). Regulation of the VEGF-system in the endometrium during steroid-replacement and early pregnancy of pigs. *Exp Clin Endocrinol Diabetes* **111**, 33-40.
- Wen, H. Y., Abbasi, S., Kellems, R. E., and Xia, Y. (2005). mTOR: a placental growth signaling sensor. *Placenta* **26 Suppl A**, S63-9.
- White, F. J., Ross, J. W., Joyce, M. M., Geisert, R. D., Burghardt, R. C., and Johnson, G. A. (2005). Steroid regulation of cell specific secreted phosphoprotein 1 (osteopontin) expression in the pregnant porcine uterus. *Biol Reprod* **73**, 1294-301.
- White, J. A., Beckett-Jones, B., Guo, Y. D., Dilworth, F. J., Bonasoro, J., Jones, G., and Petkovich, M. (1997). cDNA cloning of human retinoic acid-metabolizing enzyme (hP450RAI) identifies a novel family of cytochromes P450. *J Biol Chem* **272**, 18538-41.
- White, J. A., Beckett, B., Scherer, S. W., Herbrick, J. A., and Petkovich, M. (1998). P450RAI (CYP26A1) maps to human chromosome 10q23-q24 and mouse chromosome 19C2-3. *Genomics* **48**, 270-2.
- Widmann, C., Gibson, S., Jarpe, M. B., and Johnson, G. L. (1999). Mitogen-activated protein kinase: conservation of a three-kinase module from yeast to human. *Physiol Rev* **79**, 143-80.
- Wieduwilt, M. J., and Moasser, M. M. (2008). The epidermal growth factor receptor family: biology driving targeted therapeutics. *Cell Mol Life Sci* **65**, 1566-84.

- Wiktor-Jedrzejczak, W., Bartocci, A., Ferrante, A. W., Jr., Ahmed-Ansari, A., Sell, K. W., Pollard, J. W., and Stanley, E. R. (1990). Total absence of colony-stimulating factor 1 in the macrophage-deficient osteopetrotic (op/op) mouse. *Proc Natl Acad Sci U S A* **87**, 4828-32.
- Wilcox, A. J., Baird, D. D., and Weinberg, C. R. (1999). Time of implantation of the conceptus and loss of pregnancy. *N Engl J Med* **340**, 1796-9.
- Williams, J. B., Etches, R. J., and Rzasa, J. (1985). Induction of a pause in laying by corticosterone infusion or dietary alterations: effects on the reproductive system, food consumption and body weight. *Br Poult Sci* **26**, 25-34.
- Winther, H., Ahmed, A., and Dantzer, V. (1999). Immunohistochemical localization of vascular endothelial growth factor (VEGF) and its two specific receptors, Flt-1 and KDR, in the porcine placenta and non-pregnant uterus. *Placenta* **20**, 35-43.
- Wittig, R., Nesslering, M., Will, R. D., Mollenhauer, J., Salowsky, R., Munstermann, E., Schick, M., Helmbach, H., Gschwendt, B., Korn, B., Kioschis, P., Lichter, P., Schadendorf, D., and Poustka, A. (2002). Candidate genes for cross-resistance against DNA-damaging drugs. *Cancer Res* **62**, 6698-705.
- Wollenhaupt, K., Welter, H., Einspanier, R., Manabe, N., and Brussow, K. P. (2004). Expression of epidermal growth factor receptor (EGF-R), vascular endothelial growth factor receptor (VEGF-R) and fibroblast growth factor receptor (FGF-R) systems in porcine oviduct and endometrium during the time of implantation. *J Reprod Dev* **50**, 269-78.
- Wu, G., Bazer, F. W., Cudd, T. A., Meininger, C. J., and Spencer, T. E. (2004). Maternal nutrition and fetal development. *J Nutr* **134**, 2169-72.
- Xiao, Y., Hughes, A. L., Ando, J., Matsuda, Y., Cheng, J. F., Skinner-Noble, D., and Zhang, G. (2004). A genome-wide screen identifies a single beta-defensin gene cluster in the chicken: implications for the origin and evolution of mammalian defensins. *BMC Genomics* **5**, 56.
- Yang, K. T., Lin, C. Y., Liou, J. S., Fan, Y. H., Chiou, S. H., Huang, C. W., Wu, C. P., Lin, E. C., Chen, C. F., Lee, Y. P., Lee, W. C., Ding, S. T., Cheng, W. T., and Huang, M. C. (2007). Differentially expressed transcripts in shell glands from low and high egg production strains of chickens using cDNA microarrays. *Anim Reprod Sci* **101**, 113-24.

- Yelich, J. V., Pomp, D., and Geisert, R. D. (1997a). Detection of transcripts for retinoic acid receptors, retinol-binding protein, and transforming growth factors during rapid trophoblastic elongation in the porcine conceptus. *Biol Reprod* **57**, 286-94.
- Yelich, J. V., Pomp, D., and Geisert, R. D. (1997b). Ontogeny of elongation and gene expression in the early developing porcine conceptus. *Biol Reprod* **57**, 1256-65.
- Yuan, L., Ahn, I. S., and Davis, P. F. (2007). Inhibition of tyrosine phosphorylation of vascular endothelial growth factor receptors in human umbilical vein endothelial cells: a potent anti-angiogenic lipid-rich extract from shark. *J Med Food* **10**, 657-61.
- Yue, Z. P., Yang, Z. M., Li, S. J., Wang, H. B., and Harper, M. J. (2000). Epidermal growth factor family in rhesus monkey uterus during the menstrual cycle and early pregnancy. *Mol Reprod Dev* **55**, 164-74.
- Zagouras, P., Stifani, S., Blaumueller, C. M., Carcangiu, M. L., and Artavanis-Tsakonas, S. (1995). Alterations in Notch signaling in neoplastic lesions of the human cervix. *Proc Natl Acad Sci U S A* **92**, 6414-8.
- Zhao, Y., and Chegini, N. (1994). Human fallopian tube expresses granulocyte-macrophage colony stimulating factor (GM-CSF) and GM-CSF alpha and beta receptors and contain immunoreactive GM-CSF protein. *J Clin Endocrinol Metab* **79**, 662-5.
- Zhao, Y., and Chegini, N. (1999). The expression of granulocyte macrophage-colony stimulating factor (GM-CSF) and receptors in human endometrium. *Am J Reprod Immunol* **42**, 303-11.
- Zhuge, Y., Lagman, J. A., Ansenberger, K., Mahon, C. J., Daikoku, T., Dey, S. K., Bahr, J. M., and Hales, D. B. (2009). CYP11B1 expression in ovarian cancer in the laying hen *Gallusdomesticus*. *Gynecol Oncol* **112**, 171-8.
- Ziecik, A. J., Wacławik, A., Kaczmarek, M. M., Blitek, A., Jalali, B. M., and Andronowska, A. (2011). Mechanisms for the establishment of pregnancy in the pig. *Reprod Domest Anim* **46 Suppl 3**, 31-41.
- Zwijsen, A., van Rooijen, M. A., Goumans, M. J., Dewulf, N., Bosman, E. A., ten Dijke, P., Mummery, C. L., and Huylebroeck, D. (2000). Expression of the inhibitory Smad7 in early mouse development and upregulation during embryonic vasculogenesis. *Dev Dyn* **218**, 663-70.

초록

임신기간중 태아소실의 대부분은 착상을 전후로 한 임신초기에 집중되어 있으며, 이는 태아의 생존과 임신의 유지에 있어 착상 전후시기의 중요성을 시사한다. 포유동물의 성공적인 임신 확립에 있어 착상전후 기간동안 모체-태아간에 형성되는 긴밀한 상호 신호전달과정은 필수적이라고 할 수 있다. 돼지의 경우 비침투적 착상기전을 통해 최종적으로 상피용모성 태반을 형성하게 되며, 이 경우 다른 타입의 태반을 형성하는 종에 비해 착상까지의 기간이 길뿐만 아니라 이 기간동안 배반포가 길이적으로 신장되는 특이적인 과정을 거침으로써 향후 모체와 영양분과 가스를 교환할 수 있는 최대한의 접촉면적을 확보한다는 점에 있어서 임신초기 모체-태아간의 상호작용에 의한 태아발달이 더욱 중요하게 부각될 수 있다.

착상 전 태아 생존과 임신의 확립은 자궁강으로 분비되는 조직영양소의 공급에 의존적이며, 이러한 조직영양소에는 다양한 영양물질들과 성장인자 등이 포함된다. 이들 조직영양소들 중, 포유동물의 배아발생이나 착상과정에 EGF, IGF-I, VEGF, 및 CSF2가 중요한 역할을 한다고 보고되어 왔으나 돼지의 경우 착상전후 기간 태아에 이러한 성장인자들이 미치는 작용에 대해서는 연구가 미흡한 편이며, 특히 이러한 성장인자들에 의한 신호전달 조절메커니즘에 대해서도 알려진 바가 거의 없다. 본 연구에서는 위의 네가지 성장인자가 임신초기 돼지 태아의 발달에 미치는 영향 및 조절기전을 규명하고자 먼저, 발정주기와 임신초기 기간동안 자궁내막내 EGF, IGF-I, VEGF, CSF2 및 해당 수용체 유전자의 발현을 비교분석 하고 발현위치를 확인하였다. 다음으로 돼지 영양외배엽세포내에서 이러

한 성장인자들에 의해 활성화되는 세포내 신호전달 경로를 조사하였으며, 해당 성장인자들의 처리에 따른 돼지 영양외배엽세포의 증식 및 이동성 변화를 분석하였다.

먼저, 돼지 영양외배엽세포내에서 EGF에 의해 유도되는 기능적 효과를 연구하였다. EGF 및 수용체 EGFR은 발정기간에 비해 임신초기 자궁내막에서 발현이 크게 증가하였으며, 주로 선상피세포와 조직 내 기질에서 세포 특이적인 발현이 확인되었다. 배양중인 영양외배엽세포에 EGF를 처리하였을 때, 세포질과 핵내의 AKT, ERK1/2 MAPK, 그리고 세포질 내 P90RSK의 인산화가 빠르게 유도되었으며, 반면 이러한 효과는 EGFR siRNA를 함께 처리하였을 때 다시 억제되었다. 뿐만 아니라 EGFR siRNA를 도입한 영양외배엽세포에서는 착상에 관련된 주요 인자들 중 IFN- δ 및 TGF β -1 유전자의 발현이 감소하는 효과를 나타내었다. 또한 EGF는 배양중인 영양외배엽세포의 증식과 이동성을 증가시키는 효과를 나타내었으며, 이러한 유도효과는 각각 p38, ERK1/2 MAPK, MTOR, 및 PI3K 특이적인 억제제 처리에 의해 감소되는 것을 밝혔다.

두번째 연구에서는 배발생이나 착상 등 다양한 생식과정에서 중요한 기능을 수행하는 것으로 알려진 IGF-I이 돼지 영양외배엽세포 발달에 미치는 영향을 분석하였다. 자궁내막 IGF-I 및 IGF-IR의 발현이 조직내 선상피세포, 자궁내강 상피세포에서 특이적으로 탐지되었으며, IGF-IR의 경우 비임신 기간에 비해 임신초기 기간동안 발현이 증가함을 확인하였다. 또한 IGF-I은 영양외배엽세포의 핵과 세포질 내 AKT, ERK1/2 MAPK, 그리고 핵부근 세포질 내 RPS6의 인산화를 유도하였으며, 이러한 IGF-I에 의한 AKT 및 ERK1/2 MAPK 인산화 유도효

과는 PI3K 억제제에 의해 감소하였다. 또한 배양중인 영양외배엽세포내에 IGF-I 을 처리하였을 때, 세포의 증식과 이동성이 유도되었으며, 이러한 유도효과는 p38, ERK1/2 MAPK, MTOR, 및 PI3K를 억제시켰을 때 크게 감소되었다.

세번째로, 주로 혈관신생이나 혈관 투과성 조절에 주요한 기능을 수행하는 것으로 잘 알려진 VEGF에 대해 연구를 수행하였다. 최근 연구에서 VEGF가 초기 배아 발달을 촉진시키는 것으로 보고되었으나, 이는 주로 수정 직후 기간을 대상으로 이루어진 것이며, 착상을 전후로 한 기간동안 VEGF의 작용과 조절기전에 대해서는 알려진 바가 거의 없다. 본 연구에서 VEGF 및 VEGFR-1, VEGFR-2의 발현이 발정주기에 비해 임신초기 기간동안 높은 수준으로 유지되었으며, 주로 자궁내막 조직의 선상피세포, 자궁내강 상피세포, 조직 내 기질에서 세포 특이적인 발현이 확인되었다. 또한 VEGF는 영양외배엽세포내 AKT, ERK1/2 MAPK, P70RSK, RPS6, 및 4EBP1의 인산화를 촉진하는 효과를 나타내었고, 반면 세포내 PI3K를 억제시켰을 때 AKT뿐만 아니라 ERK1/2의 인산화 유도효과가 감소되는 것을 밝혔다. 게다가 VEGF는 배양중인 영양외배엽세포의 증식과 이동성을 증대시키는 효과를 나타내었고, 마찬가지로 p38, ERK1/2 MAPK, MTOR, 및 PI3K 억제제를 함께 처리하였을 때 이러한 VEGF의 효과가 감쇄됨을 확인하였다.

마지막으로, 과립구대식세포 증식인자로도 잘 알려진 CSF2에 대한 연구를 수행하였다. 본 연구에서 자궁내막 CSF2의 발현이 비 임신돈에비해 착상전후 기간동안 증가하였으며, CSF2의 발현이 증가하는 시기는 발달중인 태아 영양외배엽이 신장하는 기간과 시기적으로 상응한다. CSF2는 영양외배엽세포내 AKT,

ERK1/2 MAPK, MTOR, P70RSK, 및 RPS6를 활성화시키는 효과를 나타내었고, 이전 연구들에서 CSF2에 의해 활성화된다고 잘 알려진 STAT-신호전달 경로 내 STAT3의 경우 본 연구에서는 유의적인 인산화유도효과를 나타내지 않았다. 또한 PI3K를 억제시켰을 때 CSF2에 의해 유도되는 AKT, ERK1/2, 및 MTOR의 활성화 정도가 크게 감소하였다. 배양중인 영양외배엽세포에 CSF2를 처리하였을 때 세포 증식이 증대되었으며, 이러한 효과는 ERK1/2 MAPK, MTOR, 및 PI3K를 억제시킴으로써 감쇄됨을 확인하였다.

결론적으로, 본 연구의 결과는 임신초기 자궁내막 혹은 태아유래의 EGF, IGF-I, VEGF, 및 CSF2는 돼지 영양외배엽세포의 성장과 발달에 중요한 역할을 하며, 이러한 성장인자들에 의한 임신초기 태아 발달 효과는 주로 PI3K-AKT 및 ERK1/2 MAPK를 포함한 다양한 세포 내 신호전달 경로들을 통해 조절됨을 시사한다. 이러한 결과들은 임신초기 성장인자에 의해 매개되는 모체-태아간 상호작용의 보다 심도있고 종합적인 이해를 위한 선행 기초연구가 될 뿐만 아니라, 착상, 임신을 개선 및 주요 경제동물 생산성 증대를 위한 연구분야에 기여할 수 있을 것으로 사료된다.

주요어: 영양외배엽세포, peri-implantation, EGF, IGF-I, VEGF, CSF2

학번: 2010-24127